AN ABSTRACT OF THE DISSERTATION OF

Stephen R. Pacella for the degree of Doctor of Philosophy in Ocean, Earth, and Atmospheric Sciences presented on November 5, 2018.

Title: Interactions amongst Local and Global Drivers of Coastal Acidification in Estuarine Habitats of the Northern California Current

Abstract approved:

_____

George G. Waldbusser

The variability of coastal carbonate chemistry continues to provide significant hurdles for understanding interactions between anthropogenic and natural CO_2 cycling and resultant effects on coastal acidification dynamics. Attribution of the anthropogenic component is vital for identifying the impacts of increasing atmospheric carbon on coastal habitats such as coral reefs, upwelling margins, inland seas, and estuaries. The dynamic nature of these systems has led some to conclude that the baseline shift in atmospheric CO_2 is a relatively unimportant driver, but emerging evidence of rapidly acidifying coastal systems suggests otherwise. This dissertation addresses natural and anthropogenic inorganic carbon cycling interactions on diel, seasonal, and decadal time scales to determine current and future acidification trajectories in estuary habitats typical of the northern California Current. Chapter 2 focuses on alterations of diel-scale "carbonate weather" and accelerated rates of acidification in a seagrass habitat resulting from interactions between metabolic CO_2 cycling and rising atmospheric CO_2 levels. Chapter 3 quantifies how the seasonal variability of

carbonate chemistry in two seagrass habitats is altered by rising atmospheric CO_2, and how these alterations compare with perturbations driven by altered river discharge, warming temperatures, and eutrophication. Chapter 4 investigates the temporal and spatial dynamics of coastal acidification drivers in a small, open-coast estuary subject to seasonal upwelling and inputs from an agriculturally-developed watershed. This work shows that estuarine habitats are often poorly-buffered against increasing global atmospheric CO_2 levels, resulting in accelerated changes of extreme carbonate weather and enhanced CO_2 seasonality. Current and future acidification trajectories are significantly modulated by local biophysical processes, including net community metabolism and watershed chemistry. While these local processes control the variance of acidification trajectories amongst estuarine systems, our results suggests the global atmospheric CO_2 perturbation is likely the dominant anthropogenic driver of coastal acidification in many systems. Management and policymaking for coastal acidification impacts will be more effective if the spatial and temporal interactions between local and global drivers of acidification are properly accounted for.

Interactions amongst Local and Global Drivers of Coastal Acidification in Estuarine Habitats of the Northern California Current

by
Stephen R. Pacella

A DISSERTATION

submitted to

Oregon State University

in partial fulfillment of
the requirements for the
degree of

Doctor of Philosophy

Presented November 5, 2018
Commencement June 2019

Doctor of Philosophy dissertation of Stephen R. Pacella presented on November 5, 2018.

APPROVED:

Major Professor, representing Ocean, Earth, and Atmospheric Sciences

Dean of the College of Earth, Ocean, and Atmospheric Sciences

Dean of the Graduate School

I understand that my dissertation will become part of the permanent collection of Oregon State University libraries. My signature below authorizes release of my dissertation to any reader upon request.

Stephen R. Pacella, Author

ACKNOWLEDGEMENTS

This dissertation represents the research efforts and professional and moral support of many, to whom I am forever grateful. The faculty and staff in the College of Earth, Ocean, and Atmospheric Sciences have always been incredibly helpful and supportive, and there is no way I would have made it out alive without their guidance. I am proud to have been able to be a member of this world-class research community.

My advisor, George Waldbusser, has served as a scientific, professional, and moral compass since the beginning of this project. His unwavering (and high) bar for excellence in research has pushed me beyond what I had thought I was capable of. I will always be grateful for his guidance in my development as a research scientist.

My committee members, Burke Hales, Laurie Juranek, Cheryl Brown, and Skip Rochefort have all served as vital resources throughout my time at CEOAS. They have been incredibly generous with their time and advice, and their obvious interest in my personal and professional development is very appreciated. In particular, my conversations with Burke Hales have dramatically improved the science contained in this dissertation and heavily influenced my research focus.

The support of the Pacific Coastal Ecology Branch in all ways over the years has been remarkable. Their investment in my development has been pivotal for my career, and I will always be grateful for the opportunities and responsibilities they have granted me. Walt Nelson and Ted Dewitt have been encouraging and supportive mentors whom took many chances on me through the years, and are ultimately responsible for the opportunities necessary to have completed this degree. Cheryl Brown, Jim Kaldy, T Chris Mochon Collura, Jody Stecher, Pat Clinton, Nate Lewis, Darryl Marrois, Bill Rugh, Amy Zimmer-Faust, and Rochelle Labiosa all helped with field work and planning. I am also grateful for the assistance of EPA's Region 10 dive team and the Tulalip Tribes with field work and project planning. This project would not have been possible without Cheryl Brown's unwavering mentorship and generosity.

Finally, I have benefitted enormously from the incredible base of support in my family and friends. I am blessed to have been helped along in this process by more than I can name here, and I will forever be grateful for the love you have all shown me. I am especially grateful for the love and support of Annika through this process, and from afar of my parents, who have selflessly sacrificed to grant me the opportunities I have today.

CONTRIBUTION OF AUTHORS

Chapter 2:

The study was conceived of and designed by S.R. Pacella, C.A. Brown, G.G. Waldbusser, R.G. Labiosa, and B. Hales. S.R. Pacella and C.A. Brown performed the field work. B. Hales contributed new analytical tools. S.R. Pacella, G.G. Waldbusser, B.H. Hales analyzed data. S.R. Pacella wrote the first draft of the manuscript. S.R. Pacella, G.G. Waldbusser, C.A. Brown, and R.G. Labiosa provided edits for the final version of the manuscript.

Chapter 3:

The study was conceived of and designed by S.R. Pacella, C.A. Brown, G.G. Waldbusser, R.G. Labiosa, and B. Hales. S.R. Pacella, C.A. Brown, and T.C. Mochon Collura performed the field work. B. Hales contributed new analytical tools. S.R. Pacella, G.G. Waldbusser, B.H. Hales analyzed data. S.R. Pacella wrote the first draft of the manuscript. S.R. Pacella, G.G. Waldbusser, C.A. Brown, and R.G. Labiosa provided edits for the final version of the manuscript.

Chapter 4:

The study was conceived of and designed by S.R. Pacella, C.A. Brown, J.E. Kaldy, and R.G. Labiosa. S.R. Pacella, C.A. Brown, J.E. Kaldy, T.C. Mochon Collura, and H.A. Stecher performed the field work. B. Hales contributed new analytical tools. S.R. Pacella and C.A. Brown analyzed data. S.R. Pacella wrote the first draft of the manuscript. S.R. Pacella and C.A. Brown provided edits for the final version of the manuscript.

TABLE OF CONTENTS

Page

TABLE OF CONTENTS (Continued)

Page

TABLE OF CONTENTS (Continued)

Page

TABLE OF CONTENTS (Continued)

Page

LIST OF FIGURES

LIST OF FIGURES (Continued)

Figure Page

LIST OF FIGURES (Continued)

Figure Page

LIST OF TABLES

1. Introduction: Ocean acidification in estuarine habitats

Over the past ~250 years, anthropogenic CO_2 emissions primarily from land use change and fossil fuel combustion have resulted in a mean global atmospheric CO_2 increase from pre-industrial (PI) levels of ~280 ppm to presently exceeding 400 ppm, with the majority of this increase having occurred since 1950. The resulting change in the atmosphere – ocean pCO_2 gradient has driven a net accumulation of CO_2 in the ocean (C_{anth}), which in turn increases the partial pressure of seawater CO_2 (pCO_2) and decreases seawater pH_T and carbonate mineral saturations states (e.g. $\Omega_{aragonite}$). These collective changes in the CO_2 chemistry of the ocean are commonly referred to as ocean acidification (OA). The acidification of the ocean happening presently is unique when compared to past geologic events, as the current rate of atmospheric CO_2 increase severely outpaces the flux of weathered materials to the ocean, inhibiting the ability for the natural carbon cycle to buffer against increasing C_{anth} burdens and declining pH. Effectively an acid-base imbalance on the level of the global ocean, rates of ocean acidification are an order of magnitude larger than have occurred for millions of years (Doney and Schimel, 2007), open-ocean pH is lower than has occurred in the past ~2 million years (Hönisch *et al.*, 2012), and predicted acidification rates for the later 21st century are unlikely to have occurred in the past ~14 million years (Sosdian *et al.*, 2018). This oceanic sink of anthropogenic CO_2 presently accounts for nearly one third of human CO_2 emissions to the atmosphere (Sabine *et al.*, 2002), and significantly moderates rates of atmospheric CO_2 increase and global climate change dynamics as a result (Sabine *et al.*, 2004; Doney *et al.*, 2009).

Mean ocean pH has declined by ~0.1 units since the pre-industrial period, with a further 0.3-0.4 unit decrease expected by the end of the 21st century based on business-as-usual emissions pathways (Doney *et al.*, 2009). Observations of the changes in ocean chemistry driven by OA have come from analysis of high quality, long-term open ocean time series (e.g. Bates *et al.*, 2012) of marine carbonate system parameters (including pH and pCO_2). These analyses generally show that the rate of ocean pCO_2 increase tracks the rate of atmospheric CO_2 increase. This observation of relatively constant air-sea pCO_2 disequilibrium has enabled the ocean carbon community to develop modeling methods for hindcasting how C_{anth} burdens have evolved with atmospheric CO_2 increase, taking into account the ventilation age of water parcels and the atmospheric CO_2 levels at which these water parcels were last in contact with the atmosphere (Gruber *et al.*, 1996; Sabine *et al.*, 2002, 2004). More recently, these relatively simple empirical models have been supplemented with complex coupled physical/biogeochemical numerical models capable of simulating oceanic carbon cycling into the future, while also including mechanisms for potential climate and ecological feedbacks (e.g. (Gruber *et al.*, 2012; Hauri *et al.*, 2013)).

Over the past ~10 years there has been a large effort by the ocean carbon community to understand how rising atmospheric CO_2 and increasing oceanic C_{anth} affects the CO_2 chemistry of coastal ocean waters (e.g. Feely *et al.*, 2008; Waldbusser *et al.*, 2011; Duarte *et al.*, 2013). This more recent OA research has built upon a rich literature that has shown carbon cycling in coastal and estuarine waters to fundamentally differ from that of the open ocean. Coastal zones are characterized by coincident and amplified physical and biogeochemical processes relative to the open ocean, including:

vigorous aerobic and anerobic metabolic activity; hydrodynamic processes such as tidal action, riverine and groundwater discharges, and estuarine circulation; biogenic calcification and dissolution; gas exchange; and benthic-pelagic biogeochemical coupling and redox cycling. The co-occurrence and rapid rates of these processes, often on small spatial and temporal scales, results in CO_2 chemistry of coastal and estuarine waters that is characteristically far more variable, both in amplitude and frequency space, than that typically found in open-ocean biomes (Hofmann *et al.*, 2011). This high-frequency variability of the CO_2 system typical of coastal and estuarine habitats has been termed "carbonate-weather" (Waldbusser and Salisbury, 2014). The variability of pH and other CO_2 system parameters in coastal zones, along with the multiple interactions amongst drivers responsible for this variability, has called into question (Duarte *et al.*, 2013), and spurred discussions on (Wallace *et al.*, 2014; Waldbusser and Salisbury, 2014), how rising atmospheric CO_2 and oceanic C_{anth} levels will impact these systems.

The natural processes operating in coastal zones to control CO_2 chemistry have been shown to sometimes combine with anthropogenic drivers and amplify the acidifying effects in coastal waters. For example, (Cai *et al.*, 2011) demonstrated that additions of respiratory CO_2 resulting from eutrophication can enhance the depression of pH levels in subsurface waters of the Gulf of Mexico. This "enhanced acidification" is a result of the fundamental thermodynamic properties of the marine carbonate system, whereby unbuffered additions of CO_2 will titrate CO_3^{2-} ions and push the distribution of dissolved inorganic carbon (made up of $CO_{2(aq)}$ + H_2CO_3 (hereafter simply $CO_{2(aq)}$ given the vastly greater abundance of this form over H_2CO_3), HCO_3^-, and CO_3^{2-}) towards the $CO_{2(aq)}$ and HCO_3^- species. The titration of available CO_3^{2-} with CO_2 thereby results in a loss in

buffering capacity of the waters and enhances reductions in pH and increases of pCO_2 with continuing CO_2 addition. The natural buffering capacities of coastal and estuarine waters are often much less than that of the open-ocean, due to dilution with low alkalinity freshwaters, accumulation of metabolic CO_2, and presence of organic acid-base systems (Yang *et al.*, 2015) not seen in open ocean settings. This reduced buffering capacity has been well-established in the literature and shown to make coastal waters more susceptible to changes in their carbonate systems with anthropogenic CO_2 addition when compared with full-strength ocean waters (Egleston *et al.*, 2010; Cai *et al.*, 2011; Waldbusser *et al.*, 2011; Hu and Cai, 2013a).

Concurrent with the development of our understanding of how OA will change ocean chemistry, a large research effort has been underway to understand how these chemical changes will impact coastal organisms and ecosystems. Compilations of experimental results show a diverse range of physiological and behavioral responses by organisms to the lowered pH_T and $CaCO_3$ saturation states (Ω), and increased pCO_2 levels, expected with OA during the 21st century (Gazeau *et al.*, 2013; Kroeker *et al.*, 2013; Busch and McElhany, 2016). Information on these organismal and taxon-specific OA impacts have been applied to coastal ecosystems models, which have found that ecological interactions can both ameliorate and enhance the impacts of OA on organisms (Ainsworth *et al.*, 2011; Busch *et al.*, 2013). While the information gained thus far represents an enormous scientific effort and is incredibly valuable, OA experiments conducted with coastal organisms have generally been designed with static pH and pCO_2 treatments chosen to represent predicted end-of-century open ocean conditions (Gimenez *et al.*, 2018). Given the observed variability of coastal CO_2 chemistry, it is unlikely these

treatments are representative of *in-situ* conditions organisms are facing presently, nor in future high-CO_2 scenarios (Reum *et al.*, 2014). In response to this, the latest generation of OA experiments have begun to incorporate multiple stressors and high-frequency manipulations of CO_2, dissolved oxygen, and other stressors to more accurately represent the observed variability of coastal habitats (Boyd *et al.*, 2016; Clark and Gobler, 2016; Gimenez *et al.*, 2018).

Despite the variability of CO_2 chemistry in coastal habitats, the demonstrated potential for amplification of low pH conditions, and experimental evidence for susceptibility of coastal organisms to OA, there has been little mechanistic work on how natural and anthropogenic CO_2 cycling in coastal zones will interact to shape the chemical habitat of organisms on time and space scales relevant for their fitness. An improved understanding of natural and anthropogenic carbon interactions would help inform how much of the observed carbonate weather in our present-day observations is due to natural versus anthropogenic CO_2 cycling, as well as forecasting how this interaction will shape future carbonate weather of coastal habitats. Attribution of OA impacts on coastal carbonate chemistry could improve OA experimental treatments to better simulate current and future exposure of organisms to stressful CO_2 conditions. Additionally, attribution of the natural versus anthropogenic signals in present-day pH observations is of intense interest to managers and policymakers (Kelly *et al.*, 2011; Strong *et al.*, 2014) for quantifying exceedances of water quality criteria, as well as designing policies addressing current and future OA impacts in coastal habitats.

The research effort described in this dissertation was motivated by the relative lack of information on how CO_2 chemistry in estuarine habitats is likely to change with

OA, despite the demonstrated potential for enhanced impacts of C_{anth} in coastal and estuarine habitats (Egleston *et al.*, 2010; Cai *et al.*, 2011) operating on spatial and temporal scales (Waldbusser *et al.*, 2011) to be relevant for OA-sensitive coastal organisms (Waldbusser and Salisbury, 2014). I sought to investigate how additions of anthropogenic carbon have altered the CO_2 cycling of estuarine habitats on daily and seasonal time scales, and how future increases in atmospheric CO_2 will further modify present-day dynamics. I focused on estuarine habitats known to be ecologically important for many coastal organisms and ecosystems in order to specifically quantify how the chemical environments for these resident organisms have been, and will be, altered with OA.

Chapter 2 describes the temporal variability of dry season pH_T, aragonite saturation state (Ω_{arag}), and pCO_2 in a shallow, subtidal *Zostera marina* seagrass habitat of Puget Sound, WA, USA. *In-situ* observations of pH_T, dissolved oxygen, temperature, salinity, and water depth were combined with discrete samples of pCO_2 and dissolved inorganic carbon (DIC) concentrations to characterize the carbonate weather of the seagrass habitat over a span of 3 months. These observations were used to parameterize a 1-D time-dependent mechanistic model describing changes in DIC and alkalinity (Alk) with terms for aerobic photosynthesis and respiration, mixing between marine and river end-members, and gas exchange of CO_2 and O_2. This model faithfully reproduced observations of pH_T, Ω_{arag}, and pCO_2 dynamics in the habitat, and resulted in a 15-minute resolution time series of the full carbonate system for the three-month study period. This model time series was used to estimate how additions of anthropogenic carbon (C_{anth}) from rising atmospheric CO_2 between the years 1765-2100 interacts with metabolic CO_2

cycling in the habitat to alter high-frequency pH_T, Ω_{arag}, and pCO_2 dynamics. The addition of C_{anth} was found to reduce the habitat's ability to buffer against natural metabolic CO2 cycling, resulting in enhanced pH_T depressions and pCO_2 increases with increasing atmospheric CO_2 levels. Model runs both with and without the aerobic metabolism term revealed seagrass habitat metabolism to currently increase the severity of transient harmful conditions (i.e. low pH_T, low Ω_{arag}, and high pCO_2), but ultimately reduce organismal exposure to harmful conditions in future, high CO_2 scenarios. These findings suggest a complicated role of seagrass habitats as chemical refugia for OA-sensitive organisms, the efficacy of which is likely related to the time scales on which a given organism is susceptible to CO_2 system change. The interactions between metabolic and anthropogenic carbon leading to reduced buffering capacities and more extreme CO_2 levels in the seagrass habitat of this study are a function of the fundamental thermodynamics of the marine carbonate system and are therefore broadly applicable to metabolically vigorous coastal and estuarine habitats. It is likely these interactions will lead to more extreme carbonate weather in estuarine habitats with continued ocean acidification, the ecological ramifications of which are just beginning to be studied.

Chapter 3 builds upon the dataset from Chapter 2 to investigate the seasonal drivers of carbonate weather in two seagrass beds of Puget Sound, WA, USA over a ten-month period, and then simulate how the addition of C_{anth} will alter the seasonal evolution of carbonate weather in the habitats. One-dimensional mechanistic models were built to calculate the contributions of riverine dilution, temperature changes, aerobic photosynthesis and respiration, $CaCO_3$ formation and dissolution, and CO_2 gas exchange to observed pH_T, pCO_2 and Ω_{arag} levels. Aerobic metabolism was found to be responsible

for the majority of seasonal changes in CO_2 system parameters. The summer and spring seasons were characterized by large net photosynthetic removals of DIC from the water column in both habitats, raising pH_T and Ω_{arag} levels and lowering pCO_2 when compared with source water values. Winter conditions were estimated to have an approximately balanced net metabolism, with pH_T, Ω_{arag}, pCO_2 levels similar to values expected from conservative mixing between sub-surface marine waters near the study sites and the Snohomish River. The simulated addition of C_{anth} in the habitats drove variable, season-specific changes in the CO_2 system parameters, with the most rapid declines in pH_T and increase in pCO_2 during the winter for both habitats. This season-specific variability in the progression of OA in the habitats was driven by seasonal differences in the buffer factors (e.g. $\frac{\frac{\partial[H^+]}{[H^+]}}{\frac{\partial[DIC]}{[DIC]}}$), largely described the evolution of the DIC:Alk ratio of waters in the habitats. The photosynthetic removal of DIC in the summer and spring lowered DIC:Alk ratios in both habitats, making them more buffered against additions of C_{anth}. In contrast, the lack of this photosynthetic DIC removal during the winter enhanced OA-driven pH_T and pCO_2 changes in both habitats, with the most severe changes in the seagrass study site with lower net community production (and therefore higher DIC:Alk ratios). These results demonstrate the strong spatial and temporal gradients of OA impacts in estuarine habitats, and the role of net ecosystem metabolism in setting the baseline sensitivities of these habitats to rising atmospheric CO_2. From a first-order perspective, coastal habitats characterized by lower net community production and higher DIC:Alk ratios will be more sensitive to OA impacts, hastening the exceedance of physiological thresholds for OA-sensitive organisms in already naturally stressful chemical environments. The impacts of

current and future changes in river discharge, temperature increases, and eutrophication on the CO_2 systems of the study sites are estimated to be far less than those driven by rising atmospheric CO_2 and accumulation of C_{anth}. The dominance of this globally-driven C_{anth} signal in current and future changes highlights the potentially limited ability for local management actions to offset OA impacts in these estuarine habitats.

Chapter 4 builds on the methods and lessons learned from the previous work in Puget Sound to investigate rates of ocean and watershed-mediated coastal acidification in a California Current estuary. The project sought to characterize the seasonal CO_2 system dynamics of Tillamook Estuary, OR (USA), a small open-coast estuary in the northern California Current Large Marine Ecosystem subject to coastal upwelling and river discharge from an agriculturally-developed watershed. Seasonal variability in the ocean and watershed end-members was the primary control on CO_2 chemistry of the estuary, with internal bay processes acting as a seasonally variable sink and source of DIC. The highest values of river DIC and Alk in the watershed were observed in areas of agricultural activity and were hypothesized to be driven by human land use change. These watershed DIC and Alk enrichments were combined with published estimates of oceanic anthropogenic carbon burdens to estimate the magnitude and timing of human changes to present-day CO_2 chemistry in the estuary. Most of the human-driven perturbation in estuarine chemistry during our study period was due to ocean acidification-driven changes in the coastal ocean, with the impacts of altered watershed chemistry mostly constrained to areas of low salinities (i.e. reduced influence of ocean waters). Consistent with the findings in Puget Sound, the dominant role of oceanic C_{anth} and limited role of local anthropogenic drivers suggests that local management actions

(e.g. nutrient reductions) aimed at improving OA-related water quality indices in the estuary are likely to show limited results.

SEAGRASS HABITAT METABOLISM INCREASES SHORT-TERM EXTREMES AND LONG-TERM OFFSET OF CO_2 UNDER FUTURE OCEAN ACIDIFICATION

Stephen R. Pacella[a,b], Cheryl A. Brown[a], George G. Waldbusser[b], Rochelle G. Labiosa[c], and Burke Hales[b]

[a]Western Ecology Division, National Health and Environmental Effects Research Laboratory, Office of Research and Development, United States Environmental Protection Agency, Newport, OR 97365

[b]College of Earth, Ocean, and Atmospheric Sciences, Oregon State University, Corvallis, OR 97331

[c]Region 10, United States Environmental Protection Agency, Seattle, WA 98101

Proceedings of the National Academy of Sciences of the United States of America

500 Fifth Street NW, NAS 338, Washington, DC 20001 USA

Issue 115 (15)

2. Seagrass habitat metabolism increases short-term extremes and long-term offset of CO_2 under future ocean acidification

2.1 Abstract

The role of rising atmospheric CO_2 in modulating estuarine carbonate system dynamics remains poorly characterized, likely due to myriad processes driving the complex chemistry in these habitats. We reconstructed the full carbonate system of an estuarine seagrass habitat for a summer period of 2.5 months utilizing a combination of time-series observations and mechanistic modeling, and quantified the roles of aerobic metabolism, mixing, and gas exchange in the observed dynamics. The anthropogenic CO_2 burden in the habitat was estimated for the years 1765-2100 to quantify changes in observed high-frequency carbonate chemistry dynamics. The addition of anthropogenic CO_2 alters the thermodynamic buffer factors (e.g. the Revelle factor) of the carbonate system, decreasing the seagrass habitat's ability to buffer natural carbonate system fluctuations. As a result, the most harmful carbonate system indices for many estuarine organisms (minimum pH_T, minimum Ω_{arag}, and maximum $pCO_{2(s.w.)}$) change up to 1.8x, 2.3x, and 1.5x more rapidly than the medians for each parameter, respectively. In this system, the relative benefits of the seagrass habitat in locally mitigating ocean acidification increase with the higher atmospheric CO_2 levels predicted toward 2100. Presently however, these mitigating effects are mixed due to intense diel cycling of CO_2 driven by aerobic metabolism. This study provides the first estimates of how high-frequency pH_T, Ω_{arag}, and $pCO_{2(s.w.)}$ dynamics are altered by rising atmospheric CO_2 in an

estuarine habitat, and highlights non-linear responses of coastal carbonate parameters to ocean acidification relevant for water quality management.

2.2 Introduction

Ocean acidification (OA) due to increasing atmospheric CO_2 from anthropogenic emissions increases the dissolved inorganic carbon ($[TCO_2]$) and partial pressure of seawater CO_2 ($pCO_{2(s.w.)}$), and decreases seawater pH_T and carbonate mineral saturation states (e.g. Ω_{arag}). These changes in marine chemistry have been demonstrated to negatively affect acid-base balance, biocalcification, and metabolism of coastal and estuarine organisms(George G. Waldbusser *et al.*, 2015). Many observational studies of OA have focused in open ocean (Bates *et al.*, 2012) and shelf waters (Feely *et al.*, 2008; Takeshita *et al.*, 2015; Sutton *et al.*, 2016), with fewer studies investigating how rising atmospheric CO_2 interacts with estuarine carbonate chemistry (R. a. Feely *et al.*, 2010; Hales *et al.*, 2016). The carbonate chemistry in estuarine habitats is highly variable (Hinga, 1992; Hales *et al.*, 2016) due to high rates of photosynthesis and respiration, hydrodynamic processes (including tides, freshwater inputs, and estuarine circulation), biogenic calcification and dissolution, gas exchange, and strong benthic-pelagic biogeochemical coupling (Hofmann *et al.*, 2011; Waldbusser and Salisbury, 2014). The resulting dynamic range of high-frequency estuarine carbonate chemistry calls into question the impact of rising atmospheric CO_2 levels as a driver in these systems (Waldbusser and Salisbury, 2014; Wallace *et al.*, 2014), with suggestions that OA (as defined above) is predominant only in open-ocean environs (Duarte *et al.*, 2013).

There is, however, an emerging appreciation for the role of high-frequency (i.e. sub-hourly time scales) carbonate chemistry dynamics influencing organismal responses to OA (Waldbusser and Salisbury, 2014; Small *et al.*, 2016). Yet, despite the significance of the coastal zone to ecosystems and our economy, our understanding of how natural and anthropogenic processes control estuarine carbonate chemistry is generally limited to studies of large spatial and/or low temporal resolution (Provoost *et al.*, 2010; Feely *et al.*, 2010; Feely *et al.*, 2016), with relatively little mechanistic examination. Thus, our understanding of how the global baseline increase in atmospheric CO_2 interacts with habitat-specific, high-frequency carbonate chemistry dynamics, or "carbonate weather," (Waldbusser and Salisbury, 2014) to alter the chemical environment of estuarine organisms is poorly understood. The fundamental thermodynamic properties of the marine carbonate system predict that an increase in baseline [TCO_2] levels will amplify the dynamic ranges of pH and $pCO_{2(s.w.)}$, and dampen that of Ω_{arag} (Egleston *et al.*, 2010). The two studies we are aware of that have investigated this response of the carbonate system (in coral reef (Shaw *et al.*, 2013) and coastal shelf (Takeshita *et al.*, 2015) systems) to future OA have highlighted the importance of this altered buffering capacity of the carbonate system, resulting in larger modeled dynamic ranges of $pCO_{2(s.w.)}$ and pH_T, and reduced dynamic ranges of Ω_{arag} (Shaw *et al.*, 2012; Takeshita *et al.*, 2015). Attribution of the drivers of CO_2 dynamics responsible for the large dynamic ranges observed in estuaries permits a more rigorous and mechanistic analysis of how interactions between OA and nearshore, habitat-specific carbonate weather may be expected to accelerate carbonate conditions demonstrated to be harmful for coastal organisms (e.g. low pH, high $pCO_{2(s.w.)}$, low Ω_{arag}). This mechanistic

approach to attribution of natural versus anthropogenically - driven carbonate dynamics is also crucial for informing pressing management decisions related to coastal water quality (Kelly *et al.*, 2013; Strong *et al.*, 2014).

The objectives of this study were to 1) characterize the carbonate weather in a shallow seagrass habitat typical of the Puget Sound estuarine system at time scales relevant to individual organisms, 2) de-convolve the observed chemical time series into the primary biological and physical drivers through mechanistic modeling, and 3) use these model results of present-day processes to illustrate the effect of OA on carbonate weather in the seagrass habitat under pre-industrial through future emission scenario conditions. We focused on the dry season (July through September), which is a critical period of growth and recruitment for many estuarine producer and consumer species in Puget Sound (Miller *et al.*, 2016). Our analyses focused on how the interaction of OA and aerobic metabolism in this habitat controls the onset and severity of exposure to low pH_T, high $pCO_{2(s.w.)}$, and low Ω_{arag} conditions for resident organisms currently and into the future.

2.3 Results and Discussion

High-resolution (15 min^{-1}) observations of pH_T from July 15 – October 1, 2015 in a seagrass habitat of Hat Island in Puget Sound, WA showed large variability on time scales consistent with local diel photosynthesis/respiration cycles, tidal advection of metabolically-altered water parcels, and wind-driven mixing events (mean pH_T = 8.08, s.d. = 0.16, max pH_T = 8.43, min pH_T = 7.59, n = 7,455) (SI Appendix, Fig. S1). The mean diel range of pH_T for the period of observation was 0.39 (s.d.=0.16, n=78 days)

units, with a maximum observed diel range of 0.74 units, similar to published observations from other metabolically-intensive coastal systems (Hofmann *et al.*, 2011; Baumann *et al.*, 2014; Takeshita *et al.*, 2015). pH_T was significantly correlated with O_2 (R^2 =0.91, $p < 0.001$, SI Appendix, Fig.S2), demonstrating the role of aerobic metabolism (primary production + respiration) in observed carbonate chemistry variability. Tidal exchange was documented by sampling the water masses representing mixing end-members for the Hat Island site as: 1) marine deep water (sampled at 50m) entering Possession Sound to the south of Hat Island, and 2) the Snohomish River (Banas *et al.*, 2015; Yang *et al.*, 2015). The marine end-member was characterized by consistently low pH_T and elevated TCO_2 (mean=7.66, s.d. = 0.02, n=5; $[TCO_2]$ = 2,024 μmol kg^{-1}, s.d. = 9.2 μmol kg^{-1}; [Alk] = 2,061 μmol kg^{-1}, s.d. = 10.1 μmol kg^{-1}) and low O_2 (mean=194.5 μmol kg^{-1}, s.d. = 9.7 μmol kg^{-1}, n=5), consistent with published observations of deep marine waters in Puget Sound, whose ultimate source has been traced back to delivery of North Pacific Ocean waters through the Strait of Juan de Fuca via estuarine circulation (Feely *et al.*, 2010; Murray *et al.*, 2015). In contrast, the Snohomish River displayed variable pH_T and lower TCO_2 (mean=7.88, s.d. = 0.40, n=5; $[TCO_2]$ = 572 μmol kg^{-1}, s.d. = 45 μmol kg^{-1}; [Alk] = 555 μmol kg^{-1}, s.d. = 27 μmol kg^{-1}) and O_2 (mean=290.7 μmol kg^{-1}, s.d. = 9.7 μmol kg^{-1}, n=5) when compared with deep marine waters. Salinities at Hat Island (mean = 27.96, s.d. = 0.80, n = 7,455) indicated strong influence of marine deep waters, with a relatively small amount of freshwater dilution during the dry season.

To characterize the primary processes responsible for the observed variability of carbonate chemistry in the seagrass habitat, we developed a deterministic model (termed

the “Full Model”) that included tidal mixing (via salinity variance), net community metabolism (NCM; via O_2/CO_2 stoichiometry), and gas exchange processes (see Methods and Supplemental Information). The Full Model reproduced 92% of the observed variance in the pH_T time series (Pearson Product Correlation, $r = 0.957$; $p < 0.001$; Fig. 1a), and also showed good agreement with calculated values of $pCO_{2(s.w.)}$ and Ω_{arag} (Fig. 1b & 1c) from discrete samples with measured [TCO_2], $pCO_{2(s.w.)}$, and pH_T (Satlantic SeaFET) taken next to in-situ sensors ($pCO_{2(s.w.)}$ root mean squared error (R.M.S.E.) = 13.5 μatm, $r=0.99$, $p < 0.001$; Ω_{arag} R.M.S.E. = 0.19, $r = 0.94$, $p < 0.001$), and published carbonate system values observed near our study site(Pelletier *et al.*, 2018) . The NCM estimates were on average responsible for 66% (s.d. = 26%) and 35% (s.d. = 31%) of modeled [TCO_2] and [Alk] variability in the Full Model, respectively (SI Appendix, Fig. S3). Conservative mixing of the marine and riverine end members accounted for an average of 34% (s.d. = 26%) and 65% (s.d. = 31%) of modeled [TCO_2] and [Alk] variability, respectively. Gas exchange was episodically important during the observational period, but generally a small component of the high-frequency [TCO_2] variability due to low wind speeds and relatively slow exchange rates of CO_2 due to carbonate system buffering (SI Appendix, Fig. S3). Observations indicated the study site was within a stable surface mixed layer for the majority of the dry-season observational period; larger gas exchange fluxes from equilibration between locally upwelled high CO_2 waters and the atmosphere likely occurred earlier during the spring transition and shoaling/formation of the observed surface mixed layer (Moore-Maley *et al.*, 2016).

We simulated the impacts of changing atmospheric CO_2 from 1765 to 2100 using the RCP 8.5 emissions scenario(Riahi *et al.*, 2011) both to hind-cast and forecast how

carbonate weather of the system is altered. These simulations estimate the state of the observed system (based on year 2015 dynamics of aerobic metabolism and mixing) under different levels of atmospheric CO_2, with the 1765 scenario representing the carbonate chemistry of the habitat if fossil fuels were never burned. Modeled anthropogenic [TCO_2] (C_{anth}) in 2015 ranged from 47-59 μmol kg^{-1}. Estimates of C_{anth} for nearshore surface waters of the California Current in the year 2012 have been previously published as 52-58 μmol kg^{-1} (Feely *et al.*, 2016) and 62 μmol kg^{-1} (Takeshita *et al.*, 2015), which compare well with our mean model estimate of 53 μmol kg^{-1} for the same year. The small discrepancies amongst the values can be attributed to differences in temperature, salinity, and alkalinity of surface waters in the studies; warm, fresh, low alkalinity waters (such as those found at the Hat Island study site) hold relatively less C_{anth} when theoretically equilibrated with a given atmospheric CO_2 level. Results of these yearly 1765-2100 OA simulation models provide the first estimates of how pH_T, Ω_{arag}, and $pCO_{2(s.w.)}$ high-frequency dynamics (i.e. carbonate weather) in an estuarine habitat are altered by rising atmospheric CO_2.

Model results indicate that OA alters both means/medians and diel ranges of pH_T, $pCO_{2(sw)}$, and Ω_{arag} in the seagrass habitat, resulting in more rapid changes to extreme events relative to means/medians (Fig. 2). Median dry-season pH_T decreased 0.12 units from the pre-industrial (year 1765) to 2015, with a total median reduction of 0.41 units expected by the year 2100 under the RCP 8.5 emission scenario (Table S1), equivalent to an increase in acidity of 32% in 2015, and 157% by 2100. Compared to the year 1765, mean $pCO_{2(sw)}$ increased by 107 μatm (+45%) in 2015 and 548 μatm (+227%) in 2100, while mean dry-season Ω_{arag} decreased by 0.56 units (-20%) in 2015, and 1.50 units (-

54%) in 2100. In addition to these changes in the median/mean values, changes to the thermodynamic buffer factors of the carbonate system (driven by increasing C_{anth}) altered diel ranges of pH_T, $pCO_{2(sw)}$, and Ω_{arag} (SI Appendix, Table S1). Previous work(Egleston, Sabine and Morel, 2010; Hagens and Middelburg, 2016) has shown that the sensitivities of pH_T, $pCO_{2(sw)}$, and Ω_{arag} (defined here as $\frac{\Delta x}{\Delta[TCO_2]}$, where x is the carbonate parameter of interest) respond differently to changes in $[TCO_2]$. Briefly, pH_T is most sensitive near the point where $[TCO_2]$ = [Alk], $pCO_{2(s.w.)}$ is increasingly sensitive to increasing values of $[TCO_2]$, and Ω_{arag} is decreasingly sensitive to increasing levels of $[TCO_2]$. These sensitivities, delineated by the thermodynamic buffer factors of the marine carbonate system, are responsible for the behavior as illustrated in Fig. 3: diel ranges of pH_T, $pCO_{2(s.w.)}$, and Ω_{arag} of the pre-industrial, 2015, and 2100 models change through time with increasing OA, despite diel ranges of $[TCO_2]$ remaining largely unchanged for all model years. The mean diel pH_T range at the study site was amplified by 0.06 units in 2015, and 0.18 units in 2100, when compared with year 1765. Diel $pCO_{2(s.w.)}$ ranges were also amplified by OA, with increases of 176 µatm (+67%) and 932 µatm (+352%) in 2015 and 2100, respectively. Conversely, the mean diel range of Ω_{arag} was at its maximum in the pre-industrial, having decreased by 0.08 units (-5%) in 2015 and 0.40 units (-25%) in 2100 with increasing OA (note the severity of low Ω_{arag} conditions worsens with increasing OA, however, as the absolute change outweighs the decrease in range; Fig. 2). These changes in variance of carbonate weather due to altered buffering is analogous to recently predicted (Kwiatkowski and Orr, 2018) and observed (Landschützer *et al.*, 2018) amplification of carbonate system variability on seasonal time scales in open-ocean environments.

The altered carbonate system buffering capacity due to OA causes a preferential amplification of extreme conditions, and thus a more rapid change in the most harmful OA conditions to transient life stages of organisms in these environments, such as bivalve larvae. This is due to the fact that amplification of diel ranges is asymmetrical (Fig. 4); the carbonate system becomes more sensitive to a given addition of respiratory CO_2 than an equivalent photosynthetic CO_2 removal with increasing OA. Respiration-driven extremes of low pH, high $pCO_{2(s.w.)}$, and low Ω_{arag} become preferentially worse, with larger (+105%, +17%, and +53% in 2100, respectively; Fig. S4a) and more rapid (up to 1.8x, 2.3x, and 1.5x, respectively; SI Appendix, Fig. S4b) changes when compared with medians/means. These changes also outpace published changes in open-ocean carbonate parameters(Bates *et al.*, 2012), contemporary atmospheric CO_2 (Riahi *et al.*, 2011), and maximal rates of atmospheric CO_2 change during glacial-interglacial cycles in the past 800,000 years (Lüthi *et al.*, 2008). Currently, indices of Ω_{arag} have progressed farthest toward their estimated 2100 values (35-52% of expected changes; Fig. S4c) when compared with other carbonate parameters (19-26% of expected changes), indicating organisms and habitats sensitive to Ω_{arag} are more likely to respond first to OA. The extent of this effect would depend heavily on the organism's dependence on calcification; however, laboratory studies (Waldbusser *et al.*, 2015) and field observations (Barton *et al.*, 2012; Bednaršek *et al.*, 2014) support the concept of present-day calcification-related OA stress for organisms as well as ecosystems (Dove *et al.*, 2013; Albright *et al.*, 2016).

A potential OA mitigation strategy that has been proposed for shellfish and coastal environments is the preservation and restoration of submerged aquatic vegetation (Adelsman and Whitley Binder, 2012). While our modeling technique doesn't attribute

the observed net community metabolism (NCM) signal to its sub-components (e.g. seagrass vs. water column metabolism) due to the significant methodological hurdles associated with appropriate field observations (Long *et al.*, 2015), it does provide an opportunity to explore how integrated habitat-level metabolism alters the carbonate weather experienced by resident organisms of the seagrass habitat. The OA simulations suggest NCM in this seagrass habitat currently improves average conditions for all carbonate system variables, but drives transient extremes of low pH, high $pCO_{2(s.w.)}$, and low Ω_{arag}. NCM during the productive dry season in our study system is estimated to raise present-day (2015) dry season median pH_T by 0.08 units, raise median Ω_{arag} by 0.33 units, and lower median $pCO_{2(s.w.)}$ by 70 µatm (Fig. 5 a,b) . These effects of seagrass habitat metabolism will become increasingly important under worsening OA from an organismal OA-refugia perspective with respect to pH_T and $pCO_{2(s.w.)}$, but diminish with respect to Ω_{arag} (Fig. 5b). NCM will be increasingly effective at raising median pH_T (+0.07 units in 1765, +0.11 units in 2100) and reducing median $pCO_{2(s.w.)}$ (-44 µatm in 1765, -199 µatm in 2100), but less effective at raising median Ω_{arag} (+0.35 units in 1765, +0.28 units in 2100) with increasing atmospheric CO_2 levels. While NCM improves average conditions in this habitat, NCM is also responsible for driving the natural extremes of the habitat's carbonate weather; minimum dry season pH is reduced by 0.49 units, minimum dry season Ω_{arag} is reduced by 1.15 units, and maximum dry season $pCO_{2(s.w.)}$ is raised by 1,033 µatm in 2015 (Fig. 5b). As discussed, these NCM-driven extremes of low pH_T and high $pCO_{2(s.w.)}$ are amplified with increasing atmospheric CO_2 levels. Conversely, decreased sensitivity of Ω_{arag} at higher $[TCO_2]$ levels cause the

addition of anthropogenic carbon to slightly reduce the relative importance of NCM in driving minimum Ω_{arag} levels.

The decoupling of carbonate system averages and extremes illustrates a dichotomous role of NCM in metabolically-vigorous environments facing rising atmospheric CO_2: increasing the severity of transient poor carbonate chemistry in the present and near-future, while ultimately reducing organismal exposure to harmful carbonate conditions in a future, high CO_2 world. For example, our model predicts seagrass habitat NCM effectively delays median dry-season Ω_{arag} from crossing an established larval shellfish calcification threshold (Ω_{arag} = 1.4) by 26 years; equivalent to buffering against a 215 ppmv increase in atmospheric CO_2. However, low Ω_{arag} periods driven by NCM cause average dry-season daily minimums of Ω_{arag} to cross this same threshold 44 years earlier than estimated in the absence of NCM. This concept is illustrated in Fig. 6, where we compare exceedance of previously published harmful and exceptionally favorable Ω_{arag} thresholds for larval bivalves(George G Waldbusser *et al.*, 2015) due to increasing OA in the presence and absence of NCM. Presently, NCM increases the duration of time during which Ω_{arag} conditions for bio-calcification are exceptionally favorable ($\Omega_{arag} > 2.8$) by 37%, while also causing the exceedance of demonstrated harmful thresholds for calcification ($\Omega_{arag} < 1.4$) that would not be experienced for another 43 years in the absence of aerobic metabolism. However, an inflection point in time is reached in the future (year 2061, atmospheric CO_2 = 611 p.p.m.v.), at which point NCM reduces the duration of negative threshold exceedance when compared with the models run without NCM. This is due to the large diel ranges of carbonate parameters driven by NCM, resulting in windows of favorable carbonate

conditions associated with short-term photosynthetic reductions of [TCO_2]. Tolerance thresholds for carbonate parameters have been experimentally shown to be species-specific (Gazeau *et al.*, 2013); therefore, the timing of these inflection points will differ amongst species, but the general pattern illustrated in Fig. 6 can still be expected.

Conceptually, metabolically intensive coastal zones may ameliorate the negative effects of OA on organisms via temporal windows of favorable pH_T and $pCO_{2(s.w.)}$ (e.g. productive daytime hours) despite decreasing baselines, or conversely exacerbate these negative effects via the enhanced magnitudes and exposure durations of low pH_T and high $pCO_{2(s.w.)}$. While researchers are beginning to explore how short-term carbonate weather influences organismal responses to OA (Hofmann and Todgham, 2010; Shaw *et al.*, 2013), most OA experiments have focused on measuring effects due to static exposure of organisms following long experimental acclimation periods. These methodologies fail to capture the realistic carbonate weather of many nearshore habitats. The ability to cope with changing variances of carbonate chemistry will likely be an important determinant of acclimation and ultimately genetic adaptation amongst taxa with increasing OA, highlighting the need for a better understanding of organismal responses to variable conditions (Shaw *et al.*, 2013; Reum *et al.*, 2014; Clark and Gobler, 2016; Li *et al.*, 2016; Small *et al.*, 2016). This may be most important for species with temporally short, but OA-sensitive, developmental stages, such as marine bivalve larvae (Waldbusser *et al.*, 2015). Our model predicts Ω_{arag} has already reached a mean daily minimum value below established harmful thresholds ($\Omega_{arag} < 1.4$ (Ekstrom *et al.*, 2015; Waldbusser *et al.*, 2015)) for early calcification of some bivalve larvae in 2013. Organisms often live close to tolerance thresholds in estuarine habitats (Waldbusser and

Salisbury, 2014), and so while adaptation to naturally variable environments can enhance resilience to stress (Schoepf *et al.*, 2015), exceedance of these tolerance thresholds by increasingly frequent and more extreme events (as demonstrated in this study) can still be expected (Hauri *et al.*, 2013).

The decoupling of the averages and extremes of carbonate parameters with increasing anthropogenic CO_2 (Figs. 2, 4, SI Appendix S4) also poses an important question for OA-related water quality standards: what really matters? Our study has shown that the carbonate parameters previously identified as being most stressful for coastal organisms (minimum pH_T and Ω, maximum $pCO_{2(s.w.)}$) are changing more rapidly than their corresponding averages – the index frequently used in water quality standards. The U.S. Environmental Protection Agency recommended criteria for most marine waters states that pH should not be changed more than 0.2 units outside of the naturally occurring range and should not be outside the range of 6.5 to 8.5 units; Washington State includes this provision in their water quality standards (U.S. E.P.A., 1986). If we assume carbonate system variability in the 1765 model represents this "naturally occurring range," the minimum dry-season pH_T has already exceeded this $\Delta 0.2$ unit threshold in 2012, while median pH_T is not expected to exceed a $\Delta 0.2$ unit threshold until 2045. Existing standards are, therefore, likely insufficient to account for carbonate weather-scale impacts on coastal ecosystems - the very scale experienced by resident organisms. While there are currently no recommended water quality standards for other carbonate parameters, analogous issues exist for $pCO_{2(s.w.)}$ and Ω_{arag}. Additionally, environmental management resulting in nutrient reductions could be expected to help offset some OA effects on water quality (Kelly *et al.*, 2013), but may also lower baseline pH_T levels (and

raise $pCO_{2(s.w.)}$) of estuarine habitats due to reduced net ecosystem production in surface waters. Further study is necessary to understand the impact of anthropogenic nutrients in controlling carbonate chemistry dynamics in shallow, nearshore environments. Efficacy of OA-related management decisions will depend on matching time and space scales of interventions with those of system-specific drivers of carbonate chemistry, and the specific exposure duration, magnitude, and frequency of exceedance of the OA parameter(s) of interest to the most sensitive organisms.

Our analyses indicate that as anthropogenic CO_2 continues to increase in the atmosphere, the carbonate system in this seagrass habitat becomes less able to buffer natural sources of high-frequency CO_2 variance, causing non-linear amplification of naturally extreme events. Increasing OA will result in similar patterns of amplified changes in the variability and extremes of other metabolically-vigorous estuarine and marine systems due to altered buffering with increasing anthropogenic carbon (Egleston *et al.*, 2010; Hagens and Middelburg, 2016). This predicted amplification of carbonate system variability is beginning to emerge in open-ocean observations on seasonal timescales (Landschützer *et al.*, 2018), supporting the underlying mechanisms of more extreme carbonate weather in estuaries with OA. The magnitude of change in carbonate weather due to this altered buffering capacity will be a function of the initial "natural" carbonate buffer factors of the system, as well as the intensity of high-frequency carbon cycling.

2.4 Materials and Methods

The study site was located in a shallow subtidal seagrass habitat (48° 01.20'N, 122° 19.39'W) on the northern shore of Hat (Gedney) Island, WA, in Possession Sound. The seagrass habitat consisted of a dense stand of *Z. marina* (canopy height ~1 meter) typical of fringing shoreline seagrass beds, which make up ~50% of all seagrass habitat in the whole of Puget Sound (Christiaen *et al.*, 2017). Sensor packages were anchored to the benthos with sensing units ~30cm above the bottom. Water depth ranged from 0.62m to 4.98m, with a mean of 3.19m. Time series measurements of pH_T, O_2, salinity, temperature, and depth were collected every 15 minutes during the study period using YSI 6000 series sondes. Sondes were replaced with a calibrated sonde every ~4 weeks, and checked for fouling and drift after deployments. A Satlantic SeaFET sensor was deployed from July 1-July 15 to verify accuracy of the YSI pH measurements (SI Appendix, Fig. S5). Sensors were factory calibrated, and verified with Certified Reference Material CO_2 standards from the University of California, San Diego (Batch #132). Grab samples for sensor validation were stored in sealed 330-mL amber glass bottles using established protocols for dissolved gas sampling, and analyzed for $[TCO_2]$ and pCO_2 at Oregon State University. The Marine Deep end member was sampled at 50 m depth at the southern end of Possession Sound near Mukilteo (47° 58.05'N, 122° 18.08'W). The Snohomish River end member was sampled at river mile 10.6 (47° 56.25'N, 122° 10.14'W). Carbonate chemistry of the end-members was calculated with CO_2SYS (Matlab version 1.1; K1 and K2 constants of Millero *et al.* 2010; KSO_4 constants of Dickson 1990; borate:salinity of Lee 2010) using paired *in-situ* YSI pH_{NBS} and $[TCO_2]$, or paired $[TCO_2]$ and $pCO_{2(s.w.)}$ (when available) from grab samples. The

EPA Office of Research and Development will publish the data via the Environmental Dataset Gateway (htttps://edg.epa.gov).

To reconstruct the observed pH time series at Hat Island, changes from initial measured [TCO_2] and calculated [Alk] (using [TCO_2] and SeaFET pH_T) on July 1 were estimated using a model which incorporated mixing of the marine and riverine end-members, aerobic photosynthesis and respiration (i.e. net community metabolism), and gas exchange of O_2 and CO_2 (SI Appendix). Mixing ratios of riverine and marine end-member [TCO_2] and [Alk] were determined using observed salinities at Hat Island. The dissolved oxygen time series was corrected for gas exchange and mixing of riverine and marine end-members, and used to estimate aerobic metabolism using a metabolic quotient (ΔO_2:ΔTCO_2) of 1.05 (following published values for seagrass habitats (Duarte *et al.*, 2010)). Concurrent metabolic alterations of [Alk] were estimated using the Redfield ratio of 16:117 for ΔAlk:ΔTCO_2. A $CaCO_3$ calcification/dissolution term was not included due to insufficient data to constrain these processes on the time scales of the model. High correlation between model output and observations suggest these processes are not dominant drivers of carbonate weather in this system during the modeled time period. The modeled values of [TCO_2] and [Alk] for each time point were used to compute the full carbonate system using CO_2SYS (Matlab version 1.1) (SI Appendix, Dataset S1), and results were corrected for gas exchange of CO_2 to produce the Full Model final results using 2015 as a base year.

$$[TCO2]_{t+1} = [TCO2]_t + \Delta[TCO2]_{mixing} + \Delta[TCO2]_{metabolism} + \Delta[TCO2]_{gas}$$

$$[Alk]_{t+1} = [Alk]_t + \Delta[Alk]_{mixing} + \frac{16}{117}\Delta[TCO2]_{metabolism}$$

In order to isolate and quantify the effect of aerobic metabolism on carbonate weather in the seagrass habitat, we ran the model with ("Full Model") and without ("Abiotic Model") the metabolic term in the model. This procedure was repeated for all OA scenario models for the years 1765-2100.

Historic and future carbonate weather was estimated using two methods for calculating anthropogenic CO_2: an adaptation of the ΔC^* method (assuming constant air-sea disequilibrium with respect to $[TCO_2]$ (Matsumoto and Gruber, 2005)), and an adaptation of the ΔpCO_2 method (Feely *et al.*, 2010; Hales *et al.*, 2016) (assuming constant air-sea disequilibrium with respect to pCO_2) (Supplementary Information). We report the results of the $\Delta[TCO_2]$ method here for clarity, and include the results of the adapted ΔpCO_2 method in the SI Appendix. The $\Delta[TCO_2]$ method produces the more conservative results, with both methods supporting the conclusions of this manuscript (see Supplementary Information for discussion).

2.5 Acknowledgements

The authors would like to thank the Tulalip Tribes, T Chris Mochon Collura, and Dr. Jim Kaldy for assistance with field work, and Dr. Lauren Juranek and two reviewers for improving this manuscript. This project was funded by a U.S EPA RARE grant. The views expressed in this article are those of the authors and do not necessarily represent the views or policies of the U.S. Environmental Protection Agency. Any mention of trade names, products, or services does not imply an endorsement by the U.S. Government or

the U.S. Environmental Protection Agency. The EPA does not endorse any commercial products, services, or enterprises.

2.6 Supplementary Information

Mechanistic modeling of present-day observed carbonate chemistry

In order to reconstruct the full carbonate system of the seagrass bed for the period of study, a carbonate chemistry model was built using [TCO_2] and [Alk] as state variables. The model includes terms for conservative mixing of marine and riverine end members, aerobic metabolism, and gas exchange. For each model time point, [TCO_2] and [Alk] were calculated as:

$$[TCO2]_{t+1} = [TCO2]_t + \Delta[TCO2]_{mixing} + \Delta[TCO2]_{metabolism} + \Delta[TCO2]_{gas}$$

$$[Alk]_{t+1} = [Alk]_t + \Delta[Alk]_{mixing} + \Delta[Alk]_{metabolism}$$

The models began at a time point (t=1) where the full carbonate system was characterized using a grab sample analyzed for [TCO_2], and [Alk] was calculated with CO2SYS using [TCO_2] and *in-situ* pH_T from a SeaFET pH sensor.

Conservative mixing term

$\Delta[TCO2]_{mixing}$ and $\Delta[Alk]_{mixing}$ are conservative mixing terms representing mixing of the Snohomish River water with the Marine Deep end member (sampled at 50m depth in Possession Sound, north of Mukilteo, WA). Multiple vertical profiles were taken of the water column of Possession Sound during the study period and found homogenous physical (temperature, salinity) and biogeochemical (pH, dissolved oxygen) water

characteristics below the pycnocline to our 50m marine sampling station. We took samples from 50m as we wanted to quantify and characterize a true marine end-member, and avoid potential mixing effects of the river plume. Grab samples for [TCO_2] of both end members were taken on multiple occasions from July 15 – July 23, 2015 and analyzed in the laboratory of Dr. Burke Hales at Oregon State University. pH was measured *in-situ* with a YSI 6000 series sonde, and [ALK] was calculated using [TCO_2] and pH with CO2SYS for both end members. The mixing term was then calculated as:

$$\Delta[TCO2]_{mixing,t+1}$$

$$= (f_{marine,t+1} * [TCO2]_{marine} + (1 - f_{marine,t+1}) * [TCO2]_{river})$$

$$- (f_{marine,t} * [TCO2]_{marine} + (1 - f_{marine,t}) * [TCO2]_{river})$$

$$\Delta[Alk]_{mixing,t+1}$$

$$= (f_{marine,t+1} * [Alk]_{marine} + (1 - f_{marine,t+1}) * [Alk]_{river})$$

$$- (f_{marine,t} * [Alk]_{marine} + (1 - f_{marine,t}) * [Alk]_{river})$$

Where f_{marine} is equal to the fraction of marine water observed at the study site based on salinity:

$$f_{marine} = \left(\frac{S_{obs} - S_{river}}{S_{marine} - S_{river}}\right)$$

and S_{obs}=observed salinity at Hat Island study site, S_{marine} = salinity of Marine Deep end member (S = 29.89, T = 12.05 °C, $[TCO_2]_{marine}$ = 2,024 µmol kg^{-1}, $[Alk]_{marine}$ = 2,061 µmol kg^{-1}), and S_{river} = salinity of the Snohomish River (S = 0, T = 21.79 °C, $[TCO_2]_{river}$= 572 µmol kg^{-1}, $[Alk]_{river}$ = 555 µmol kg^{-1}).

Aerobic metabolism term

$\Delta[TCO2]_{metabolism}$ and $\Delta[Alk]_{metabolism}$represent the changes in dissolved inorganic carbon and alkalinity due to photosynthesis and respiration observed at the study site, and are based on the observed *in-situ* dissolved oxygen time series. This method therefore represents a complete integration of all aerobic metabolic processes at the study site, and is unable to parse out the metabolism specific to the seagrass species (*Zostera marina*) at the site. These NCM estimates therefore represent the whole seagrass community metabolism (e.g.,. benthos, epiphytes, water column), and all references to NCM in the text should be understood to represent this. In order to calculate the changes in O_2 due to photosynthesis and respiration, the observed O_2 time series was corrected for gas exchange and mixing of the marine and riverine end members (which had distinct O_2 levels) as follows:

$$\Delta[O2]_{metabolism} = \Delta[O2]_{observed} + \Delta[O2]_{gas} - \Delta[O2]_{mixing}$$

$$\Delta[O2]_{observed} = [O2]_{YSI,t+1} - [O2]_{YSI,t}$$

$$\Delta[O2]_{mixing} = (f_{marine,t+1} * [O2]_{marine} + (1 - f_{marine,t+1}) * [O2]_{river}) - (f_{marine,t} * [O2]_{marine} + (1 - f_{marine,t}) * [O2]_{river})$$

The $\Delta[O2]_{gas}$ term was calculated using the Wanninkhof 1992 gas exchange parameterization for oxygen with wind speeds (corrected to a reference height of 10 m using the relationship of Hsu et al. 1994) from a nearby station located in Tulalip, WA. The metabolic change in dissolved oxygen was related to the change in dissolved inorganic carbon using a metabolic quotient of 1.05 for TCO_2:O_2. This value is a median from a meta-analysis of metabolic quotients in seagrass ecosystems (Duarte *et al.*, 2010):

$$\Delta[TCO2]_{metabolism} = \Delta[O2]_{metabolism} * 1.05$$

The change in TCO_2 due to aerobic metabolism was then used to calculate the change in alkalinity using the well-known Redfield Ratio for aerobic organic matter production/respiration:

$$\Delta[Alk]_{metabolism} = \Delta[TCO2]_{metabolism} * 16/117$$

Gas exchange term

$\Delta[TCO2]_{gas}$ was calculated using the Wanninkhof (1992) gas exchange parameterization for CO_2 with wind speeds (corrected to a reference height of 10m using the relationship of Hsu et al. 1994) from a nearby station located in Tulalip, WA. We acknowledge that wind-based gas transfer velocity parameterizations in shallow estuarine environments are likely to underestimate gas fluxes due to additional turbulence driven by mixing and bottom shear forces. We chose this wind-based parameterization due to a lack of current velocity data at our study site. Therefore, our O_2 and CO_2 gas flux estimates are likely underestimates at times of low wind speeds and large tidal exchange, resulting in our O_2-based NCM estimates to likely be conservative.

2015 Model

Results for TCO_2 and Alkalinity at each 15-minute time point were then used as input to CO2SYS (Matlab version 1.1) to calculate the full carbonate system (e.g. pH, pCO_2, Ω) at each time point. Calculated pH from model results were compared with the *in-situ* pH time series from the YSI sonde. Note that the YSI pH time series is not used for any model parameterization, and is completely independent of model results.

Comparison of model output with observations from grab samples

Grab samples were taken directly adjacent to the *in-situ* sensor package at the study site, with a total of 29 samples (including replicates) spread over a period of 11 days (shown in Fig. 1). All samples were analyzed for [TCO2] at the Oregon State University Chemical Analysis Lab. pCO_2 analyses are available for 11 of the samples. In-situ pH_T (SeaFET) is available for 24 of the time points at which the grab samples were collected. The full carbonate system was calculated for all 29 grab samples using paired [TCO_2] and pCO_2 values when available, and paired [TCO_2] and pH_T when pCO_2 was not available. All measured and calculated values for grab samples are reported in the SI Excel file sheet "Grab sample data". Pearson correlation coefficients (r) and root mean squared errors (RMSE) were calculated to compare grab sample carbonate parameters with those predicted by the Full Model. Means of replicates for each time point were used in these analyses.

1765-2100 OA scenario modeling

OA scenario models were calculated using an adaptation of the ΔC* method (here referred to as the ΔTCO_2 method), outlined in Matsumoto and Gruber 2005, as well as the ΔpCO2 method (assuming constant air-sea pCO2 disequilibrium) (Feely *et al.,* 2010, Hales *et al.*, 2016). The ΔTCO_2 method method is also similar to the methodology of Takeshita *et al.* 2015 for estimating future carbonate weather of coastal shelf habitats. The key component of the ΔTCO_2 method is that it assumes constant disequilibrium between observed [TCO_2] and atmospheric-equilibrated [TCO_2], rather than assuming constant disequilibrium with respect to pCO_2 as used by others (e.g. Feely *et al.*, 2010).

This method reduces errors associated with altered Revelle factors with increasing anthropogenic CO_2, therefore maintaining diurnal TCO_2 ranges known to be largely driven by aerobic metabolism from the results of our mechanistic modeling. Aerobic metabolism directly alters the TCO_2 pool through photosynthetic uptake of $CO_{2(aq)}$ and HCO_3^- and respiratory release of $CO_{2(aq)}$. pCO_2 responds to this TCO_2 uptake and release through its dependence on $[CO_{2(aq)}]$, but it is also a function of temperature, salinity, pressure, and thermodynamically-determined carbonate system speciation (as described by the Revelle factor). By altering the conservative TCO_2 term in our OA scenario models, we maintain the metabolic transformations of the TCO_2 pool, and allow pCO_2 to respond according to the Revelle factor. We believe this is a more conservative method for modeling past and future high-frequency carbonate chemistry dynamics in systems dominated by metabolic processes and often far from atmospheric equilibrium, but more work is required to further understand the most appropriate applications of the ΔTCO_2 and ΔpCO_2 methods in coastal areas. Below we describe the modeling of both methods for this manuscript.

ΔTCO_2 method

The $[TCO_2]$ disequilibrium was calculated at each model time point (15-minute intervals, n=7,455) for the 2015 model year as:

$$\Delta[TCO2]_{diseq} = [TCO2]_{eq}^{2015} - [TCO2]_{obs}^{2015}$$

Where $[TCO2]_{obs}^{2015}$ is the modeled $[TCO_2]$ for model year 2015 and $[TCO2]_{eq}^{2015}$ is the theoretical equilibrated TCO2 for model year 2015 calculated using modeled [Alk] at that time point, and pCO2 = 400 µatm. [TCO2] time series were then recreated for each year

from 1765-2100 by subtracting off the $\Delta[TCO2]_{diseq}$ time series from the theoretical equilibrated TCO2 for each model year, as follows:

$$[TCO2]_{obs}^{year} = [TCO2]_{eq}^{year} - \Delta[TCO2]_{diseq}$$

$$[TCO2]_{eq}^{year} \sim f(pCO2_{year}, [Alk]_{obs})$$

Where $pCO2_{year}$ is equal to the atmospheric CO2 concentration of that year from the RCP 8.5 scenario, and $[Alk]_{obs}$ is the modeled [Alk] from the 2015 model. The alkalinity time series is the same for all OA model scenarios, as we assume the only change amongst model years is equilibration with a different atmospheric CO_2.
The full carbonate system was then calculated using the calculated time series of $[TCO2]_{obs}^{year}$ and $[Alk]_{obs}$ for each OA scenario model year (1765-2100).

ΔpCO_2 method

The ΔpCO_2 method assumes a constant air-sea disequilibrium with respect to CO_2, effectively tying the rate of seawater pCO_2 increase to that of the atmosphere. Using the RCP 8.5 scenario model for atmospheric CO_2 levels, we calculated the rate of atmospheric pCO_2 increase from 1765 to 2100. We then altered the observed pCO2 time series from 2015 according to these rates to create a pCO2 time series for each model year. The pCO2 time series of 2015 was first smoothed to reduce high-frequency variability associated with short-term biological modification, reducing the effect of the Revelle factor on incorrectly altering diurnal ranges of TCO_2.

Anthropogenic carbon was calculated for each year from 1765-2100 by:

1). Altering the smoothed pCO2 time series for 2015 ($pCO_{2\ smooth,\ 2015}$) by the relative change in atmospheric CO2:

$$pCO_{2\ seawater,\ year} = pCO_{2\ smooth,\ 2015} - (pCO_{2\ atm,\ 2015} - pCO_{2\ atm,\ year})$$

2). Calculating the TCO_2 time series for each model year using this estimated seawater pCO_2 and the alkalinity time series from 2015:

$$TCO_{2\ seawater,\ year} \sim f(pCO_{2\ seawater,\ year}, Alk_{obs})$$

3). Subtracted the calculated TCO_2 time series for year 1765 (which we assume to be representative of the PI and have no anthropogenic carbon) from the calculated TCO_2 time series from 1766 to 2100

$$TCO_{2\ anth,\ year} = TCO_{2\ seawater,\ year} - TCO_{2\ seawater,\ 1765}$$

The anthropogenic carbon time series ($TCO_{2\ anth,\ year}$) for each year was then subtracted (pre-2015) or added (post-2015) to the 2015 modeled time series of the Full Model ($[TCO2]_{obs}^{2015}$) to produce high-resolution time series of TCO2 for each year from 1765-2100. These TCO_2 time series were combined with the alkalinity time series (Alk_{obs}) to calculate the full carbonate system for each year.

ΔpCO_2 method results

Figures S8 and S9 display the output of models utilizing the ΔpCO_2 method to estimate anthropogenic carbon for each year from 1765-2100, and comparing the output of models using the ΔpCO_2 method and ΔTCO_2 methods.

2.7 References

Adelsman, H. and Whitley Binder, L. (2012) *Ocean Acidification : From Knowledge to Action, Washington State's Strategic Response*. Olympia, WA.

Albright, R. *et al.* (2016) 'Reversal of ocean acidification enhances net coral reef calcification', *Nature*. Nature Publishing Group, 531(7594), pp. 362–365. doi: 10.1038/nature17155.

Banas, N. S. *et al.* (2015) 'Patterns of River Influence and Connectivity Among Subbasins of Puget Sound, with Application to Bacterial and Nutrient Loading', *Estuaries and Coasts*, 38(3), pp. 735–753. doi: 10.1007/s12237-014-9853-y.

Barton, A. *et al.* (2012) 'The Pacific oyster, Crassostrea gigas, shows negative correlation to naturally elevated carbon dioxide levels: Implications for near-term ocean acidification effects', *Limnology and Oceanography*, 57(3), pp. 698–710. doi: 10.4319/lo.2012.57.3.0698.

Bates, N. R. *et al.* (2012) 'Detecting anthropogenic carbon dioxide uptake and ocean acidification in the North Atlantic Ocean', *Biogeosciences*, 9(7), pp. 2509–2522. doi: 10.5194/bg-9-2509-2012.

Baumann, H. *et al.* (2014) 'Large Natural pH, CO_2 and O_2 Fluctuations in a Temperate Tidal Salt Marsh on Diel, Seasonal, and Interannual Time Scales', *Estuaries and Coasts*, pp. 220–231. doi: 10.1007/s12237-014-9800-y.

Bednaršek, N. *et al.* (2014) '*Limacina helicina* shell dissolution as an indicator of declining habitat suitability owing to ocean acidification in the California Current Ecosystem.', *Proceedings. Biological sciences / The Royal Society*, 281(1785), p. 20140123. doi: 10.1098/rspb.2014.0123.

Christiaen, B. *et al.* (2017) 'Puget Sound Seagrass Monitoring Report Monitoring Year 2015'. Available at: http://www.dnr.wa.gov/programs-and-services/aquatics/aquatic-science/nearshore-habitat-publications%0AThis.

Clark, H. and Gobler, C. (2016) 'Do diurnal fluctuations in CO_2 and dissolved oxygen concentrations provide a refuge from hypoxia and acidification for early life stage bivalves?', *Marine Ecology Progress Series*, 558, pp. 1–14. doi: 10.3354/meps11852.

Dove, S. G. *et al.* (2013) 'Future reef decalcification under a business-as-usual CO_2 emission scenario.', *Proceedings of the National Academy of Sciences of the United States of America*, 110(38), pp. 15342–7. doi: 10.1073/pnas.1302701110.

Duarte, C. M. *et al.* (2010) 'Seagrass community metabolism: Assessing the carbon sink capacity of seagrass meadows', *Global Biogeochemical Cycles*, 24(4), pp. 1–8. doi: 10.1029/2010GB003793.

Duarte, C. M. *et al.* (2013) 'Is Ocean Acidification an Open-Ocean Syndrome? Understanding Anthropogenic Impacts on Seawater pH', *Estuaries and Coasts*, 36(2), pp. 221–236. doi: 10.1007/s12237-013-9594-3.

Egleston, E. S. *et al*. (2010) 'Revelle revisited: Buffer factors that quantify the response of ocean chemistry to changes in DIC and alkalinity', *Global Biogeochemical Cycles*, 24(1), pp. 1–9. doi: 10.1029/2008GB003407.

Ekstrom, J. A. *et al.* (2015) 'Vulnerability and adaptation of US shellfisheries to ocean acidification', *Nature Climate Change*. Nature Publishing Group, 5(3), pp. 207–214. doi: 10.1038/nclimate2508.

Feely, R. A. *et al.* (2008) 'Evidence for upwelling of corrosive "acidified" water onto the continental shelf.', *Science*, 320(5882), pp. 1490–1492. doi: 10.1126/science.1155676.

Feely, R. A. *et al.* (2010) 'The combined effects of ocean acidification, mixing, and respiration on pH and carbonate saturation in an urbanized estuary', *Estuarine, Coastal and Shelf Science*. Elsevier Ltd, 88(4), pp. 442–449. doi: 10.1016/j.ecss.2010.05.004.

Feely, R. A. *et al.* (2016) 'Chemical and biological impacts of ocean acidification along the west coast of North America', *Estuarine, Coastal and Shelf Science*, pp. 1–11. doi: 10.1016/j.ecss.2016.08.043.

Gazeau, F. *et al.* (2013) 'Impacts of ocean acidification on marine shelled molluscs', *Marine Biology*, 160(8), pp. 2207–2245. doi: 10.1007/s00227-013-2219-3.

Hagens, M. and Middelburg, J. J. (2016) 'Generalised expressions for the response of pH to changes in ocean chemistry', *Geochimica et Cosmochimica Acta*. Elsevier Ltd, 187, pp. 334–349. doi: 10.1016/j.gca.2016.04.012.

Hales, B. *et al.* (2016) 'The Carbonate Chemistry of the "Fattening Line," Willapa Bay, 2011–2014', *Estuaries and Coasts*. Estuaries and Coasts, pp. 2011–2014. doi: 10.1007/s12237-016-0136-7.

Hauri, C. *et al.* (2013) 'The intensity, duration, and severity of low aragonite saturation state events on the California continental shelf', *Geophysical Research Letters*, 40(13), pp. 3424–3428. doi: 10.1002/grl.50618.

Hinga, K. R. (1992) 'Co-occurrence of dinoflagellate blooms and high pH in marine enclosures', *Marine Ecology Progress Series*, 86(2), pp. 181–187. doi:

10.3354/meps087181.

Hofmann, G. E. *et al.* (2011) ‘High-frequency dynamics of ocean pH: a multi-ecosystem comparison.’, *PloS one*, 6(12), p. e28983. doi: 10.1371/journal.pone.0028983.

Hofmann, G. E. and Todgham, A. E. (2010) ‘Living in the Now: Physiological Mechanisms to Tolerate a Rapidly Changing Environment’, *Annual Review of Physiology*, 72(1), pp. 127–145. doi: 10.1146/annurev-physiol-021909-135900.

Kelly, M. W. *et al.* (2013) ‘Natural variation and the capacity to adapt to ocean acidification in the keystone sea urchin Strongylocentrotus purpuratus’, *Global Change Biology*, 19(8), pp. 2536–2546. doi: 10.1111/gcb.12251.

Kwiatkowski, L. and Orr, J. C. (2018) ‘Diverging seasonal extremes for ocean acidification during the twenty-first centuryr’, *Nature Climate Change*. Springer US, 8(2), pp. 141–145. doi: 10.1038/s41558-017-0054-0.

Landschützer, P. *et al.* (2018) ‘Strengthening seasonal marine CO 2 variations due to increasing atmospheric CO 2’. doi: 10.1038/s41558-017-0057-x.

Li, F. *et al.* (2016) ‘Physiological responses of coastal and oceanic diatoms to diurnal fluctuations in seawater carbonate chemistry under two CO_2 concentrations’, *Biogeosciences Discussions*, (July), pp. 1–39. doi: 10.5194/bg-2016-281.

Long, M. H. *et al*. (2015) ‘Seagrass metabolism across a productivity gradient using the eddy covariance, Eulerian control volume, and biomass addition techniques’, *Journal of Geophysical Research: Oceans*, 120(5), pp. 3624–3639. doi: 10.1002/2014JC010352.

Lüthi, D. *et al.* (2008) ‘High-resolution carbon dioxide concentration record 650,000-800,000 years before present.’, *Nature*, 453(7193), pp. 379–382. doi: 10.1038/nature06949.

Matsumoto, K. and Gruber, N. (2005) ‘How accurate is the estimation of anthropogenic carbon in the ocean? An evaluation of the ΔC* method’, *Global Biogeochemical Cycles*, 19(3), pp. 1–17. doi: 10.1029/2004GB002397.

Miller, J. J. *et al.* (2016) ‘Exposure to low pH reduces survival and delays development in early life stages of Dungeness crab (Cancer magister)’, *Marine Biology*. Springer Berlin Heidelberg, 163(5), pp. 1–11. doi: 10.1007/s00227-016-2883-1.

Moore-Maley, B. L. *et al.* (2016) ‘Locally driven interannual variability of near-surface pH and OmegaA in the Strait of Georgia’, *Journal of Geophysical Research: Oceans*, (121), pp. 1600–1625. doi: 10.1002/2015JC011118.Received.

Murray, J. W. *et al.* (2015) ‘An inland sea high nitrate-low chlorophyll (HNLC) region

with naturally high pCO_2', *Limnology and Oceanography*, 60(3), pp. 957–966. doi: 10.1002/lno.10062.

Pelletier, G. *et al.* (2018) 'Seasonal variation in aragonite saturation in surface waters of Puget Sound – a pilot study', *Elem Sci Anth*, 6(1), p. 5. doi: 10.1525/elementa.270.

Provoost, P. *et al.* (2010) 'Seasonal and long-term changes in pH in the Dutch coastal zone', *Biogeosciences*, 7(11), pp. 3869–3878. doi: 10.5194/bg-7-3869-2010.

Reum, J. C. P. *et al.* (2014) 'Interpretation and design of ocean acidification experiments in upwelling systems in the context of carboante chemsitry co-variation with temperature and oxygen', *ICES Journal of Marine Science*, 71(3), pp. 528–536. doi: 10.1093/icesjms/fst176.

Riahi, K. *et al.* (2011) 'RCP 8.5-A scenario of comparatively high greenhouse gas emissions', *Climatic Change*, 109(1), pp. 33–57. doi: 10.1007/s10584-011-0149-y.

Schoepf, V. *et al.* (2015) 'Limits to the thermal tolerance of corals adapted to a highly fluctuating, naturally extreme temperature environment.', *Scientific reports*. Nature Publishing Group, 5(November), p. 17639. doi: 10.1038/srep17639.

Shaw, E. C. *et al.* (2013) 'Anthropogenic changes to seawater buffer capacity combined with natural reef metabolism induce extreme future coral reef CO2 conditions', *Global Change Biology*, 19(5), pp. 1632–1641. doi: 10.1111/gcb.12154.

Shaw, E. C., McNeil, B. I. and Tilbrook, B. (2012) 'Impacts of ocean acidification in naturally variable coral reef flat ecosystems', *Journal of Geophysical Research: Oceans*, 117(3), pp. 1–14. doi: 10.1029/2011JC007655.

Shaw, E. C., Munday, P. L. and McNeil, B. I. (2013) 'The role of CO_2 variability and exposure time for biological impacts of ocean acidification', *Geophysical Research Letters*, 40(17), pp. 4685–4688. doi: 10.1002/grl.50883.

Small, D. P. *et al.* (2016) 'Temporal fluctuations in seawater pCO_2 may be as important as mean differences when determining physiological sensitivity in natural systems', *ICES Journal of Marine Science: Journal du Conseil*, 73, pp. 604–612. doi: 10.1093/icesjms/fsv232.

Strong, A. L. *et al.* (2014) 'Ocean acidification 2.0: Managing our Changing Coastal Ocean Chemistry', *BioScience*, 64(7), pp. 581–592. doi: 10.1093/biosci/biu072.

Sutton, A. J. *et al.* (2016) 'Using present-day observations to detect when anthropogenic change forces surface ocean carbonate chemistry outside pre-industrial bounds',

Biogeosciences Discussions, (March), pp. 1–30. doi: 10.5194/bg-2016-104.

Takeshita, Y. *et al.* (2015) 'Including high-frequency variability in coastal ocean acidification projections', *Biogeosciences*, 12(19), pp. 5853–5870. doi: 10.5194/bg-12-5853-2015.

U.S. E.P.A., O. of W. R. and S. (1986) *Quality Criteria for Water 1986 (EPA Publication No. 440/5-86-001)*. Washington, DC.

Waldbusser, G. G. *et al.* (2015a) 'Ocean acidification has multiple modes of action on bivalve larvae', *PLoS ONE*, 10(6). doi: 10.1371/journal.pone.0128376.

Waldbusser, G. G. *et al.* (2015b) 'Saturation-state sensitivity of marine bivalve larvae to ocean acidification', *Nature Climate Change*, 5(3), pp. 273–280. doi: 10.1038/NCLIMATE2479.

Waldbusser, G. G. and Salisbury, J. E. (2014) 'Ocean acidification in the coastal zone from an organism's perspective: multiple system parameters, frequency domains, and habitats.', *Annual review of marine science*, 6, pp. 221–47. doi: 10.1146/annurev-marine-121211-172238.

Wallace, R. B. *et al.* (2014) 'Coastal ocean acidification: The other eutrophication problem', *Estuarine, Coastal and Shelf Science*. Elsevier Ltd, 148, pp. 1–13. doi: 10.1016/j.ecss.2014.05.027.

Yang, Z. *et al.* (2015) 'Estuarine response to river flow and sea-level rise under future climate change and human development', *Estuarine, Coastal and Shelf Science*. Elsevier Ltd, 156(1), pp. 19–30. doi: 10.1016/j.ecss.2014.08.015.

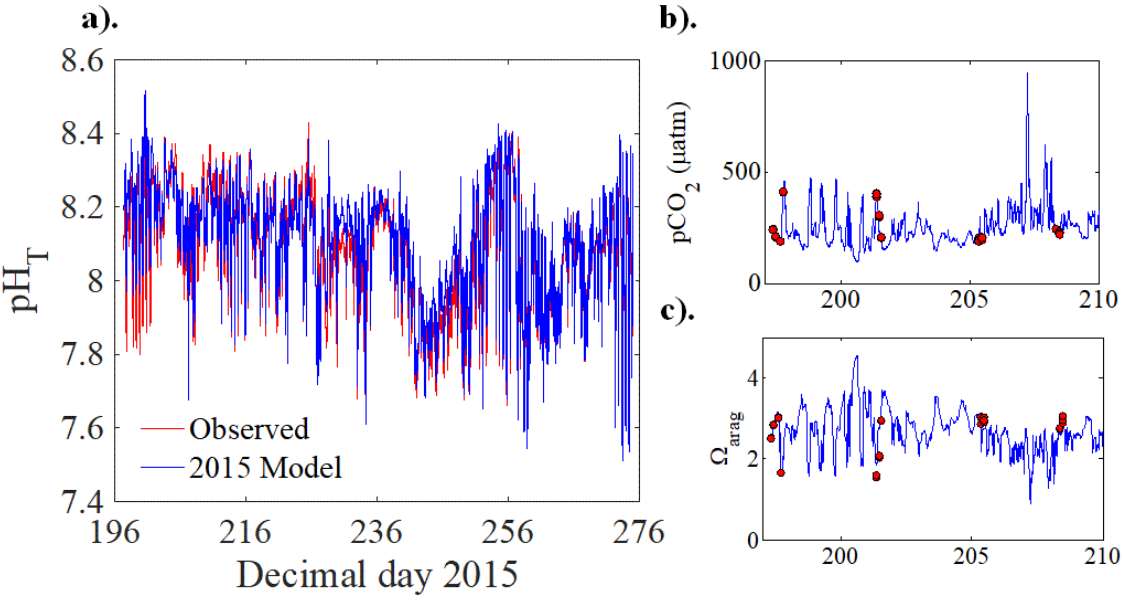

Figure 2.1. a). Time series (15-min frequency) of measured pH (red) at Hat Island and modeled pH (blue) of the full model. The Pearson correlation coefficient for the model was r = 0.957, p < 0.001. **b).** Modeled pCO_2 (blue line) with calculated values (red dots) from grab samples taken at the study site. **c).** Modeled $\Omega_{aragonite}$ (blue line) with calculated values (red dots) from grab samples taken at the study site. Calculated parameters used SeaFET pH, and measured pCO_2 and $[TCO_2]$ values for calculation of the carbonate system using CO2SYS.

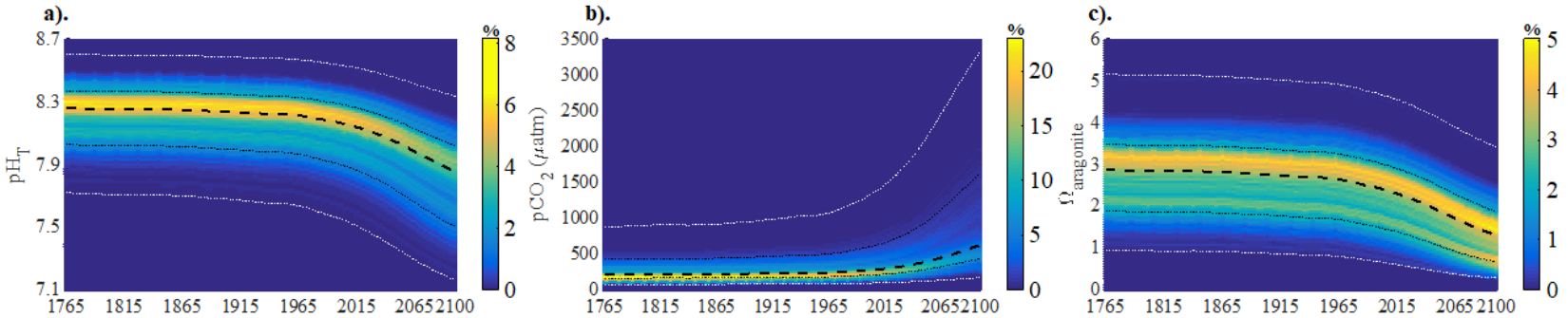

Figure 2.2. Results of OA scenario models from 1765 to 2100. Color maps represent the percent occurrence for **a).** pH_T, **b).** $pCO_{2(s.w.)}$, and **c).** Ω_{arag} as a function of time. Bold dashed lines represent the annual dry-season median, black dotted lines are the average daily dry-season minimum and maximum observations, and white dotted lines are annual dry-season maximum and minimum observations. Note the differences between medians and means for each parameter, indicative of the non-normal distributions of each parameter for a given year.

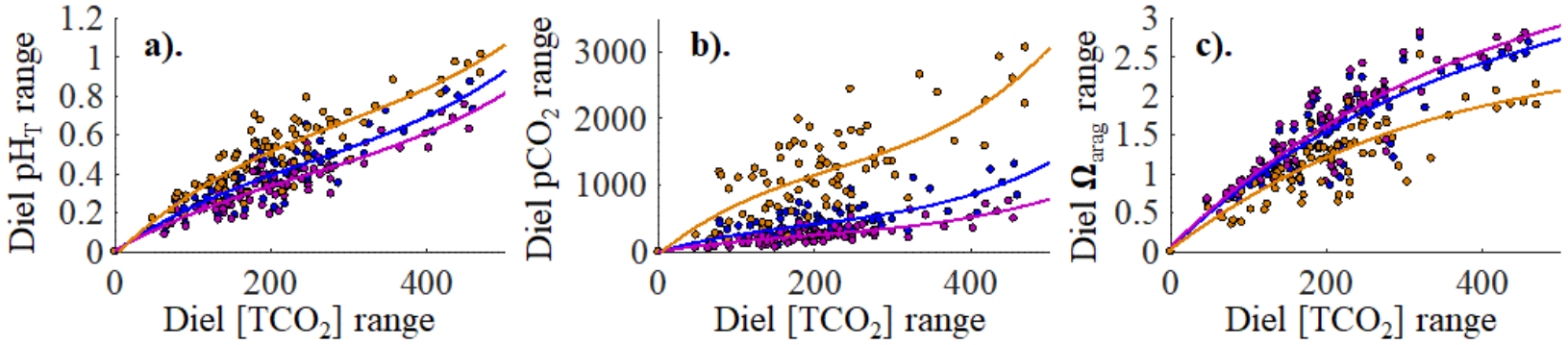

Figure 2.3. Scatterplots of daily **a).** pH_T, **b).** pCO_2, and **c).** Ω_{arag} ranges versus daily [TCO_2] ranges for the pre-industrial (1765, purple), present-day (2015, blue), and 2100 (orange) model scenarios. Each point represents a single day (July 15 – October 1) in the model (n = 78). Lines are third-degree polynomial lines of best fit for each of the model scenarios.

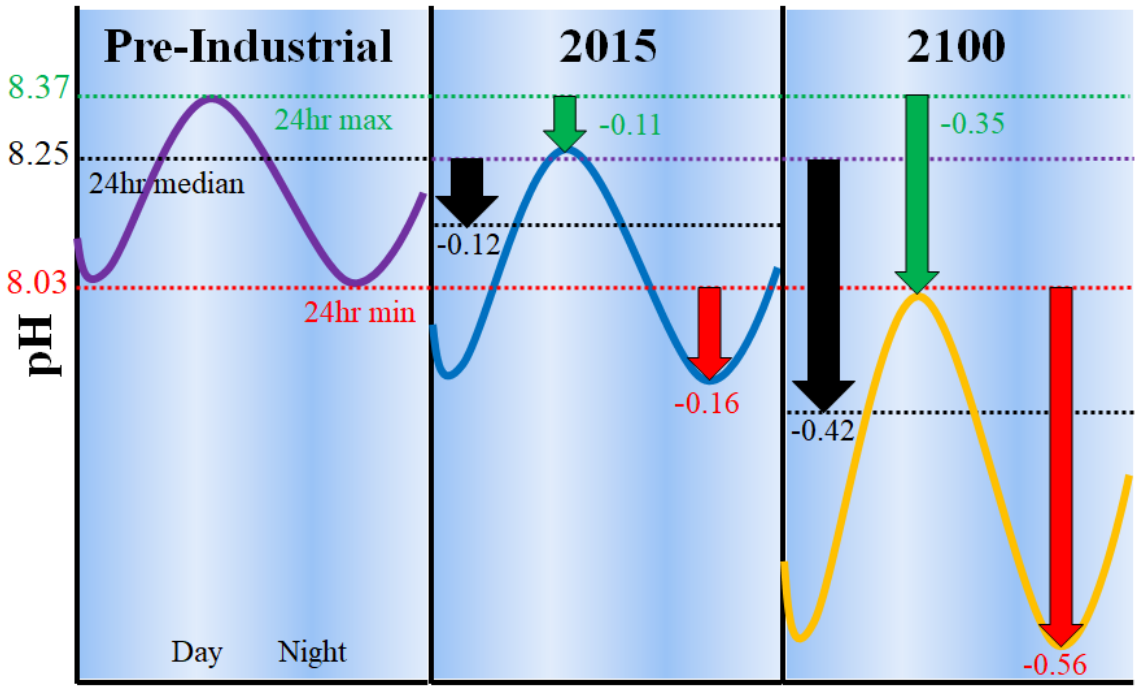

Figure 2.4. Representative diel curves illustrating changes in daily pH medians (black), maximums (green), and minimums (red) from pre-industrial values for years 2015 and 2100. Daily pH minimums have larger reductions than corresponding medians and maximums due to the additive anthropogenic and respiratory carbon reducing the pH buffering capacity of the system. Values shown are mean changes for the dry season of the designated year.

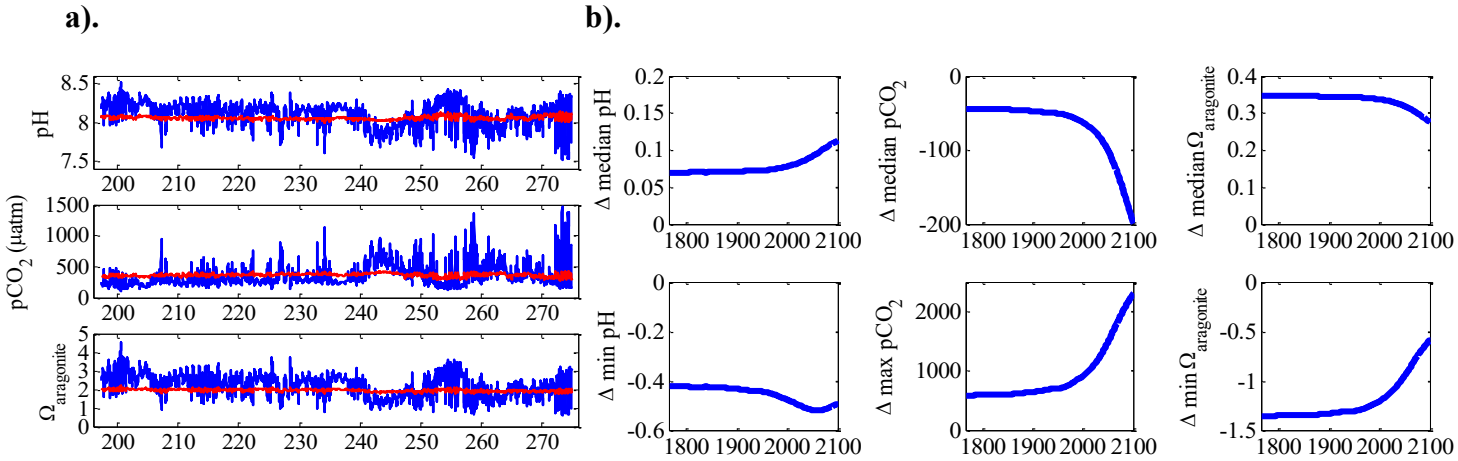

Figure 2.5. Comparison of OA simulation models with (full) and without (abiotic) the net community metabolism term. **a).** shows a comparison of model output for the full model (blue) and the abiotic model (red) of model year 2015 (July 15 – October 1). **b).** illustrates the differences in median and extremes of carbonate parameters between the full and abiotic models from 1765 to 2100. The y-axis deltas are equal to the full model parameter minus the abiotic model parameter. For example, NCM elevates median dry-season pH by ~0.07 units in 1765, but decreases minimum dry-season pH by ~0.42 units.

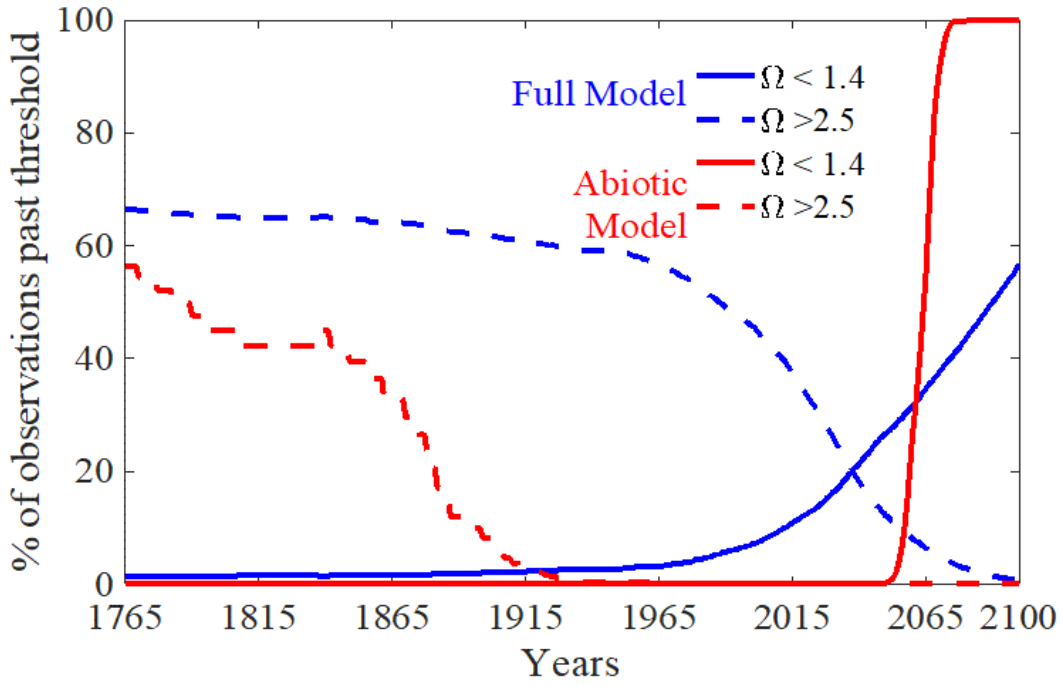

Figure 2.6. Percentage of observations for each OA model simulation year exceeding published harmful (solid lines) and exceptionally favorable (dashed lines) thresholds of $\Omega_{aragonite}$ for biocalcification of larval bivalves. Compared is output from all model simulations for the full (with NCM; blue lines) and abiotic (without NCM; red lines) models. The $\Omega_{aragonite}$ thresholds are from Waldbusser et al. 2015a,b. Conditions were similarly favorable for biocalcification in the pre-industrial with or without NCM's influence on carbonate chemistry. Currently, NCM increased incidence of exceptionally favorable and harmful conditions. In future high-CO2 scenarios, incidences of exceptionally favorable conditions are nearly absent, regardless of NCM; however, NCM greatly reduces the incidence of harmful conditions.

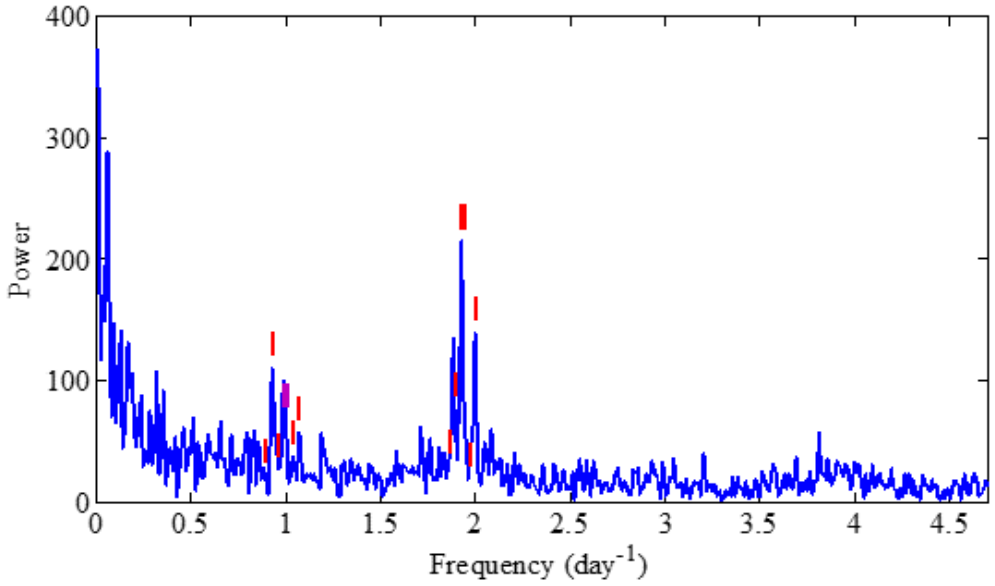

Figure S2.1. Fast Fourier Transform of observed YSI pH data (n=7,455) for full study period (July 15 – October 1, 2015). Major tidal constituent frequencies are shown by red dashes (M2 (bold), K1, S2, O1, M1, N2, Q1, L2, 2N2, J1, OO1) and the 24-hour frequency is indicated by purple dash.

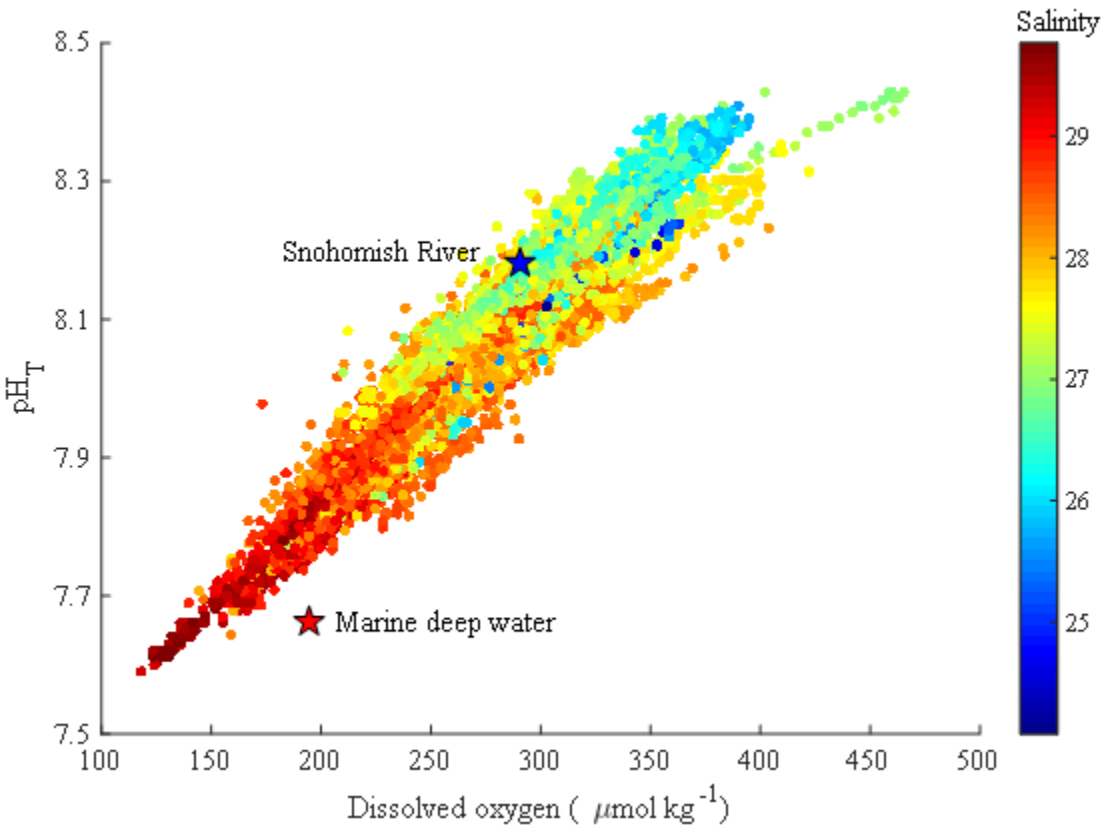

Figure S2.2. Scatterplot of observed dissolved oxygen and pH (total scale) as a function of salinity in the seagrass bed study site at Hat Island, WA from July 1-October 1 2015 (filled circles, n=7,455). Also shown are mean pH and dissolved oxygen (O_2) values for the marine deep water (salinity = 29.64, n=6) and the Snohomish River (salinity = 0, n=6) observed during the study period.

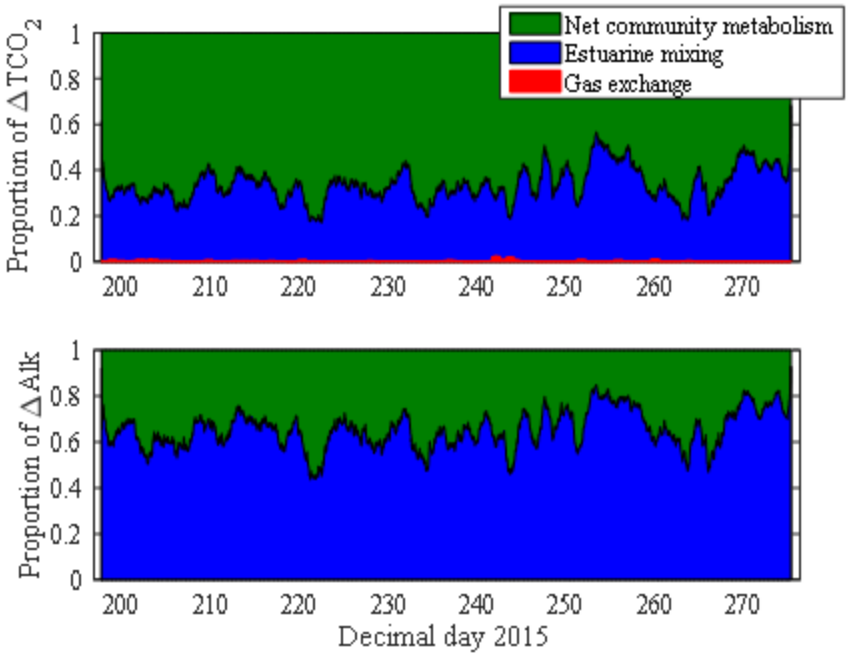

Figure S2.3. Proportion of modeled [TCO_2] and [Alk] variability explained by the net community metabolism, estuarine mixing, and gas exchange components of the Full Model for the year 2015. Proportions are plotted as 24-hr smoothed areas to clearly illustrate the patterns.

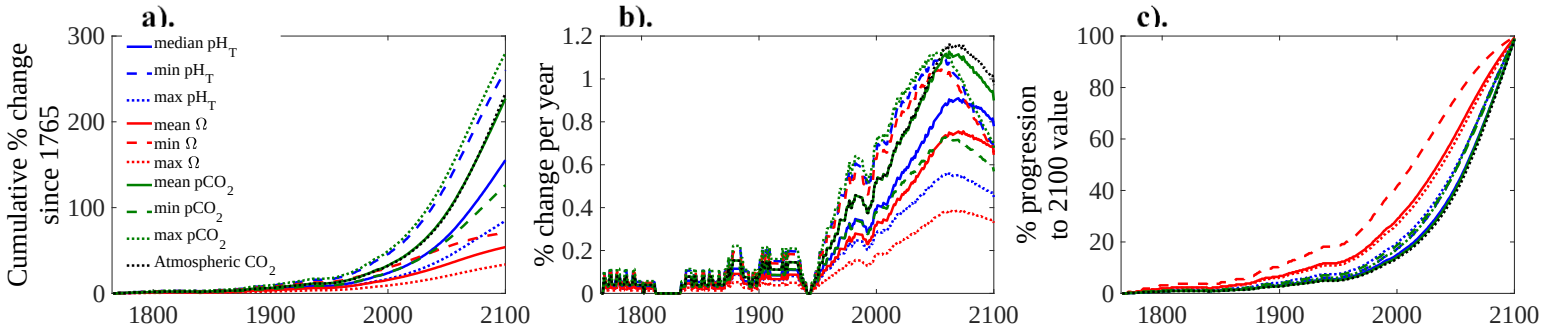

Figure S2.4. Magnitudes and rates of change for indices of pH, pCO2, and Ωaragonite calculated from the 1765-2100 Scenario models. **a).** Modeled cumulative percent changes in carbonate parameters since 1765. **b).** modeled percent yearly rates of change for each carbonate parameter. Values shown are 10-year smoothed values to more clearly show trends and reduce noise due to variable rates of yearly atmospheric CO2 change for RCP 8.5. **c).** Percent of total changes in carbonate parameters expected from 1765-2100.

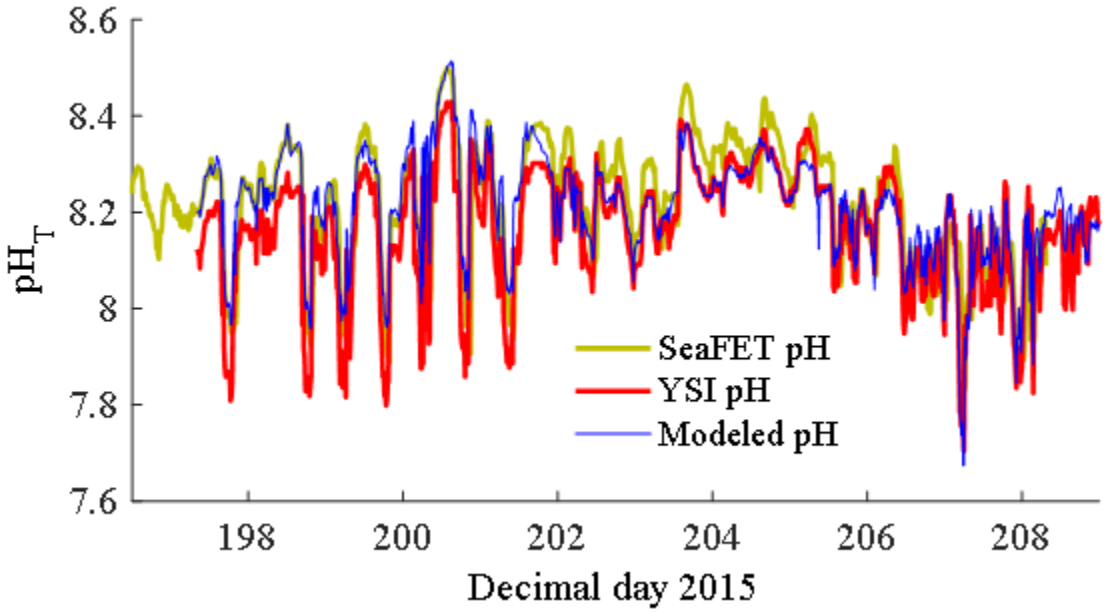

Figure S2.5. Partial pH time series at the Hat Island seagrass bed study site, showing comparison of observed pH from YSI and SeaFET sensors and modeled pH from this study (model year 2015) from July 15-July 29, 2015. YSI pH was converted from the NBS pH scale to the Total pH scale using CO2SYS (v. 1.1).

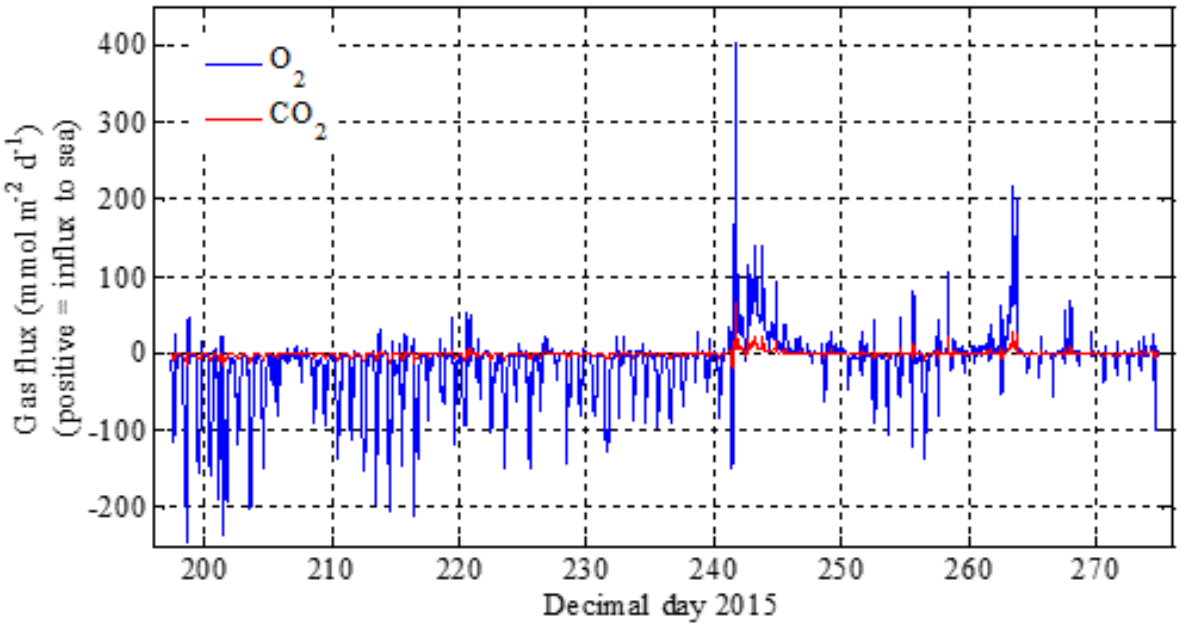

Figure S2.6. Time series of modeled gas exchange fluxes for O_2 and CO_2 used in the Full Model. Positive fluxes represent net fluxes from atmosphere to seawater. See SI methods text for information on parameterization of gas exchange models.

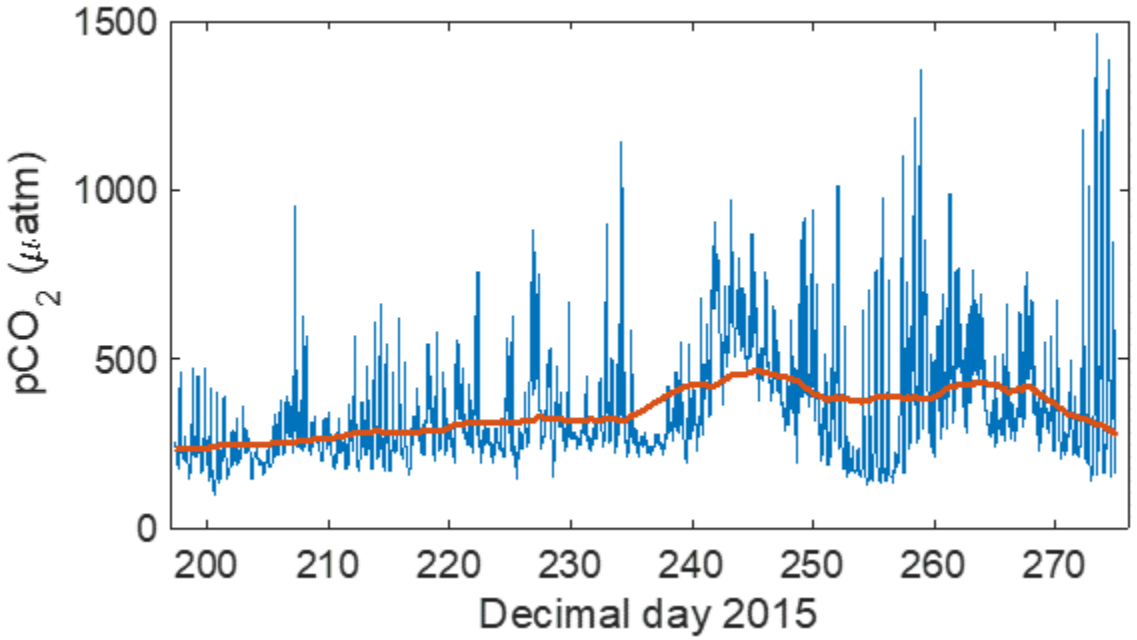

Figure S2.7. Full 15-minute time series of pCO_2 for model year 2015 (blue), and 14-day averaged pCO_2 (red).

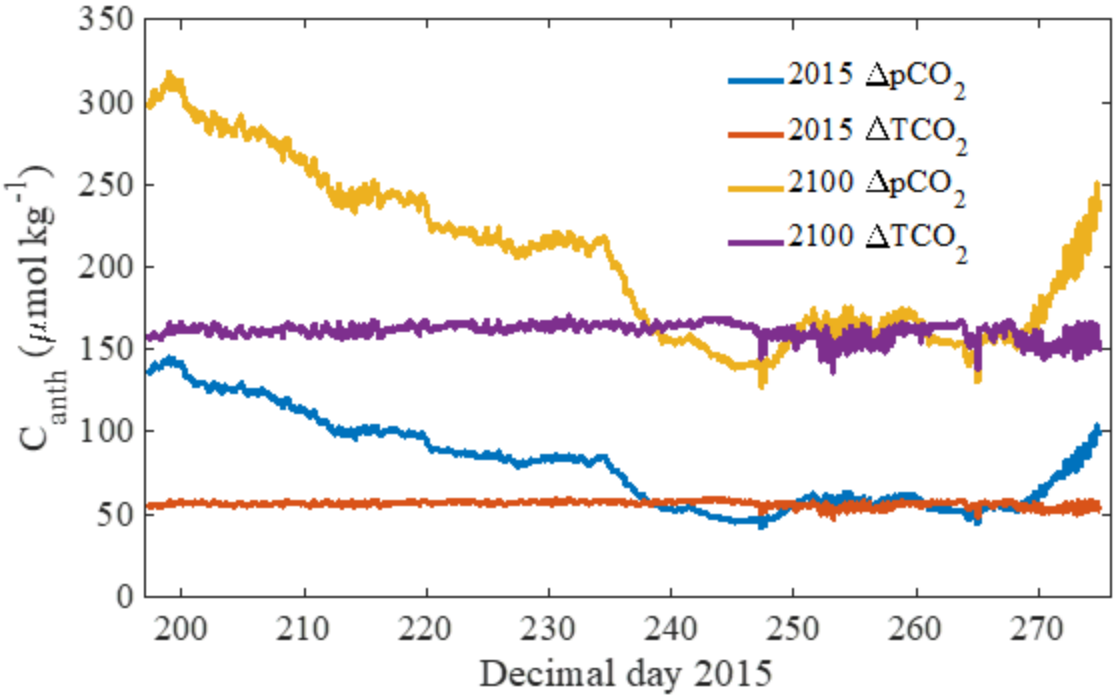

Figure S2.8. Time series of anthropogenic carbon for the years 2015 and 2100 using the ΔpCO$_2$ and ΔTCO$_2$ methods.

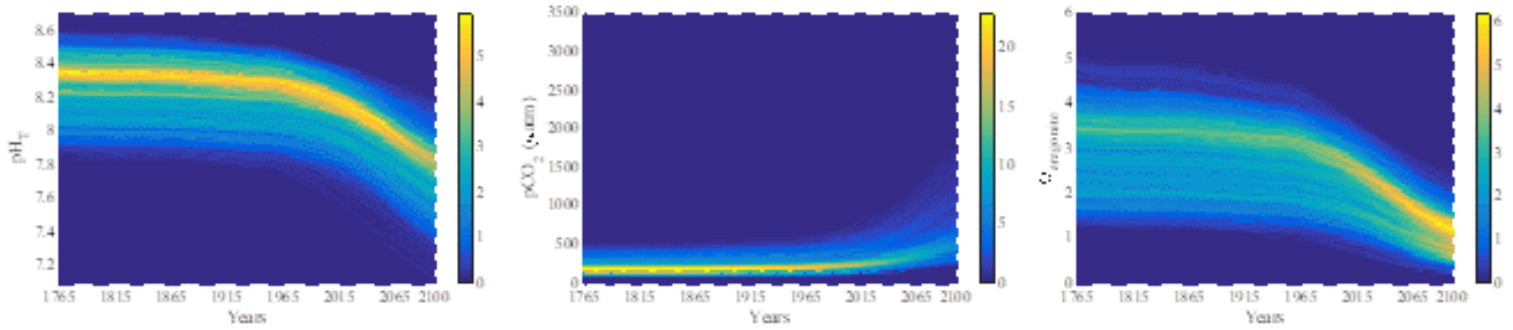

Figure S2.9. Results of OA scenario models from 1765-2100 using the ΔpCO_2 method. Colormaps represent the percent frequency of observations for each parameter as a function of time.

Table S2.1. Summary statistics of carbonate system parameters from OA scenario models for the years 1765, 2015, and 2100. Shown are medians, means (standard deviations), mean diurnal range as defined by the daily maximum-minimum observations, and extreme values during the modeled period (July 1-October 1) for each year. Extreme values are defined as the minimum observed pHT, maximum observed pCO2, and minimum observed Ωaragonite. Medians were calculated for pHT to avoid known issues when calculating means and standard deviations for pH data (Boutilier and Shelton 1980).

Year	pH_{total}			pCO_2 (µatm)			$\Omega_{aragonite}$		
	Median	**Diurnal range**	**Extreme**	**Mean (s.d.)**	**Diurnal range**	**Extreme**	**Mean (s.d.)**	**Diurnal range**	**Extreme**
1765	8.26	0.34	7.72	241 (102)	262	872	2.79 (0.65)	1.60	0.94
2015	8.14	0.40	7.51	348 (170)	434	1,460	2.23 (0.62)	1.52	0.60
2100	7.85	0.52	7.16	789 (469)	1,190	3,315	1.28 (0.50)	1.20	0.28

Table S2.2. Comparison of summary statistics between ΔpCO_2 and ΔTCO_2 methods.

Modeling method	1765 mean pH_T	1765 mean pCO_2	1765 mean Ω	2015 mean pH_T	2015 mean pCO_2	2015 mean Ω	2100 mean pH_T	2100 mean pCO_2	2100 mean Ω
ΔpCO_2	8.28	215	3.04	8.11	349	2.22	7.74	918	1.11
ΔTCO_2	8.23	241	2.79	8.11	349	2.22	7.81	789	1.28

INTERACTIONS BETWEEN LOCAL METABOLISM AND ATMOSPHERIC CO_2 DETERMINE THE SEASONAL BUFFER CAPACITIES AND RATES OF OCEAN ACIDIFICATION IN ESTUARINE HABITATS

Stephen R. Pacella[a,b], Cheryl A. Brown[a], Rochelle G. Labiosa[c], Burke Hales[b], T Chris Mochon Collura[a], and George G. Waldbusser[b],

[a]Western Ecology Division, National Health and Environmental Effects Research Laboratory, Office of Research and Development, United States Environmental Protection Agency, Newport, OR 97365

[b]College of Earth, Ocean, and Atmospheric Sciences, Oregon State University, Corvallis, OR 97331

[c]Region 10, United States Environmental Protection Agency, Seattle, WA 98101

In preparation for submission to: *Journal of Geophysical Research: Oceans*

2000 Florida Avenue N.W. Washington, D.C. 20009-1227 USA

3. Interactions between local metabolism and atmospheric CO_2 determine the seasonal buffer capacities and rates of ocean acidification in estuarine habitats

3.1 Abstract

The characteristic variability of coastal carbonate chemistry continues to provide significant hurdles for understanding interactions between anthropogenic and natural CO_2 cycling. Attribution of the anthropogenic component is vital for identifying the impacts of increasing atmospheric carbon on coastal habitats such as coral reefs, upwelling margins, inland seas, and estuaries. The dynamic nature of these systems has led some to conclude that the baseline shift in atmospheric CO_2 is a relatively unimportant driver, but emerging evidence of rapidly acidifying coastal systems suggests otherwise. Here, we present *in-situ* sensor and discrete sample data of carbonate chemistry covering a 10-month period from two subtidal seagrass bed sites in Puget Sound, WA, USA. We used mass balance mechanistic models to evaluate seasonal drivers of carbonate system parameters in the seagrass beds. Model simulations of anthropogenic carbon (C_{anth}) loading from 1765 to 2100 reveal seasonal differences in the magnitude of carbonate system responses, driven by a seasonal evolution of the thermodynamic buffer factors (e.g. $\frac{\frac{\partial[H^+]}{[H^+]}}{\frac{\partial[DIC]}{[DIC]}}$), We highlight how the interaction of local CO_2 cycling and C_{anth} control these buffer factors and determine the susceptibility of each habitat to OA impacts. Rising atmospheric CO_2 has the net effect of increasing the seasonal variability of pH_T and pCO_2, decreasing the seasonal variability of Ω_{arag}, and accelerating rates of acidification in these habitats when compared with open-ocean estimates. These changes in seasonal

variability impact the time to exceedance of established thresholds for both the physiology of endemic organisms and water quality management. Contrary to some previous studies of coastal systems, our results suggest that rising atmospheric CO_2 is likely the dominant driver of current and future changes to pH_T, pCO_2, and $CaCO_3$ saturation states in these habitats when compared with projected changes in river discharge, water temperature, and eutrophication. The accelerating carbonate system changes in estuarine habitats, as demonstrated here, highlight the need for a continuing effort to elucidate the relative roles of anthropogenic forcings in these systems.

3.2 Introduction

The susceptibility of coastal species and ecosystems to impacts of ocean acidification (OA) is an active and rapidly-evolving topic of scientific research and policy discussions. Our emerging understanding of these observed (Waldbusser *et al.*, 2015; Bednaršek *et al.*, 2016; Feely *et al.*, 2016) and predicted (e.g. Busch *et al.*, 2013) harmful ecological impacts has shifted much of the focus of the OA research community to coastal and estuarine ecosystems, but quantitative projections of likely carbonate chemistry changes in estuaries are difficult (Cai *et al.*, 2017) and still lacking. The observational work in these environments shows that the carbonate system is controlled by multiple and co-occurring physical, chemical, and biological processes at rates far exceeding typical oceanic conditions (Hofmann *et al.*, 2011; Waldbusser and Salisbury, 2014; Hales *et al.*, 2016). Additionally, emerging research on rates of coastal carbonate system change show that rates of acidification in coastal habitats can significantly exceed that of the open ocean (e.g. Carstensen *et al.*, 2018). The observed variability in the

carbonate system of coastal habitats has inspired two overarching research challenges to characterizing OA: 1) How do we discern between the "natural" and "anthropogenic" signals in carbonate chemistry observations in coastal environments? and, 2) How does natural variability of the carbonate system in coastal habitats combine with rising baseline CO_2 levels to exceed stress thresholds for OA-sensitive organisms and ecosystems? The first question begs to improve our understanding of how (and how much) OA currently manifests in coastal carbonate chemistry observations, with important implications for interpretation and development of water quality standards. The second question is vital to address to quantify the magnitude, duration, and frequency of exceedance of physiological thresholds derived from laboratory-based OA experiments. Identifying spatial and temporal patterns of these exceedances may provide insight into the relative vulnerability of coastal ecosystems to OA, as well as highlight focal areas for management and research.

Here, we used high-frequency carbonate system observations from two sites in temperate seagrass habitats in Puget Sound, WA, USA over a period of 10 months (July 2015-April 2016) to characterize the physical and biogeochemical mechanisms for seasonal variability of pH_T, pCO_2, and $CaCO_3$ saturation state ($\Omega_{aragonite}$). We then modeled how the removal and addition of anthropogenic carbon (C_{anth}) corresponding to atmospheric CO_2 levels from 1765 to 2100 (RCP 8.5 scenario) alter the observed carbonate system dynamics in the seagrass habitats during summer, winter, and spring conditions. Our prior work has highlighted how diel-scale metabolic CO_2 cycling in a seagrass habitat creates periods of additive anthropogenic and metabolic carbon, causing accelerated depression of pH_T and $\Omega_{aragonite}$ and amplified increases in pCO_2 (Pacella *et*

al., 2018). We focus our analyses here on how OA alters pH_T, pCO_2, and $\Omega_{aragonite}$ dynamics on seasonal time scales, and how these OA-driven alterations influence the crossing of physiological thresholds for endemic coastal organisms as well as water quality management thresholds. The mechanistic roles of local processes in observed carbonate chemistry dynamics are compared with estimates of C_{anth} to address the relative importance of rising atmospheric CO_2 as a control on current and future carbonate chemistry dynamics.

3.3 Methods

3.3.1 Study Sites

Our two seagrass habitat study sites ("Mission Beach" and "Hat Island") are located ~4.7 km apart in shallow, subtidal areas of Puget Sound, WA, USA near the mouth of the Snohomish River. The Snohomish River is the second largest river in Puget Sound, with an annual average flow of 270 $m^3 s^{-1}$ (Yang *et al.*, 2015). The Mission Beach site (48°2'35" N, 122°16'25" W) is located in a continuous *Zostera marina* bed on the Snohomish River delta. The benthos at this site is characterized by fine, muddy sediments and an active infaunal community with high concentrations of ghost shrimp (*Neotrypaea californiensis*) burrows. It is an area known to be important habitat for juvenile dungeness crab (*Cancer magister*), juvenile salmonids, and feeding grounds of seasonal resident gray whales (*Eschrichtius robustus*). The Hat Island site (48°1'20" N, 122°19'39"W) is located in a fringing *Z. marina* bed on the northern shore of Hat Island in Possession Sound. The benthos at this site was characterized by sandy gravel and shell hash substrate and lacked the vigorous infaunal community present at the Mission Beach

site. Water depths at both sites were similar, with Mission Beach ranging from 0.51-5.09-m (mean = 3.15-m) and Hat Island from 0.62 to 4.98-m (mean = 3.19-m).

3.3.2 In-situ sensors and discrete sampling

The measurements and methods have been partially described elsewhere (Pacella et al., 2018), so we will briefly review and expand where needed. Sensor packages (YSI 6000 series sonde with pH, optical dissolved oxygen, conductivity, temperature, and pressure probes, as well as SeaFET pH and SAMI pH sensors) were anchored to the benthos with sensing units ~30cm above the bottom. All sensors were programmed to record simultaneously at a 15-minute frequency. Sensor packages were deployed at Hat Island from 1 July 2015 – 14 April 2016 and at Mission Beach from 28 July 2015 – 14 April 2016. Gaps in YSI data coverage are due to battery failure. SeaFET and SAMI sensors were deployed for shorter periods of time in July/August 2015 and February-March 2016. SeaFET and SAMI sensors were factory calibrated and verified prior to deployment with Certified Reference Material CO_2 standards from the University of California, San Diego (Batch 132). Deployed YSI sondes were replaced with a newly calibrated sonde every ~4 weeks and checked for fouling and sensor drift after every deployment. YSI pH output was corrected using a constant pH offset calculated using concurrent readings from the SAMI pH sensor and the YSI sonde at each site. This pH offset was calculated as the mean difference between SAMI and YSI pH readings at each site and resulted in pH corrections ranging from -0.033 to -0.077 units on the total pH scale. All reported pH values in this manuscript are on the total hydrogen ion scale (pH_T).

Cruises were conducted during the summer (July/August 2015), winter (February 2016), and spring (April 2016) to collect discrete samples adjacent to the sensor packages at both sites, and to characterize the mixing end-members: the Snohomish River and the Possession Sound deep waters (PSDW). Samples to characterize the Snohomish River end-member were taken at river mile 10.6 (47°56'25" N, 122°10'14" W) and samples of PSDW were collected at 50-m depth at the southern end of Possession Sound (47°58'5" N, 122°18'8" W). Water samples from all sites were collected using a General Oceanics 8-L Niskin bottle following established protocols for dissolved gas sampling. Sample water for paired analysis of CO_2 partial pressure ($pCO_{2(s.w.)}$) and total dissolved inorganic carbon (TCO_2) were transferred to 330-mL amber glass bottles and immediately poisoned with 30-µL of a saturated mercuric chloride solution. Analysis for $pCO_{2(s.w.)}$ and TCO_2 was conducted using non-dispersive infra-red absorption, as described by (Hales *et al.*, 2004; Bandstra *et al.*, 2006), in the laboratory of Burke Hales at Oregon State University. Samples for dissolved inorganic nutrients ($[NO_3+NO_2]$, $[NH_4]$, $[PO_4]$) were immediately filtered with 0.2-µm syringe filters and frozen in the field. Nutrient concentrations were colorimetrically determined by flow injection analysis at the MSI Analytical Laboratory at the University of California - Santa Barbara. pH_T time series and discrete samples of pCO_2/TCO_2 from the Hat Island site for July-September 2015 have been previously reported in Pacella *et al.*, 2018.

3.3.3 Calculating the present-day carbonate system

Using the grab samples from both seagrass sites, the Snohomish River, and the PSDW for all seasons, we created an empirical relationship between calculated alkalinity

(using the paired $pCO_{2(s.w.)}$ and TCO_2 analyses) and salinity for the full range of salinity observed at the study sites (Supplementary Information). The empirical relationship found was:

$$Alk_{sal} = 58.6 * S + 391;$$

$$n=38,\ R^2=0.992,\ p<0.001,\ RMSE=38\ \mu eq\ kg^{-1}$$

where Alk_{sal} is the salinity-derived alkalinity in μeq kg^{-1}, and *S* is the observed *in-situ* salinity (Supplementary Information). This relationship allowed for calculating Alk_{sal} values for the full time series at both sites. We then used Alk_{sal} and the observed *in-situ* pH_T time series to calculate the full carbonate system using CO_2SYS (Matlab version 1.1; K_1 and K_2 constants of Millero, 2010; KSO_4 constants of Dickson 1990; borate:salinity of Lee *et al.*, 2010). Propagation of the estimated errors of both the *in-situ* pH_T measurements and Alk_{sal} values when calculating the full carbonate system results in uncertainties of ~2% for TCO_2, ~5% for $pCO_{2(s.w.)}$, and ~4% for $\Omega_{aragonite}$. Note these uncertainty estimates do not include uncertainties associated with the equilibrium constants of the carbonate system (~0.5-2% for pCO_2 calculated from pH_T and Alk; Williams et al., 2017). The resultant time series of the full carbonate system in both habitats is referred to throughout the manuscript as the "present-day" observations.

3.3.4 Mechanistic mass-balance models

Mechanistic models of TCO_2 and Alk mass budgets were used to quantify the relative roles of riverine dilution, temperature changes, aerobic photosynthesis/respiration, $CaCO_3$ formation/dissolution, and gas exchange in controlling observed carbonate chemistry dynamics in the seagrass habitats for the summer and

spring seasons. PSDW was assumed to be the primary marine source waters to both sites. The carbonate chemistry, salinity, and temperature of the PSDW was relatively invariant during the 2015-16 study period and therefore provides a relevant baseline to compare the role of local physical and biogeochemical drivers of carbonate chemistry in the seagrass habitats. We present the changes in pH_T, $pCO_{2(s.w.)}$, and Ω_{arag} due to each of these local drivers as the departures from observed PSDW values. The non-additive nature of these carbon system parameters means that the contributions of each individual driver do not perfectly sum to the total observed deviation from PSDW. The mass balance equations used were:

$$Alk_{obs} = Alk_{PSDW} + Alk_{dil} + Alk_{bio} + Alk_{calc}$$

$$TCO_{2,obs} = TCO_{2,PSDW} + TCO_{2,dil} + TCO_{2,bio} + TCO_{2,calc} + TCO_{2,gas}$$

where Alk_{obs} and $TCO_{2,obs}$ are observed values from the two seagrass study sites. Changes to TCO_2 and Alk by each of the mechanisms were calculated as found below:

Riverine dilution:

$$TCO_{2,dil} = (f_m * TCO_{2,PSDW} + (1\text{-}f_m) * TCO_{2,river}) - TCO_{2,PSDW}$$

$$Alk_{dil} = (f_m * Alk_{PSDW} + (1\text{-}f_m) * Alkriver) - Alk_{,PSDW}$$

where f_m is the fraction of PSDW present at the study site based on observed salinity, $TCO_{2,PSDW}$ and Alk_{PSDW} are the observed values for the PSDW, and $TCO_{2,river}$ and Alk_{river} are the observed values for the Snohomish River.

Photosynthesis/Respiration:

$$TCO_{2,bio} = 106C{:}1P * ([PO_4]_{mix} - [PO_4]_{obs})$$

$$[PO_4]_{mix} = f_m * [PO_4]_{marine} + (1-f_m) * [PO_4]_{river}$$

$$Alk_{bio} = -16/117 * TCO_{2,bio}$$

Where 106C:1P is the Redfield/Ketchum stoichiometric ratio of carbon to phosphorus for aerobic photosynthesis and respiration, $[PO_4]_{obs}$ is the observed phosphate concentration in the seagrass study site, $[PO_4]_{marine}$ and $[PO_4]_{river}$ are the observed phosphate concentrations of the PSDW and Snohomish River, and -16/117 is the stoichiometric ratio of alkalinity to TCO_2 change during aerobic photosynthesis and respiration.

CaCO3 formation/dissolution:

$$Alk_{calc} = Alk_{obs} – Alk_{dil} – Alk_{bio} – Alk_{PSDW}$$

$$TCO_{2,calc} = Alk_{calc} / 2$$

Where Alk_{calc} and $TCO_{2,calc}$ are the changes in Alk and TCO_2 as a result of $CaCO_3$ formation and dissolution.

Gas exchange:

$$TCO_{2,gas} = TCO_{2,obs} – TCO_{2,dil} – TCO_{2,bio} - TCO_{2,calc\Delta} – TCO_{2,PSDW}$$

Where $TCO_{2,gas}$ is the change due to CO_2 gas exchange, found by difference using the mass balance equation.

Temperature change:

$$\Delta T_i = T_{PSDW} – T_{i,obs}$$

The effect of changes in temperature (ΔT_i) from PSDW to those observed (*in-situ*) in each seagrass study sites was found by recalculating the carbonate chemistry of PSDW at

the *in-situ* temperature in the seagrass habitats for each point of the time series ($T_{i,obs}$). Changes to pH, $pCO_{2(s.w.)}$, and Ω_{arag} were calculated at each time point of the times series of both habitats as the change in PSDW with ΔT_i.

3.3.5. Ocean acidification simulations

We modeled the removal and addition of anthropogenic carbon from present-day observations to simulate the carbonate chemistry dynamics in the seagrass habitats under altered atmospheric CO_2 levels from 1765-2100. Anthropogenic carbon concentrations were calculated for each point of the time series for both habitats using an adaptation of the ΔC* method used in other coastal ocean studies (Gruber *et al.*, 1996), as explained in detail in Pacella *et al.*, 2018 and briefly here. We assumed atmospheric CO_2 levels from the Representative Concentration Pathway 8.5 scenario (Riahl *et al.*, 2011). The TCO_2 disequilibrium at each time point for the present-day observations was calculated as:

$$[TCO_2]_{diseq} = [TCO_2]_{eq}^{2015} - [TCO_2]_{obs}^{2015}$$

Where $[TCO_2]_{obs}^{2015}$ is the present-day observed [TCO_2], and $[TCO_2]_{eq}^{2015}$ is the theoretical atmospheric-equilibrated value calculated using the observed [Alk] and pCO_2 = 402 μatm. New [TCO_2] time series for each habitat were calculated for each year from 1765 to 2100 by subtracting off the $[TCO_2]_{diseq}$ time series from the theoretical atmospheric-equilibrated values (e.g., $[TCO_2]_{eq}^{2015}$) for each year, as follows:

$$[TCO_2]_{obs}^{year} = [TCO_2]_{eq}^{year} - [TCO_2]_{diseq}$$

$$[TCO_2]_{eq}^{year} \sim f(pCO_{2,year}, [Alk]_{obs})$$

Where "year" is each year from 1765 to 2100, $pCO2_{year}$ is equal to the atmospheric CO_2 mole fraction of that year from the RCP 8.5 scenario, and $[Alk]_{obs}$ is the present-day observed value. The full carbonate system was then calculated for each year using the time series of $[TCO_2]_{obs}^{year}$ and $[Alk]_{obs}$. Anthropogenic carbon concentrations were thereby calculated at each time point for every simulation year as the difference from the 1765 model:

$$C_{anth} = [TCO_2]_{year} - [TCO_2]_{1765}$$

3.4 Results

3.4.1 Present-day time series observations

Time series of pH_T from both seagrass habitat sites (Fig. 1, Table 1) show the highest average pH values and largest daily variances during the summer (July - November 1, 2015) and spring (March 1, 2016 - April 16, 2016) seasons, with winter (November 1, 2015 – March 1, 2016) conditions characterized by lower average and less variable pH_T. pH_T and O_2 at Mission Beach were on average lower than observations from Hat Island, despite similar salinity patterns at both sites (Table 1). Daily and seasonal variability in pH_T is generally consistent with previous studies of seagrass habitats (e.g. Hendriks *et al.*, 2014; Challener *et al.*, 2016). Calculated values of $pCO_{2(s.w.)}$ and $\Omega_{aragonite}$ show distinct seasonal patterns, similar to those of pH_T (Table 1; Figure 1). Summer and spring conditions displayed lower mean $pCO_{2(s.w.)}$ and higher mean $\Omega_{aragonite}$ when compared with winter conditions, which were characterized by high $pCO_{2(s.w.)}$ and consistently low $\Omega_{aragonite}$. Mission Beach showed consistently higher

$pCO_{2(s.w.)}$ and lower $\Omega_{aragonite}$ when compared with Hat Island, in agreement with observed patterns of pH_T. Maximum $pCO_{2(s.w.)}$, minimum pH_T, and minimum $\Omega_{aragonite}$ values were observed in the fall during the transition from summer to winter conditions at both sites. These observed seasonal differences in pH_T, $pCO_{2(s.w.)}$, and $\Omega_{aragonite}$ magnitude and variability are in agreement with samples taken in 2014/2015 by the Washington State Department of Ecology's (WADOE) marine monitoring program Station PSS019 (~2.3 km from our Hat Island site) (Pelletier *et al.*, 2018), which are reported in Fig. 1. The correlation of pH_T and O_2 displayed a seasonal evolution at both sites. Summer pH_T and O_2 were highly correlated at Hat Island and Mission Beach (Pearson correlation coefficient (r)=0.928, $p<0.001$; r=0.907, $p<0.001$, respectively). Winter pH_T and O_2 observations were less variable and poorly correlated at Hat Island (r=0.249, $p<0.001$), while Mission Beach displayed similarly low variability but stronger correlation (r=0.746, $p<0.001$). Both sites displayed a transition into spring-time conditions in late March/early April with larger variability and higher correlation of pH_T and O_2 (r=0.957, $p<0.001$; r=0.788, $p<0.001$, respectively). The lower correlation at Mission Beach in spring was seemingly due to the later timing of this transition. Hypoxic conditions were not observed at either study site (Table 1).

3.4.2 Mechanistic drivers of seasonal dynamics

We used multiple methods to estimate the season-specific drivers of observed carbonate chemistry at the seagrass sites: Property-property plots to illustrate correlation of chemical parameters, 1-D mechanistic mass-balance models utilizing carbonate system and nutrient data from the seasonal cruises, and quantifying departures from expected

values due to conservative mixing between the Snohomish River and PSDW end-members. Percentage contributions of each driver calculated by the mechanistic mass balance models do not add to 100% due to the non-linear behavior of pH_T, pCO_2, and $\Omega_{aragonite}$ with changes in TCO_2 and Alk, but are directly comparable with one another due to their common starting point for the calculations (the PSDW). Below we report results by season using each of these methods. In summary, photosynthesis/respiration was the dominant driver of observed carbonate chemistry in the summer and spring at both sites, while winter conditions displayed balanced net aerobic metabolism and more closely reflected mixing between the river and marine end members.

Summer (July 2015-November 1 2015):

Summer carbonate chemistry at both sites was characterized by relatively low CO_2 values on average but displayed large dynamic ranges on daily time scales consistent with diel production/respiration. Observed pH_T and apparent oxygen utilization (AOU; calculated as O_2 at 100% saturation minus observed O_2) at the Hat Island ($r = -0.929$, $p < 0.001$) and Mission Beach ($r = -0.913$, $p < 0.001$) sites were significantly correlated (Fig. 2). Nutrient concentrations at both sites were highly depleted when compared to the conservative mixing line between the Snohomish River and PSDW end-members (Fig. 3). pH_T and $\Omega_{aragonite}$ were consistently higher and more variable, and $pCO_{2(s.w.)}$ depressed and more variable, when compared with expected values from conservative mixing of the end-members (Fig. 1). The mechanistic mass-balance models estimated that both the sign and magnitude of each driver in altering PSDW source waters were similar between the two study sites with the exception of gas exchange (Fig. 4). Photosynthesis and respiration explained the majority of changes in pH_T (90-104%), pCO_2 (94-104%), and

$\Omega_{aragonite}$ (77-89%) from PSDW source waters at Hat Island and Mission Beach, respectively. Gas exchange was less important for changes to pH_T (21-32%), pCO_2 (43-45%), and $\Omega_{aragonite}$ (8-21%), with Hat Island estimated to be a net source of CO_2 and Mission Beach a net sink of CO_2 with respect to atmospheric exchange. However, the Mission Beach gas exchange term may be confounded by inputs of CO_2 from sediment respiration and is discussed further in section 4.1. Riverine dilution, temperature changes, and $CaCO_3$ formation/dissolution were all relatively minor drivers of pH_T, pCO_2, and $\Omega_{aragonite}$ dynamics in both habitats.

Winter (November 1, 2015 – March 1, 2016):

Winter carbonate chemistry at both sites was characterized by high CO_2 levels and lower daily variability, driven largely by conservative mixing with less net metabolic influence. pH_T and AOU showed poor correlation ($R=-0.363$, $p<0.001$) at Hat Island, but the correlation at Mission Beach remained reasonably strong ($R=-0.838$, $p<0.001$) (Fig. 2). This suggests aerobic metabolism continues to be an important driver of carbonate system variability at Mission Beach, but much less so at Hat Island. Nutrient concentrations at both sites showed only small departures from conservative mixing (Fig. 3). Time series of *in-situ* pH_T, calculated pCO_2, and calculated $\Omega_{aragonite}$ agree with magnitudes predicted by conservative mixing models (Fig. 1), but show more high-frequency variability. Unfortunately, discrete samples of pCO_2/TCO_2 used to calculate the full carbonate system did not agree with *in-situ* pH_T, pCO_2, or $\Omega_{aragonite}$ time series (Figure 1). Calculated pH_T from the discrete samples was substantially higher (~0.2 units) than *in-situ* sensor measurements of pH_T, while discrete pCO_2 values were lower and discrete $\Omega_{aragonite}$ values were higher when compared with time series values at both

sites. We have attempted to account for the anomalous nature of these discrete samples, and briefly discuss here. Procedures for sample collection, poisoning, and storage were identical for the full study and conducted by the same researchers, making improper sampling technique unlikely given the good agreement for summer and spring discrete samples with *in-situ* measurements. A review of the instrument performance during the period these samples were analyzed in the laboratory revealed good calibration curves and accurate analysis of gas and liquid standards for both pCO_2 and TCO_2. Samples from both the winter and spring cruises were intermixed and run in the same batches, but only spring discrete samples showed good agreement with *in-situ* measurements. We therefore ruled out analytical issues related to instrument performance, as we would expect to have seen poor agreement in the spring samples run in these intermixed batches. It was later realized that some of the bottle caps used to seal the winter cruise sample bottles were faulty and did not properly seal, sometimes audibly off-gassing if the cap was bumped. We therefore think it is possible that the batch of caps used for our winter cruise did not create gas-tight seals and allowed exchange with the room air (~400 μatm) in which they were stored. If the bottles did off-gas CO_2 (given calculated pCO_2 at the sites was ~600-1000 μatm during the winter cruise), the samples would be expected to show anomalously low pCO_2, high pH_T, high $\Omega_{aragonite}$, low TCO_2, but correct alkalinity. We indeed observe this behavior when we compare discrete samples with *in-situ* values (Figure 1) for pCO_2, pH_T, and $\Omega_{aragonite}$. Alkalinity values calculated from the discrete samples fall directly along the alkalinity-salinity relationship created from summer and spring samples in this study. Given this evidence for poor sample reliability and possible leaking bottles, we have chosen to not interpret the winter cruise discrete

samples. We report the values in Figure 3 however, given the fact that we cannot definitively identify the cause for the anomalous sample behavior. Despite these issues, we can estimate the role of photosynthesis/respiration as our methods rely only on the nutrient and salinity data (Methods 2.4). We estimate photosynthesis/respiration to be responsible for -3.3 (+/- 10.4) μmol TCO_2 kg^{-1} at Hat Island and +5.1 (+/- 5.8) μmol TCO_2 kg^{-1} at Mission Beach. This would alter the pH_T, pCO_2, and $\Omega_{aragonite}$ of PSDW by +0.01, -28 μatm, and +0.02 units respectively at Hat Island, and -0.02, +47 μatm, and -0.03 units respectively at Mission Beach.

Spring (March 1, 2016 – April 16, 2016):

The spring period displayed a strong transition from mixing-dominant winter conditions (higher average pCO_2 and lower average pH_T and $\Omega_{aragonite}$, with lower diel variability amongst all parameters) to net autotrophic conditions similar to those observed in summer 2015 (lower average pCO_2 and higher average pH_T and $\Omega_{aragonite}$, with higher diel variability amongst all parameters). pH_T and AOU at Mission Beach retained similar correlation in the spring ($R=-0.828$, $p<0.001$) as for the winter, with late spring values displaying the highest correlation (Fig. 2). Hat Island showed a similar pH_T-AOU correlation ($R=-0.963$, $p<0.001$) as observed in the summer. Nutrient concentrations at both sites showed significant, but variable, drawdown when compared with conservative mixing lines (Fig. 3); DIN and phosphate at Hat Island were more depleted than those of Mission Beach at comparable salinities, likely reflecting more complete photosynthetic assimilation of available nutrients and driving the higher observed pH_T and O_2 at Hat Island. Observed pH_T and $\Omega_{aragonite}$ were higher and more variable, and pCO_2 depressed and more variable, when compared with expected values from conservative mixing of the

end-members (Fig. 1). The magnitude of these local modifications from expected mixing values were similar to those observed in summer 2015. Also similar to the summer period, photosynthesis/respiration was the dominant driver of pH_T (81-86%), pCO_2 (83-88%), and $\Omega_{aragonite}$ (101-148%) alteration at both sites (Fig. 4). Both sites were net sinks of atmospheric CO_2, causing 12-38% of observed pH_T changes, 26-67% of observed pCO_2 changes, and 8-40% of $\Omega_{aragonite}$ changes. Temperature changes and $CaCO_3$ formation/dissolution were again relatively minor drivers of pH_T, pCO_2, and $\Omega_{aragonite}$ dynamics in both habitats. Riverine dilution was more prominent than in the summer due to higher spring-time river discharge, resulting in 21-24% of observed pH_T changes, 44-50% of observed pCO_2 changes, and 2-19% of observed $\Omega_{aragonite}$ changes.

3.4.3 Ocean acidification simulations

Simulations of anthropogenic carbon loading and resultant carbonate system alterations reveal that the summer season had higher and more rapidly increasing C_{anth} when compared with the winter and spring (Figs. 5 & 6) at both sites. Estimates of average C_{anth} in 2015-16 for Hat Island (Mission Beach) were 57 (58) μmol kg^{-1} in the summer, 38 (45) μmol kg^{-1} in the winter, and 39 (42) μmol kg^{-1} in the spring. For all seasons, the rates and magnitudes of change of pH_T and $pCO_{2(s.w.)}$ were higher, and $\Omega_{aragonite}$ lower, at the Mission Beach site when compared with the Hat Island site (Fig. 6, Table 2). Despite the higher concentrations of C_{anth} in the summer, rates of pH_T decline and $pCO_{2(s.w.)}$ increase were greatest during the winter for both sites (Fig. 6). This difference in the seasonal carbonate system rate of change resulted in altered intra-annual seasonality of pH_T (as $[H^+]$), $pCO_{2(s.w.)}$, and $\Omega_{aragonite}$ at the study sites. We quantified

these changes in seasonality by looking at the absolute difference between summer and winter conditions (e.g. minimum summer $pCO_{2(s.w.)}$ minus maximum winter $pCO_{2(s.w.)}$), and how this seasonality has been altered from estimated pre-industrial conditions. Our OA simulations estimate that present-day seasonal variation in $[H^+]$ and $pCO_{2(s.w.)}$ have increased ~51-60% and 68-70%, respectively, from pre-industrial conditions (Figure 7), while the seasonal variation in $\Omega_{aragonite}$ is reduced by ~14-20%. End-of-century projections estimate 214-239% and 273-338% increases in seasonal variation of $[H^+]$ and $pCO_{2(s.w.)}$, respectively, and 43-58% reductions in seasonal $\Omega_{aragonite}$ variation. We also normalized the magnitude of seasonality by the annual mean value for pH_T (as $[H^+]$), $pCO_{2(s.w.)}$, and $\Omega_{aragonite}$ (Fig. 7b) in order to account for the increasing $[CO_{2(aq)}]$ and $[H^+]$, and declining $[CO_3^{2-}]$ with OA as:

$$\frac{\frac{\Delta x_i}{\bar{x}_i}}{\frac{\Delta x_{1765}}{\bar{x}_{1765}}}$$

where *i* is the year from 1765 to 2100, Δx_i is the magnitude of seasonality of the carbonate parameter of interest ($[H^+]$), $pCO_{2(s.w.)}$, or $\Omega_{aragonite}$), $\bar{x}_i$ is average for the carbonate parameter x in year *i*. This effectively quantifies how the magnitudes of seasonality have been altered since the pre-industrial, while normalizing for the interannual changes in baseline $[CO_{2(aq)}]$, $[H^+]$, and $[CO_3^{2-}]$. We refer to these values as the "relative seasonality". Using this perspective, the relative seasonality of $\Omega_{aragonite}$ increases with OA through the year 2100, while the relative seasonalities of $[H^+]$ and pCO_2 reach maximum values before the end of the century. Mission Beach is predicted to reach these maximum values of $[H^+]$ and pCO_2 relative seasonality earlier than Hat

Island, and drop below pre-industrial values by 2100. This behavior demonstrates how these habitats will reach their minimum buffering capacities with respect to $[H^+]$ and pCO_2 before 2100 under a business-as-usual emissions scenario.

3.5 Discussion

3.5.1 Drivers of seasonal carbonate chemistry and buffering capacity

Our previous worked showed NCM to be the dominant driver of high-frequency (e.g. diel) dynamics at the Hat Island site (Pacella *et al.*, 2018). This study demonstrates that NCM is also responsible for most of the seasonal variability in carbonate chemistry in these habitats by removing large amounts of CO_2 from waters in the habitats during summer (-144 μmol C kg^{-1}) and spring (-116 μmol C kg^{-1}), with little net removal in the winter (+/- 0 μmol C kg^{-1}) on average. Spring and summer observations at both sites show large departures from conservative mixing, improving pH_T, pCO_2, and $\Omega_{aragonite}$ conditions with respect to organismal stress tolerances. Winter observations more closely matched conditions predicted from conservative mixing between the marine and riverine end-members, with seemingly low or balanced NCM. This seasonal progression of low summer and high winter TCO_2 agrees with previous modeling work in the nearby Strait of Georgia (Moore-Maley *et al.*, 2016), which was significantly related to chlorophyll *a* biomass. Our findings support the concept of seagrass habitats improving chemical conditions during the summer and spring periods when compared with source waters (Cyronak *et al.*, 2018), but having a more limited amelioration role during the winter period. This is likely due to limited winter-time

primary production and more vigorous mixing resulting in shorter residence times of water in these habitats. The coherence between our observations and those of WADOE's larger survey of Puget Sound surface waters (Pelletier *et al.*, 2018) conducted the previous year suggests that seasonal patterns in carbonate chemistry reported in this study may be more broadly representative of conditions in these habitats, and not just specific to the 2015-2016 study period.

Net community metabolism (and its seasonal variation) is not only the dominant control of carbonate system magnitude and variability in these habitats, it is also the primary driver controlling the sensitivity of these habitats to rising atmospheric CO_2. The sensitivity of pH_T, $pCO_{2(s.w.)}$, and $CaCO_3$ mineral solubilities in marine and estuarine waters is largely described by the ratio of TCO_2:Alk (Egleston *et al.*, 2010; Hu and Cai, 2013; Cai *et al.*, 2017). A given change in TCO_2 will cause the largest pH_T perturbation at TCO_2:Alk ratios of approximately 1, cause increasing perturbations of $pCO_{2(s.w.)}$ with increasing TCO_2:Alk, and cause decreasing perturbations in $CaCO_3$ mineral solubilities with increasing TCO_2:Alk. Thereby, local physical and biogeochemical controls of the TCO_2 and Alk pools will have non-uniform effects on pH_T, $pCO_{2(s.w.)}$, and $CaCO_3$ saturation states as the TCO_2:Alk ratio is increased in ambient waters due to increasing C_{anth}. It is therefore useful to understand how local drivers alter the buffering capacity of ambient waters, as this will dictate the extent to which C_{anth} will perturb carbonate system parameters. Aerobic metabolism has the largest relative impact on the TCO_2:Alk ratio based on the stoichiometry of TCO_2:Alk alteration (approximately 117:-16), while $CaCO_3$ formation/dissolution (1:2) and gas exchange (1:0) have relatively smaller impacts. The extent that mixing between marine and river end members will alter

TCO_2:Alk will depend on the site-specific difference between their respective ratios; mixing between PSDW and the Snohomish River results in a small, near 1:1 change in TCO_2:Alk. In the seagrass habitats of this study, NCM exerts the strongest control on the seasonal variation of the TCO_2:Alk ratio (Figs. 4 & 8), thereby controlling the sensitivity of the carbonate system to increasing C_{anth} not just on diel timescales (Pacella *et al.*, 2018), but also on seasonal timescales. The net photosynthetic removal of CO_2 during the summer and spring seasons reduces the TCO_2:Alk ratio, reducing the relative sensitivity (i.e. raising buffering capacity) of these habitats to increasing C_{anth} with respect to pH_T and $pCO_{2(s.w.)}$ while increasing the sensitivity of $\Omega_{aragonite}$. The lack of this net CO_2 removal in the winter results in higher TCO_2:Alk ratios, making this season the most sensitive to increasing C_{anth} with respect to pH and $pCO_{2(s.w.)}$, and slightly less sensitive with respect to Ω_{arag}. Seasonal differences in buffering capacities have the net effect of increasing the inter-seasonal variability of pH and $pCO_{2(s.w.)}$ and dampening that of $\Omega_{aragonite}$, while also driving the inter-annual rates of seasonal change in pH, $pCO_{2(s.w.)}$, and $\Omega_{aragonite}$ (Fig. 8). The reported changes in seasonal variability predicted here have not been previously reported for coastal/estuarine environments, but are consistent with recently modeled (McNeil and Sasse, 2016) and observed (Landschützer *et al.*, 2018) responses in the open ocean. These changes in carbonate system seasonality ultimately result in earlier and more severe exceedance of physiological and water quality thresholds (see discussion below).

A possible source of error in our mechanistic mass balance modeling, however, is the assumption of mixing between only two end members (Snohomish River and PSDW), with no explicit accounting for inputs of nutrients, TCO_2, and Alk from benthic

respiration. If there is indeed an appreciable amount of benthic respiration, and a decoupling of the sediment efflux of CO_2 and inorganic nutrients from Redfield ratios as our models assume, this sedimentary CO_2 addition would manifest in our mechanistic models as an error in the gas exchange term (biasing the gas exchange term towards a greater influx of CO_2). A recent synthesis of sediment-water interface fluxes calculated that O_2 and nutrient fluxes show large departures from Redfield ratios for the majority of observations (Boynton *et al.*, 2018), supporting the possible exchange of sedimentary CO_2 and O_2 without concurrently remineralized nutrients into the water column. The observed soft-bottom infaunal community and higher AOU values at Mission Beach when compared with Hat Island demonstrate that benthic-pelagic coupling may play an important role in controlling the carbonate system of this seagrass habitat. We therefore tentatively hypothesize that our estimates of net community metabolism (NCM) at Mission Beach are upper bounds and possibly biased towards net autotrophy, while gas exchange is biased towards larger net influxes of CO_2. It is regrettable we were unable to characterize the contribution of benthic metabolism, and future mechanistic work in these types of habitats would greatly benefit from doing so.

3.5.2 Implications for OA impacts in estuarine habitats

Our results highlight how OA impacts in coastal environments have strong spatial and temporal gradients. Our study sites were in closely located *Z. marina* habitats, yet displayed large differences in observed carbonate system dynamics (Fig. 1) and OA-driven impacts to these dynamics (Figs. 5 & 6; Table 2). TCO_2:Alk ratios were higher at the Mission Beach site (Fig. 8), resulting in this habitat being more sensitive to

addition of C_{anth} with respect to pH_T and $pCO_{2(s.w.)}$ change, and less sensitive with respect to $\Omega_{aragonite}$ change. The higher TCO_2:Alk ratios are likely a result of reduced net community metabolism (primary production - autotrophic and heterotrophic respiration; NCM) when compared with Hat Island, as supported by the consistently higher AOU levels and mechanistic model results. We hypothesize the reduced NCM at Mission Beach was driven by higher rates of benthic metabolism, resulting in larger effluxes of TCO_2 and O_2 drawdown (as previously discussed).

A potentially disturbing conclusion from this line of reasoning is that habitats which are naturally characterized by low pH_T, high pCO_2, and low $\Omega_{aragonite}$ (and reduced buffering capacities) due to lower net ecosystem production (or net heterotrophy) and/or low-Alk freshwater inputs are likely to be the most impacted by OA. If this is indeed true, this would mean that habitats existing naturally close to organismal tolerance thresholds will be disproportionately impacted by increasing C_{anth}. The fact that these potentially harmful conditions are dependent upon the metabolic activity of the habitat illustrates a possible negative feedback, whereby heterotrophic systems facing OA would result in reduced secondary productivity (assuming reduced populations) and therefore lower community respiration rates, easing the metabolically-enhanced OA effect of reduced buffering capacities. This suggests that feedbacks between ecosystem metabolism and OA-driven alterations to carbonate system buffering capacity may be an important modulator of ecosystem responses. Indeed, recent work shows evidence that the response of phytoplankton communities to OA is dependent upon the buffering characteristics of ambient waters (Richier *et al.*, 2018), highlighting the need for

continuing research on how higher-order (e.g. community) metabolism interacts with increasing C_{anth} levels to determine ambient carbonate chemistry conditions.

Our OA simulations estimate that, despite lower average C_{anth} concentrations, average rates of acidification for all seasons are higher at both sites when compared with reported rates from open-ocean sites. The inherent reduced buffering capacity of estuarine waters with respect to anthropogenic CO_2 addition has been previously realized and well-discussed (Egleston *et al.*, 2010; Cai *et al.*, 2011; Waldbusser *et al.*, 2011; Hu and Cai, 2013), outlining the theoretical basis for faster rates of acidification in estuaries and coasts when compared to the open ocean. A given change in pCO_2 (and atmospheric CO_2) will result in larger changes in [TCO_2] (and therefore C_{anth}) at higher alkalinity and lower Revelle factors, the magnitude of which is proportional to the initial Revelle factor (see (Fassbender *et al.*, 2017) for discussion). The waters in our study sites are characterized by lower alkalinity and higher Revelle factors when compared to open ocean values. They therefore are estimated to hold less C_{anth} than full-strength ocean waters, but this C_{anth} results in larger relative changes to pH_T, pCO_2. Average rates of atmospheric CO_2-driven acidification estimated in this study for Hat Island and Mission Beach are -0.0021 & -0.0027, -0.0027 & -0.0028, and -0.0020 & -0.0024 pH units yr^{-1} for summer, winter, and spring respectively for the period 2001-2012. These are larger than the reported rates of -0.0020 pH_T units yr^{-1} for the Northeast Pacific (2001-2012; Chu *et al.*, 2016) and -0.0018 pH_T units yr^{-1} for the Bermuda Atlantic Time Series (1983-2011; (Bates *et al.*, 2012)). Currently, estimated OA-driven pH_T changes since the pre-industrial range from -0.128 to -0.189, again larger than open-ocean estimates of -0.1 to -0.12 often cited in coastal acidification literature. While we report average rates of

change in this study for comparison purposes, rates of change of low pH_T and high pCO_2 conditions in the seagrass habitats will be higher than these averages for all seasons due to altered buffering (Pacella *et al.,* 2018). The higher natural variability of the carbonate system in estuarine habitats such as our study sites make these sorts of trends difficult to observationally detect by effectively lengthening the time of emergence (Keller *et al.*, 2014). This does not negate the role of atmospheric CO_2-driven changes in these habitats, however, but instead supports the need for further development of methods for monitoring and detection of these changes in dynamic coastal systems.

3.5.3 Exceedance of physiological thresholds for resident organisms

To explore how OA-driven changes in the carbonate system of seagrass habitats predicted by this study may impact endemic organisms, we compared carbonate parameters from the OA simulation model output to physiological thresholds for pH_T, $pCO_{2(s.w.)}$, and $\Omega_{aragonite}$ previously shown to negatively affect coastal species based on laboratory studies. It has been demonstrated that OA-driven changes to the carbonate system can negatively affect organisms through a variety of physiological, behavioral, and trophic mechanisms (e.g. Kroeker *et al.*, 2013; Busch and McElhany, 2016; Marshall *et al.*, 2017), and these mechanisms may act concurrently effectively making OA a multi-stressor itself (Waldbusser *et al.*, 2015). We acknowledge the application of laboratory-based biological thresholds to natural systems is overly-simplistic and ignores the likely emergent properties of OA impacts in the real world (e.g. Kroeker *et al.*, 2017). We nonetheless believe illustrating the variability and progression of threshold exceedances with rising atmospheric CO_2 is useful for characterizing potential OA hotspots (both

spatial and temporal) of vulnerability for organisms and ecosystems, and interpret our analyses from this perspective. A pH_T threshold of < 7.5 was chosen based on a previous study demonstrating increased *Cancer magister* larval mortality (Miller *et al.*, 2016). A $pCO_{2(s.w.)}$ threshold of >1000 μatm was chosen as a general hypercapnia threshold (e.g. McNeil and Sasse, 2016; Feely *et al.*, 2018). An $\Omega_{aragonite}$ threshold of <1.4 was chosen based on previous studies showing acute negative effects on early larval bivalve development (Waldbusser *et al.*, 2015a; Waldbusser *et al.*, 2015b). Figure 9 shows the percent exceedance of these thresholds for each season at both sites, as well as for the full period of observation. Immediately apparent is the difference between the Mission Beach and Hat Island sites with regards to the timing and duration of exceedance – the Mission Beach site is predicted to exceed all thresholds earlier and/or more frequently with rising atmospheric CO_2 levels. This is due to the lower observed NCM (evidenced by higher AOU; Fig. 4) and therefore lower average pH_T and $\Omega_{aragonite}$, and higher $pCO_{2(s.w.)}$. Additionally, the lower NCM at Mission Beach results in higher TCO_2:Alk ratios in this habitat, resulting in lower buffering capacity and faster rates of acidification and $pCO_{2(s.w.)}$ increase when compared with Hat Island as previously discussed.

Despite this difference in timing and magnitude of threshold exceedance, the seasonal patterns of relative chemical favorability are similar between the two sites. Winter conditions are expected to exceed the pH_T and $pCO_{2(s.w.)}$ thresholds earliest and most frequently, with 100% exceedance for both thresholds at atmospheric CO_2 levels predicted by 2100 (RCP 8.5 scenario). Spring and summer threshold exceedances for both pH_T and $pCO_{2(s.w.)}$ are predicted to have been rare at pre-industrial atmospheric CO_2 levels, with rapid increases in percent exceedance by 2050 at both sites. Exceedances of

the $\Omega_{aragonite}$ threshold display different behavior; our simulations predict winter-time $\Omega_{aragonite}$ would always have been below 1.4 even at pre-industrial atmospheric CO_2 levels at both sites. Summer and spring conditions are also predicted to have exceeded this $\Omega_{aragonite}$ threshold 7-40% and 37-61% of the time, respectively, prior to the addition of $C_{anth.}$ However, our simulations predict that exceedance of the $\Omega_{aragonite}$ threshold has recently accelerated at both sites and is currently most frequent when compared with pH_T and pCO_2 thresholds.

The extent of organismal impacts in these habitats would likely depend on the synchronous timing of stressful chemical conditions driven by OA (as illustrated here by seasonal percent threshold exceedances) with the phenology of OA-sensitive life stages, as well as other environmental drivers affecting organismal fitness (Hales *et al.*, 2017). Larval and juvenile stages of many coastal species (e.g. shellfish, crab, salmonids) are known to be associated with seagrass, and are often found to be the most OA-sensitive based on laboratory experiments (e.g. Waldbusser and Salisbury, 2014; Waldbusser *et al.*, 2015; Miller and Waldbusser, 2016), with the potential for carry-over effects in later life stages (Hettinger *et al.*, 2012). For example, *C. magister* eggs hatch and enter the larval stage between February and May (Rasmuson, 2013) in Puget Sound. We show that winter-time conditions are expected to exceed the pH_T threshold for *C. magister* larval mortality earliest and most frequently when compared to summer and spring, with >50% exceedance predicted by 2063 at Hat Island and by 2045 at Mission Beach. End-of-century projections show 100% exceedance of this threshold at both sites. It is important to reiterate that our projections only simulate the impact of changing atmospheric CO_2, and the real-world timing of these exceedances will be modified by natural inter-annual

variability of carbonate chemistry drivers at the sites, altered river discharge, warming, anthropogenic nutrient additions or reductions, as well as large-scale regional drivers (e.g. ENSO, PDO) (see below for further discussion). However, if the conditions observed in 2015/2016 can be considered "typical" for these habitats, the patterns in the seasonality of acidification rates and relative chemical favorability for resident organisms should hold true. There is good reason to believe our observations reflect "typical" conditions in these habitats based on recent work in Puget Sound characterizing the seasonal dynamics of carbonate chemistry in surface waters (Pelletier *et al.*, 2018), as well as general agreement with other observational studies from coastal and estuarine systems (Baumann *et al.*, 2014; Baumann and Smith, 2017; Cyronak *et al.*, 2018). It therefore seems likely that the lower buffering capacity of estuarine waters in Puget Sound, and asymmetric amplification of low pH_T, high $pCO_{2(s.w.)}$, and low $\Omega_{aragonite}$ (Pacella *et al.*, 2018), will ultimately result in earlier and more severe exposure to stressful conditions for OA-sensitive resident organisms.

3.5.4 Importance of rising atmospheric CO_2 in comparison with other anthropogenic drivers of carbonate system change

A confounding factor in studying coastal acidification is the magnitude of the C_{anth} signal relative to other anthropogenic "press" disturbances (Bender *et al.*, 1984) acting in the coastal zone to alter carbonate chemistry. We evaluate here the potential relative importance of projected alterations of river discharge, increases in temperature, and eutrophication in comparison with C_{anth} in controlling current and future changes to carbonate chemistry in our study sites. Discharge data for the Snohomish River indicates

that winter flows have currently increased ~2% since 1963, and summer flows have decreased ~51% during the same time period (Supplementary Information). In the future, the Snohomish River is expected to transition from a double peak (December and spring snow-melt high flows) hydrograph to one with a single peak in December, with the net effect of ~50% increased winter river flows and ~50% reduced summer flows (Vano *et al.*, 2008; Mauger *et al.*, 2015). We simulated the impacts of these estimated changes to river discharge on the carbonate chemistry in the habitats by recalculating the carbonate system in 2015 and 2100 assuming this percentage increase/decrease in the fraction of riverine water at both sites. To simulate increases in temperature, we recalculated the carbonate system assuming a 1°C baseline increase in water temperature from 1765 to 2015, and a 5°C baseline increase in water temperature from 2015 to 2100 following estimated changes in air temperature for the region (Vano *et al.*, 2008; Mauger *et al.*, 2015). We compare the estimated current (from 1765 to 2015) and future (year 2015 to 2100) changes in pH_T, $pCO_{2(s.w.)}$, and $\Omega_{aragonite}$ driven by changes in river discharge, temperature, and C_{anth} alone in Table 3 for the summer and winter seasons.

Currently, altered river discharge is estimated to have change observed carbonate chemistry by 0-11% of the change driven by C_{anth}, and warming is estimated to be 2-12% of the change driven by C_{anth}. Projections for 2100 estimate that changes in river discharge will be 1-45% of the estimated C_{anth} signal, and warming will be 4-25% of the estimated C_{anth} signal. While changes to net community metabolism would likely be important for the summer and spring seasons (and possibly less so for winter), estimates of the magnitude of both current and future changes are lacking. Our analysis estimates photosynthesis/respiration is currently responsible for the average (s.d) net removal of

144 (+/-22) and 116 (+/-28) μmol C kg^{-1} in the summer and spring, respectively, and a net balance of 0 (+/- 9) μmol C kg^{-1} in the winter. We can compare these NCM- driven changes in [TCO_2]with average predicted C_{anth} concentrations for each season in 2015 (38-58 μmol C kg-1) and 2100 (113-166 μmol C kg-1). This shows a roughly 50% change in summer and spring NCM since the pre-industrial would be currently required to have a comparable effect on observed carbonate chemistry as present levels of C_{anth}. Longer-term projections estimate a >100% change in NCM would be required in order to have a comparable impact on future (year 2100) carbonate chemistry as rising atmospheric CO_2. Recent work estimates anthropogenic nutrient sources currently contribute only ~13% of the total dissolved inorganic nitrogen (DIN) load to Whidbey Basin (where our study sites were located), with a maximum ~31% increase in DIN loads due to anthropogenic inputs in Puget Sound (Mohamedali *et al.*, 2011). If we assume no other ecological limitations such that an increase in available nutrients would result in a 1:1 change in NCM (i.e. a 13% increase in available nutrients would increase gross primary production by 13%) via increased photosynthetic activity, these percentage increases of DIN are insufficient to alter the carbonate system as much as current estimates of C_{anth}. Assuming no drastic alterations of the ecosystems' stabilities, it therefore seems likely that the addition of C_{anth} into the waters of these seagrass habitats via rising atmospheric CO_2 has been and will be the dominant driver of current and future changes to the "natural" carbonate system of these habitats. The similarity in observed carbonate chemistry magnitudes and seasonal dynamics of the seagrass habitats in this study when compared with broader surface waters of Puget Sound (Pelletier *et al.,* 2018) suggests this may also be generally true for surface waters of the Salish Sea.

This finding seems at first to counter previous work from the Belgian coast showing eutrophication has a stronger control on coastal carbonate chemistry than rising atmospheric CO_2 levels (Borges and Gypens, 2010). We think that our study does not run counter to the findings of this previous work however for two reasons: 1). The study of Borges and Gypens covered a period of continuously and rapidly rising nutrient levels (~+500% increase in river DIN loading) well above those estimated for Puget Sound, and 2). The model time period of 1951-1998 encompassed a time period where atmospheric CO_2 was rising ~50% as quickly (+1.2 ppmv yr^{-1}) as more recent rates in the past 20 years (+2.25 ppmv yr^{-1} for 1998-2018), necessarily resulting in lower anthropogenic carbon burdens and slower rates of acidification. Therefore, we do not think the findings of our study conflict with those of Borges and Gypens (2010), but instead support a renewed effort to better understand the relative role of atmospheric CO_2 forcing in estuarine and coastal systems, and a reconsideration of the potential for atmospheric CO_2 to currently be or soon become the dominant driver of long-term anthropogenic perturbation of carbonate chemistry in similar systems.

3.5.5 Exceedance of existing recommended water quality criteria and management implications

Quantifying the roles of natural and anthropogenic drivers in shaping coastal carbonate chemistry dynamics provides an opportunity to estimate the potential efficacy of OA management strategies – a critical need for managers and policymakers currently (Strong *et al.*, 2014). The relative importance of a given driver in a coastal system will dictate the upper bound by which management action can influence that

driver to alter the chemistry of a system. For example, nutrient reductions in systems where nutrients are likely not a limiting factor for organic metabolism (e.g. San Francisco Bay, (Cloern, 2018)), or metabolism is a relatively unimportant driver, would likely have limited effects on the carbonate chemistry of that system, whereas nutrient limited, metabolically vigorous systems would likely see larger changes. While a simple concept, the elucidation of system-specific drivers required to estimate these efficacies is difficult due to the highly complex spatial and temporal variability present in estuaries, as exemplified by this study. Our analysis estimates that net community metabolism is the dominant driver in summer and spring, elevating pH_T and $\Omega_{aragonite}$ and reducing $pCO_{2(s.w)}$ when compared with source water values. Nutrient availability also appears to be a limiting factor for photosynthesis during these seasons, as exemplified by the depleted DIN and phosphate concentrations observed at both sites (Fig. 3). Management actions to reduce nutrient loading to these habitats may therefore reduce the net autotrophy in these shallow habitats during the growing season, effectively reducing the seasonal OA-ameliorating effects of photosynthesis in these habitats (Carstensen *et al.*, 2018) as well as reducing their buffering capacity (i.e. increasing TCO_2:Alk) to resist long-term acidification with increasing C_{anth}. As previously discussed, changes in global atmospheric CO_2 levels seem to be the dominant anthropogenic driver in these habitats, possibly limiting the efficacy of local management actions. The limited scope of our dataset preclude us from forming broader conclusions for habitats of Puget Sound. Utilization of models capable of faithfully reproducing the hydrodynamics, biogeochemistry, and anthropogenic forcings to the system (e.g. (Bianucci *et al.*, 2018) will likely be useful for assessing the utility of local management actions at this scale.

The habitat-specific nature of OA impacts (as demonstrated in this study) will require fine spatial and temporal model resolutions to understand the effects of management actions in meaningful ways for organisms and ecosystems.

Despite increasing concern about OA impacts from various governance and management entities (Strong et al., 2014), there are currently no OA-specific recommended water quality criteria. The most relevant existing criteria are likely the US Environmental Protection Agency's marine aquatic life recommended criteria, which partially state that the pH of marine waters may change "not more than 0.2 units outside of the normally occurring range" (U.S. E.P.A., 1986). If we assume our 1765 simulations to represent the "normally occurring range" of these systems, we can calculate the timing at which the pH_T is reduced by >0.2 units solely due to the addition of C_{anth}. Figure 10 shows the percent of observations for both seagrass sites which have been reduced by >0.2 pH_T units for each year. As with the physiological thresholds, there is a distinct seasonal pattern to the rate of exceedance: winter conditions are predicted to cross this threshold most frequently in both sites, with 100% exceedance by the year 2040. Currently (year 2015), the total exceedance for all observations is estimated to be 2% at Hat Island, and 20% at Mission Beach. The differences in percent exceedance amongst seasons and between seagrass sites illustrates how the variable rates of acidification in these habitats, driven by the wide range of buffering capacities on daily (Pacella *et al.*, 2018) and seasonal (this study) time scales, challenge interpretation of existing water quality criteria recommendations.

3.6 Conclusion

Our findings argue that the carbonate systems in estuarine habitats are more sensitive to rising atmospheric CO_2 than is often appreciated in the coastal acidification literature. Our analysis estimates that the pH_T, $pCO_{2(s.w)}$, and $CaCO_3$ saturation states in estuarine habitats typical of the Salish Sea are currently being altered at rates exceeding current estimates from open-ocean habitats, with most of these changes being driven by rising atmospheric CO_2 levels. Therefore, rates of acidification from open-ocean studies (e.g. Doney *et al.*, 2010) that are commonly cited in coastal and estuarine acidification literature (e.g. Duarte *et al.*, 2013) as comparisons to local drivers likely underestimate the atmospheric CO_2 impact in coastal zones. The inherent reduced buffering capacity of the waters in these habitats (when compared with oceanic waters), combined with natural metabolic cycling of CO_2 on diel and seasonal scales, leads to accelerated reductions in pH_T and $\Omega_{aragonite}$, and increases in $pCO_{2(s.w)}$, for a given change in atmospheric CO_2. Exceedances of physiological thresholds for OA-sensitive coastal organisms, as well as existing recommended water quality criteria, will therefore happen earlier and with greater magnitudes than would otherwise be expected in these habitats. The dominance of the globally-driven C_{anth} signal in current and future estimated changes to the carbonate systems of these habitats highlights the potential difficulties for local scale management actions to offset these impacts.

3.7 Acknowledgements

The authors would like to thank the Tulalip Tribes, the US EPA Region 10 Dive Team, and Dr. Jim Kaldy for assistance with field work. Dr. Richard Feely and Dr. Jason Grear provided valuable comments and feedback to a previous version of this manuscript. This project was funded by a U.S EPA RARE grant. The views expressed in this article are those of the authors and do not necessarily represent the views or policies of the U.S. Environmental Protection Agency. Any mention of trade names, products, or services does not imply an endorsement by the U.S. Government or the U.S. Environmental Protection Agency. The EPA does not endorse any commercial products, services, or enterprises.

3.8 Supplementary Information

River discharge:

Present-day changes in Snohomish River discharge were calculated using United States Geological Survey (USGS) Water Resources Data average monthly discharge data from station 12150800 “Snohomish River near Monroe, WA” dating back to 1963 (https://waterdata.usgs.gov/nwis/uv?site_no=12150800). The percent change in summer discharge was calculated using a linear regression of monthly average July, August, and September discharge data from 1963 to 2015 (Fig. S1). The linear regression gives an average dry season discharge of 5,276 cfs in 1960 and 3,487 cfs in 2015, resulting in a calculated 51% reduction. The same methods were used to calculate the change in winter discharge for the months of January, February, and March (Fig. S2). The winter

discharge linear regression gives an average discharge of 11,093 cfs in 1960 and 11,370 cfs in 2015, an increase of 2%. Future changes (2015 to 2100) to river discharge were estimated from climate changes reports for Puget Sound (Mauger et al., 2015). Figure S3 shows historic monthly average streamflow for the Snohomish River compared with low and high greenhouse scenarios, reproduced from Mauger et al., 2015.

Changes in river influence at each study site were calculated assuming changes in salinity would be proportional to changes in river discharge; i.e. a 50% increase in river discharge would result in a 50% increase in the fraction of fresh water (f_{riv}) at the study sites. Changes in TCO_2 and Alk for each observed time point were assumed to change due to these altered mixing fractions as shown below using the example of a 51% reduction in dry season river flow since the preindustrial:

$$f_{mar,2015} = S_{obs}/S_{PSDW}$$

$$f_{riv,2015} = 1 - f_{PSDW}$$

$$f_{riv,dry,PI} = f_{riv,2015} * 1.51$$

$$f_{mar,dry,PI} = 1 - f_{riv,dry,PI}$$

$$S_{obs,PI} = f_{mar,dry,PI} * S_{PSDW}$$

$$[TCO_2]_{mix,2015} = f_{mar,2015} * [TCO_2]_{PSDW} + f_{riv,2015} * [TCO_2]_{riv}$$

$$[Alk]_{mix,2015} = f_{mar,2015} * [Alk]_{PSDW} + f_{riv,2015} * [Alk]_{riv}$$

$$[TCO_2]_{mix,PI} = f_{mar,dry,PI} * [TCO_2]_{PSDW} + f_{riv,dry,PI} * [TCO_2]_{riv}$$

$$[Alk]_{mix,PI} = f_{mar,dry,PI} * [Alk]_{PSDW} + f_{riv,dry,PI} * [Alk]_{riv}$$

$$\Delta[TCO_2]_{mix,PI\rightarrow2015} = [TCO_2]_{mix,2015} - [TCO_2]_{mix,PI}$$

$$\Delta[Alk]_{mix,PI\rightarrow2015} = [Alk]_{mix,2015} - [Alk]_{mix,PI}$$

$$[TCO_2]_{obs,PI} = [TCO_2]_{obs,2015} - \Delta[TCO_2]_{mix,PI \rightarrow 2015}$$

$$[Alk]_{obs,PI} = [Alk]_{obs,2015} - \Delta[Alk]_{mix,PI \rightarrow 2015}$$

Where $f_{mar,2015}$ is the fraction of marine water (i.e. PSDW) at the study site during one time point of the observations period, S_{obs} is the salinity observed at the study site, S_{PSDW} is the observed salinity of the PSDW, $f_{riv,2015}$ is the fraction of river water present at the study site, $f_{riv,dry,PI}$ is the estimated fraction of river water present at the study site in the pre-industrial period, $f_{mar,dry,PI}$ is the estimated fraction of marine water present at the study site in the pre-industrial period, $S_{obs,PI}$ is the estimated salinity at the study site in the pre-industrial period, $[TCO_2]_{mix,2015}$ and $[Alk]_{mix,2015}$ are the estimated present-day $[TCO_2]$ and [Alk] at the study site based on conservative mixing alone of the PSDW ($[TCO_2]_{PSDW}$ & $[Alk]_{PSDW}$) and Snohomish River ($[TCO_2]_{riv}$ & $[Alk]_{riv}$), $[TCO_2]_{mix,PI}$ and $[Alk]_{mix,PI}$ are the estimated pre-industrial $[TCO_2]$ and [Alk] at the study site based on conservative mixing alone of the PSDW and Snohomish River, $\Delta[TCO_2]_{mix,PI \rightarrow 2015}$ and $\Delta[Alk]_{mix,PI \rightarrow 2015}$ are the estimated present-day changes to $[TCO_2]$ and [Alk] at the study sites due to altered mixing of the PSDW and Snohomish River, and $[TCO_2]_{obs,PI}$ and $[Alk]_{obs,PI}$ are the estimated pre-industrial $[TCO_2]$ and [Alk] used to calculate the pre-industrial carbonate system using present-day temperature and $S_{obs,PI}$.

Temperature change:

Changes in water temperature were assumed to follow air temperature trends, due to a lack of site-specific hindcast and forecast data for water temperatures. Changes in air temperature from the pre-industrial (1895) to present-day (2014) are estimated to be ~+1°C (Mauger et al. 2015). Future air temperature changes are dependent upon

emissions pathways; for this study we chose to use a high-end estimate of temperature change in 2100 (+5°C, Fig. S4) as our study utilized business-as-usual atmospheric CO_2 projections from RCP 8.5. The carbonate system at both study sites for the full period of observation was recalculated with these changes in temperature, where the pre-industrial and 2100 temperatures were calculated as:

$$T_{PI,i} = T_{obs,i} - 1$$

$$T_{2100,i} = T_{obs,i} + 5$$

Where $T_{PI,I}$ is the estimated pre-industrial water temperature at time point i, $T_{obs,i}$ is the present-day observed water temperature at time point i, and $T_{2100,I}$ is the estimated year 2100 water temperature at time point i.

3.9 References

Bandstra, L. *et al*. (2006) 'High-frequency measurements of total CO2: Method development and first oceanographic observations', *Marine Chemistry*, 100(1–2), pp. 24–38. doi: 10.1016/j.marchem.2005.10.009.

Bates, N. R. *et al.* (2012) 'Detecting anthropogenic carbon dioxide uptake and ocean acidification in the North Atlantic Ocean', *Biogeosciences*, 9(7), pp. 2509–2522. doi: 10.5194/bg-9-2509-2012.

Baumann, H. *et al.* (2014) 'Large Natural pH, CO_2 and O_2 Fluctuations in a Temperate Tidal Salt Marsh on Diel, Seasonal, and Interannual Time Scales', *Estuaries and Coasts*, pp. 220–231. doi: 10.1007/s12237-014-9800-y.

Baumann, H. and Smith, E. M. (2017) 'Quantifying Metabolically Driven pH and Oxygen Fluctuations in US Nearshore Habitats at Diel to Interannual Time Scales', *Estuaries and Coasts*, (October), pp. 1–16. doi: 10.1007/s12237-017-0321-3.

Bednaršek, N. *et al.* (2016) 'Pteropods on the edge: Cumulative effects of ocean acidification, warming, and deoxygenation', *Progress in Oceanography*, 145, pp. 1–24. doi: 10.1016/j.pocean.2016.04.002.

Bender, E. A. *et al.* (1984) 'Perturbation Experiments in Community Ecology: Theory and Practice', *Ecology*, 65(651), pp. 1–13. doi: 10.2307/1939452.

Bianucci, L. *et al.* (2018) 'Sensitivity of the regional ocean acidification and carbonate system in Puget Sound to ocean and freshwater inputs', *Elem Sci Anth*, 6(1), p. 22. doi: 10.1525/elementa.151.

Borges, A. V. and Gypens, N. (2010) 'Carbonate chemistry in the coastal zone responds more strongly to eutrophication than ocean acidification', *Limnology and Oceanography*, 55(1), pp. 346–353. doi: 10.4319/lo.2010.55.1.0346.

Boynton, W. R. *et al.* (2018) 'Oxygen and Nutrient Exchanges at the Sediment-Water Interface: a Global Synthesis and Critique of Estuarine and Coastal Data', *Estuaries and Coasts*. doi: 10.1007/s12237-017-0275-5.

Busch, D. *et al.* (2013) 'Potential impacts of ocean acidification on the Puget Sound food web', *ICES Journal of Marine Science*, 70, pp. 823–833. Available at: http://icesjms.oxfordjournals.org/content/70/4/823.short.

Busch, D. S. and McElhany, P. (2016) 'Estimates of the direct effect of seawater pH on the survival rate of species groups in the California current ecosystem', *PLoS ONE*, 11(8), pp. 1–28. doi: 10.1371/journal.pone.0160669.

Cai, W.-J. *et al.* (2011) 'Acidification of subsurface coastal waters enhanced by eutrophication', *Nature Geoscience*. Nature Publishing Group, 4(11), pp. 766–770. doi: 10.1038/ngeo1297.

Cai, W. J. *et al.* (2017) 'Redox reactions and weak buffering capacity lead to acidification in the Chesapeake Bay', *Nature Communications*, 8(1), pp. 1–12. doi: 10.1038/s41467-017-00417-7.

Carstensen, J. *et al.* (2018) 'Long-Term and Seasonal Trends in Estuarine and Coastal Carbonate Systems', *Global Biogeochemical Cycles*, 32, pp. 497–513.

Cloern, J. E. (2018) 'Patterns, pace, and processes of water-quality variability in a long-studied estuary', *Limnology and Oceanography*, pp. 1–17. doi: 10.1002/lno.10958.

Cyronak, T. *et al.* (2018) 'Short-Term Spatial and Temporal Carbonate Chemistry Variability in Two Contrasting Seagrass Meadows: Implications for pH Buffering Capacities', *Estuaries and Coasts*. Estuaries and Coasts, pp. 1–15. doi: 10.1007/s12237-017-0356-5.

Egleston, E. S. *et al.* (2010) 'Revelle revisited: Buffer factors that quantify the response of ocean chemistry to changes in DIC and alkalinity', *Global Biogeochemical Cycles*, 24(1), pp. 1–9. doi: 10.1029/2008GB003407.

Fassbender, A. J. *et al.* (2017) 'Nonuniform ocean acidification and attenuation of the ocean carbon sink', *Geophysical Research Letters*, 44(16), pp. 8404–8413. doi: 10.1002/2017GL074389.

Feely, R. A. *et al.* (2016) 'Chemical and biological impacts of ocean acidification along the west coast of North America', *Estuarine, Coastal and Shelf Science*, 183, pp. 260–270. doi: 10.1016/j.ecss.2016.08.043.

Hales, B. *et al.* (2017) 'The Carbonate Chemistry of the "Fattening Line," Willapa Bay, 2011–2014', *Estuaries and Coasts*. Estuaries and Coasts, 40(1), pp. 173–186. doi: 10.1007/s12237-016-0136-7.

Hales, B., Chipman, D. W. and Takahashi, T. T. (2004) 'High-frequency measurement of partial pressure and total concentration of carbon dioxide in seawater using microporous hydrophobic membrane contactors', *Limnology and Oceanography: Methods*, 2(Weiss 1974), pp. 356–364. doi: 10.4319/lom.2004.2.356.

Hettinger, A. *et al.* (2012) 'Persistent carry-over effects of planktonic exposure to ocean acidification in the Olympia oyster', *Ecology*, 93(12), pp. 2758–2768. doi: 10.1890/12-0567.1.

Hofmann, G. E. *et al.* (2011) 'High-frequency dynamics of ocean pH: a multi-ecosystem comparison.', *PloS one*, 6(12), p. e28983. doi: 10.1371/journal.pone.0028983.

Hu, X. and Cai, W. J. (2013) 'Estuarine acidification and minimum buffer zone - A conceptual study', *Geophysical Research Letters*, 40(19), pp. 5176–5181. doi: 10.1002/grl.51000.

Kroeker, K. J. *et al.* (2013) 'Impacts of ocean acidification on marine organisms: Quantifying sensitivities and interaction with warming', *Global Change Biology*, 19(6), pp. 1884–1896. doi: 10.1111/gcb.12179.

Kroeker, K. J., Kordas, R. L. and Harley, C. D. G. (2017) 'Embracing interactions in ocean acidification research: confronting multiple stressor scenarios and context dependence', *Biology Letters*, 13(3), p. 20160802. doi: 10.1098/rsbl.2016.0802.

Landschützer, P. *et al.* (2018) 'Strengthening seasonal marine CO2 variations due to increasing atmospheric CO2', *Nature Climate Change*. Springer US, 8(February). doi: 10.1038/s41558-017-0057-x.

Lee, K. *et al.* (2010) 'The universal ratio of boron to chlorinity for the North Pacific and North Atlantic oceans', *Geochimica et Cosmochimica Acta*. Elsevier Ltd, 74(6), pp. 1801–1811. doi: 10.1016/j.gca.2009.12.027.

Marshall, K. N. *et al.* (2017) 'Risks of ocean acidification in the California Current food web and fisheries: ecosystem model projections', *Global Change Biology*, 23(4), pp. 1525–1539. doi: 10.1111/gcb.13594.

Mauger, G. S. *et al.* (2015) *State of Knowledge: Climate Change in Puget Sound*. doi: 10.7915/CIG93777D.

McNeil, B. I. and Sasse, T. P. (2016) 'Future ocean hypercapnia driven by anthropogenic amplification of the natural CO_2 cycle.', *Nature*. Nature Publishing Group, 529(7586), pp. 383–6. doi: 10.1038/nature16156.

Miller, C. and Waldbusser, G. (2016) ‘A post-larval stage-based model of hard clam Mercenaria mercenaria development in response to multiple stressors: temperature and acidification severity’, *Marine Ecology Progress Series*, 558, pp. 35–49. doi: 10.3354/meps11882.

Miller, J. J. *et al.* (2016) ‘Exposure to low pH reduces survival and delays development in early life stages of Dungeness crab (Cancer magister)’, *Marine Biology*. Springer Berlin Heidelberg, 163(5), pp. 1–11. doi: 10.1007/s00227-016-2883-1.

Millero, F. J. (2010) ‘Carbonate constants for estuarine waters’, (Millero 2001), pp. 139–142.

Mohamedali, T., *et al.* (2011) *Puget Sound Dissolved Oxygen Model Nutrient Load Summary for 1999-2008, Washington Department of Ecology*. Available at: https://fortress.wa.gov/ecy/publications/documents/1103057.pdf.

Moore-Maley, B. L. *et al.* (2016) ‘Locally driven interannual variability of near-surface pH and XA in the Strait of Georgia’, *Journal of Geophysical Research: Oceans*, (121), pp. 1600–1625. doi: 10.1002/2015JC011486.Received.

Pacella, S. R. *et al.* (2018) ‘Seagrass habitat metabolism increases short-term extremes and long-term offset of CO 2 under future ocean acidification’, 115(15), pp. 1–6. doi: 10.23719/1407616.

Pelletier, G. *et al.* (2018) ‘Seasonal variation in aragonite saturation in surface waters of Puget Sound – a pilot study’, *Elem Sci Anth*, 6(1), p. 5. doi: 10.1525/elementa.270.

Rasmuson, L. K. (2013) *The biology, ecology and fishery of the dungeness crab, cancer magister, Advances in Marine Biology*. doi: 10.1016/B978-0-12-410498-3.00003-3.

Richier, S. *et al.* (2018) ‘Geographical CO 2 sensitivity of phytoplankton correlates with ocean buffer capacity’, *Global Change Biology*, (December 2017), pp. 1–15. doi: 10.1111/gcb.14324.

U.S. E.P.A., O. of W. R. and S. (1986) *Quality Criteria for Water 1986 (EPA Publication No. 440/5-86-001)*. Washington, DC.

Vano, J. a *et al.* (2008) ‘Climate Change Impacts on Water Management in the Puget Sound Region, Washington, USA’.

Waldbusser, G. G. *et al.* (2011) ‘Biocalcification in the Eastern Oyster (Crassostrea virginica) in Relation to Long-term Trends in Chesapeake Bay pH’, *Estuaries and Coasts*, 34(2), pp. 221–231. doi: 10.1007/s12237-010-9307-0.

Waldbusser, G. G. *et al.* (2015) ‘Ocean acidification has multiple modes of action on bivalve larvae’, *PLoS ONE*, 10(6). doi: 10.1371/journal.pone.0128376.

Waldbusser, G. G. *et al.* (2015) ‘Saturation-state sensitivity of marine bivalve larvae to ocean acidification’, *Nature Climate Change*, 5(3), pp. 273–280. doi: 10.1038/NCLIMATE2479.

Waldbusser, G. G. and Salisbury, J. E. (2014) ‘Ocean acidification in the coastal zone from an organism’s perspective: multiple system parameters, frequency domains, and habitats.’, *Annual review of marine science*, 6, pp. 221–47. doi: 10.1146/annurev-marine-121211-172238.

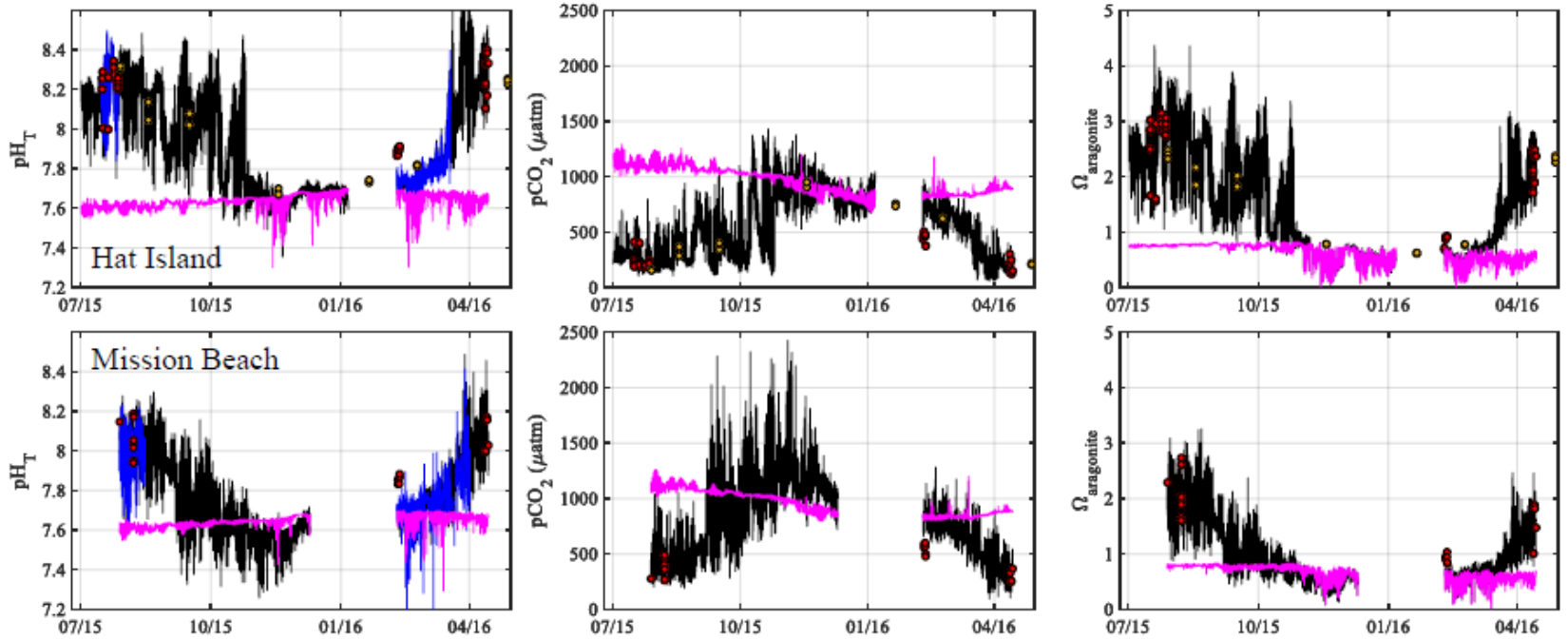

Figure 3.1. Time series from Hat Island (a-c) and Mission Beach (d-f) of observed YSI pH_T (a & d), calculated pCO_2 (b & e) and calculated Ω_{arag} (c & f) shown in black. Blue lines are from SeaFET pH (July-August 2015) and SAMI pH (February-April 2016) sensors deployed adjacent to the YSIs at both sites. Pink lines represent expected values based on conservative mixing of TCO_2 and Alk between marine (PSDW) and riverine (Snohomish River) end members, at observed temperatures in both seagrass sites. Red dots represent calculated values from paired pCO_2/TCO_2 analyses on discrete water samples taken adjacent to the sensor packages. Orange dots represent calculated values from paired TCO2/Alk analyses from Washington Department of Ecology's marine monitoring program station PSS019 in 2014 and 2015. Station PSS019 was located on the southeast side of Hat Island, near our study site.

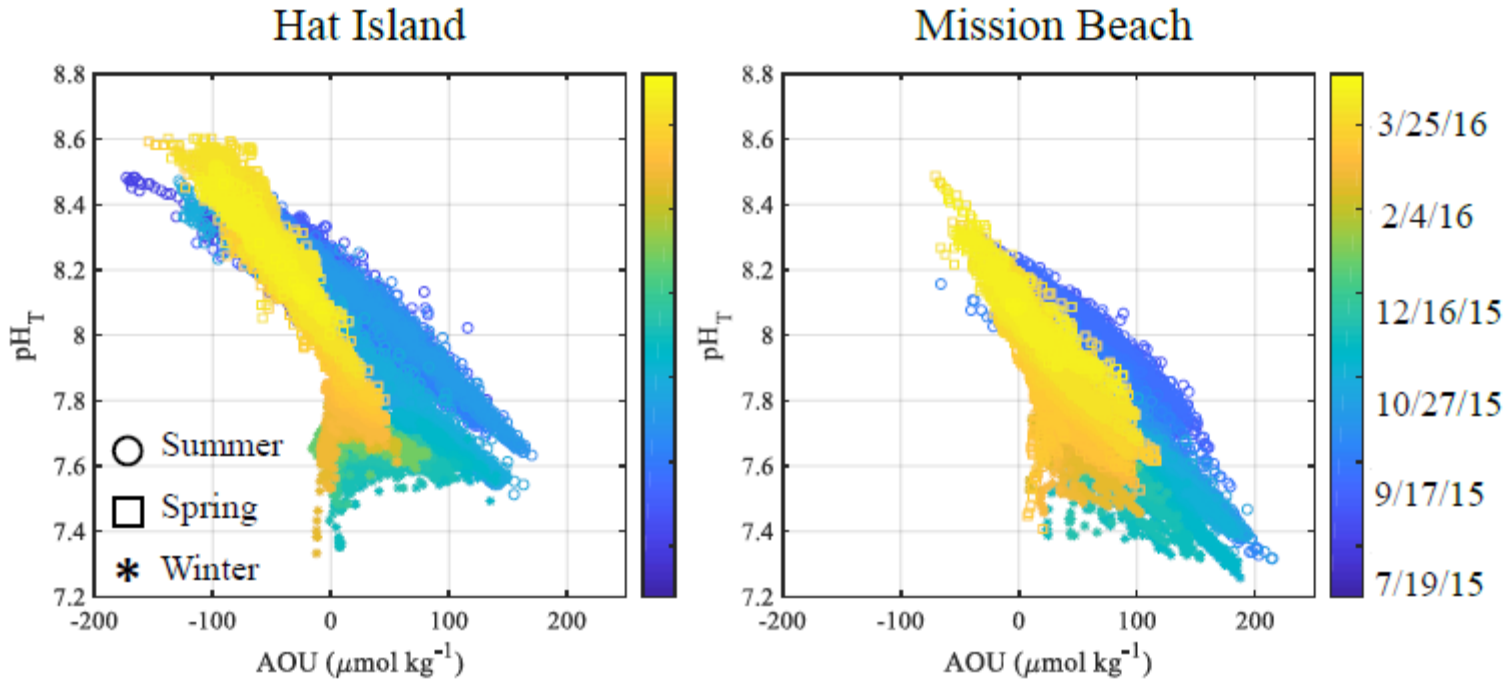

Figure 3.2. Property-property plot of observed apparent oxygen utilization (AOU) versus pH_T at the a). Hat Island and b). Mission Beach seagrass sites. Colorbar represents time of observation, from July 2015-April 2016. Symbol type denotes season of observation.

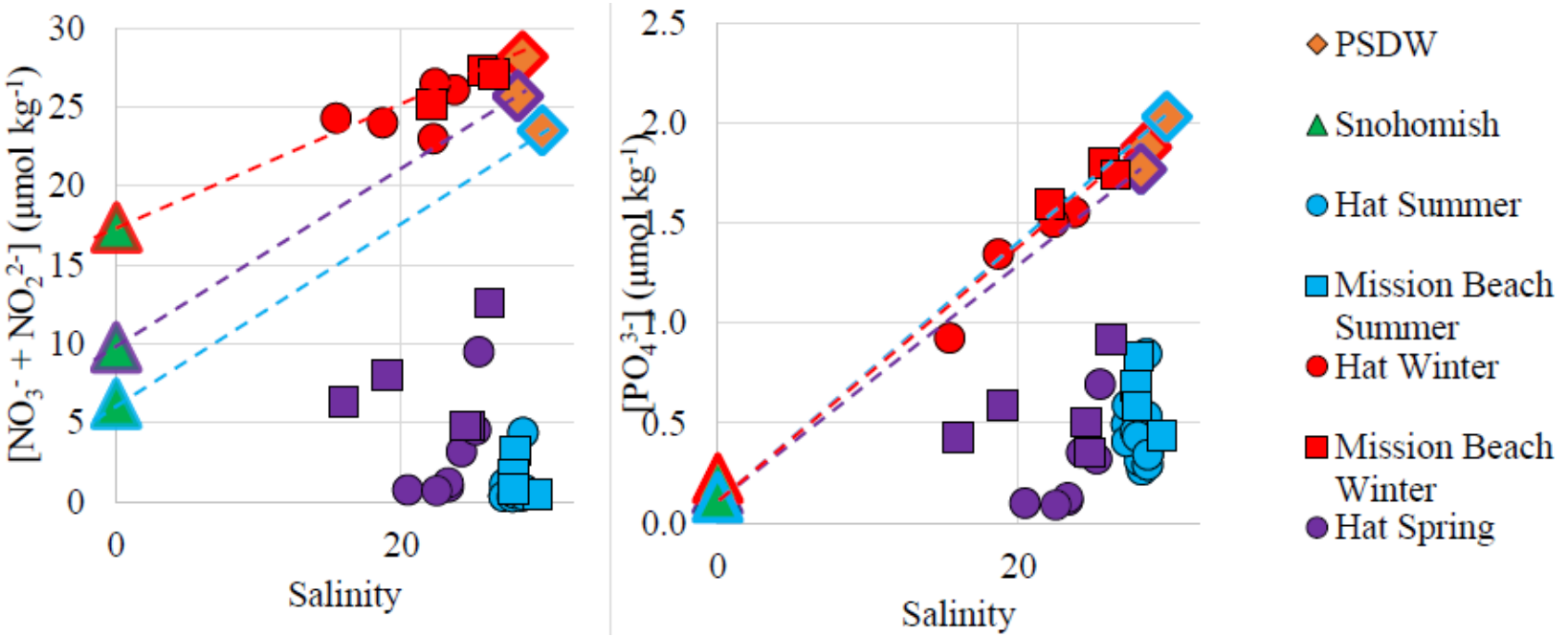

Figure 3.3. Property-property plots of observed salinity versus observed a).nitrate plus nitrite, and b). phosphate in the Hat Island and Mission Beach seagrass sites. Dashed lines represent conservative mixing lines between marine (PSDW) and riverine (Snohomish River) end-members for summer (blue), winter (red), and spring (purple).

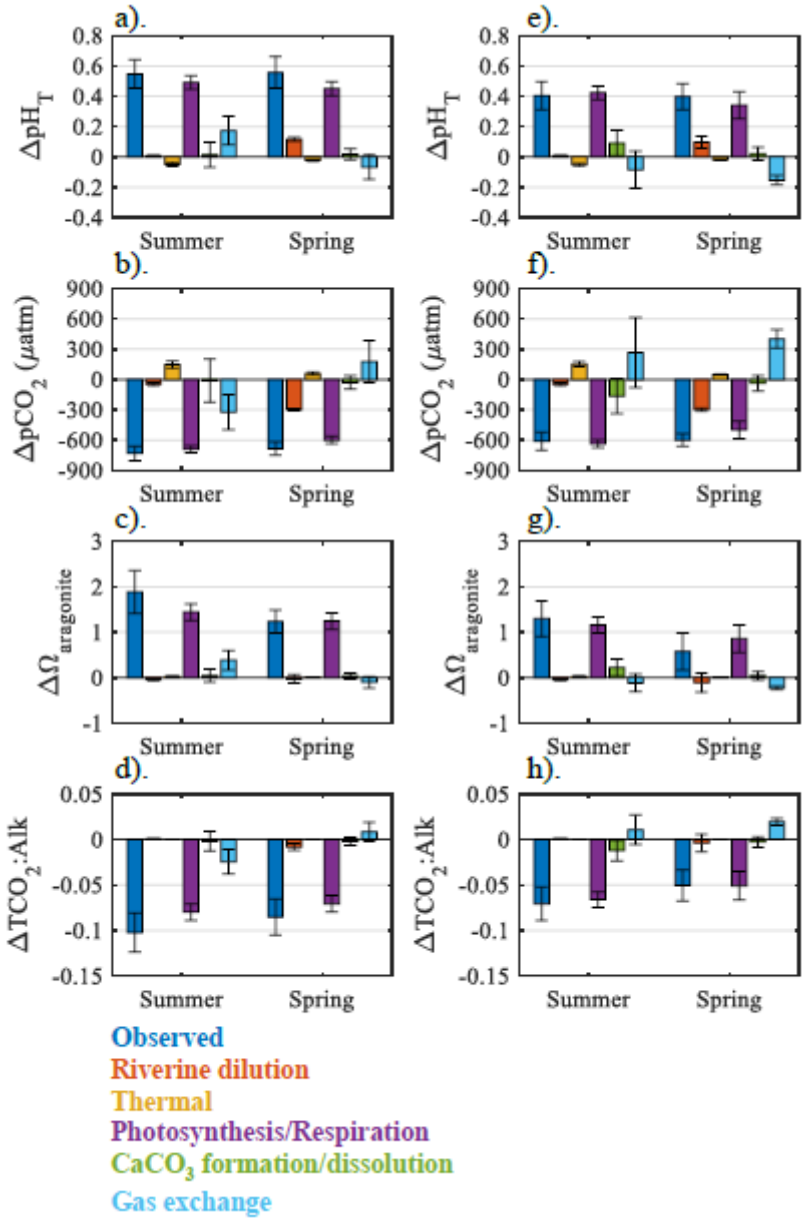

Figure 3.4. Bar graphs quantifying the role of the modeled mechanistic drivers of carbonate chemistry in the Hat Island (a-d) and Mission Beach (e-g) seagrass sites in the summer and spring seasons. Magnitudes represent the effect of each driver in observations made in the seagrass habitats, quantified as the departure from PSDW source water carbonate chemistry. Values are averages +/- one standard deviation.

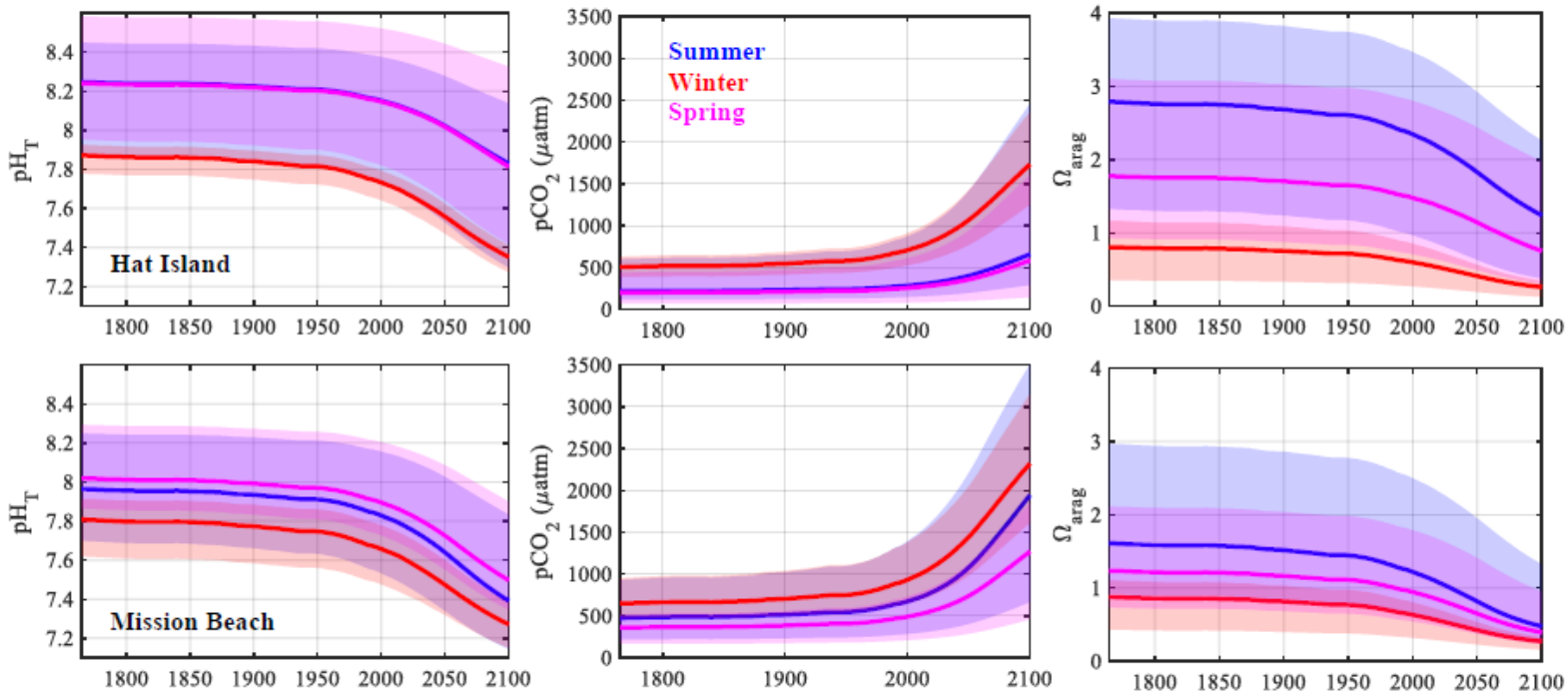

Figure 3.5. Results of yearly OA simulation models from 1765-2100 for Hat Island (a-c) and Mission beach (d-f). Results are partitioned by season. Lines represent seasonal medians of each year, with shaded regions representing 90% interquantile ranges.

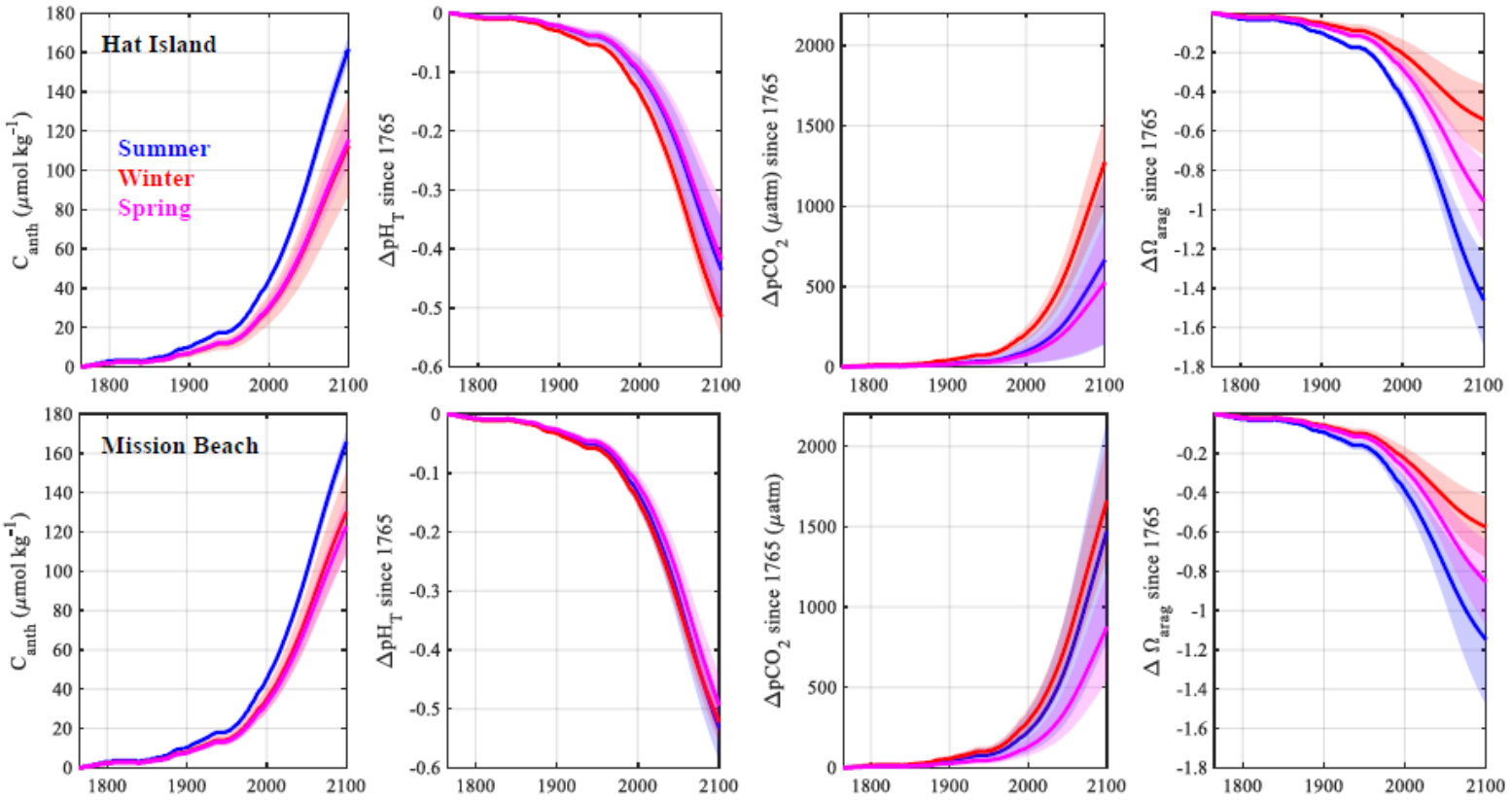

Figure 3.6. Simulated changes in C_{anth}, pH_T, pCO_2, and Ω_{arag} for both seagrass sites since 1765, separated into summer, winter, and spring seasons. Lines represent seasonal average changes of each year, with shaded regions representing +/- one standard deviation.

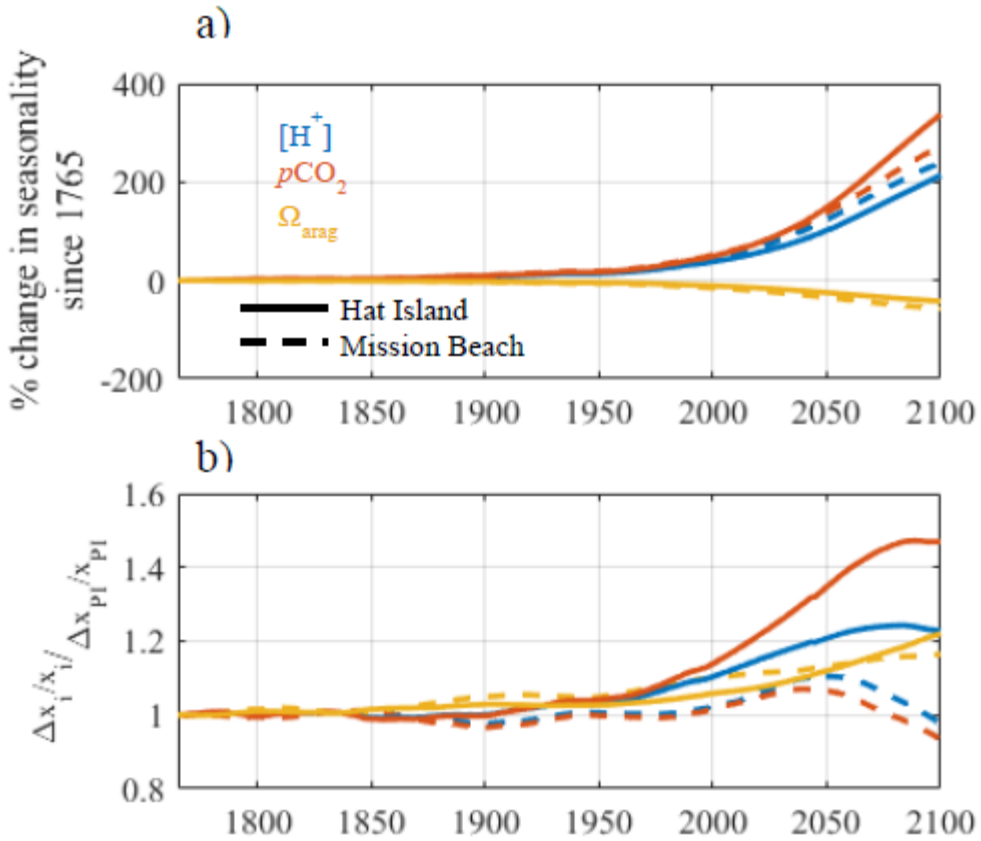

Figure 3.7. a). Annual percent change in seasonal variability of carbonate system parameters since 1765. Seasonal variability is defined as the absolute value of 7-day smoothed summer minus winter conditions (e.g., maximum summer pH – minimum winter pH). Hat Island parameters indicated by solid lines; Mission Beach parameters indicated by dashed lines. **b).** Changes in relative seasonalities of carbonate system parameters since 1765. See Section 3.3 for explanation of calculations.

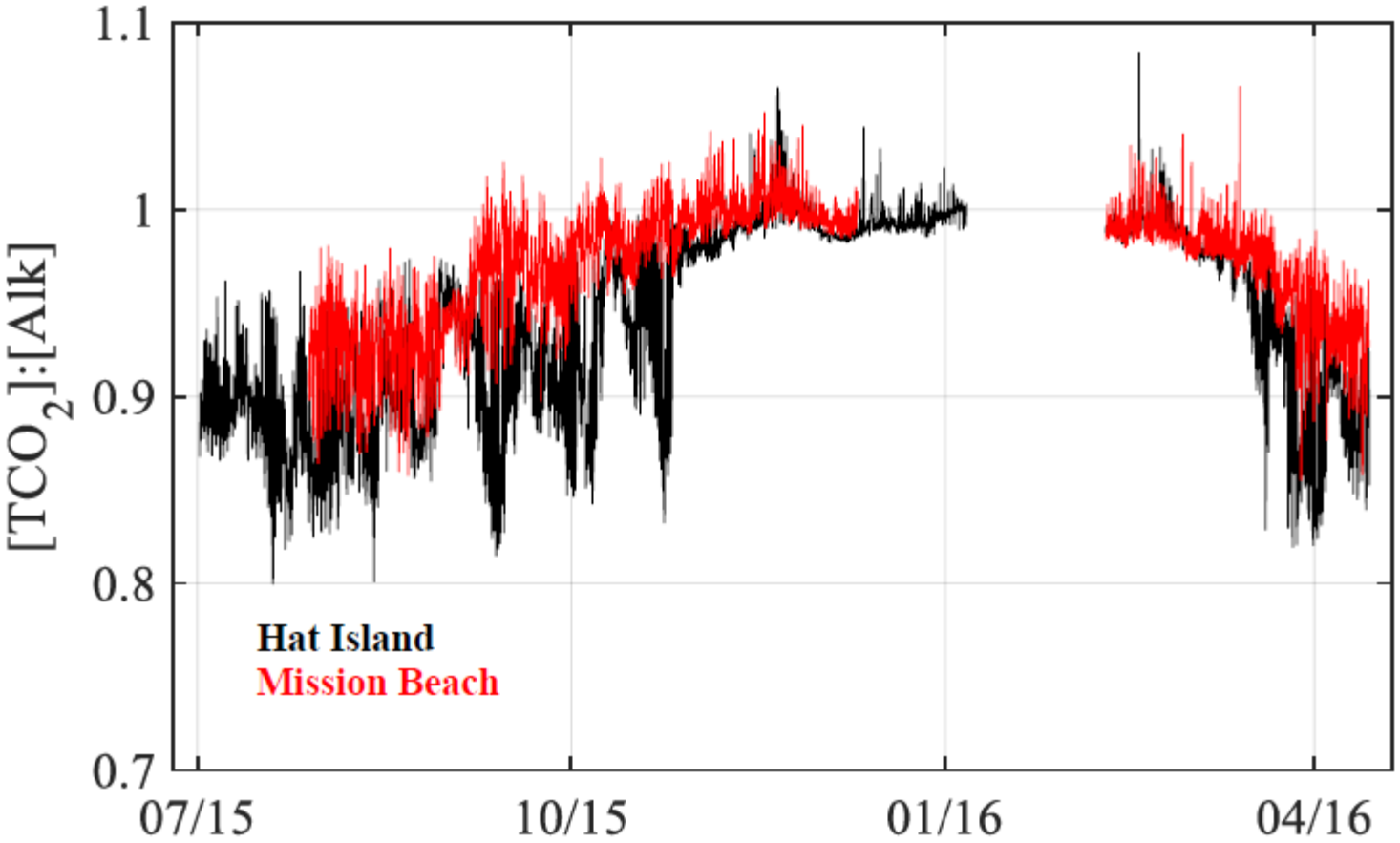

Figure 3.8. Time series of ratios of TCO_2:Alk for the Hat Island and Mission Beach sites for the period of observation (July 2015-April 2016).

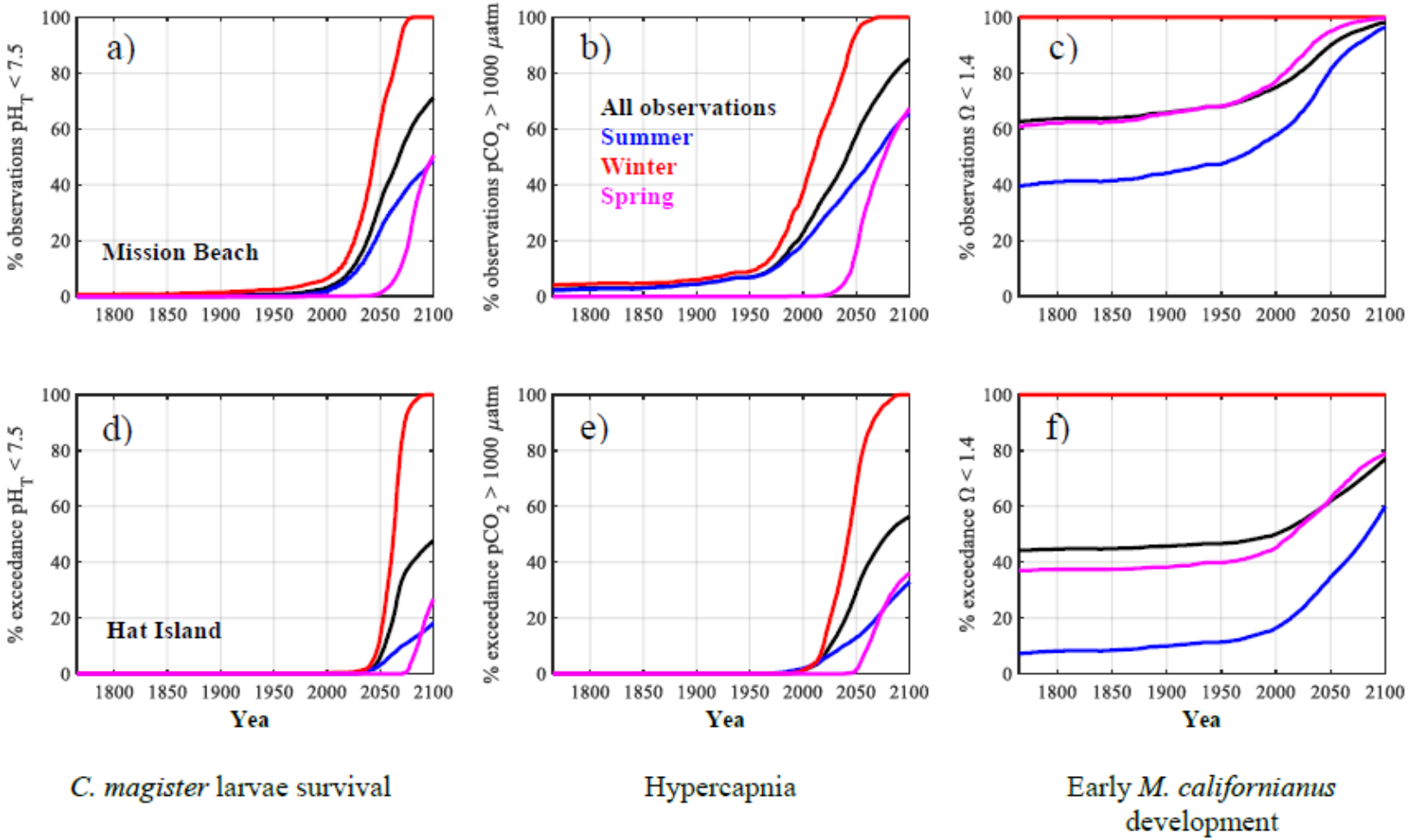

Figure 3.9. Annual and seasonal percent exceedances of physiological thresholds for pH_T (a, d), pCO_2 (b, e), and Ω_{arag} (c, f) at Mission Beach (a-c) and Hat Island (d-f) from 1765-2100. Threshold values of parameters from text.

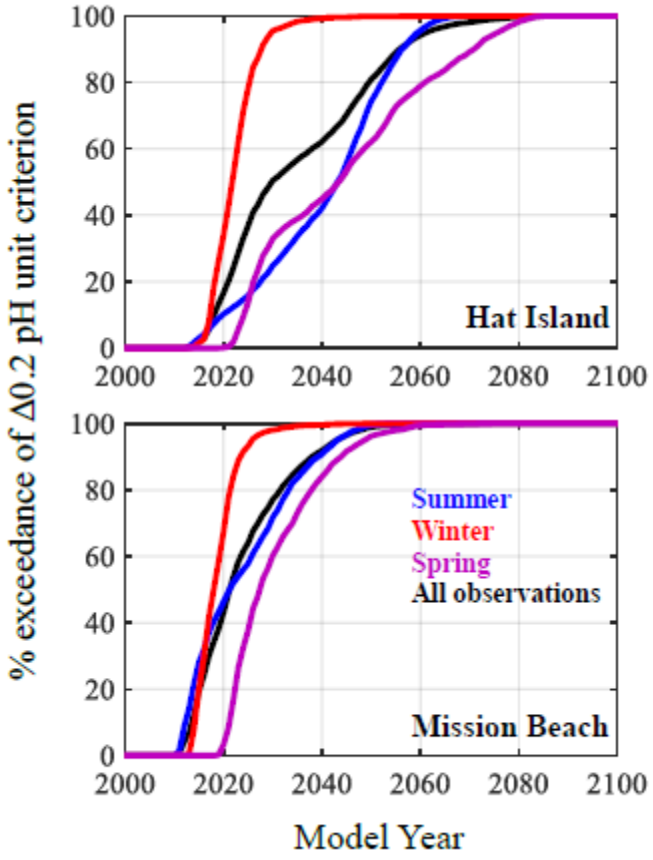

Figure 3.10. Annual and seasonal percent exceedances of Δ0.2 pH unit threshold for Hat Island (a) and Mission Beach (b) from 2000-2100.

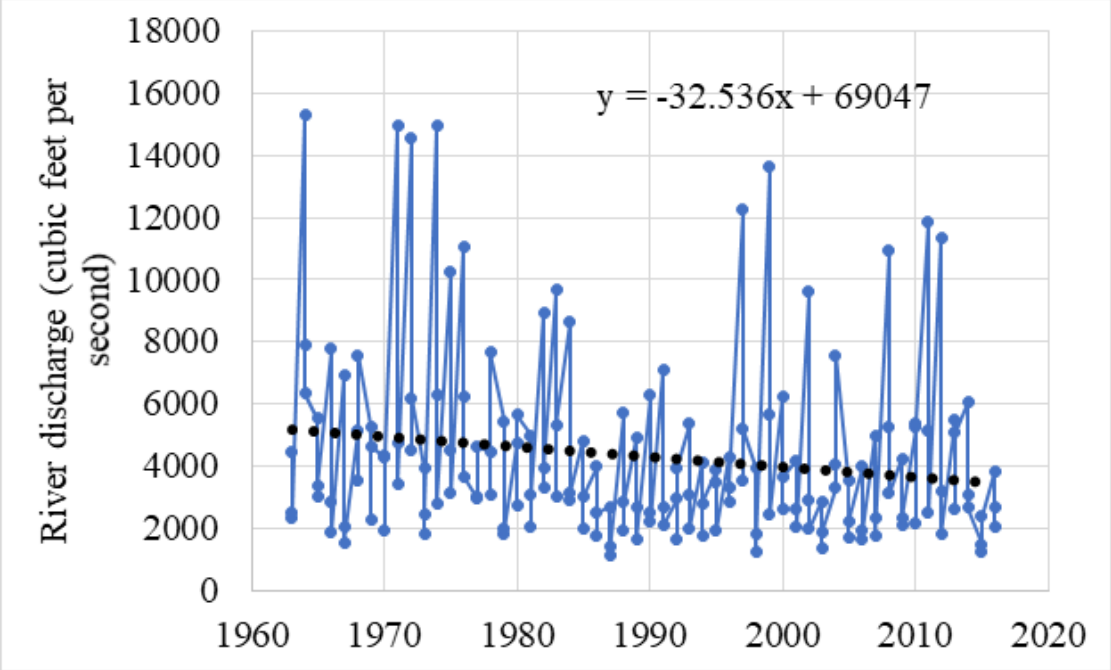

Figure S3.1. Monthly average July, August, and September discharge for the Snohomish River from 1963-2015. Data from USGS station 12150800 (https://waterdata.usgs.gov/nwis/uv?site_no=12150800).

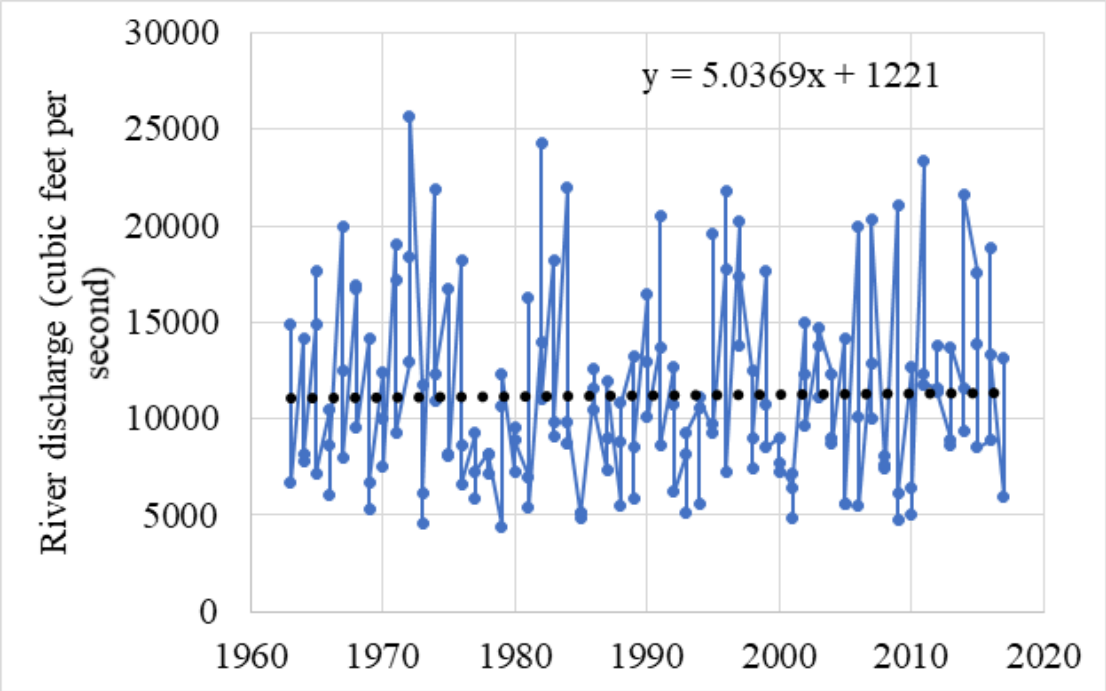

Figure S3.2. Monthly average January, February, and March discharge for the Snohomish River from 1963-2015. Data from USGS station 12150800 (https://waterdata.usgs.gov/nwis/uv?site_no=12150800).

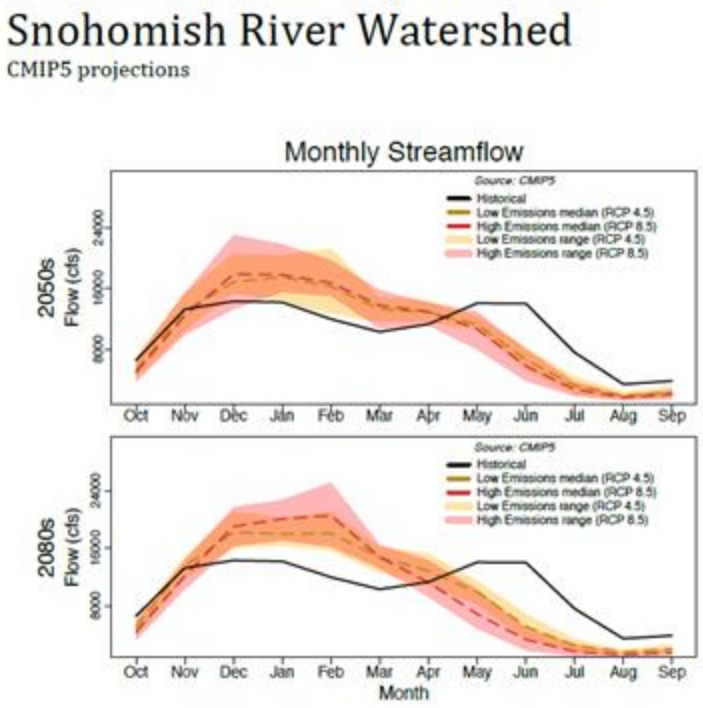

Figure S3.3. Monthly average Snohomish River discharge scenarios used to calculate future (~2100) changes in dry season and wet season discharge from historic conditions. Figure from Mauger et al., 2015.

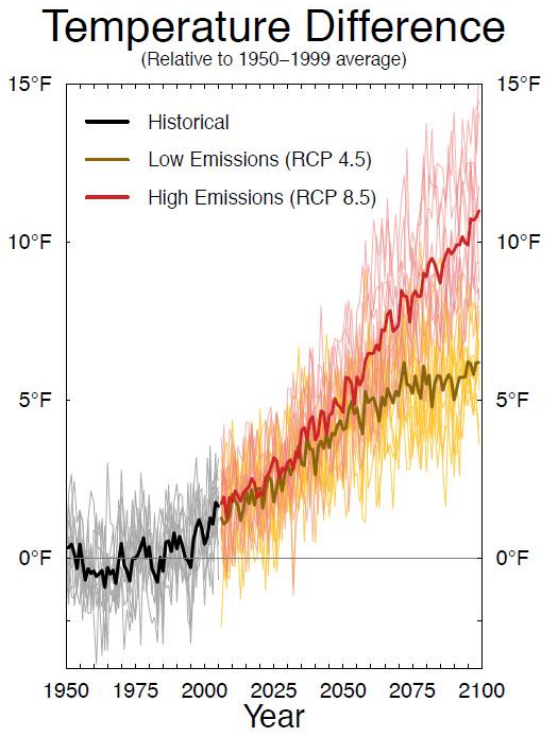

Figure S3.4. Projections of air temperature changes for the Puget Sound region. Figure from Mauger et al., 2015.

Table 3.1. Summary statistics of observations for the Hat Island and Mission Beach study sites during 2015-2016. Values indicated are mean (standard deviation). Ranges are observed minimum-observed maximum.

	Annual		**Summer**		**Winter**		**Spring**	
	Hat Island	Mission Beach	Hat Island	Mission Beach	Hat Island	Mission Beach	Hat Island	Mission Beach
pH_T	7.95 (0.26)	7.76 (0.20)	8.07 (0.20)	7.79 (0.20)	7.68 (0.05)	7.61 (0.09)	8.10 (0.24)	7.89 (0.16)
pH_T range	7.33-8.60	7.26-8.49	7.51-8.48	7.32-8.30	7.33-7.85	7.26-7.79	7.72-8.60	7.41-8.49
O_2 (µmol kg-1)	282 (52.8)	222 (48.3)	277 (57.8)	197 (43.3)	266 (34.1)	223 (35.2)	328 (41.9)	273 (29.9)
O_2 range (µmol kg-1)	118-465	75.0-378	118-465	75.0-356	149-360	110-328	245-462	185-378
Salinity	24.94 (4.00)	26.38 (3.04)	27.91 (0.94)	28.62 (0.74)	21.93 (4.33)	24.73 (3.15)	22.61 (2.28)	23.88 (2.45)
Salinity Range	3.15-29.90	2.61-30.00	23.71-29.90	24.71-30.00	3.15-29.44	8.09-29.41	10.87-28.13	2.61-27.60
Temperature (°C)	12.18 (3.08)	12.14 (2.46)	14.98 (1.45)	14.43 (1.15)	9.33 (1.67)	10.38 (1.34)	10.03 (0.98)	9.69 (0.71)
Temperature Range (°C)	3.83-20.19	7.18-19.72	12.15-20.19	12.74-19.72	3.83-12.84	7.18-12.87	7.94-13.40	7.85-12.44
$\Omega_{aragonite}$	1.47 (0.94)	0.99 (0.53)	2.13 (0.76)	1.26 (0.57)	0.54 (0.16)	0.55 (0.13)	1.48 (0.69)	0.99 (0.38)
$\Omega_{aragonite}$ range	0.02-4.36	0.02-3.25	0.59-4.36	0.39-3.25	0.02-0.95	0.08-0.81	0.38-3.17	0.02-2.46
pCO_2 (µatm)	527 (285)	829 (374)	403 (250)	823 (398)	797 (129)	1,061 (265)	341 (199)	530 (185)
pCO_2 range (µatm)	61-1,430	94-2,425	106-1,430	192-2,320	437-1,378	599-2,425	61-804	94-1,173

Table 3.2. Changes to carbonate system parameters since 1765 from results of the OA simulation models for both seagrass study sites. Values displayed are mean (standard deviation).

		Summer		**Winter**		**Spring**	
		Change in 2015	Change in 2100	Change in 2015	Change in 2100	Change in 2015	Change in 2100
Hat Island	C_{anth}	+57 (2.3)	+162 (6.5)	+38 (9.7)	+113 (25)	+39 (5)	+115 (13)
	pH_T	-0.133 (0.030)	-0.435 (0.087)	-0.178 (0.013)	-0.516 (0.032)	-0.128 (0.033)	-0.418 (0.097)
	pCO_2	+132 (105)	+666 (525)	+282 (62)	+1,274 (282)	+106 (75)	+527 (379)
	Ω_{arag}	-0.55 (0.05)	-1.46 (0.23)	-0.26 (0.09)	-0.54 (0.18)	-0.36 (0.06)	-0.96 (0.21)
Mission Beach	C_{anth}	+58 (1.9)	+166 (5.4)	+45 (7.8)	+130 (20)	+42 (5.4)	+123 (14)
	pH_T	-0.174 (0.030)	-0.533 (0.053)	-0.189 (0.01)	-0.522 (0.035)	-0.155 (0.023)	-0.494 (0.050)
	pCO_2	+308 (174)	+1,472 (683)	+393 (106)	+1,660 (360)	+177 (74)	+876 (335)
	Ω_{arag}	-0.49 (0.09)	-1.15 (0.33)	-0.28 (0.07)	-0.57 (0.15)	-0.35 (0.07)	-0.85 (0.21)

Table 3.3. Estimated changes to current and future carbonate system parameters driven by altered river discharge, warming temperatures, and increasing C_{anth}. Values displayed are average seasonal changes. See Supplementary Material for additional information on assumptions.

		Summer						Winter					
		Hat Island			Mission Beach			Hat Island			Mission Beach		
		ΔpH	**ΔpCO_2**	**ΔΩ_{arag}**	**ΔpH**	**ΔpCO_2**	**ΔΩ_{arag}**	**ΔpH**	**ΔpCO_2**	**ΔΩ_{arag}**	**ΔpH**	**ΔpCO_2**	**ΔΩ_{arag}**
1765→ 2015	**Δ River discharge**	-0.013	+14	+0.04	-0.002	+9	+0.03	-0.002	+0	-0.01	-0.001	+0	-0.00
	Δ Temperature	-0.015	+16	+0.01	-0.014	+31	+0.01	-0.014	+31	+0.01	-0.014	+40	+0.01
	Δ C_{anth}	-0.133	+132	-0.55	-0.174	+308	-0.49	-0.178	+282	-0.26	-0.189	+393	-0.28
2015→ 2100	**Δ River discharge**	-0.012	+15	+0.04	-0.002	+9	+0.03	-0.053	+24	-0.13	-0.029	+14	-0.08
	Δ Temperature	-0.074	+89	+0.07	-0.070	+170	+0.05	-0.068	+168	+0.03	-0.066	+216	+0.03
	Δ C_{anth}	-0.302	+534	-0.91	-0.533	+1,472	-1.15	-0.338	+992	-0.29	-0.522	+1,660	-0.57

OCEANIC AND WATERSHED CONTROLS OF COASTAL ACIDIFICATION IN A SMALL, AGRICULTURALLY DEVELOPED CALIFORNIA CURRENT ESTUARY

Stephen R. Pacella[a,b], Cheryl A. Brown[a], James E. Kaldy[a], Rochelle G. Labiosa[c], Burke Hales[b], T Chris Mochon Collura[a], Hilmar A. Stecher[a], and George G. Waldbusser[b]

[a]Western Ecology Division, National Health and Environmental Effects Research Laboratory, Office of Research and Development, United States Environmental Protection Agency, Newport, OR 97365

[b]College of Earth, Ocean, and Atmospheric Sciences, Oregon State University, Corvallis, OR 97331

[c]Region 10, United States Environmental Protection Agency, Seattle, WA 98101

In preparation for submission to: *Limnology & Oceanography*

4. Oceanic and watershed controls of coastal acidification in a small, agriculturally developed California Current estuary

4.1 Abstract

This study characterized the seasonal CO_2 system dynamics of Tillamook Estuary, OR (USA), a small open-coast estuary in the northern California Current Large Marine Ecosystem subject to coastal upwelling and river discharge from an agriculturally-developed watershed. From July 2017 through July 2018, we conducted a series of sampling cruises to characterize the CO_2 biogeochemistry of the estuary as well as the coastal ocean and watershed end-members. We quantified the roles of allochthonous input of oceanic and riverine dissolved inorganic carbon (DIC), as well as internal bay carbon cycling, in controlling the seasonal pH, $CaCO_3$ saturation state, and pCO_2 dynamics of the estuary. Variability in the ocean and watershed end-members was the primary control on CO_2 chemistry of the estuary, with internal bay processes acting as a seasonally variable sink and source of DIC. Observed watershed DIC enrichments in areas of increased agricultural activity were hypothesized to be driven by human land use change. These watershed DIC enrichments were combined with published estimates of oceanic anthropogenic carbon burdens to estimate the magnitude and timing of human changes to present-day CO_2 chemistry in the estuary. We estimate that most of the human-caused perturbation in estuarine chemistry during our study period was due to ocean acidification-driven changes in the coastal ocean waters. We discuss how

attribution of changes in CO_2 chemistry to ocean, bay, and watershed drivers informs the potential efficacy of management actions operating at local versus global scales.

4.2 Introduction

Coastal acidification is broadly defined as the lowering of pH in coastal ocean and estuarine waters resulting from human activities, including fossil fuel combustion, land use change, and eutrophication (e.g. Kelly et al., 2011). The concentration of these human activities in the coastal zone, and their resultant interacting effects on coastal carbonate chemistry, sets coastal acidification dynamics apart from purely atmospheric CO_2 emissions-driven ocean acidification. The interaction of these processes in the coastal zone can amplify pH changes (e.g. Cai *et al.*, 2011; Hu and Cai, 2013b; Waldbusser *et al.*, 2011) in a synergistic manner due to the thermodynamics of the marine carbonate system (Egleston *et al.*, 2010), resulting in acidification rates which outpace those of the open ocean (Provoost *et al.*, 2010; Carstensen *et al.*, 2018). Water quality impacts (defined here as alterations of pH_T, $CaCO_3$ saturation states (Ω_{arag}), and pCO_2) due to coastal acidification have been studied in a variety of coastal systems, including the Chesapeake Bay (Waldbusser *et al.*, 2011; Cai *et al.*, 2017), the Gulf of Mexico (Cai *et al.*, 2011; Laurent *et al.*, 2018), the northeast coast of the United States (Wallace *et al.*, 2014), western European coasts (Borges and Gypens, 2010; Hagens *et al.*, 2015), and recently in a northern California Current estuary (Hales et al., 2017). These changes in water quality have been shown to impair the fitness of coastal species through a variety of physiological and behavioral mechanisms (e.g. Gazeau *et al.*, 2013;

Busch and McElhany, 2016), negatively impact commercial fisheries of the California Current (Barton *et al.*, 2015), and are hypothesized to alter the structure and function of coastal food webs (Ainsworth *et al.*, 2011; Busch *et al.*, 2013; Marshall *et al.*, 2017).

The documented and projected impacts of coastal acidification have inspired research to attribute changes in coastal water quality to the multiple anthropogenic stressors (Kelly *et al.*, 2011) in these systems. There is a growing number of studies exploring mechanisms controlling CO_2 chemistry in coastal and estuarine environments, including the role of oceanic and watershed forcings (e.g. Hu *et al.*, 2017; Reimer *et al.*, 2017; Xue *et al.*, 2017). In addition to the role of global atmospheric CO_2 increases in acidifying oceanic waters, recent papers have discussed the importance of watershed delivery of alkalinity and inorganic carbon (and the ratio between these levels) in modulating coastal pH_T and $CaCO_3$ saturation states (Joesoef *et al.*, 2017; Moore-Maley *et al.*, 2018). The human modification of carbon (both organic and inorganic) and nutrient transport from land to sea is well-established (Regnier *et al.*, 2013), but how this affects coastal acidification dynamics is less clear. Research to date has shown disparate effects on coastal biogeochemistry, where altered watershed delivery of carbon and nutrients can lead to enhanced coastal acidification (e.g. Cai *et al.*, 2011; Laurent *et al.*, 2018), but also long-term coastal basification due to enhanced riverine alkalinity delivery and primary production (Borges and Gypens, 2010; Duarte *et al.*, 2013). Therefore, impacts of anthropogenically-altered watershed chemistry on coastal acidification dynamics appear to be system-specific. This lack of generality poses challenges for predicting how urbanization, agricultural activities, and other human land use changes

known to alter watershed chemistry are likely to interact with acidified ocean waters in coastal and estuarine habitats.

Creating effective management strategies, policies, and understanding decision tradeoffs for addressing coastal acidification will therefore require system-specific attribution of drivers controlling acidification dynamics, as well the spatial and temporal variability of those drivers. Attribution of the drivers of acidification allows management actions to be tailored to most efficiently target the primary drivers of water quality degradation. A rigorous understanding of the anthropogenic drivers of coastal acidification in both space and time will also help to inform the nature of the system response to potential management actions: i.e., what are the magnitude, duration, and frequency of change in water quality endpoints (e.g. pH_T) for a given management action, and what is the spatial "footprint" of efficacy of that management action? Attribution research thereby improves our fundamental understanding of carbon cycling in coastal and estuarine environments, as well as provides timely and necessary information for managers and policymakers addressing coastal acidification (Strong *et al.*, 2014).

The Pacific Northwest (PNW) region of the United States has been a focus of coastal acidification research activity due to its location in the northern California Current Large Marine Ecosystem and exposure to seasonal upwelling of naturally high CO_2 waters, as well as documented OA impacts on coastal resources (Barton *et al.*, 2015). The coastal ocean in the PNW is known to be highly productive and supports large commercial and recreational fisheries (Marshall *et al.*, 2017), but is also especially sensitive to ocean acidification (Feely *et al.*, 2018) and is rapidly acidifying (Feely *et al.*, 2016; Chan *et al.*, 2017) with rising atmospheric CO_2 levels. While there has been a

large effort to establish high-quality CO_2 monitoring stations in this region (Fassbender *et al.*, 2018), to our knowledge there has been no analysis of long-term CO_2 system dynamics in PNW estuaries outside of the Salish Sea (but see Hales *et al.*, 2017). This lack of long-term data records makes it difficult to quantify how changes in ocean and watershed conditions have impacted estuarine CO_2 chemistry in the region. There has been extensive study of how coastal ocean conditions of the California Current have been altered by ocean acidification (e.g. Feely *et al.*, 2008, 2016; Gruber *et al.*, 2012; Sutton *et al.*, 2016; Chan *et al.*, 2017), with general agreement that surface waters are accumulating anthropogenic carbon with concomitant decreasing pH_T and $CaCO_3$ mineral saturation states. These changes to CO_2 chemistry have been widely implicated in recent difficulties associated with shellfish aquaculture in the PNW (Barton *et al.*, 2012; Barton *et al.*, 2015), highlighting the urgency of the issue to regional stakeholders (Mabardy *et al.*, 2015). In contrast to our relatively advanced understanding of ocean acidification in the California Current, limited information is available on how urban development and land use change in coastal watersheds have altered the inorganic carbon composition of rivers discharging to PNW estuaries. However, previous studies have shown that urban and agricultural development can enhance delivery of dissolved inorganic carbon (DIC) and alkalinity (Alk) through metabolic and enhanced weathering processes in temperate watersheds of the United States (Barnes and Raymond, 2009; Oh and Raymond, 2006) and Europe (Perrin *et al.*, 2008). These observed DIC and Alk enrichments suggest the need for research to investigate if similar enrichments are characteristics of developed coastal watersheds, as well as how these enrichments interact with upwelled high CO_2 waters in estuaries of the California Current. Improving our understanding of these ocean

– watershed interactions would likely lead to more robust forecasting of estuarine responses to watershed and upwelling forcings in the face of climate change, growing coastal populations, and land use change.

This study characterized the seasonal carbonate system dynamics in Tillamook Estuary, OR, USA, a small open-coast estuary in the northern California Current Large Marine Ecosystem, subject to coastal upwelling and river discharge from an agriculturally-developed watershed. From July 2017 – July 2018, we conducted ten cruises in the bay, with concurrent sampling of the five rivers entering the bay, to quantify the carbonate biogeochemistry dynamics of Tillamook Estuary. The bay has a large tidal prism (Colbert and McManus, 2003) and receives riverine discharges from watersheds which have been modified by human land use primarily for dairy farming (Shanks *et al.*, 2006). Tillamook Estuary is also home to commercial shellfish aquaculture operations (Tillamook Estuaries Partnership, 2015) and is considered an "estuary of national significance" as part of the US Environmental Protection Agency's National Estuary Program. Our primary goal was to quantify the roles of allochthonous input of oceanic and riverine dissolved inorganic carbon, as well as autochthonous bay carbon cycling, in controlling the seasonal variations of carbonate chemistry in the estuary. We estimated how local carbon cycling within the bay drives departures of estuarine pH_T, pCO_2, and Ω_{arag} from conservative mixing between the coastal ocean and river end members. Previously published estimates of oceanic anthropogenic carbon burdens (driven by ocean acidification) were combined with observed watershed DIC and Alk enrichments, hypothesized to be driven by human land use change, to quantify the magnitude and timing of changes to the carbonate chemistry in Tillamook Bay since pre-

industrial times. We discuss how attribution of changes in estuarine CO_2 chemistry to ocean and watershed drivers informs the potential efficacy of management actions operating at local versus global scales.

4.3 Methods

4.3.1 Study site

Tillamook Estuary is a shallow (~2 m average depth), relatively small (34 km^2) drowned river mouth estuary on the coast of Oregon, USA. There is close connection between the estuary and coastal ocean due to strong tidal forcing (mean tidal volume is 1.23×10^8 m^3 d^{-1}; http://ian.umces.edu/neea/siteinformation.php), with semi-diurnal tides averaging 1.7 m in range (Colbert and McManus, 2003). The estuary receives coastal ocean waters subject to seasonal upwelling typical of the California Current system, with summers characterized by delivery of high CO_2, high nutrient, low pH, low dissolved oxygen oceanic waters (Feely *et al.*, 2003). There are five rivers draining into the bay: the Miami, Kilchis, Wilson, Trask, and Tillamook rivers in order from north to south (Figure 1). Their combined annual average discharge is $\sim 7.6 \times 10^6$ m^3 d^{-1}, with maximal discharge during the winter wet season (November – March; $\sim 1.71 \times 10^7$ m^3 d^{-1}) and minimum discharges during the summer dry season (June – September; $\sim 7.82 \times 10^5$ m^3 d^{-1}). The watersheds of all five rivers lie in the Oregon Coast Range and drain similar geologic features consisting of Tertiary marine sediments and volcanic rocks (Komar *et al.*, 2004). The watersheds are subject to human activities via managed forest lands and commercial timber harvest in the upper watersheds, and agricultural activity consisting primarily of dairy farming in the lower watersheds. The 2011 Multi-Resolution Land

Characteristics land cover (MRLC) layer for the conterminous United States as modified in 2014 was used to provide a summary of land cover within the sub-watersheds of each of the five rivers in the Tillamook Estuary watershed (Homer *et al.*, 2015; https://www.mrlc.gov/nlcd2011.php). As a whole, land cover within the Tillamook Estuary watershed are classified as 2% open water, 7% developed, 70% forest, 16% shrub/scrub and grassland/herbaceous, 3% pasture/hay, <1% cultivated crops, and 3% wetlands. The relative area of pasture/hay land use in the Tillamook watershed (which captures livestock grazing areas) is ~500% of the average for US west coast estuarine systems. Most of the agricultural and urban areas are within the lower watersheds of the Wilson, Kilchis, Trask, and Tillamook Rivers, while the Miami River watershed contains relatively little agricultural land cover and is primarily forested. The bay has a single jettied ocean inlet at its northwest corner, with the majority of river discharge (Kilchis, Wilson, Trask, and Tillamook) enters the bay's southeastern portion. This sets up a dominant counterclockwise flow in the bay, with oceanic waters flooding through the western portion of the bay, while the riverine discharge primarily travels northward along the eastern side of the bay and exits at the single northwestern inlet (Komar *et al.*, 2004). Seasonal changes in river discharge to the bay (winter maximum and summer minimum discharges) creates a two-layer stratified system during the winter period, and a well-mixed system during the summer (Burt and McAllister, 1958). Freshwater flushing times for the bay have been estimated to vary from a few days during the wet season with high river discharges, to approximately one month during the dry season with low river discharge (Colbert and McManus, 2003). The bay is known for its recreational and commercial shellfish harvesting, with Oregon's largest commercial Pacific Oyster

(*Crassostrea gigas*) production by area and value, yielding >54,000 bushels and a value of nearly $2M in 2017 (Oregon Department of Agriculture). The bay is also recognized for being important native salmon and steelhead habitat (Tillamook Estuaries Partnership, 2015). The Tillamook Bay watershed has a history of bacterial contamination and hypoxia issues resulting from a combination of wastewater treatment plant discharge, agricultural runoff, septic system discharge, and direct animal inputs (Sullivan *et al.*, 2005). As a result, shellfish harvesting is restricted to the northern portion of the bay and is periodically closed during periods of high precipitation and river discharge (Tillamook Estuaries Partnership, 2015).

4.3.2 Water quality survey cruises

Ten sampling cruises were conducted in Tillamook Estuary approximately monthly from July 2017 through July 2018 and occupied nine bay stations (Fig. 4.1), including a "marine" station at the inlet which targeted incoming coastal ocean waters on flood tides. The marine station (station "M") was used as the coastal ocean end-member for all analyses. Concurrent with the bay cruises, an additional land-based team collected water samples from the five river systems entering Tillamook Bay at both "upriver" stations above major agricultural influences, and "downriver" stations shortly before the rivers entered the bay (Fig. 4.1). The upriver sampling stations were in forested sections of the watersheds, with minimal human urban and agricultural influence upstream of these sites. The upstream station of the Tillamook River was likely influenced by some urban/agricultural development, but sampling further upstream was unfortunately not feasible due to the highly branched nature of the upriver streams which form the river.

Downriver sampling stations were located in areas of urban and agricultural land use, and the locations were chosen to be as far downstream the rivers as possible while still being able to sample all stations in a single day without tidal salt intrusion. The Miami River was sampled only at a single downriver station, as the river's watershed is primarily forested and previous pilot work had shown minimal downriver gradients in water chemistry. All downstream sites were tidally influenced with salt intrusion at high tide, but were always sampled during low tides with no salt influence (salinities were always <0.02).

Water samples at all stations were collected with Niskin (bay stations) or Van-Dorn (river stations) gas-tight water sampling devices. Water was sampled from ~1 m depth at all bay stations except for the marine station, which was sampled at ~5-m depth and always below any observed surface stratification. At each station, sample water for CO_2 analysis was transferred to triplicate 330-mL amber glass bottles using best-practices for dissolved gas sampling (Riebesell *et al.*, 2010), immediately poisoned with 30-µL of a saturated mercuric chloride solution, and sealed with urethane-lined crimp sealed metal caps (see Hales *et al.*, 2017 for a discussion of the storage and preservation techniques). Water for inorganic nutrient (NO_3 + NO_2, NH_4, PO_4) analyses was filtered through a pre-rinsed 0.4µm capsule filter, collected in triplicate polyethylene centrifuge tubes, stored on ice in the field, and frozen within 12 hours of collection. A YSI 6000 series sonde was used to measure *in-situ* salinity, temperature, pH_{NBS}, dissolved oxygen, and chlorophyll of the sample waters. Inorganic nutrient analyses were colorimetrically determined by flow injection analysis at the Marine Chemistry Laboratory at the University of Washington, WA, USA. Analysis of paired pCO_2 and DIC for water samples was

conducted at Oregon State University in the laboratory of Burke Hales using non-dispersive infra-red absorption, as described by (Hales *et al.*, 2004; Bandstra *et al.*, 2006). The full carbonate system (including alkalinity (Alk), pH_T and Ω_{arag}) was calculated utilizing these paired pCO_2 and DIC measurements, along with *in-situ* salinity and temperature following procedures outlined in Hales et al., 2017. We used the CO_2SYS program (Matlab version 1.1), K_1 and K_2 constants of Millero *et al.*, 2010, K_{SO4} constants of Dickson, 1990, and the borate:salinity relationship of Lee *et al.*, 2010 for the carbonate system calculations. To account for the acidic effect of the mercuric chloride preservative, a +27.3 ueq kg^{-1} correction factor was applied to the Alk of samples with salinity <10, and then this corrected Alk and the measured DIC were combined to recalculate the *in-situ* conditions. This corresponded to the amount of $HgCl_2$ that was added to each bottle during poisoning, assuming an $HgCl_2$ solubility of 7.4 g/100 mL and complete reaction of Hg^{2+} with H_2O to give $HgOH^+$ and H^+.

4.3.3 Calculating departures from conservative behavior of Tillamook Estuary biogeochemistry

For each cruise, we calculated departures from conservative mixing of DIC, Alk, DIN (dissolved inorganic nitrogen, $NO_3 + NO_2 + NH_4$), and PO_4 at each bay station. The ocean end member was assumed to be represented by flood tide waters sampled at our marine station on each cruise. Flow-weighted average river DIC, Alk, DIN, and PO_4 end members were calculated for each cruise using observations from the downriver stations, following the technique used by Colbert and McManus 2003. The

fraction of total river discharge contributed by each river (e.g. f_{Trask} for the Trask River) was found by:

$$f_{Trask} = Q_{Trask}/Q_{Total}$$

where Q_{Trask} is the mean daily river discharge for a given month of the Trask River, and Q_{total} is the total average monthly river discharge into Tillamook Bay from all five rivers. Mean daily river discharge for each month of the study was downloaded from the Oregon Water Resources Department Near Real Time Hydrographics Data portal (https://apps.wrd.state.or.us/apps/sw/hydro_near_real_time/). The flow weighted average river end member was then calculated for each chemical constituent (using DIC as an example) as:

$$DIC_{fwa,down} = f_{Miami}*DIC_{Miam} + f_{Wilson}*DIC_{Wilson,down} + f_{Kilchis}*DIC_{Kilchis,down} +$$

$$f_{Trask}*DIC_{Trask,down} + f_{Tillamook}*DIC_{Tillamook,down}$$

where DIC_{fwa} is the flow-weighted average DIC river end member, and $DIC_{Trask,down}$ is the observed DIC from the downriver station. Departures from conservative mixing for bay stations were calculated as:

$$f_{mar} = S_{obs,i}/S_{mar}$$

$$\Delta DIC_i = DIC_{obs,i} – (f_{mar}*DIC_{mar} + (1-f_{mar})*DIC_{fwa})$$

Where f_{mar} is the fraction of marine waters present at the bay station i, $S_{obs,i}$ is the observed salinity at bay station i, S_{mar} is the observed salinity of the marine station, ΔDIC_i is the departure from conservative mixing at bay station i, and $DIC_{obs,i}$ is the observed DIC at bay station i. This same procedure was used to calculate departures from conservative mixing of Alk, DIN, and PO_4.

4.3.4 Garibaldi YSI mooring time series

A mooring was established in July 2017 at the Port of Garibaldi Dock (northern end of Tillamook Bay, station "G" in Fig. 4.1) containing a YSI 6000 series sonde sampling continuously at a 15-minute interval for salinity, temperature, pressure, pH_{NBS}, and dissolved oxygen. The mooring was located ~1.5 m above the benthos and ranged in depth from 1.5 m to 5.9 m depending upon tidal stage. Sondes were replaced approximately every 2 - 4 weeks with a freshly calibrated sonde, and laboratory tests were performed immediately following deployments to quantify instrument drift and identify possible fouling issues. The pH probe was calibrated using NIST standards of pH_{NBS} 7 and 10 following manufacturer recommendations. The pH_{NBS} readings from the sondes were converted to the Total scale (pH_T) using CO2SYS, and all reported mooring observations in this manuscript refer to these converted pH_T values. A bay cruise sampling station "G" was located at the mooring, and calculated pH_T from discrete samples was used as an *in-situ* validation of the sondes' pH_T readings. Root mean squared error between calculated pH_T from discrete bottle samples (using pCO_2 and DIC) and converted YSI pH_T was 0.05 (n = 7).

An alkalinity-salinity regression was used to create an alkalinity time series for the full period of mooring observations and allow for calculation of the full carbonate system, including pCO_2 and Ω_{arag}. The regression (R^2 = 0.986, Root mean square error = 60.5 $\mu eq\ kg^{-1}$) was formed using all discrete bottle samples (n = 80) from the bay cruises with calculated alkalinity from the paired pCO_2 and DIC data:

$$Alk_{sal,i} = 54.5 * Salinity_i + 470$$

where $Salinity_i$ is the observed salinity at the Garibaldi mooring at time point i. The full carbonate system was then calculated using pH_T converted from the YSI data and Alk_{sal} in CO2SYS (Matlab version 1.1). Propagation of the uncertainty in YSI pH_T (0.054, as stated above) and calculated Alk_{sal} results in calculated pCO_2 uncertainties of ~17% and calculated Ω_{arag} uncertainties of ~8% at average mooring conditions (salinity = 27.6, temperature = 11.4, pH_T = 7.89, Alk = 1,967 μeq kg^{-1}).

4.3.5 Calculating watershed and oceanic anthropogenic alterations of bay chemistry

We applied previously published values of ocean C_{anth} and observed watershed DIC and Alk enrichments from this study to estimate present-day human alterations of pH_T, Ω_{arag}, and pCO_2 in Tillamook Bay. Previously published values of oceanic C_{anth} in nearshore waters of the California Current (Feely *et al.*, 2016; Chan *et al.*, 2017) were used to estimate how coastal ocean waters have been altered by ocean acidification. The C_{anth} (Feely *et al.*, 2016) concentrations in coastal ocean waters are known to vary between ~37 μmol kg^{-1} and ~55 μmol kg^{-1} , with the highest values found in surface waters and the lowest values in recently upwelled waters. Freshly upwelled waters contain less C_{anth} due to exposure to and gas exchange with lower past atmospheric CO_2 values at the time of formation and subduction of the water parcel, and insufficient time to gain C_{anth} from exchange with the modern atmosphere. The physical and chemical characteristics of coastal ocean waters entering Tillamook Bay during the July (2017 and 2018) and August cruises suggest these waters were recently upwelled, and so we assume an ocean end-member C_{anth} concentration of 37 μmol C kg^{-1} (Chan *et al.*, 2017), which is a conservative estimate of this perturbation. Fall, winter, and spring cruises were not

during periods of upwelling favorable conditions and we therefore assume an ocean end-member C_{anth} concentration of 55 μmol C kg^{-1}. We calculated the present-day anthropogenic alteration of the ocean end-member carbonate system by subtracting these C_{anth} concentrations from observed DIC concentrations, and assumed no change in Alk.

Maximum anthropogenic changes in watershed delivery of DIC and Alk, are assumed to be bounded by the difference between the flow-weighted averages of upstream and downstream station DIC and Alk concentrations, such that:

$$C_{enrich,riv} = DIC_{fwa,down} - DIC_{fwa,up},$$

$$Alk_{enrich,riv} = Alk_{fwa,down} - Alk_{fwa,up},$$

where $C_{enrich,riv}$ is the magnitude of watershed end-member carbon enrichment in μmol kg^{-1}, $DIC_{fwa,up}$ is the flow-weighted average DIC concentration of the upriver stations, $Alk_{fwa,up}$ is the flow-weighted average Alk concentration of the upriver stations, and $Alk_{enrich,riv}$ is the magnitude of watershed end-member alkalinity enrichment in μmol kg^{-1}. Conservative mixing values of pH_T, Ω_{arag}, and pCO_2 were calculated for the full estuarine salinity spectrum assuming 1) modern C_{anth} concentrations in the ocean end-member and upriver DIC and Alk concentrations ($DIC_{fwa,up}$ and $Alk_{fwa,up}$) for the watershed end-member, 2) Modern C_{anth} concentrations removed from the ocean end-member and downriver DIC and Alk concentrations ($DIC_{fwa,up} + C_{enrich,riv}$ and $Alk_{fwa,up} + Alk_{enrich,riv}$) for the watershed end-member 3) modern C_{anth} concentrations in the ocean end-member and downriver DIC and Alk concentrations ($DIC_{fwa,up} + C_{enrich,riv}$ and $Alk_{fwa,up} + Alk_{enrich,riv}$) for the watershed end-member. pH_T, Ω_{arag}, and pCO_2 were recalculated with the same assumptions for all bay stations using the cruise specific values of watershed $C_{enrich,riv}$ and $Alk_{enrich,riv}$, and oceanic C_{anth}.

While we were able to apply cruise-specific observations of watershed $C_{enrich,riv}$ and $Alk_{enrich,riv}$ to each set of bay cruise observations, the variability of these enrichment values among cruises prevented us from choosing a single representative value for each to apply to the Garibaldi mooring time series. Given the excellent predictability of $C_{enrich,riv}$ and $Alk_{enrich,riv}$ with river discharge and availability of average daily discharge data for the Trask River for the full period of the mooring time series, we calculated a time series of daily $C_{enrich,riv}$ and $Alk_{enrich,riv}$ for the full mooring period (August 2017 – July 2018) based on Trask River discharge. They were calculated using the reported relationships between downriver enrichments and river discharge as:

$$DIC_{enrich,riv,j} = 2{,}192 * Q_{Trask,j}^{-0.5238}$$

$R^2 = 0.91$, root mean square error (RMSE) = 23 μmol kg^{-1} DIC,

$$Alk_{enrich,riv,j} = 3{,}703 * Q_{Trask,j}^{-0.7301}$$

$R^2 = 0.89$, RMSE = 18 μeq kg^{-1} Alk

Where $DIC_{enrich,riv,j}$ and $Alk_{enrich,riv,j}$ are daily flow-weighted average downriver enrichments of DIC and Alk as previously defined with units of μmol kg^{-1}, j is the day of year, and Q_{Trask} is the average daily discharge of the Trask River in cubic feet per second for day j. We then calculated a time series of present-day DIC and Alk perturbations at the Garibaldi mooring (ΔDIC_{anth} and ΔAlk_{anth}, respectively) using the values of daily river and ocean end-member DIC and Alk as:

$$\Delta DIC_{anth,i} = C_{anth} * f_{mar,i} + (1-f_{mar,i}) * DIC_{enrich,riv,j}$$

$$\Delta Alk_{anth,i} = (1-f_{mar,i}) * Alk_{enrich,riv,j}$$

where *i* is a 15-minute frequency mooring observation, *j* is the day of year, $f_{mar,i}$ is the fraction of oceanic water at the Garibaldi mooring at time point *i*. We subtracted

these changes in DIC_{anth} and Alk_{anth} from the calculated mooring time series of observed DIC and Alk (See Methods 2.4) and recalculated pH_T, pCO_2, and Ω_{arag} to estimate how the present-day Garibaldi times series has been altered by anthropogenic DIC and Alk from ocean and watershed sources. We refer to this recalculated time series as the "Pre-Industrial" (PI) conditions (e.g. $pH_{T,PI}$, $pCO_{2,PI}$, and $\Omega_{arag,PI}$) to follow literature conventions, but acknowledge that changes in the watershed delivery of DIC and Alk observed here are likely governed by land use changes not commonly encompassed by this term. The PI time series of DIC and Alk used to recalculate pH_T, pCO_2, and Ω_{arag} and was calculated as:

$$DIC_{PI,i} = DIC_{obs,i} - DIC_{anth,i}$$

$$Alk_{PI,i} = Alk_{sal,i} - Alk_{anth,i}$$

where $DIC_{obs,i}$ and $Alk_{sal,i}$ are the calculated present-day DIC and Alk at time point i. We assumed no changes to salinity or temperature for this exercise.

4.4 Results

4.4.1 Seasonal variations of watershed and ocean end-member chemistry

For our analyses, we define the "summer" season as the July (2017 and 2018) and August cruises, the "fall" season as the September and October cruises, the "winter" season as the January, February, and March cruises, and the "spring" season as the May cruise. DIC and Alk concentrations were highest during the late summer and fall, and lowest during the winter (Fig. 4.2, Table 4.1) at both upstream and downstream stations of the Kilchis, Wilson, Trask, and Tillamook rivers and the single station of the

Miami river. Upriver DIC ranged from 312 to 699 µmol C kg^{-1}, and Alk from 268 to 657 µeq kg^{-1}, with the Trask River having the highest average concentrations. DIC and Alk were higher at the downriver sampling sites when compared with the upriver sampling sites in the Kilchis, Trask, Wilson, and Tillamook rivers in all seasons with one exception: Alk at the Tillamook River downriver site was slightly lower than the upriver site in January. Downriver DIC ranged from 317 to 939 µmol kg^{-1}, and Alk from 228 to 841 µeq kg^{-1}, with the Trask River again having the highest average concentrations. The differences between downriver and upriver DIC and Alk for each river were maximal during the summer/fall and spring, with smaller downriver gradients in the winter. These downriver DIC and Alk "enrichments" were variable for each river, but the Trask and Tillamook rivers displayed the largest upriver to downriver enrichments for all seasons. The sub-watersheds of the Tillamook and Trask rivers had the largest proportion of agricultural land use of the five river systems, and the Trask river also had the largest proportion of pasture/hay land use in the watershed area between the upstream and downstream sampling sites (27%) of all rivers. Flow-weighted averages of downriver enrichments of DIC_{fwa} and Alk_{fwa} were well-described with power functions of average daily river discharge (using the Trask River gauging station) for each cruise date (Fig. 4.3). pH_T was always higher at the upriver stations for all rivers (Table 4.1), with downriver stations often ~0.4 units lower. pH_T variability amongst the rivers was higher than the annual variability within each river, resulting in a wide pH_T range of river water entering Tillamook Bay at a given time. The river end member DIN_{fwa} concentrations were always >40 µM and seasonally variable, with the highest values in the fall and winter (56-69 µM) (Fig. 4.4). River DIN_{fwa} concentrations were lower and similar for the

spring and summer (44-46 μM). The upper forested areas of the watershed are known to have nitrogen-fixing red alder, which is likely responsible for the high river DIN_{fwa} levels as DIN concentrations were also high at the Upriver sampling stations. Riverine phosphate concentrations showed less seasonal variability (0.33-0.49 μM) than those of DIN (Fig. 4).

Coastal ocean waters entering Tillamook Bay sampled at station "M" in July and August 2017, and July 2018, displayed low pH_T, low temperatures, and nutrient values consistent with seasonally upwelled waters of the northern California Current (Table 4.2; Hales *et al.*, 2005; Chan *et al.*, 2018). Ocean waters entering the bay during the wet season and spring cruises were higher in dissolved oxygen and pH_T and depleted of nutrients (May cruise ocean DIN = 0.1 μM) when compared with the dry season (14 – 25 μM); this was likely a result of surface mixed layer metabolic (net autotrophy) and gas exchange processes. Ω_{arag} was near undersaturation during July and August (0.92 – 1.25), with winter and spring values near or above 2 (1.70 – 2.45). Salinities were lower (< 32) during the winter and lowest in spring (May cruise ocean salinity = 26.82), possibly due to intrusion of the Columbia River plume which has been shown to influence winter and spring-time shelf waters in this region (Hickey and Banas 2003). Oceanic DIC and Alk concentrations followed the same pattern as observed salinity: highest during the dry season, lower in the wet season, and lowest in the spring (Table 4.2). pCO_2 values indicated the oceanic waters were a source of CO_2 to the atmosphere in July, August, and September, near atmospheric levels in October and January, and a sink in February, March, and May. Coastal ocean waters entered the bay with a wide range of DIN (0.1 – 24.3 μM) and phosphate (0.02 – 1.78 μM) concentrations during the

study (Fig. 4.4, Table 4.2). Ocean DIN (18 – 24 μM) and phosphate (1.45 – 1.78 μM) concentrations were highest during the summer, consistent with published values for recently upwelled waters (Chase, 2002). Nutrient concentrations observed during the fall and winter cruises were similar and more depleted than the summer, with DIN and phosphate ranging from 2.74 – 6.43 μM and 0.61 – 0.67 μM, respectively. Ocean waters in the spring were the most nutrient depleted of all cruises, with DIN and phosphate observations of 0.1 μM (below the mean detection limit of 0.29 μM) and 0.02 μM, respectively.

4.4.2 Seasonal observations of carbonate chemistry in Tillamook Estuary, OR

4.4.2a Garibaldi mooring observations

The Garibaldi Dock mooring provided a high temporal resolution of physical and chemical variability within Tillamook Bay not captured by the seasonal bay cruises (Fig. 4.5). pH_T, Ω_{arag}, and pCO_2 at the mooring were highly variable on diel, weekly, and seasonal time scales, with observed ranges of 6.93 – 8.35, ~0 – 2.97, and 152 – 3,766 μatm, respectively. The lowest pH_T observations were associated with two types of environmental conditions: 1) short-duration events in the fall, winter, and spring associated with low salinities (< 10), which coincided with spikes in the hydrographs of the Trask and Wilson Rivers, and northward winds often associated with the passing of low pressure systems (Bane *et al.,* 2004) and precipitation events; and 2). longer duration events in the summer of 2018 associated with high salinity (>32), low temperatures (< 12°C), and high pCO_2 characteristic of freshly upwelled coastal ocean waters. The low salinity events were also characterized by undersaturated values of Ω_{arag} and high (>1000

μatm) pCO_2 values. During the full period of observation, pCO_2 values exceeded 400 μatm for 76% of observations, with the highest values during summer 2018 upwelling events. Waters at the mooring were undersaturated with respect to Ω_{arag} (<1.0 units) in 31% of the observations, and only exceeded 1.5 units for 28% of the observed period. Discrete observations of pH_T, Ω_{arag}, and pCO_2 from the bay cruises showed generally good agreement with the Garibaldi mooring observations at comparable salinities (Fig. 5).

4.4.2b Bay cruise observations and internal carbon cycling

Salinities at the Garibaldi YSI mooring and on the bay cruises exhibited strong seasonality reflecting variability in river discharge. The coherence of salinity patterns between the mooring and cruise data, and correlation with river discharge, suggest our limited cruise samplings captured seasonal changes in the bay. Salinities at the bay stations were highest during July through early October 2017, and late May to July 2018, which coincided with periods of low river discharge (Fig. 4.5). During the January cruise, river discharge was highest and resulted in the lowest bay salinities (mean = 8.61, std = 6.42). Bay station salinities were highest during the August 2017 cruise (mean = 29.55, std = 2.54) and July 2018 cruise (mean = 28.95, std = 7.48), which coincided with the highest salinities observed for the ocean end member (32.47 and 33.35, respectively). The July 2017 and 2018 and August 2017 cruises occurred during periods of upwelling-favorable southward wind stress (Fig. 4.5).

For all seasons, pH_T, Ω_{arag}, and pCO_2 observations at the bay stations largely followed patterns expected from observed variability in the carbonate chemistry of both ocean and riverine end-members (Fig. 4.6). The carbonate chemistry variability of the

ocean end-member reflected the seasonal dynamics of coastal upwelling/downwelling conditions. The lowest pH_T, lowest Ω_{arag}, and highest pCO_2 observations during this study at salinities >20 occurred during the July and August (summer) cruises. Bay stations during these summer cruises had a mean pH_T of 7.77, mean Ω_{arag} of 1.09, and meanpCO_2 of 780µatm. Fall (September and October) cruises had a mean pH_T of 7.86, mean Ω_{arag} of 1.25, and mean pCO_2 of 587 µatm. Winter (January, February, and March) cruise observations had a mean pH_T of 7.87, mean Ω_{arag} of 0.81, and mean pCO_2 of 502µatm. The spring (May) cruise had a mean pH_T of 7.92 units, mean Ω_{arag} of 1.34 units, and mean pCO_2 of 423 µatm.

While the seasonal variations of bay chemistry largely reflected end-member variability, departures from conservative mixing were observed in the bay for DIC, Alk, pH_T, Ω_{arag}, and pCO_2 for all cruises (Fig. 4.6) with variability amongst stations. The largest departures were typically during the summer cruises, with apparent sinks of DIC and Alk within the bay resulting in elevated pH and Ω_{arag}, and depressed pCO_2. The August cruise, likely during a period of active upwelling, had smaller departures from conservative mixing than the July cruises. Fall and winter cruises showed a mix of bay sources and sinks of DIC and Alk, usually resulting in a net lowered pH_T and Ω_{arag}, and net elevated pCO_2 (Fig. 4.6). The bay was a net sink of Alk and mixed sink/source of DIC during the May cruise, usually resulting in lowered pH_T, elevated pCO_2, and relatively large reductions in Ω_{arag}.

4.4.3 Dissolved inorganic nutrient observations

Nutrient concentrations at the bay stations departed from expected conservative mixing concentrations during all cruises, indicating the bay can be a significant sink or source of DIN and phosphate (Fig. 4.4). DIN concentrations in the river end member were always higher than those of the ocean end-member, but river phosphate concentrations were generally lower than the ocean (except for the May cruise). Departures from conservative mixing for DIN and phosphate did not always agree in sign, suggesting aerobic metabolism was not the dominant driver of these observations. This decoupling in the signs of internal DIN and phosphate cycling within the bay were also observed in a previous study of nutrient dynamics in Tillamook Bay (Colbert and McManus, 2003). The bay was generally a source of phosphate during the fall, winter, and spring cruises, but appeared to be a sink during the summer. Alternatively, the bay appeared to be a mixed source/sink for DIN during the fall, winter, and spring (with both positive and negative departures from conservative mixing behavior), and a sink during the summer. The largest excess DIN was observed in the October and February cruises, during which some bay stations were also apparent DIN sinks.

4.4.4 Anthropogenic alterations of estuarine carbonate chemistry from watershed and oceanic influences

Using the estimates of ocean and watershed end-member anthropogenic alterations of DIC and Alk (see Methods 2.5), we calculated resultant changes in present-day conservative mixing curves of pH_T, Ω_{arag}, and pCO_2 in Tillamook Bay (Fig. 4.7). As expected, oceanic C_{anth} is the dominant driver of perturbations to bay pH_T, Ω_{arag}, and

pCO_2 at high salinities (>18) for all cruises. However, along the salinity gradient there is a crossover point at which watershed alterations have an equal effect on altering bay chemistry as does mixing in of oceanic C_{anth}. At salinities below this crossover point, watershed $C_{enrich,riv}$ and $Alk_{enrich,riv}$ are responsible for most of the changes in bay CO_2 chemistry. The total changes in pH_T, Ω_{arag}, and pCO_2 driven by the sum of both ocean and watershed anthropogenic inputs are always greater than the changes driven by either the ocean or watershed inputs. The additional alkalinity delivered to the bay from the lower watershed (i.e. $Alk_{enrich,riv}$) is insufficient to fully buffer against the inputs of ocean C_{anth} and $DIC_{enrich,riv}$, and anthropogenic perturbation of the end-members always results in lower pH_T, lower Ω_{arag}, and higher pCO_2.

We also applied the cruise and salinity-specific anthropogenic perturbations of DIC and Alk to discrete samples from each bay cruise to assess how observations of present-day carbonate chemistry in Tillamook Bay have been changed by human activity (see Methods 2.5). The addition of ocean C_{anth} to the bay waters sampled by the cruises always resulted in lower pH_T, lower Ω_{arag}, and higher pCO_2 (Fig. 4.8). Present-day levels of oceanic C_{anth} are estimated to have lowered pH_T from -0.09 units (+/- 0.02 units; July 2017 cruise) to -0.15 units (+/-0.02 units; October cruise) on average amongst bay stations, lowered Ω_{arag} from -0.08 units (+/-0.07 units; January cruise) to -0.42 units (+/-0.17 units; September cruise), and increased pCO_2 from +83 μatm (+/-50 μatm; January cruise) to +218 μatm (+/-13 μatm; August cruise). Note these estimated changes assume summer upwelling C_{anth} values of ~37 μmol kg^{-1}, but estimates of ocean-driven changes assuming higher summer surface C_{anth} values are also indicated in Fig. 4.8. Present-day watershed additions of $C_{enrich,riv}$ and $Alk_{enrich,riv}$ to the bay always

resulted in lower pH_T and higher pCO_2, with mostly negative changes to Ω_{arag}. Watershed-driven pH_T alterations ranged from -0.02 units (+/-0.01 units; February cruise) to -0.10 units (+/-0.215 units; July 7th cruise), Ω_{arag} alterations from -0.07 units (+/-0.08 units; July 7th cruise) to +0.03 units (+/-0.03 units; May cruise), and pCO_2 alterations from +54 μatm (+/-43 μatm; July 18th cruise) to +135 μatm (+/-347 μatm; May cruise). Changes to the bay carbonate system driven by internal DIC and Alk cycling were highly variable with occasional decoupling amongst the signs of pH_T, Ω_{arag}, and pCO_2 changes. This internal carbon cycling caused the largest effects during the July cruises, when pH_T was increased by +0.19 units (+/-0.06 units), Ω_{arag} increased by +0.34 units (+/-0.12 units), and pCO_2 decreased by -451 μatm (+/-137 μatm). The May cruise saw the largest internally-driven decreases in pH_T (-0.13, +/-0.144) and Ω_{arag} (-0.47, +/-0.30), while the September cruise saw the largest increase in pCO_2 (+76 μatm, +/-253 μatm).

The comparison of watershed enrichments, oceanic C_{anth} addition from ocean acidification, and internal bay carbon cycling at each of the bay stations illustrates that oceanic C_{anth} is responsible for most of the present-day perturbation to Tillamook Bay carbonate chemistry, with changes in watershed carbon delivery driving relatively smaller pH_T and pCO_2 changes and nearly negligible changes in Ω_{arag}. The watershed-driven changes in Ω_{arag} were always <0.1 units, and highlights the complicated nature of carbonate system decoupling in estuarine systems (Hales *et al.*, 2017). Figures 4.7 g-i demonstrate how internal bay carbon cycling interacts with ocean and watershed changes to either enhance or ameliorate ΔpH_T, $\Delta\Omega_{arag}$, and ΔpCO_2 predicted from conservative mixing alone. Internal bay carbon cycling both enhances and reduces the depressions of

pH_T and Ω_{arag} and increases of pCO_2 driven by changes in the ocean and watershed end members.

Results of the calculations of estimated daily anthropogenic alterations of watershed CO_2 chemistry ($DIC_{enrich,riv}$ and $Alk_{enrich,riv}$) for the period of observation from August 2017 to July 2018 are shown in Figure 4.9a, along with the oceanic end-member C_{anth} value for California Current surface waters (Methods 4.2.5). $DIC_{enrich,riv}$ and $Alk_{enrich,riv}$ are highest at low flows during the summer of 2017, decrease during periods of higher river discharge in the fall and winter season, and increase again during the spring of 2018 to dry season values. Resulting perturbations to DIC and Alk at the Garaibaldi mooring (ΔDIC_{anth} and ΔAlk_{anth}) were maximal in the dry seasons (Fig. 4.9b), during periods of high riverine $DIC_{enrich,riv}$ and $Alk_{enrich,riv}$. Seasonal variability of ΔDIC_{anth} and ΔAlk_{anth} at the mooring is largely controlled by changes in watershed delivery of DIC and Alk, despite salinities >25 at the mooring for ~78% of the observations. However, the addition of oceanic C_{anth} is responsible for the majority of changes in frequency distributions of observed pH_T, Ω_{arag}, and pCO_2 at the mooring (Fig. 4.10), while watershed additions of $DIC_{enrich,riv}$ and $Alk_{enrich,riv}$ had relatively little net effect on these parameters. The magnitude of changes in pH_T, Ω_{arag}, and pCO_2 were highly variable on high-frequency time scales, and ranged from -0.04 to -0.39, ~0 to -0.67, and +49 to +1,501 μatm, respectively. The median pH_T decline was -0.19 units (from a PI value of 8.09 to 7.90), median Ω_{arag} decline was -0.55 units (from a PI value of 1.78 to 1.23), and median pCO_2 increase of 196 μatm (from a PI value of 319 μatm to 516 μatm). Ω_{arag} at this site is currently undersaturated 31% of the observations, but was undersaturated only 8% of the time in the PI. This is in general agreement with a

previous study (Hauri, Gruber, McDonnell, *et al.*, 2013) that estimated a quadrupling of aragonite undersaturation events in nearshore bottom waters of the California Current since the PI.

4.5 Discussion

4.5.1 Tillamook Estuary carbonate chemistry

The carbonate chemistry dynamics of Tillamook Bay are mostly dominated by mixing between coastal ocean and river waters, with internal bay carbon processing a secondary control on observed variability. The range of carbonate system parameters between the ocean and river end-members is greater than observed departures from conservative mixing due to internal bay carbon cycling for all seasons, and underlines the importance of end-member variability in controlling the carbonate chemistry experienced in the bay. Coastal ocean waters entering the bay exhibited broad ranges of pH_T (7.68 – 8.21 units), pCO_2 (243 – 1,009 μatm), and Ω_{arag} (0.87 – 2.45 units). Seasonal pCO_2 variability of the downstream river end-member (870 – 3,344 μatm) exceeded that of the ocean end-member due to the low buffering capacity of the river waters and high sensitivity of pCO_2 to carbonate system changes, while seasonal pH_T (7.07 – 7.39 units) and Ω_{arag} (~ 0 for all seasons) variability was less than that of the ocean. Internal carbon cycling alterations of pH_T were usually less than 0.2, alterations of Ω_{arag} usually less than 0.4, and alterations of pCO_2 usually less than 300 μatm (Fig. 4.8). Departures from conservative mixing of DIC and Alk within the estuary (Fig. 4.6) are often of similar magnitudes, suggesting that aerobic metabolism alone is not the primary mechanism of

internal bay carbon cycling for all seasons. If aerobic metabolism was dominant, proportionally larger changes in the DIC pool as compared with Alk would have been expected. This was true only during the dry season, when the bay was a relatively large apparent sink for DIC, DIN, and phosphate with smaller changes in the Alk pool, consistent with net autotrophic metabolism. However, net autotrophy would be expected to increase Alk and make the bay appear as a net Alk source; instead the bay was still a net sink of Alk during the dry season. These observations may be explained by net calcification, which would be a net sink of both DIC and Alk. There are large shellfish populations within the bay, making this a plausible explanation. Assuming a reasonable bay residence time of ~3 weeks for the dry season, an observed Alk anomaly of -100 μeq kg^{-1} would correspond to a net calcification rate of ~130 mg $CaCO_3$ m^{-2} d^{-1}. This value is well within previously published net calcification rates of ~367 mg $CaCO_3$ m^{-2} d^{-1} for *C. gigas* populations in a temperate estuary (Lejart *et al.*, 2012). It is also likely that sediment metabolism and benthic-pelagic coupling is important in the Tillamook estuary given its shallow depths (Colbert and McManus, 2003), and may be a possible explanation for the sign decoupling of DIN and phosphate anomalies (Fig. 4.4).

The dominance of end-member variability in controlling bay CO_2 chemistry likely reflects the relatively short residence times of water in the bay, decreasing the amount of time available for internal biogeochemical cycling to alter the chemistry of the end-members. Observed non-conservative behavior of DIC, Alk, and inorganic nutrients within the bay was most pronounced during the summer and spring cruises when river discharge was lowest, in agreement with past findings of freshwater flushing time as a dominant control of Tillamook Bay nutrient dynamics (Colbert and McManus, 2003).

Water residence time (amongst other hydrologic characteristics) has been used as a framework for classifying the susceptibility of estuaries to pollutant effects (Engle *et al.*, 2007). Analogously, we propose that estuarine residence time is a valuable first-order predictor of end-member biogeochemical variability versus autochthonous biogeochemical cycling as drivers of estuarine acidification. Estuaries with shorter residence times will more closely reflect the biogeochemical signatures of their end members, while systems with longer residence times will depart from these source water signatures due to autochthonous biogeochemical processing. Tillamook Estuary represents a short to moderate residence time system dominated by the variability of its end members. In contract, coastal acidification studies in systems like the Chesapeake Bay with long residence times (~180 days; (Du and Shen, 2016)) have shown that autochthonous biogeochemical processing can be a dominant driver of acidification rates (e.g. (Cai *et al.*, 2011; Cai *et al.*, 2017)). Given the need to identify coastal systems vulnerable to acidification, but large research efforts required for coastal acidification studies, it may be useful to develop a residence-time framework to classify the likely drivers of anthropogenic acidification in coastal systems. This effort could be valuable for ranking the relative susceptibility of these systems to local (e.g. eutrophication) versus regional (e.g. upwelling systems) stressors (e.g. (Ekstrom *et al.*, 2015)), and identifying priority locations for future research and management efforts.

With the exception of prior work in the Salish Sea, there are few studies of carbonate chemistry dynamics in California Current estuaries (Hales *et al.*, 2017; Paulsen *et al.*, 2018). A relevant comparison with our study is that of Hales et al. 2017, which characterized a multiple year dataset of carbonate chemistry in Willapa Bay, WA, USA.

Willapa Bay is similar to Tillamook Bay in that it is a shallow, open coast estuary (~120km north of Tillamook), subject to similar coastal oceanographic conditions (including seasonal upwelling and Columbia River plume influence) and river inputs from small mountainous watersheds, and is home to extensive aquaculture of Pacific oysters (*Crassostrea gigas*) (Dumbauld *et al.*, 2011). There are similarities in the carbonate chemistry of Willapa and Tillamook bays. For example, DIC and Alk largely follow observed salinity patterns; pCO_2 is highly variable and often above atmospheric levels; pH_T is highly variable, shows no clear seasonal trend, and is rarely above 8.1 units; Ω_{arag} is most frequently below an established developmental threshold for *C. gigas* larvae of ~1.4 units (Waldbusser *et al.*, 2015) and nearly always below 2.0 units; and there is a strong decoupling of the variance in carbonate system parameters. The coherence in carbonate system observations between Tillamook and Willapa Bays suggests that coastal ocean and watershed boundary conditions are similar, and that these boundary conditions are dominant controls of pH_T, pCO_2, and Ω_{arag} in open-coast, short residence time, small mountainous river systems typical of the west coast of the United States.

4.5.2 Influence of coastal upwelling dynamics on bay chemistry

The broad ranges in the carbonate chemistry of coastal ocean waters entering the estuary (sampled at station M), with relatively high CO_2 conditions in the summer and lower CO_2 in the winter, show how coastal ocean upwelling dynamics can be significant modulators of carbonate chemistry not just on the shelf (e.g. Feely *et al.*, 2008; Harris *et al.*, 2013; Feely *et al.*, 2016), but also of estuaries in the California

Current ((Barton *et al.*, 2012; Hales *et al.*, 2017); this study). Indeed, a 1,000 km network of nearshore pH monitoring in open-coast habitats of the California Current showed strong correspondence between shelf pH and nearshore pH values attributable to upwelling dynamics (Chan *et al.*, 2017). The advection of upwelled waters into California Current estuaries can be significant as shown by this study and others (Brown and Ozretich, 2009; Roegner *et al.*, 2011; Murray *et al.*, 2015), and it is known that the lowest pH_T and most corrosive upwelled waters occur in the most nearshore regions of the shelf (Feely *et al.*, 2016). Thereby, estuarine organisms and ecosystems are naturally exposed to some of the most extreme CO_2 conditions experienced in the California Current system. This is important for a few reasons: 1). While these ecosystems have likely always experienced naturally stressful conditions (Hales *et al.*, 2017), upwelled waters may be especially prone to accelerated anthropogenic acidification (Chan *et al.*, 2017; Feely *et al.*, 2018); 2). Freshly upwelled, high CO_2 waters have a high DIC:Alk ratio, which can enhance carbonate system perturbations due to local carbon cycling (e.g. eutrophication-enhanced watershed carbon delivery or bay metabolism) (Pacella *et al.*, 2018); and 3). Corrosive conditions in estuaries of the California Current during periods of upwelling have been shown to significantly impair Pacific oyster hatchery operations due to larval mortality attributed to low Ω_{arag} (Barton *et al.*, 2012; Barton *et al.*, 2015). It therefore seems likely that future variability and rates of coastal acidification in California Current estuaries will be largely modulated by coastal ocean upwelling dynamics. The timing and duration of upwelling events are controlled by equatorward wind stress, and are predicted to become less frequent, stronger, and longer in duration with ongoing climate change (Iles *et al.*, 2012). The physical and chemical

characteristics of upwelled waters are largely controlled by the relative contributions of North Pacific Waters (higher pH, lower CO_2) and Equatorial Pacific Water (lower pH, higher CO_2) to upwelling source waters in the California Current (Meinvielle and Johnson, 2013). An increasing fraction of Equatorial Pacific Water has been shown to contribute to waters of the California Undercurrent in the past ~30 years (Meinvielle and Johnson, 2013), resulting in more acidic source waters delivered to coastal and estuarine habitats. Additionally, the carbonate chemistry of source waters at the time of initial formation and subduction will likely be altered by climate change, potentially including altered NCM. Warming surface waters would both enhance stratification and reduce nutrient availability for primary production in the surface mixed layer, as well as drive thermally-induced alterations of community metabolic rates (e.g. Q_{10} effects; Bruno *et al.*, 2015) These less-appreciated upwelling dynamics will likely be an important control on the interannual and decadal variability of future coastal acidification dynamics of California Current coastal habitats. Interpretation of long-term pH and CO_2 system changes in these habitats would benefit from accounting for these dynamics (Turi *et al.*, 2016).

4.5.3 Watershed carbonate chemistry and human land use

The five rivers discharging into Tillamook Bay were characterized by relatively low DIC and Alk concentrations when compared with previously published values from large river systems (e.g. Stets *et al.*, 2014), but are similar to recently published values from the Fraser River in British Columbia (Moore-Maley *et al.*, 2018). The watersheds of the Oregon coast range drain largely volcanic and sedimentary rock

formations and export less alkalinity when compared with watersheds with limestone lithology (e.g. Suchet and Ludwig, 2003; Mcgrath *et al.*, 2016). However, the DIC:Alk ratios of the rivers at their downstream stations were relatively high (1.15 – 1.2; Fig. 2) when compared to other river systems in North America (<1.1; Joesoef *et al.*, 2017; Moore-Maley *et al.*, 2018).

Our study design sought to characterize the influence of human land use on the carbonate chemistry of the rivers discharging to Tillamook Bay by sampling both upstream of and amongst areas with human land use modification. We are unaware of other studies characterizing land use effects on the CO_2 chemistry of coastal rivers discharging to the California Current, but previous work has shown that DIC content of temperate streams is strongly related to watershed land use (e.g. Barnes and Raymond, 2009; Zhang *et al.*, 2009). DIC concentrations in streams with dominant urban and agricultural land use have been found to be up to 4.7 and 3.3 times higher, respectively, than in streams of forested watersheds (Barnes and Raymond, 2009). These increased DIC concentrations have been attributed to waste water and septic inputs (Barnes and Raymond, 2009) and agricultural activities (Oh and Raymond, 2006; Perrin *et al.*, 2008), including delivery of HCO_3^- via enhanced chemical weathering fueled by nitrogenous fertilizer applications and liming practices. Tillamook County contained 36,551 acres of farmland as of the 2012 Census of Agriculture (USDA-NASS, 2012), of which 4,582 acres are treated with “commercial fertilizer, lime and soil conditioners”, and 12,261 acres are treated with manure. While these numbers are county-wide, the bulk of this agricultural activity is concentrated in the lower Tillamook Estuary watershed encompassed by our study sites. The bacterial contamination issues previously

documented in the bay (Shanks *et al.*, 2006), thought to be related to agricultural runoff, septic system discharges, and wastewater discharges, demonstrate a direct link between anthropogenic land use in the watershed and water quality in the bay. It therefore seems plausible that other water quality indices in Tillamook Bay, including pH_T and other carbonate parameters, may be affected by these same land use practices.

The strong relationship observed between river discharge and downstream enrichments of DIC and Alk (Fig. 4.3) suggests dilution of a downstream source in the area of agricultural influence. A concurrent study in Tillamook Bay (Brown *et al.*, *in prep*) found downstream DIN enrichments with elevated $\delta^{15}N\text{-}NO_3$ values (a common indicator of anthropogenic influence) in the Tillamook river systems. These DIN enrichments were significantly correlated with microbial markers of cows observed at the same downstream stations, supporting a physical/biogeochemical link between agricultural activities and riverine water quality during our study period. Observed river DIC concentrations are also significantly correlated with human land use metrics, including the number of cows upstream of each sampling site during all seasons (Fig. 4.11a,b), as well as the estimated proportion of DIN loading from anthropogenic sources (septic discharge, fertilizers, manure, developed land, and waste water treatment plant discharge) using the USGS SPARROW model (Fig. 4.11c; https://water.usgs.gov/nawqa/sparrow/) during the summer. The majority of downriver DIC enrichments are as HCO_3^- with smaller additions of $CO_{2(aq)}$, resulting in the ratios of downriver DIC and Alk enrichments to nearly always fall above a 1:1 DIC to Alk ratio line (Fig. 4.12). The addition of HCO_3^- in temperature streams and rivers has generally been interpreted as resulting from weathering of carbonate and silicate minerals (Oh and

Raymond, 2006; Barnes and Raymond, 2009; Joesoef *et al.*, 2017), sometimes anthropogenically enhanced by lime additions and acids produced by metabolic processing of agricultural fertilizers and manure (Oh and Raymond, 2006). Alternatively, a study in a temperate salt marsh interpreted changes in DIC and Alk, and the ratio between the two, as resulting from aerobic ($+CO_{2(aq)}$) and anaerobic (HCO_3^-) metabolic processes, respectively (Wang *et al.*, 2016). The downstream DIC and Alk enrichments in the Tillamook watershed (primarily HCO_3^- with smaller amounts of $CO_{2(aq)}$) would be consistent with the delivery of anerobic (including sulfate reduction) and aerobic metabolites to the lower rivers, likely via exchange with subsurface runoff from agricultural areas. This explanation is supported by the observations of elevated DIN concentrations in most areas of the watershed with enriched DIC, with the exception of the Tillamook River (Fig. 4.11d). However, the DIC enrichments could also be explained by carbonate dissolution in the lower watershed, with smaller additions of metabolic $CO_{2(aq)}$ and/or organic acids. A third explanation is that the downriver enrichments resulted from in-stream respiratory processes. If stream respiration were primarily responsible for downriver enrichments, we would have expected the increases in DIC to be accompanied by relatively small changes in Alk (assuming stoichiometry close to Redfield ratios). Instead, DIC enrichments were accompanied by large changes in Alk – a result of the majority of the DIC additions being HCO_3^- ion which contributes to the Alk and DIC pools in a 1:1 ratio. Unfortunately, the number of possible explanations for observed downstream DIC enrichments is under-constrained by our current dataset, and a full accounting and interpretation of these changes in DIC and Alk is not possible at this time. It is important to note that we fully constrained the inorganic

carbon system with our measurement technique (using pCO_2 and DIC), and so while a better understanding of the mechanisms resulting in the downriver DIC enrichments is intriguing and potentially illuminating from a management perspective (as we further discuss below), new information on these mechanisms would not change the conclusions of the paper as to how enrichments in DIC and Alk alter bay chemistry.

Given the literature demonstrating agricultural enrichment of river DIC consistent with our observations and the correlations of observed DIC enrichments with indices of agricultural influence (Fig. 4.11; Brown *et al., in prep*), this evidence taken together suggests human activities in the watershed are responsible for a portion of the downstream enrichments in DIC and Alk. Attributing the totality of these changes to human activities is not possible with the current dataset. Much of the lowland agricultural areas lie in flood plains, which may naturally deliver higher DIC and Alk loads to the rivers when compared with the upper forested watersheds via degradation of accumulated organic matter-rich soils. This would not explain the elevated $\delta^{15}N\text{-}NO_3$ values or microbial markers of cow influence by Brown et al. (*in prep*), however. We therefore posit that the observed downstream enrichments can be viewed as upper bounds of the human influence on river chemistry in the Tillamook Bay watershed, and are useful for understanding potential "worst-case scenario" human impacts on the carbonate chemistry of the bay.

4.5.4 Present-day human alterations of ocean and watershed end-members and their controls on acidification of Tillamook Bay

The combined effects of watershed DIC and Alk enrichments and oceanic C_{anth} on CO_2 chemistry within the salinity spectrum of Tillamook Estuary are highly non-linear (Fig. 4.7) despite the assumption of conservative mixing of both DIC and Alk between oceanic and river end-members. This behavior is a result of the non-linear responses of pH_T, Ω_{arag}, and pCO_2 with changes in DIC and Alk concentrations, as described by their respective buffer factors (Egleston *et al.*, 2010). The salinity range at which this non-linear behavior is most pronounced, and ΔpH_T (Fig. 4.7) has the greatest magnitude, has been previously discussed and termed the "Maximum Estuarine Acidification Zone" (MEAZ; Hu and Cai, 2013; Cai *et al.*, 2017) . The MEAZ for pH_T in Tillamook Bay varies due to the unique chemical signatures of the ocean and river end members on each cruise, but always occurs at low salinities (<12) and is generally centered at a salinity of 4 (Fig. 4.7d). Conversely, $\Delta\Omega_{arag}$ is greatest at high salinities due to the extremely low CO_3^{2-} concentrations and Ω_{arag} values at low salinities. ΔpCO_2 is maximal at the lowest salinities due to the low Alk and CO_2 buffering capacity of these waters. ΔpH_T throughout the bay is much greater than the ~0.1 unit change often attributed to ocean acidification impacts (Duarte *et al.*, 2013), and consistent with emerging evidence of more rapid acidification in coastal and estuarine environments (e.g. Robbins and Lisle, 2018).

Observed watershed enrichments of DIC and Alk drive the largest changes in bay chemistry at low- to mid-salinities, and amplify changes in oceanic C_{anth} across the full salinity spectrum (Fig. 4.7). However, changes in observed carbonate chemistry from the

bay cruises (Fig. 4.8) and the Garibaldi mooring time series (Fig. 4.10) show that most of the present-day changes in the waters of Tillamook Bay have been driven by oceanic C_{anth} despite downstream enrichments of DIC ($DIC_{enrich,riv}$) exceeding oceanic C_{anth} for much of the year (Fig. 4.9a). The dominance of oceanic conditions dictating perturbations to bay chemistry is due to the large difference in ocean versus river water delivery to the bay. The tidal volume exchanged with the coastal ocean (mean of 1.23 x 10^8 m^3 d^{-1}; http://ian.umces.edu/neea/siteinformation.php) is usually an order of magnitude larger than the total river discharge to the bay (7.82 x 10^5 m^3 d^{-1} to 1.71 x 10^7 m^3 d^{-1}). This results in mostly high salinity waters in the bay, especially during the dry season periods of low river discharge, and dilution of the downstream watershed DIC and Alk enrichments once mixed into the bay. Additionally, enriched DIC concentrations in river waters are primarily composed of HCO_3^-, and so drive relatively smaller changes in bay chemistry for a given addition of DIC when compared with OA-driven ocean C_{anth}.

4.5.5 Relevance of ocean and watershed interactions in Tillamook Estuary for broader understanding of coastal acidification dynamics

The potential for enhanced acidification of estuarine waters due to ocean acidification has been long known, but descriptions of the spatial and temporal dynamics of how this enhancement alters estuarine CO_2 chemistry from "natural" conditions has received relatively little attention until recently (e.g. Cai *et al.*, 2017; Pacella *et al.*, 2018). This is surprising, given that the observed magnitude of enhanced response in the carbonate systems of coastal areas (Cai *et al.*, 2011; Waldbusser *et al.*, 2011; Sunda and Cai, 2012) can be relatively large, and hasten the exceedance of water quality and

organismal tolerance thresholds (Pacella *et al.*, 2018). The non-linear pH_T alteration along estuarine salinity gradients driven by mixing in of oceanic C_{anth} has been recently discussed (Cai *et al.*, 2017), highlighting how the interaction of oceanic C_{anth} and local metabolic carbon cycling governs the salinity zone of minimum buffering and maximum acidification (termed the MEAZ). However, the location and magnitude of the MEAZ within an estuary is also a function of the DIC and Alk concentrations of the watershed/river end-member, where systems with low Alk and buffering capacity have more dramatic amplifications of the MEAZ in low and mid-salinity areas (Cai *et al.*, 2017). Our work builds upon these well-established concepts by incorporating how anthropogenic changes in the watershed end-member may interact with ocean C_{anth} to alter CO_2 chemistry along an estuarine salinity gradient.

The magnitude of estuarine ΔpH_T, $\Delta\Omega_{arag}$, and ΔpCO_2 resulting from human alterations of watershed chemistry alone can be as large, or larger, than those changes driven by ocean C_{anth}, with the combined effects of the two end-members being additive. Watershed drivers are most important in areas of the estuary with lower salinities, however (Fig. 4.7), making the spatial domain over which human watershed alterations dominate estuarine acidification dependent upon river discharge and circulation dynamics. Human watershed alterations can also shift the MEAZ along the estuarine salinity gradient, combining with oceanic C_{anth} to alter the spatial footprint of the most perturbed areas within an estuary. The magnitude and location of the MEAZ within an estuary will therefore vary on seasonal time scales due to changes in anthropogenically-enhanced watershed delivery of DIC and Alk, as well as interannual time scales due to the 1). rate of long-term C_{anth} accumulation in coastal ocean waters, 2). rate of future

human watershed development and land use change, and 3). changes in regional oceanography and hydrology resulting from climate change. Holding watershed perturbations at estimated present-day levels, increasing oceanic C_{anth} levels will expand the salinity range over which oceanic C_{anth} dominates anthropogenic changes in estuary CO_2 chemistry to lower salinities, while also raising DIC:Alk ratios in the bay and shifting the MEAZ to higher salinities. Future changes in watershed perturbation are likely to create a more complex response in estuarine CO_2 chemistry. From a first-order perspective, ocean acidification drives monotonically increasing DIC levels with no Alk response in coastal ocean waters. However, human-driven perturbations of river chemistry have been shown to alter both DIC and Alk pools, and the balance between the rates of change in these two pools would likely be a function of the underlying mechanisms creating these perturbations. For example, if enhanced carbonate dissolution via nitrification (Oh and Raymond, 2006) or other metabolic acid production is primarily responsible for anthropogenic alterations of river chemistry, the increased export of HCO_3^- resulting from this process would increase DIC and Alk pools in a 1:1 ratio, with relatively muted impacts to estuarine pH_T, Ω_{arag}, and pCO_2. Alternatively, if perturbations of river chemistry are dominated by metabolic processes, the increased delivery of metabolic CO_2 would increase DIC levels with minimal change in Alk. This would increase the DIC:Alk ratio and lower the buffer capacity of receiving waters, enhancing downstream impacts of lowered pH_T and Ω_{arag} and increased pCO_2 in the estuary. A similar enhancement of estuary impacts would occur if atmospheric acid deposition (Doney *et al.*, 2007) is an important process in anthropogenically altering river chemistry, where the net result is a reduction in Alk (and buffering capacity) with no

change in DIC. It therefore seems necessary to understand the system-specific mechanisms underlying changes in watershed CO_2 chemistry to reliably forecast how changes in anthropogenic watershed utilization will impact estuarine and coastal pH_T, Ω_{arag}, and pCO_2. Unfortunately, our current dataset for the Tillamook Bay system is inadequate for these types of predictions..

Anthropogenic alterations of estuarine CO_2 chemistry will be system-specific and dependent upon how human actions have altered watershed and ocean end-members, but some generalizations are possible. As previously discussed, there are zones within the estuarine salinity gradient whose alteration will be dominated by either watershed or oceanic forcings, and a crossover point exists at which the roles of the watershed and ocean anthropogenic components are equivalent in their alteration of estuarine CO_2 chemistry. The location of this point within the estuarine salinity gradient is a function of the magnitudes of perturbation in the watershed and ocean end-members, with the balance amongst the mechanisms underlying watershed perturbations modulating the inorganic carbon speciation and resultant effects on estuarine pH_T, Ω_{arag}, and pCO_2. These dynamics of watershed-ocean interactions will also be locally modulated by seasonal changes in the forcings from both the watershed and oceanic sides. For example in Tillamook Bay, downriver enrichments of DIC and Alk have relatively larger effects at higher salinities during the summer than during the winter due to the much higher $C_{enrich,riv}$ and $Alk_{enrich,riv}$ values (Fig. 4.9). It is also likely that during times of active upwelling (when the oceanic C_{anth} burden is lower (Feely *et al.*, 2016), anthropogenically-driven pH_T depressions at higher salinities will be less than at other times of the year (despite the pH_T of upwelled waters being naturally low). While there is variability in

oceanic C_{anth} in coastal zones of the United States (Feely *et al.*, 2018), this variability is often smaller than the CO_2 chemistry variability amongst natural and anthropogenically-altered watersheds studied to date (e.g. Raymond *et al.*, 2008; Carstensen *et al.*, 2018; Moore-Maley *et al.*, 2018). Therefore, variance in rates of acidification amongst estuaries and coastal habitats, and the relative susceptibility to changes in the CO_2 system, is likely to be primarily determined by local watershed chemistry and biophysical (e.g. metabolic rates, estuarine residence and freshwater flushing times, stratification) drivers.

4.5.6 Implications for water quality management in Tillamook Estuary

Ocean acidification is the result of anthropogenic CO_2 emissions to the atmosphere on a global scale, and will therefore require a coordinated international effort to reduce global emissions and their impact on ocean chemistry (Strong *et al.*, 2014). Given the political, economic, and technological hurdles to this sort of coordinated response, there is intense interest in the efficacy of targeted, local management and policy actions which may act to ameliorate acidification impacts in coastal and estuarine areas (Kelly *et al.*, 2011; Strong *et al.*, 2014; Weisberg *et al.*, 2016). Many of the proposed management actions for curtailing coastal acidification involve reduction of land-based nutrients and other pollutants associated with human land use change and urban development. The scope of the potential efficacy of these local management actions will depend upon the spatial and temporal "footprint" of acidification (and changes in other carbonate parameters, e.g. Ω_{arag}) attributable to human alterations of watershed chemistry.

This study identifies the salinity zones and seasonality of watershed and oceanic anthropogenic perturbations to the carbonate system of Tillamook Bay, thereby constraining the spatial and temporal efficacy of management actions acting upon ocean and watershed end-members to ameliorate coastal acidification in the estuary. The salinity zones where ocean acidification of the coastal ocean end-member dominates are seasonally variable (Fig. 4.7), but are typically found at salinities of 18 and above. Anthropogenic perturbations in fresher waters (salinity <18) in the estuary are driven primarily by watershed DIC and Alk enrichments. Despite the larger salinity range (~0-18) in which watershed enrichments dominate the anthropogenic perturbations in the estuary, most of the waters observed in the estuary during this study were of higher salinity (>18; Figs. 4.5 & 4.6) and were therefore more impacted by C_{anth} in the ocean end-member.

The dominance of oceanic forcing in present-day perturbations of Tillamook Bay carbonate chemistry suggests that local management actions targeted at reducing watershed DIC loading to the bay will have a limited ability to improve coastal acidification-related water quality end points. On one hand, the increased sensitivity of the carbonate system at higher DIC:Alk ratios (typical of upwelled waters) can enhance the relative amelioration role of local CO_2 removal techniques (e.g. macrophyte CO_2 removal) (Pacella *et al.*, 2018). Despite this though, local actions will be working against an accelerating change in the coastal ocean, whose influence is large in the CO_2 chemistry of estuaries and nearshore habitats of the California Current (this study; (Barton *et al.*, 2012; Hales *et al.*, 2016; Chan *et al.*, 2017)). Nutrients do not appear to be limiting in the bay for the majority of observations made during the study period (Fig.

4.4) , making management of nutrient delivery likely limited in its effects on estuary metabolism. It seems that nutrient-enhanced acidification, such as observed in the Gulf of Mexico (Cai *et al.*, 2011) and Chesapeake Bay (Waldbusser *et al.*, 2011), is unlikely in Tillamook Estuary given its short residence times, shallow depths, and general lack of stratification during the productive dry season with which to accumulate respired CO_2. While accumulation and respiration of eutrophication-fueled organic matter in bay sediments is possible, observed effects of internal bay carbon cycling on the CO_2 system are also usually smaller than those forced by oceanic C_{anth} (Fig. 4.8), constraining any anthropogenic enhancement of internal bay metabolic CO_2 production to be less than oceanic C_{anth}. If the enhanced downstream delivery of DIC and Alk in Tillamook Bay was somehow reduced to levels consistent with areas in the watershed with little human influence, this would still not offset the acidifying effects of oceanic C_{anth} in the bay at moderate and high salinities (Figs. 4.6, 4.10).

Recent efforts have focused on understanding how the magnitude, duration, and frequency of acidification-driven changes in coastal carbonate chemistry affect coastal organisms (e.g. Clark *et al.*, 2016; Bednaršek *et al.*, 2017; Gimenez *et al.*, 2018). However, application of the experimentally-derived stress metrics resulting from these efforts to *in-situ* environmental responses remains an open challenge in the coastal acidification field. Our study estimates how carbonate chemistry within the bay has been altered due to human activities, but is unable to address resulting ecological impacts in the bay. It is possible that shellfish reproduction and growth in the estuary has been hampered by acidifying conditions in the estuary, as Hales *et al*. (2017) have hypothesized for Willapa Bay, WA. We are unaware of shellfish mortality issues in

Tillamook Bay, but acidification can result in sub-lethal impacts to shellfish, including significantly reduced growth and calcification (e.g. Waldbusser *et al.*, 2010; Amaral *et al.*, 2012; Hettinger *et al.*, 2012). The seemingly insidious nature of coastal acidification effects on organisms and ecosystems, as well as the multitude of co-stressors in estuarine environments, make it difficult to attribute *in-situ* impacts of coastal acidification. However, given the documented shellfish aquaculture issues in Netarts Bay, OR attributable to low Ω_{arag} (Barton *et al.*, 2012; Barton *et al.*, 2015), it seems likely that coastal acidification is a co-stressor in Tillamook Bay where there is already a well-documented history of microbial contamination issues affecting shellfish aquaculture operations (Shanks *et al.*, 2006).

4.6 Conclusion

Using estuarine CO_2 system observations over the course of a year, this study shows that the seasonal pH_T, Ω_{arag}, and pCO_2 dynamics of Tillamook Estuary are largely controlled by variability in the coastal ocean and watershed end-members. The strong ocean-estuary connection and relatively short estuarine residence times limit the expression of internal estuary biogeochemical cycling on seasonal pH_T, Ω_{arag}, and pCO_2 variability. Rivers in the watershed displayed elevated DIC and Alk in areas with agricultural land use, which altered the conservative mixing dynamics of carbonate parameters within the estuary. Estimates of the magnitudes of anthropogenic changes in estuary chemistry driven by enriched watershed DIC and Alk versus coastal ocean C_{anth} suggest that the delivery of acidified ocean waters is the dominant driver of human

perturbation in the estuary. The response of estuarine pH_T, Ω_{arag}, and pCO_2 to local management for reductions in watershed carbon delivery are likely to be restricted to low salinity areas, and of limited importance in northern portions of the bay with greater oceanic influence and the majority of shellfish aquaculture. These findings highlight the importance of accounting for anthropogenic changes in watershed chemistry when estimating rates of estuarine acidification across a full salinity spectrum.

4.7 References

Ainsworth, C. H. *et al.* (2011) 'Potential impacts of climate change on Northeast Pacific marine foodwebs and fisheries', *ICES Journal of Marine Science*, 68(6), pp. 1217–1229. doi: 10.1093/icesjms/fsr043.

Amaral, V. *et al.* (2012) 'Moderate acidification affects growth but not survival of 6-month-old oysters', *Aquatic Ecology*, 46(1), pp. 119–127. doi: 10.1007/s10452-011-9385-5.

Bandstra, L. *et al.* (2006) 'High-frequency measurements of total CO2: Method development and first oceanographic observations', *Marine Chemistry*, 100(1–2), pp. 24–38. doi: 10.1016/j.marchem.2005.10.009.

Barnes, R. T. and Raymond, P. A. (2009) 'The contribution of agricultural and urban activities to inorganic carbon fl uxes within temperate watersheds'. Elsevier B.V., 266, pp. 318–327. doi: 10.1016/j.chemgeo.2009.06.018.

Barton, A. *et al.* (2012) 'The Pacific oyster, Crassostrea gigas, shows negative correlation to naturally elevated carbon dioxide levels: Implications for near-term ocean acidification effects', *Limnology and Oceanography*, 57(3), pp. 698–710. doi: 10.4319/lo.2012.57.3.0698.

Barton, A. *et al.* (2015) 'Impacts of coastal acidification on the Pacific Northwest shellfish industry and adaptation strategies implemented in response', *Oceanography*, 28(2), pp. 146–159. doi: 10.5670/oceanog.2015.38.

Barton, A. *et al.* (2015) 'Impacts of Coastal Acidification on the Pacific Northwest Shellfish Industry and Adaptation Strategies Implemented in Response', *Oceanography*, 25(2), pp. 146–159. doi: 10.5670/oceanog.2015.38.

Bates, N. R. *et al.* (2012) 'Detecting anthropogenic carbon dioxide uptake and ocean acidification in the North Atlantic Ocean', *Biogeosciences*, 9(7), pp. 2509–2522. doi: 10.5194/bg-9-2509-2012.

Bednaršek, N. *et al.* (2017) 'Exposure history determines pteropod vulnerability to ocean acidification along the US West Coast article', *Scientific Reports*, 7(1), pp. 1–12. doi: 10.1038/s41598-017-03934-z.

Borges, A. V. and Gypens, N. (2010) 'Carbonate chemistry in the coastal zone responds more strongly to eutrophication than ocean acidification', *Limnology and Oceanography*, 55(1), pp. 346–353. doi: 10.4319/lo.2010.55.1.0346.

Boyd, P. W. *et al.* (2016) 'Biological responses to environmental heterogeneity under future ocean conditions', *Global Change Biology*, pp. 2633–2650. doi: 10.1111/gcb.13287.

Brown, C. A. and Ozretich, R. J. (2009) 'Coupling between the coastal ocean and yaquina bay, oregon: Importance of oceanic inputs relative to other nitrogen sources', *Estuaries and Coasts*, 32(2), pp. 219–237. doi: 10.1007/s12237-008-9128-6.

Busch, D. (2013) 'Potential impacts of ocean acidification on the Puget Sound food web', *ICES Journal of Marine Science*, 70, pp. 823–833. Available at: http://icesjms.oxfordjournals.org/content/70/4/823.short.

Busch, D. S. and McElhany, P. (2016) 'Estimates of the direct effect of seawater pH on the survival rate of species groups in the California current ecosystem', *PLoS ONE*, 11(8), pp. 1–28. doi: 10.1371/journal.pone.0160669.

Bruno, J.L. *et al.* (2015) 'Exploring the role of temperature in the ocean through metabolic scaling', *Ecology*, 96(12), pp. 3126-3140. doi: 10.1890/14-1954.1.

Cai, W.-J. *et al.* (2011) 'Acidification of subsurface coastal waters enhanced by eutrophication', *Nature Geoscience*. Nature Publishing Group, 4(11), pp. 766–770. doi: 10.1038/ngeo1297.

Cai, W. J. *et al.* (2017) 'Redox reactions and weak buffering capacity lead to acidification in the Chesapeake Bay', *Nature Communications*, 8(1), pp. 1–12. doi: 10.1038/s41467-017-00417-7.

Carstensen, J. *et al.* (2018) 'Long-Term and Seasonal Trends in Estuarine and Coastal Carbonate Systems', *Global Biogeochemical Cycles*, 32, pp. 497–513.

Chan, F. *et al.* (2017) 'Persistent spatial structuring of coastal ocean acidification in the California Current System', *Scientific Reports*, 7(September 2016), p. 2526. doi: 10.1038/s41598-017-02777-y.

Chase, Z. (2002) 'Iron, nutrient, and phytoplankton distributions in Oregon coastal waters', *Journal of Geophysical Research*, 107(C10), p. 3174. doi: 10.1029/2001JC000987.

Clark, H. and Gobler, C. (2016) 'Do diurnal fluctuations in CO2 and dissolved oxygen concentrations provide a refuge from hypoxia and acidification for early life stage bivalves?', *Marine Ecology Progress Series*, 558, pp. 1–14. doi: 10.3354/meps11852.

Colbert, D. and McManus, J. (2003) 'Nutrient Biogeochemistry in an Upwelling-Influenced Estuary of the Pacific Northwest (Tillamook Bay , Oregon , USA)', *Estuaries*, 26(5), pp. 1205–1219.

Doney, S. C. *et al.* (2007) 'Impact of anthropogenic atmospheric nitrogen and sulfur deposition on ocean acidification and the inorganic carbon system.', *Proceedings of the National Academy of Sciences of the United States of America*, 104(37), pp. 14580–5. doi: 10.1073/pnas.0702218104.

Doney, S. C. *et al.* (2009) 'Ocean Acidification: The Other CO 2Problem', *Annual Review of Marine Science*, 1(1), pp. 169–192. doi: 10.1146/annurev.marine.010908.163834.

Doney, S. C. and Schimel, D. S. (2007) 'Carbon and climate system coupling on timescales from the Precambrian to the anthropocene', *Annual Review of Environment and Resources*, 32, pp. 31–66. doi: 10.1146/annurev.energy.32.041706.124700.

Du, J. and Shen, J. (2016) 'Water residence time in Chesapeake Bay for 1980 – 2012 Water residence time in Chesapeake Bay for 1980 – 2012', *Journal of Marine Systems*. Elsevier B.V., 164(December 2017), pp. 101–111. doi: 10.1016/j.jmarsys.2016.08.011.

Duarte, C. M. *et al.* (2013) 'Is Ocean Acidification an Open-Ocean Syndrome? Understanding Anthropogenic Impacts on Seawater pH', *Estuaries and Coasts*, 36(2), pp. 221–236. doi: 10.1007/s12237-013-9594-3.

Duarte, C. M. *et al.* (2015) 'Reconsidering ocean calamities', *BioScience*, 65(2), pp. 130–139. doi: 10.1093/biosci/biu198.

Dumbauld, B. R. *et al.* (2011) 'The Willapa Bay Oyster Reserves in Washington State: Fishery Collapse, Creating a Sustainable Replacement, and the Potential for Habitat Conservation and Restoration', *Journal of Shellfish Research*, 30(1), pp. 71–83. doi: 10.2983/035.030.0111.

Egleston, E. S., Sabine, C. L. and Morel, F. M. M. (2010) 'Revelle revisited: Buffer factors that quantify the response of ocean chemistry to changes in DIC and alkalinity', *Global Biogeochemical Cycles*, 24(1), pp. 1–9. doi: 10.1029/2008GB003407.

Ekstrom, J. A. *et al.* (2015) 'Vulnerability and adaptation of US shellfisheries to ocean acidification', *Nature Climate Change*. Nature Publishing Group, 5(3), pp. 207–214. doi: 10.1038/nclimate2508.

Engle, V. D. *et al.* (2007) 'A Classification of U . S . Estuaries Based on Physical and Hydrologic Attributes', pp. 397–412. doi: 10.1007/s10661-006-9372-9.

Fassbender, A. J. *et al.* (2018) 'Seasonal Carbonate Chemistry Variability in Marine Surface Waters of the Pacific Northwest', *Earth System Science Data Discussions*, (March), pp. 1–49.

Feely, R. A. *et al.* (2008) 'Evidence for upwelling of corrosive "acidified" water onto the continental shelf.', *Science*, 320(5882), pp. 1490–1492. doi: 10.1126/science.1155676.

Feely, R. A. *et al.* (2016) 'Chemical and biological impacts of ocean acidification along the west coast of North America', *Estuarine, Coastal and Shelf Science*, 183, pp. 260–270. doi: 10.1016/j.ecss.2016.08.043.

Feely, R. A. *et al.* (2018) 'The combined effects of acidification and hypoxia on pH and aragonite saturation in the coastal waters of the California current ecosystem and the northern Gulf of Mexico', *Continental Shelf Research*, 152(July 2017), pp. 50–60. doi: 10.1016/j.csr.2017.11.002.

Gazeau, F. *et al.* (2013) 'Impacts of ocean acidification on marine shelled molluscs', *Marine Biology*, 160(8), pp. 2207–2245. doi: 10.1007/s00227-013-2219-3.

Gimenez, I. *et al.* (2018) 'Ocean acidification stress index for shellfish (OASIS): Linking Pacific oyster larval survival and exposure to variable carbonate chemistry regimes', *Elementa Science of the Anthropocene*, 6(51). doi: 10.1525/elementa.306.

Gruber, N. *et al.* (2012) 'Rapid progression of ocean acidification in the California Current System', *Science*, 337(6091), pp. 220–3. doi: 10.1126/science.1216773.

Gruber, N. *et al.* (1996) 'An improved method for detecting anthropogenic CO2 in the oceans', *Global Biogeochemical Cycles*, 10(4), pp. 809–837.

Hagens, M. *et al.* (2015) 'Biogeochemical processes and buffering capacity concurrently affect acidification in a seasonally hypoxic coastal marine basin', pp. 1561–1583. doi: 10.5194/bg-12-1561-2015.

Hales, B. *et al.* (2017) 'The Carbonate Chemistry of the "Fattening Line," Willapa Bay, 2011–2014', *Estuaries and Coasts*. Estuaries and Coasts, 40(1), pp. 173–186. doi: 10.1007/s12237-016-0136-7.

Hales, B. *et al.* (2004) 'High-frequency measurement of partial pressure and total concentration of carbon dioxide in seawater using microporous hydrophobic membrane contactors', *Limnology and Oceanography: Methods*, 2(Weiss 1974), pp. 356–364. doi: 10.4319/lom.2004.2.356.

Hauri, C. *et al.* (2013) 'Spatiotemporal variability and long-term trends of ocean acidification in the California Current System', *Biogeosciences*, 10(1), pp. 193–216. doi: 10.5194/bg-10-193-2013.

Hauri, C. *et al.* (2013) 'The intensity, duration, and severity of low aragonite saturation state events on the California continental shelf', *Geophysical Research Letters*, 40(13), pp. 3424–3428. doi: 10.1002/grl.50618.

Hettinger, A. *et al.* (2012) 'Persistent carry-over effects of planktonic exposure to ocean acidification in the Olympia oyster', *Ecology*, 93(12), pp. 2758–2768. doi: 10.1890/12-0567.1.

Hofmann, G. E. *et al.* (2011) 'High-frequency dynamics of ocean pH: a multi-ecosystem comparison.', *PloS one*, 6(12), p. e28983. doi: 10.1371/journal.pone.0028983.
Hönisch, B. *et al.* (2012) 'The Geological record of ocean acidification', *Science*, 335(6072), pp. 1058–1063. doi: 10.1126/science.1208277.

Hu, X. *et al.* (2017) 'Effects of eutrophication and benthic respiration on water column carbonate chemistry in a traditional hypoxic zone in the Northern Gulf of Mexico', *Marine Chemistry*. Elsevier, 194(April), pp. 33–42. doi: 10.1016/j.marchem.2017.04.004.

Hu, X. and Cai, W. J. (2013) 'Estuarine acidification and minimum buffer zone - A conceptual study', *Geophysical Research Letters*, 40(19), pp. 5176–5181. doi: 10.1002/grl.51000.

Iles, A. C. *et al.* (2012) 'Climate-driven trends and ecological implications of event-scale upwelling in the California Current System', *Global Change Biology*, 18(2), pp. 783–796. doi: 10.1111/j.1365-2486.2011.02567.x.

Joesoef, A. *et al.* (2017) 'Seasonal variability of the inorganic carbon system in a large coastal plain estuary', pp. 4949–4963.

Kelly, R. P. *et al.* (2011) 'Mitigating Local Causes of Ocean Acidification with Existing Laws', *Science*, 332(6033), pp. 1036–1037. doi: 10.1126/science.1203815.

Kroeker, K. J. *et al.* (2013) 'Impacts of ocean acidification on marine organisms: Quantifying sensitivities and interaction with warming', *Global Change Biology*, 19(6), pp. 1884–1896. doi: 10.1111/gcb.12179.

Laurent, A. *et al.* (2018) 'Climate Change Projected to Exacerbate Impacts of Coastal Eutrophication in the Northern Gulf of Mexico', *Journal of Geophysical Research: Oceans*, pp. 3408–3426. doi: 10.1002/2017JC013583.

Lejart, M. *et al.* (2012) 'Respiration and Calcification of Crassostrea gigas: Contribution of an Intertidal Invasive Species to Coastal Ecosystem CO_2 Fluxes', *Estuaries and Coasts*, 35(2), pp. 622–632. doi: 10.1007/s12237-011-9462-y.

Mabardy, R. A. *et al.* (2015) 'Perception and Response of the U.S. West Coast Shellfish Industry to Ocean Acidification: The Voice of the Canaries in the Coal Mine', *Journal of Shellfish Research*, 34(2), pp. 565–572. doi: 10.2983/035.034.0241.

Marshall, K. N. *et al.* (2017) 'Risks of ocean acidification in the California Current food web and fisheries: ecosystem model projections', *Global Change Biology*, 23(4), pp. 1525–1539. doi: 10.1111/gcb.13594.

Mcgrath, T. *et al.* (2016) 'The Inorganic Carbon Chemistry in Coastal and Shelf Waters Around Ireland', pp. 27–39. doi: 10.1007/s12237-015-9950-6.

Meinvielle, M. and Johnson, G. C. (2013) 'Decadal water-property trends in the California Undercurrent, with implications for ocean acidification', *Journal of Geophysical Research: Oceans*, 118(12), pp. 6687–6703. doi: 10.1002/2013JC009299.

Moore-Maley, B. L. *et al.* (2018) 'The sensitivity of estuarine aragonite saturation state and pH to the carbonate chemistry of a freshet-dominated river', pp. 3743–3760.

Murray, J. W. *et al.* (2015) 'An inland sea high nitrate-low chlorophyll (HNLC) region with naturally high pCO2', *Limnology and Oceanography*, 60(3), pp. 957–966. doi: 10.1002/lno.10062.

Oh, N. and Raymond, P. A. (2006) 'Contribution of agricultural liming to riverine bicarbonate export and CO 2 sequestration in the Ohio River basin', 20(August), pp. 1–17. doi: 10.1029/2005GB002565.

Pacella, S. R. *et al.* (2018) 'Seagrass habitat metabolism increases short-term extremes and long-term offset of CO 2 under future ocean acidification', 115(15), pp. 1–6. doi: 10.23719/1407616.

Paulsen, M.-L. *et al.* (2018) 'Temporal Changes in Seawater Carbonate Chemistry and Carbon Export from a Southern California Estuary', *Estuaries and Coasts*. Estuaries and Coasts, 41(4), pp. 1050–1068. doi: 10.1007/s12237-017-0345-8.

Perrin, A., *et al.* (2008) 'Impact of nitrogenous fertilizers on carbonate dissolution in small agricultural catchments : Implications for weathering CO 2 uptake at regional and global scales', 72, pp. 3105–3123. doi: 10.1016/j.gca.2008.04.011.

Provoost, P. *et al.* (2010) 'Seasonal and long-term changes in pH in the Dutch coastal zone', *Biogeosciences*, 7(11), pp. 3869–3878. doi: 10.5194/bg-7-3869-2010.

Raymond, P. A. *et al.* (2008) 'Anthropogenically enhanced fluxes of water and carbon from the Mississippi River', *Nature*, 451(7177), pp. 449–452. doi: 10.1038/nature06505.

Regnier, P. *et al.* (2013) 'Anthropogenic perturbation of the carbon fluxes from land to ocean', *Nature Geoscience*, 6(8), pp. 597–607. doi: 10.1038/ngeo1830.

Reimer, J. J. *et al.* (2017) 'Time series pCO2 at a coastal mooring: Internal consistency, seasonal cycles, and interannual variability', *Continental Shelf Research*. doi: 10.1016/j.csr.2017.06.022.

Reum, J. C. P. *et al.* (2014) 'Interpretation and design of ocean acidification experiments in upwelling systems in the context of carboante chemsitry co-variation with temperature and oxygen', *ICES Journal of Marine Science*, 71(3), pp. 528–536. doi: 10.1093/icesjms/fst176.

Riebesell, U. *et al.* (2010) *Guide to best practices for ocean acidification research and data reporting*, *European commission*. doi: 10.2777/66906.

Robbins, L. L. and Lisle, J. T. (2018) 'Regional Acidification Trends in Florida Shellfish Estuaries : a 20 + Year Look at pH , Oxygen , Temperature , and Salinity'. Estuaries and Coasts, pp. 1268–1281.

Roegner, G. C. *et al.* (2011) 'Coastal upwelling supplies oxygen-depleted water to the columbia river estuary', *PLoS ONE*, 6(4). doi: 10.1371/journal.pone.0018672.

Sabine, C. L. *et al.* (2002) 'Distribution of anthropogenic CO2 in the Pacific Ocean', *Global Biogeochemical Cycles*, 16(4), pp. 30-1-30–17. doi: 10.1029/2001GB001639.
Sabine, C. L. *et al.* (2004) 'The oceanic sink for anthropogenic CO2', *Science*, 305(5682), pp. 367–371. doi: 10.1126/science.1097403.

Shanks, O. C. *et al.* (2006) 'Basin-wide analysis of the dynamics of fecal contamination and fecal source identification in Tillamook Bay, Oregon', *Applied and Environmental Microbiology*, 72(8), pp. 5537–5546. doi: 10.1128/AEM.03059-05.

Sosdian, S. M. *et al.* (2018) 'Constraining the evolution of Neogene ocean carbonate chemistry using the boron isotope pH proxy', *Earth and Planetary Science Letters*. Elsevier B.V., 498, pp. 362–376. doi: 10.1016/j.epsl.2018.06.017.

Stets, E. G. *et al.* (2014) 'Long-term trends in alkalinity in large rivers of the conterminous US in relation to acidification, agriculture, and hydrologic modification', *Science of the Total Environment*. Elsevier B.V., 488–489(1), pp. 280–289. doi: 10.1016/j.scitotenv.2014.04.054.

Strong, A. L. *et al.* (2014) 'Ocean acidification 2.0: Managing our Changing Coastal Ocean Chemistry', *BioScience*, 64(7), pp. 581–592. doi: 10.1093/biosci/biu072.

Suchet, P. A. and Ludwig, W. (2003) 'Worldwide distribution of continental rock lithology : Implications for the atmospheric / soil CO 2 uptake by continental weathering and alkalinity river transport to the oceans', 17(2). doi: 10.1029/2002GB001891.

Sullivan, T. J. *et al.* (2005) 'Assessment of water quality in association with land use in the Tillamook Bay Watershed, Oregon, USA', *Water, Air, and Soil Pollution*, 161(1–4), pp. 3–23. doi: 10.1007/s11270-005-2443-7.

Sunda, W. G. and Cai, W. (2012) 'Eutrophication Induced CO_2 -Acidification of Subsurface Coastal Waters: Interactive Effects of Temperature, Salinity, and Atmospheric pCO_2', *Environmental Science & Technology*, 46(19), pp. 10651–10659. doi: 10.1021/es300626f.

Sutton, A. J. *et al.* (2016) 'Using present-day observations to detect when anthropogenic change forces surface ocean carbonate chemistry outside pre-industrial bounds', *Biogeosciences Discussions*, (March), pp. 1–30. doi: 10.5194/bg-2016-104.

Takeshita, Y. *et al.* (2015) 'Including high-frequency variability in coastal ocean acidification projections', *Biogeosciences*, 12(19), pp. 5853–5870. doi: 10.5194/bg-12-5853-2015.

Tillamook Estuaries Partnership (2015) 'State of the Bays 2015: Health Report', pp. 1–58. Available at: http://www.tbnep.org/reports-and-publications.php.

Turi, G. *et al.* (2016) 'Climatic modulation of recent trends in ocean acidification in the California Current System', *Environmental Research Letters*. IOP Publishing, 11(1), p. 14007. doi: 10.1088/1748-9326/11/1/014007.

USDA-NASS (2012) 'Census of Agriculture County Profile Tillamook County – Oregon'.

Waldbusser, G. G. *et al.* (2011) 'Biocalcification in the Eastern Oyster (Crassostrea virginica) in Relation to Long-term Trends in Chesapeake Bay pH', *Estuaries and Coasts*, 34(2), pp. 221–231. doi: 10.1007/s12237-010-9307-0.

Waldbusser, G. G., Hales, B., Langdon, C. J., *et al.* (2015) 'Ocean acidification has multiple modes of action on bivalve larvae', *PLoS ONE*, 10(6). doi: 10.1371/journal.pone.0128376.

Waldbusser, G. G., Hales, B., Langdon, C. J., *et al.* (2015) 'Saturation-state sensitivity of marine bivalve larvae to ocean acidification', *Nature Climate Change*, 5(3), pp. 273–280. doi: 10.1038/NCLIMATE2479.

Waldbusser, G. G., Bergschneider, H. and Green, M. A. (2010) 'Size-dependent pH effect on calcification in post-larval hard clam Mercenaria spp', *Marine Ecology Progress Series*, 417(x), pp. 171–182. doi: 10.3354/meps08809.

Waldbusser, G. G. and Salisbury, J. E. (2014) 'Ocean acidification in the coastal zone from an organism's perspective: multiple system parameters, frequency domains, and habitats.', *Annual review of marine science*, 6, pp. 221–47. doi: 10.1146/annurev-marine-121211-172238.

Wallace, R. B. *et al.* (2014) 'Coastal ocean acidification: The other eutrophication problem', *Estuarine, Coastal and Shelf Science*. Elsevier Ltd, 148, pp. 1–13. doi: 10.1016/j.ecss.2014.05.027.

Wang, Z. A. *et al.* (2016) 'Intertidal salt marshes as an important source of inorganic carbon to the coastal ocean', *Limnology and Oceanography*, 61(5), pp. 1916–1931. doi: 10.1002/lno.10347.

Weisberg, S. B. *et al.* (2016) 'Water quality criteria for an acidifying ocean: Challenges and opportunities for improvement', *Ocean & Coastal Management*, 126, pp. 31–41. doi: 10.1016/j.ocecoaman.2016.03.010.

Xue, L. *et al.* (2017) 'Sea surface aragonite saturation state variations and control mechanisms at the Gray's Reef time-series site off Georgia, USA (2006–2007)'. doi: 10.1016/j.marchem.2017.05.009.

Yang, B., Byrne, R. H. and Lindemuth, M. (2015) 'Contributions of organic alkalinity to total alkalinity in coastal waters: A spectrophotometric approach', *Marine Chemistry*. doi: 10.1016/j.marchem.2015.09.008.

Zhang, S. *et al.* (2009) 'Major ion chemistry and dissolved inorganic carbon cycling in a human-disturbed mountainous river (the Luodingjiang River) of the Zhujiang (Pearl River), China', *Science of the Total Environment, The*. Elsevier B.V., 407(8), pp. 2796–2807. doi: 10.1016/j.scitotenv.2008.12.036.

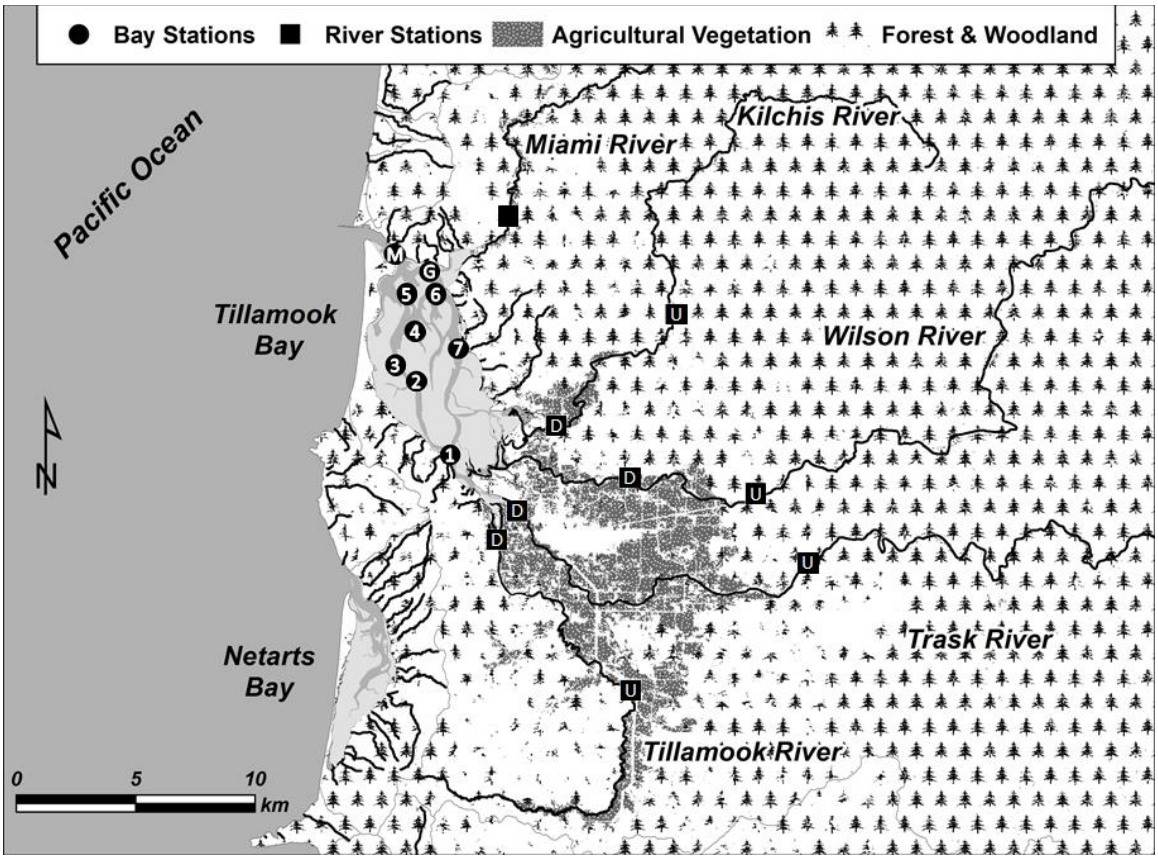

Figure 4.1. Map of study sites in Tillamook Estuary, OR, USA. Bay stations are indicated by numbered and lettered circles. Upriver sampling stations indicated by "U" and downriver sampling stations indicated by "D". Agricultural land use and forested areas of the watershed indicated as in the legend.

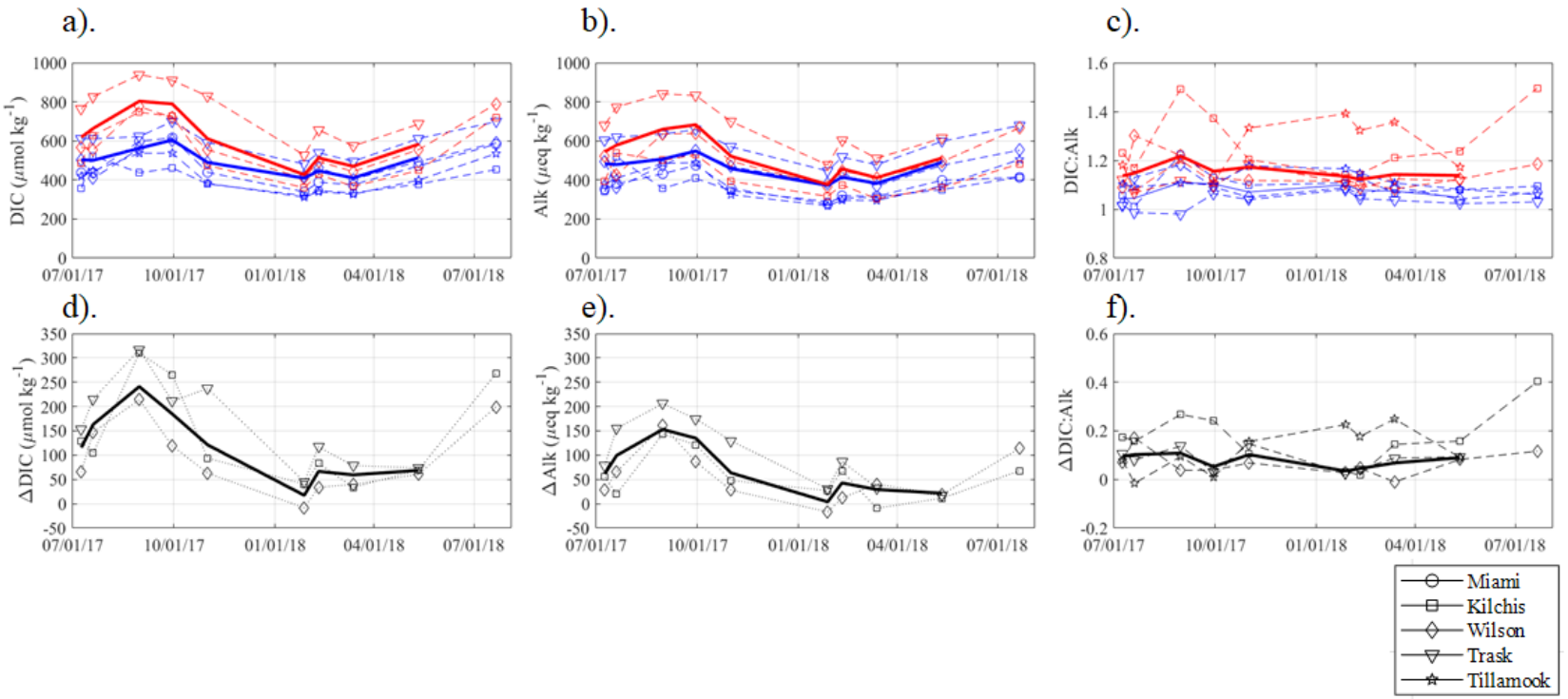

Figure 4.2. Observations of upriver (red) and downriver (blue) **a).** DIC and **b).** Alk for all sampling dates from July 2017 – July 2018. Flow-weighted averages amongst all rivers indicated by bold lines. **c).** DIC:Alk ratios for upriver (red) and downriver (blue) sampling stations. Flow-weighted averages indicated by bold lines. **d).** Downriver enrichments of DIC for each river and flow-weighted average (bold). Enrichments calculated as downriver DIC – upriver DIC. **e).** Downriver enrichments of Alk for each river and flow-weighted average (bold). Enrichments calculated as downriver Alk – upriver Alk. **f).** Changes in DIC:Alk ratio between downstream and upstream stations, including the flow-weighed average (bold).

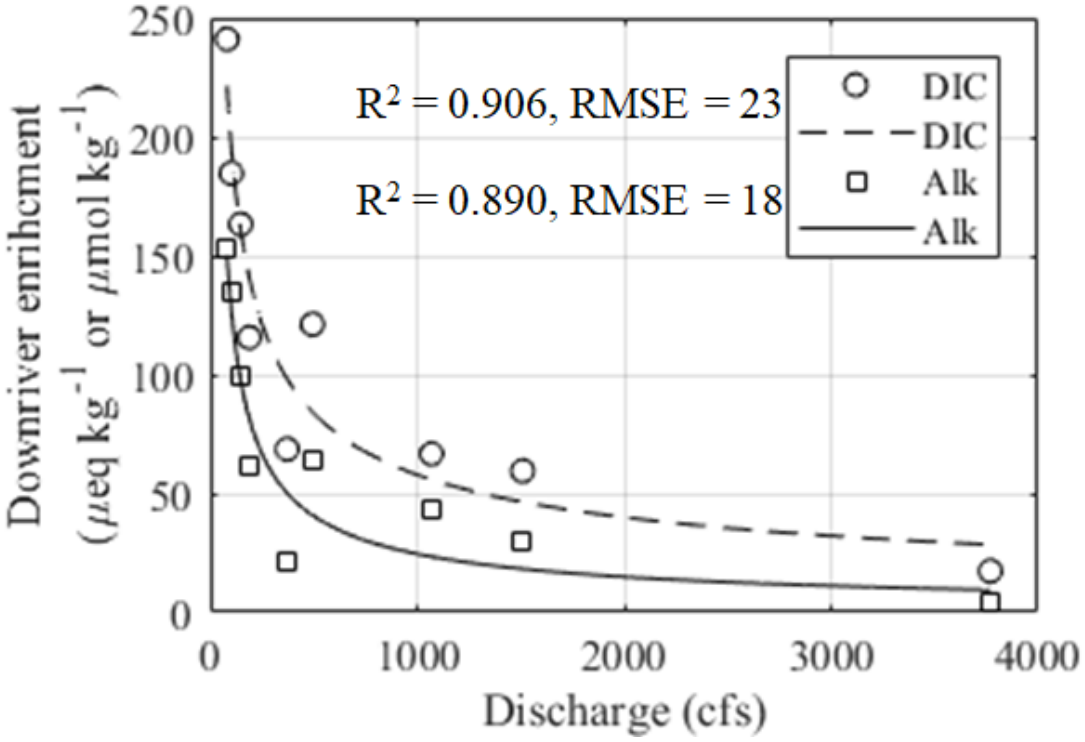

Figure 4.3. Scatter plot of flow-weighted average downriver DIC and Alk enrichments for each cruise as a function of Trask River discharge with fitted power functions.

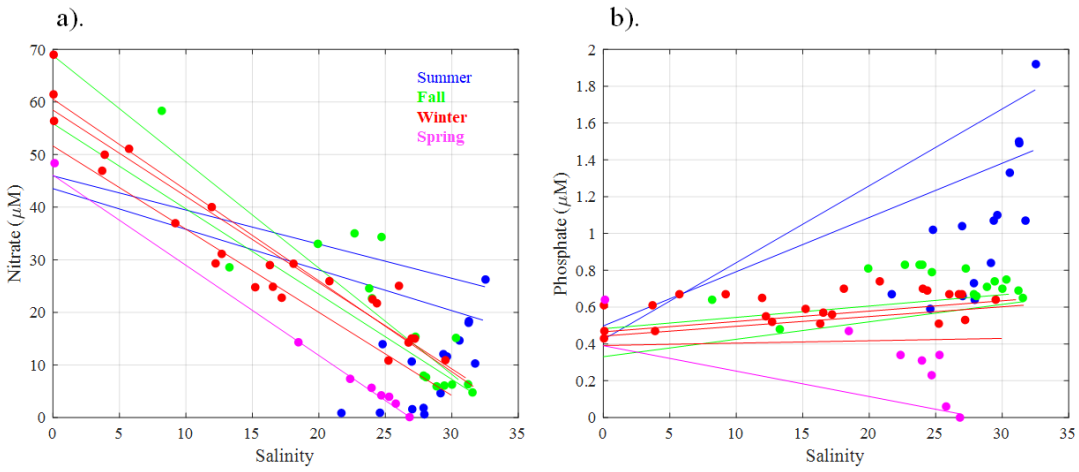

Figure 4.4. Observations of **a).** DIN and **b).** phosphate concentrations in Tillamook Estuary for all cruises, color-coded by season. Conservative mixing lines between coastal ocean and flow-weighted average river end-members are plotted using same color-coding.

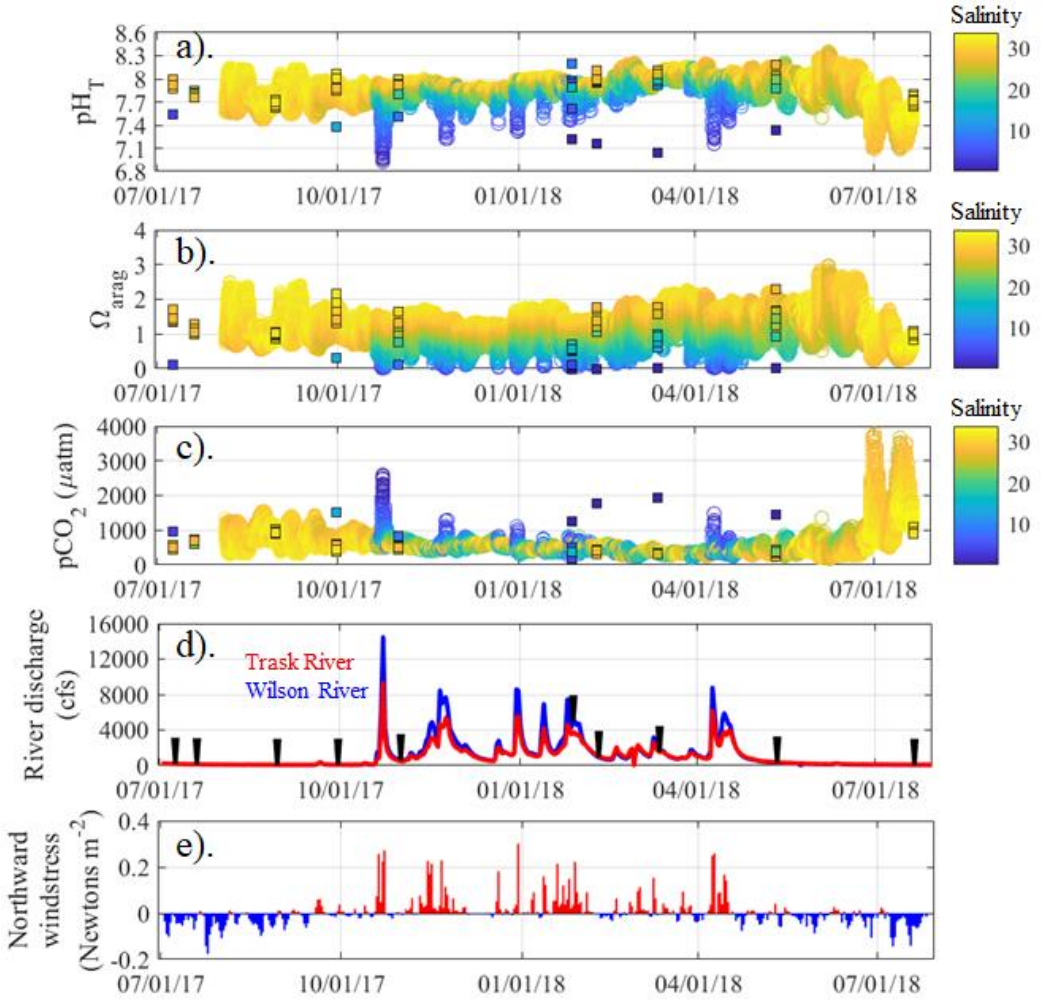

Figure 4.5. Times series from the Garibaldi mooring of **a).** observed pH_T, **b).** calculated Ω_{arag}, and **c).** calculated pCO_2. Salinity for each observation indicated by shading in legends. Squares indicate observations from bay cruises. **d).** Time series of discharge from Trask and Wilson Rivers, with timing of bay cruises indicated by black arrows. **e).** Northward wind stress during study period. Negative (blue) values indicate upwelling-favorable conditions.

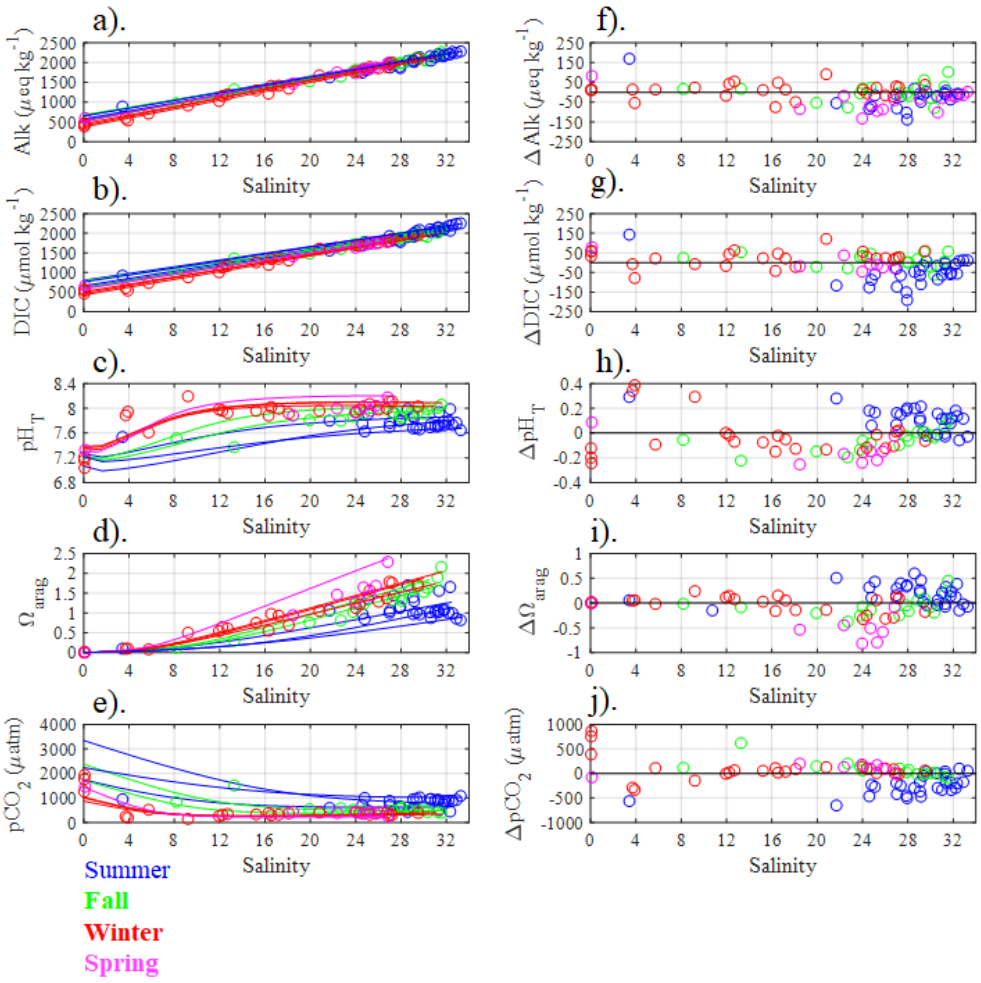

Figure 4.6. Observations of **a).** Alk, **b).** DIC, **c).** pH_T, **d).** Ω_{arag}, and **e).** pCO_2 from the bay cruises. Lines are conservative mixing lines between the coastal ocean and flow-weighted average river end-members. **f-j).** Departures of observed carbonate system indices from conservative mixing values. Positive values indicate bay values were higher than estimated from conservative mixing alone, while negative values indicate bay values were lower than estimated.

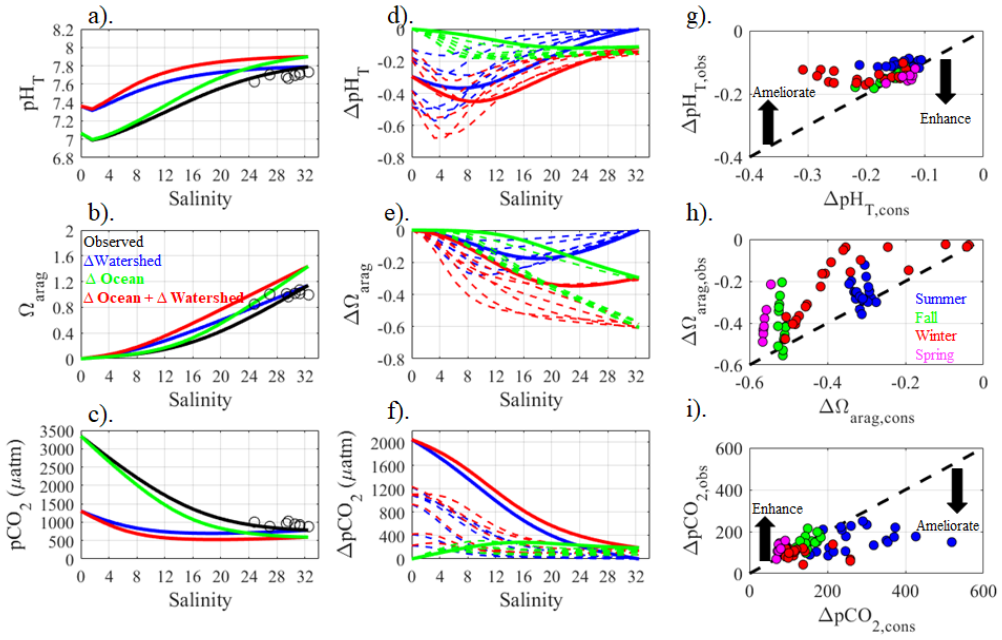

Figure 4.7. Observed and predicted conservative mixing lines for **a).** pH_T, **b).** Ω_{arag}, and **c).** pCO_2 for the August 2017 cruise. Black circles are observations from bay cruises, and black lines are conservative mixing curves between the observed coastal ocean and flow-weighted average river end-members. Blue lines are mixing curves assuming no watershed human influence, green lines are mixing curves assuming no coastal ocean human influence, and red lines are mixing curves assuming no human influence in both watershed and coastal ocean. **d-f).** Changes in mixing curves of carbonate parameters with varying levels of watershed and coastal ocean human influences, as in a-c. Curves represent the change in present-day conditions due to human influence with varying combination of watershed and coastal ocean perturbations. **g-h).** Changes in bay cruise chemistry predicted by conservative mixing alone ($\Delta pH_{T,cons}$, $\Delta\Omega_{arag,cons}$, and $\Delta pCO_{2,cons}$), and the interactions of conservative mixing plus local bay carbon cycling ($\Delta pH_{T,obs}$, $\Delta\Omega_{arag,obs}$, and $\Delta pCO_{2,obs}$). 1:1 lines indicated by dotted lines. Arrows indicate directions in which local bay carbon cycling either ameliorates or enhances the effects of watershed and oceanic human influences on bay carbonate parameter changes. Arrows for $\Delta\Omega_{arag}$ are same as for ΔpH_T but are excluded for clarity.

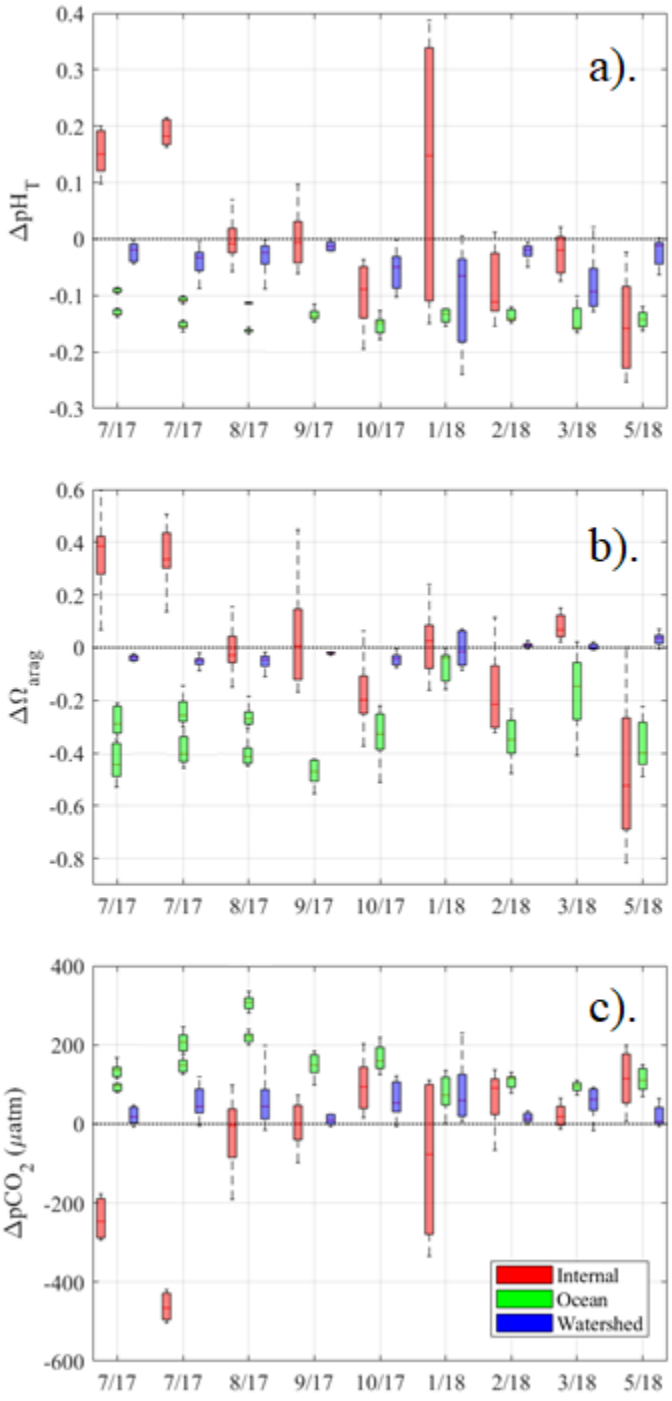

Figure 4.8. Changes in bay **a).** pH_T, **b).** Ω_{arag}, and **c).** pCO_2 driven by internal carbon cycling (red), coastal ocean C_{anth} (green), and watershed downstream DIC and Alk enrichments ($DIC_{enrich,riv}$ and $Alk_{enrich,riv}$). Summer cruises show two boxplots for oceanic influence, representing changes predicted based on C_{anth} levels of both upwelled and surface ocean waters.

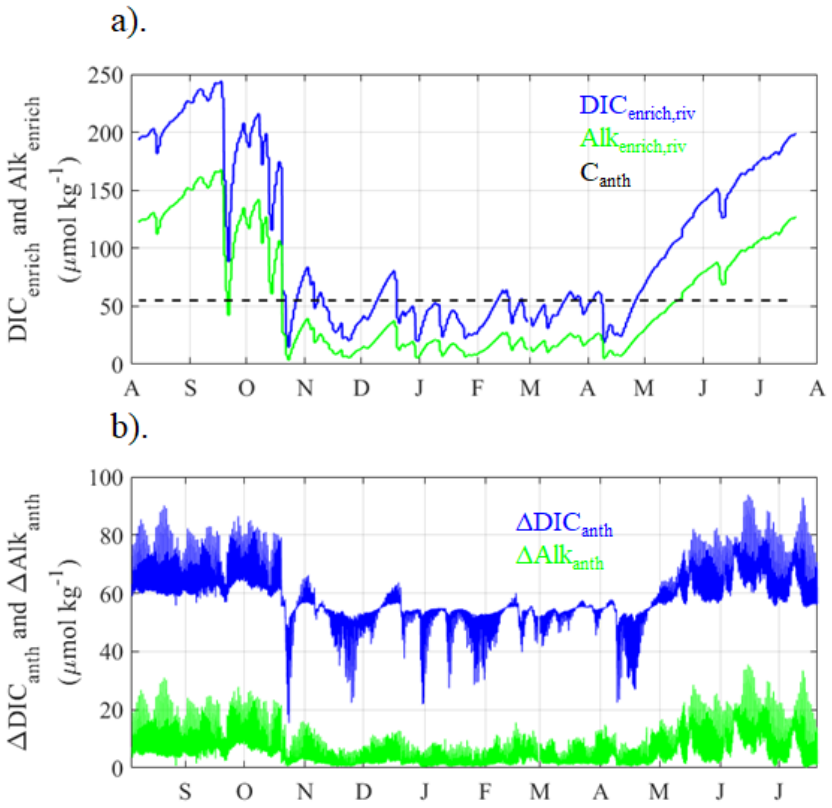

Figure 4.9. a). Time series of downstream watershed enrichments of DIC (blue) and Alk (green) calculated from river discharge during the study period. Dotted line indicates ocean C_{anth} value for surface waters. **b).** Time series of anthropogenic DIC (blue) and Alk (green) at the Garibaldi mooring. These values represent the sum of ocean and watershed human influences at the mooring.

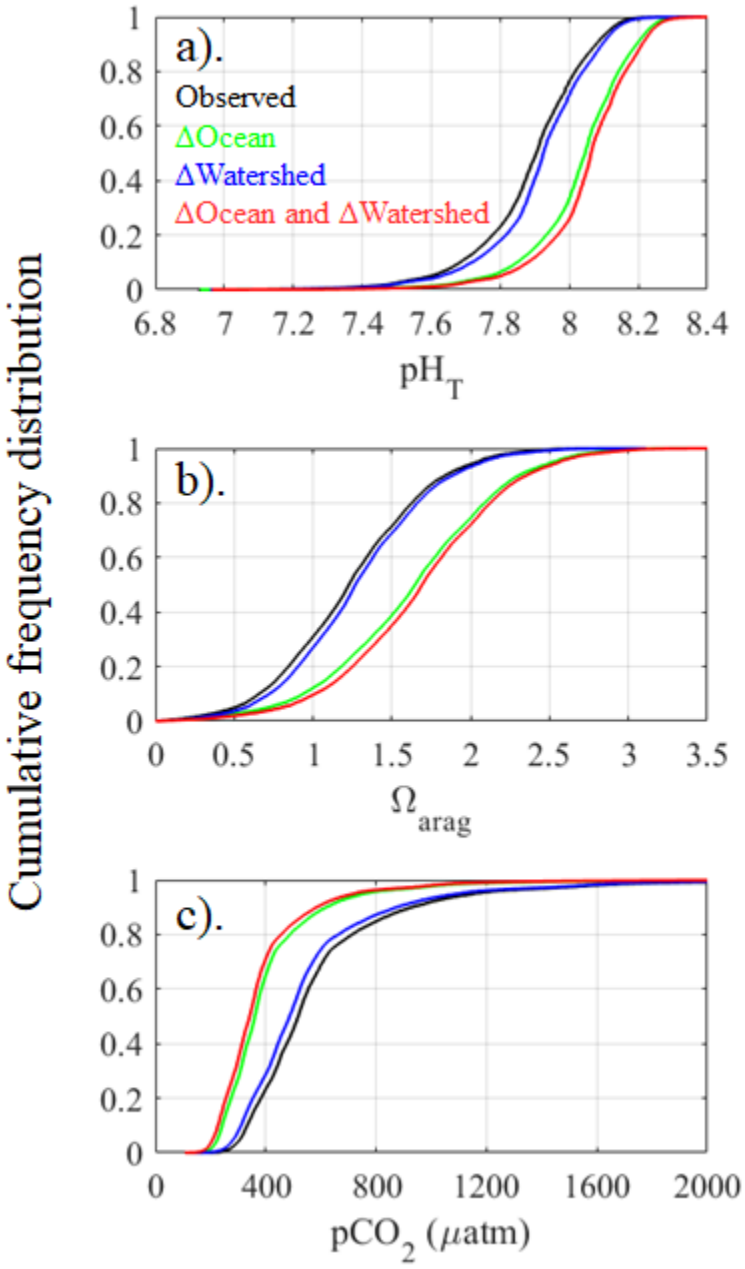

Figure 4.10. Frequency distributions of **a).** pH_T, **b).** Ω_{arag}, and **c).** pCO_2 at the Garibaldi mooring observed during this study (black), with removal of oceanic C_{anth} influence (green), with removal of watershed human influence (blue), and removal of both oceanic and watershed human influences (red).

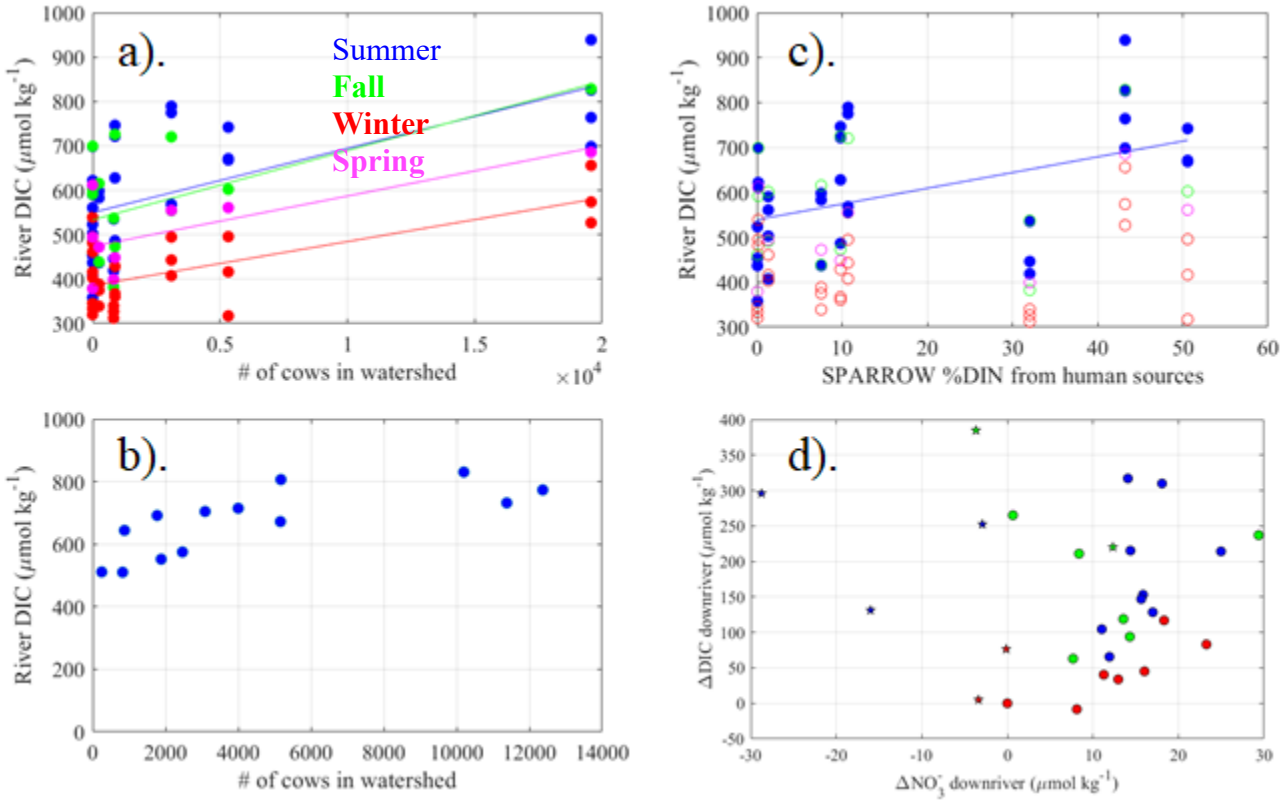

Figure 4.11. Observed river DIC concentrations compared with **a).** the number of cows in the watershed of each sampling sites for all cruises during this study, and **b).** a separate targeted river sampling during August 2017 without a concurrent bay cruise. Lines in panel a). represent significant correlations (summer $r = 0.64$, $p < 0.001$; fall $r = 0.57$, $p = 0.013$; winter $r = 0.67$, $p < 0.001$; spring $r = 0.72$, $p = 0.019$). **c).** Observed river DIC concentrations compared with proportions of anthropogenic nitrogen sources at the river sampling sites as predicted by the USGS SPARROW model. **d).** Comparison of downriver DIC enrichments and downriver NO_3^- enrichments for each river and all cruises.

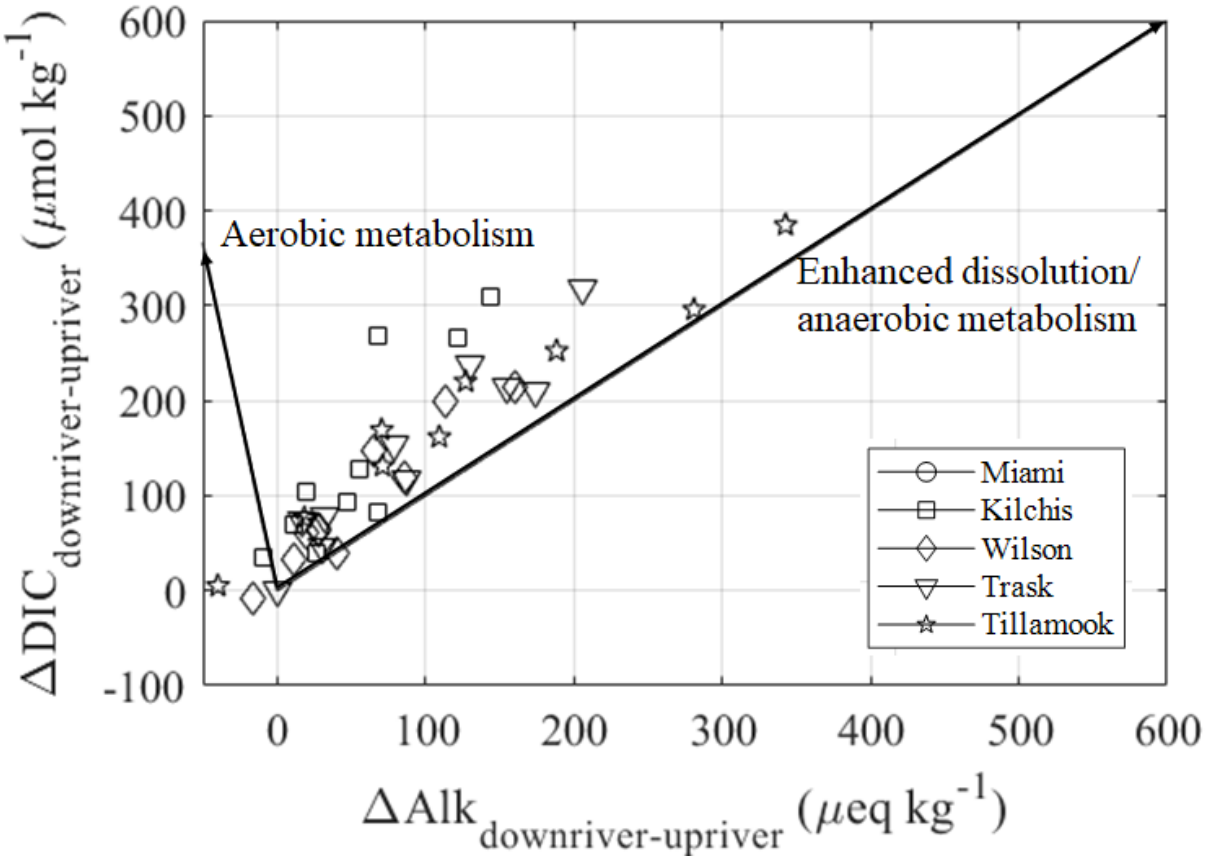

Figure 4.12. Scatterplot of downriver Alk and DIC enrichments for each river and all cruises during the study. Arrows represent theoretical DIC:Alk enrichment ratios for potential biogeochemical processes responsible for observed enrichments.

Table 4.1. Carbonate chemistry parameters of upriver and downriver sampling stations during the study period.

	Sampling date	Miami River	Wilson River		Kilchis River		Trask River		Tillamook River	
			Upriver	Downriver	Upriver	Downriver	Upriver	Downriver	Upriver	Downriver
Alk (µeq kg^{-1})	7/7/2017	353	339	395	493	522	602	681	380	569
	7/18/2017	N/A	517	537	360	426	619	774	409	690
	8/9/2017	432	356	500	474	635	635	841	485	556
	9/28/2017	475	408	N/A	552	N/A	657	N/A	488	N/A
	10/30/2017	356	345	393	468	496	569	699	325	452
	1/25/2017	276	289	316	382	365	446	476	268	228
	2/9/2018	319	306	374	435	447	517	604	296	315
	3/12/2018	316	312	303	369	409	478	510	295	365
	5/10/2018	398	350	362	475	494	598	614	369	478
	7/20/2018	413	414	482	552	666	678	678	505	1,046
DIC (µmol kg^{-1})	7/7/2017	437	358	486	503	568	611	764	419	671
	7/18/2017	N/A	523	628	407	554	611	826	446	742
	8/9/2017	598	437	746	561	775	622	939	537	668
	9/28/2017	615	461	N/A	601	N/A	699	N/A	537	N/A
	10/30/2017	439	379	473	491	554	591	829	382	602
	1/25/2017	339	320	360	416	408	482	527	312	317
	2/9/2018	388	345	428	461	495	539	656	340	416
	3/12/2018	375	333	367	403	443	495	574	327	496
	5/10/2018	472	379	448	494	555	612	686	399	561
	7/20/2018	583	453	722	590	789	698	N/A	535	1,115

Table 4.1 (Continued).

	Sampling date	Miami River	Wilson River		Kilchis River		Trask River		Tillamook River	
			Upriver	Downriver	Upriver	Downriver	Upriver	Downriver	Upriver	Downriver
pH_T	7/7/2017	7.02	7.63	7.03	7.98	7.41	8.05	7.28	7.38	7.07
	7/18/2017	N/A	8.13	7.17	7.26	6.89	8.57	7.50	7.43	7.44
	8/9/2017	6.82	7.03	6.70	7.10	7.03	8.62	7.27	7.34	7.02
	9/28/2017	6.94	7.29	N/A	7.43	N/A	7.59	N/A	7.38	N/A
	10/30/2017	7.07	7.45	7.13	7.73	7.37	7.82	7.15	7.19	6.88
	1/25/2017	7.11	7.43	7.32	7.52	7.41	7.56	7.44	7.24	6.87
	2/9/2018	7.14	7.37	7.32	7.69	7.45	7.83	7.54	7.31	6.96
	3/12/2018	7.19	7.64	7.15	7.51	7.55	7.88	7.36	7.42	6.88
	5/10/2018	7.17	7.52	7.05	7.77	7.32	7.98	7.34	7.50	7.15
	7/20/2018	6.80	7.57	6.85	7.52	7.10	7.85	7.85	7.59	7.17
$pCO_{2\ (\mu atm)}$	7/7/2017	1,827	439	2,003	289	1,153	291	2,004	871	2,550
	7/18/2017	N/A	212	1,990	1,111	3,118	87	1,312	840	1,322
	8/9/2017	3,476	1,874	5,441	2,138	3,363	83	2,436	1,243	2,783
	9/28/2017	2,865	1,125	N/A	1,108	N/A	901	N/A	1,100	N/A
	10/30/2017	1,558	640	1,510	449	1,098	439	2,501	1,094	2,969
	1/25/2017	1,094	538	769	576	714	613	861	776	1,538
	2/9/2018	1,244	692	969	473	851	408	939	779	1,853
	3/12/2018	1,025	360	1,099	578	578	314	1,115	571	2,452
	5/10/2018	1,406	558	1,691	426	1,245	330	1,483	618	1,840
	7/20/2018	3,429	512	3,107	951	2,976	519	519	728	2,165

Table 4.2. Observations of physical and biogeochemical parameters at bay stations (including the marine station "M") during the full study period.

		Station ID									
	Sampling Date	**1**	**2**	**3**	**4**	**5**	**6**	**7**	**G**	**Bay mean**	**M**
Alk (µeq kg^{-1})	7/7/2017	891	1,827	2,041	2,175	2,210	2,042	N/A	1,940	**1,875**	2,223
	7/18/2017	N/A	1,747	1,895	2,015	2,159	1,863	1,628	1,874	**1,883**	2,224
	8/9/2017	1,821	2,109	2,135	2,210	2,269	2,161	1,990	2,206	**2,113**	2,275
	9/28/2017	1,325	1,985	2,062	2,067	2,270	2,129	1,989	2,180	**2,001**	2,171
	10/30/2017	972	1,855	1,648	1,777	2,050	1,812	1,525	1,966	**1,701**	2,138
	1/25/2017	388	712	1,345	917	1,031	598	541	1,219	**844**	2,122
	2/9/2018	475	1,776	1,679	1,856	2,099	1,953	1,777	1,890	**1,688**	2,175
	3/12/2018	429	1,159	1,197	1,299	2,004	1,413	1,416	1,887	**1,350**	2,136
	5/10/2018	601	1,731	1,844	1,880	1,985	1,840	1,469	1,755	**1,638**	2,025
	7/20/2018	N/A	2,050	2,207	2,249	2,283	2,195	2,043	2,141	**2,167**	2,285
DIC (µmol kg^{-1})	7/7/2017	921	1,725	1,933	2,045	2,067	1,901	N/A	1,827	**1,774**	2,128
	7/18/2017	N/A	1,686	1,815	1,916	2,088	1,779	1,561	1,803	**1,807**	2,174
	8/9/2017	1,782	2,052	2,085	2,144	2,211	2,102	1,933	2,146	**2,057**	2,199
	9/28/2017	1,361	1,888	1,935	1,942	2,081	1,995	1,881	2,016	**1,887**	2,025
	10/30/2017	1,003	1,767	1,601	1,708	1,910	1,723	1,485	1,865	**1,633**	1,980
	1/25/2017	461	733	1,306	878	1,005	604	542	1,197	**841**	1,971
	2/9/2018	572	1,695	1,608	1,755	1,954	1,800	1,684	1,780	**1,606**	1,993
	3/12/2018	534	1,127	1,170	1,256	1,862	1,346	1,354	1,757	**1,301**	1,972
	5/10/2018	667	1,638	1,733	1,743	1,788	1,709	1,412	1,647	**1,542**	1,815
	7/20/2018	N/A	2,038	2,186	2,235	2,252	2,124	1,989	2,078	**2,129**	2,244

Table 4.2. (Continued).

	Station ID										
	Sampling Date	**1**	**2**	**3**	**4**	**5**	**6**	**7**	**G**	**Bay mean**	**M**
pH_T	7/7/2017	7.537	7.910	7.876	7.937	7.988	7.988	N/A	7.924	**7.880**	7.860
	7/18/2017	N/A	7.753	7.796	7.852	7.782	7.810	7.802	7.764	**7.794**	7.719
	8/9/2017	7.626	7.683	7.662	7.726	7.732	7.695	7.702	7.706	**7.692**	7.788
	9/28/2017	7.374	7.845	7.920	7.916	8.060	7.930	7.876	8.007	**7.866**	7.965
	10/30/2017	7.516	7.923	7.798	7.869	7.990	7.936	7.808	7.921	**7.845**	8.026
	1/25/2017	7.212	7.610	7.917	8.195	7.983	7.888	7.946	7.884	**7.829**	8.027
	2/9/2018	7.161	7.945	7.961	7.979	8.032	8.113	7.980	7.993	**7.896**	8.092
	3/12/2018	7.039	7.964	7.924	7.960	8.114	8.022	7.994	8.072	**7.886**	8.084
	5/10/2018	7.329	7.934	7.961	8.042	8.179	8.035	7.882	7.998	**7.920**	8.207
	7/20/2018	N/A	7.744	7.798	7.767	7.648	7.727	7.677	7.708	**7.724**	7.677
$pCO_{2\ (\mu atm)}$	7/7/2017	944	486	574	511	450	431	N/A	488	**555**	627
	7/18/2017	N/A	697	658	601	745	626	594	712	**662**	889
	8/9/2017	1,002	963	1,026	891	880	947	885	932	**941**	770
	9/28/2017	1,509	609	519	521	388	520	565	430	**633**	475
	10/30/2017	843	474	584	524	423	451	542	495	**542**	402
	1/25/2017	1,262	520	371	148	263	248	193	382	**423**	395
	2/9/2018	1,766	428	401	404	389	299	391	395	**559**	340
	3/12/2018	1,946	308	348	331	311	298	322	323	**523**	343
	5/10/2018	1,262	520	371	148	263	248	193	382	**423**	243
	7/20/2018	N/A	963	894	922	1,083	881	951	907	**943**	1,009

Table 4.2. (Continued).

	Station ID										
	Sampling Date	**1**	**2**	**3**	**4**	**5**	**6**	**7**	**G**	**Bay mean**	**M**
Ω_{arag}	7/7/2017	0.10	1.36	1.40	1.56	1.66	1.70	N/A	1.44	**1.31**	1.25
	7/18/2017	N/A	0.98	1.13	1.30	1.06	1.16	1.06	1.06	**1.11**	0.92
	8/9/2017	0.85	1.01	0.96	1.07	0.99	1.02	1.01	1.02	**0.99**	1.12
	9/28/2017	0.30	1.31	1.59	1.53	2.16	1.67	1.41	1.89	**1.48**	1.70
	10/30/2017	0.13	1.22	0.81	1.03	1.63	1.22	0.76	1.33	**1.02**	1.84
	1/25/2017	0.00	0.08	0.69	0.50	0.54	0.10	0.10	0.55	**0.32**	1.73
	2/9/2018	0.00	1.12	1.05	1.28	1.70	1.79	1.22	1.37	**1.19**	2.02
	3/12/2018	0.02	0.64	0.61	0.75	1.76	0.98	0.93	1.56	**0.91**	1.85
	5/10/2018	0.00	1.27	1.43	1.69	2.29	1.65	0.94	1.46	**1.34**	2.45
	7/20/2018	N/A	0.87	0.99	0.86	0.82	1.09	0.97	1.04	**0.95**	0.87
Salinity	7/7/2017	3.42	25.08	29.06	31.35	32.33	28.58	20.21	27.36	**24.67**	32.45
	7/18/2017	N/A	24.59	27.87	29.15	31.75	27.93	21.69	27.02	**27.14**	32.32
	8/9/2017	24.79	29.36	29.63	31.26	32.53	30.57	26.98	31.28	**29.55**	32.47
	9/28/2017	13.27	28.06	28.85	30.01	31.55	29.43	27.87	31.22	**27.53**	31.62
	10/30/2017	8.18	24.71	22.68	23.78	30.31	23.99	19.92	27.26	**22.60**	30.48
	1/25/2017	0.04	5.72	18.09	9.20	11.94	3.70	3.89	16.31	**8.61**	31.02
	2/9/2018	0.05	24.03	20.79	26.02	29.51	26.97	24.36	26.74	**22.31**	31.60
	3/12/2018	0.08	12.23	12.69	15.21	27.21	16.54	17.20	25.23	**15.80**	29.94
	5/10/2018	0.12	23.96	25.28	25.78	26.82	24.69	18.46	22.35	**20.93**	26.82
	7/20/2018	N/A	30.63	32.21	32.88	33.26	31.82	29.07	31.02	**31.56**	33.35

Table 4.2. (Continued).

	Station ID										
	Sampling Date	**1**	**2**	**3**	**4**	**5**	**6**	**7**	**G**	**Bay mean**	**M**
Temperature (°C)	7/7/2017	18.7	16.3	14.9	12.1	10.2	14.2	18.0	14.9	**14.9**	9.6
	7/18/2017	N/A	17.6	16.0	14.7	10.5	16.3	19.6	16.6	**15.9**	9.4
	8/9/2017	19.8	16.1	15.7	13.5	10.0	14.6	17.1	13.2	**15.0**	10.1
	9/28/2017	18.9	15.9	15.7	14.6	13.2	15.4	16.3	13.6	**15.5**	13.0
	10/30/2017	10.8	12.4	12.3	12.3	12.4	12.6	12.9	12.5	**12.3**	12.4
	1/25/2017	7.6	7.8	9.0	7.9	8.1	7.4	7.7	8.8	**8.0**	10.7
	2/9/2018	9.1	10.4	10.2	10.4	10.7	10.4	10.5	10.6	**10.3**	10.7
	3/12/2018	9.7	10.0	9.9	10.0	9.7	10.4	10.7	10.1	**10.1**	9.5
	5/10/2018	14.9	15.0	14.7	14.0	13.3	14.6	15.9	15.2	**14.7**	13.2
	7/20/2018	N/A	15.0	13.3	11.1	9.4	14.0	16.4	14.6	**13.4**	9.3
DIN (µM)	7/7/2017	24.6	6.4	10.7	11.3	10.3	7.8	4.0	7.4	**10.3**	13.8
	7/18/2017	N/A	1.0	1.9	4.7	10.4	0.7	0.9	1.7	**3.0**	18.7
	8/9/2017	14.2	12.3	11.9	18.3	26.5	14.9	10.9	18.6	**15.9**	25.1
	9/28/2017	28.9	7.9	6.1	6.4	4.9	6.3	8.2	6.5	**9.4**	4.7
	10/30/2017	58.6	34.6	35.3	24.8	15.4	22.9	33.3	15.6	**30.1**	7.4
	1/25/2017	61.6	51.3	29.4	37.1	40.2	47.1	50.0	29.1	**43.2**	7.8
	2/9/2018	69.1	22.7	26.2	25.3	11.2	15.3	22.0	14.5	**25.8**	6.2
	3/12/2018	56.4	29.3	31.1	24.8	15.0	24.9	22.8	10.9	**26.9**	4.3
	5/10/2018	48.6	5.8	4.1	2.7	0.1	4.3	14.5	7.5	**10.9**	0.1
	7/20/2018	N/A	N/A	N/A	N/A	N/A	N/A	N/A	N/A	N/A	N/A

Table 4.2. (Continued).

	Station ID										
	Sampling Date	**1**	**2**	**3**	**4**	**5**	**6**	**7**	**G**	**Bay mean**	**M**
PO_4^{3-} (µM)	7/7/2017	0.53	0.69	1.16	1.09	1.05	0.89	0.54	0.80	**0.84**	1.30
	7/18/2017	N/A	0.59	0.73	0.84	1.07	0.64	0.67	0.66	**0.74**	1.45
	8/9/2017	1.02	1.07	1.10	1.50	1.92	1.33	1.04	1.49	**1.31**	1.78
	9/28/2017	0.48	0.66	0.71	0.70	0.65	0.74	0.67	0.69	**0.66**	0.63
	10/30/2017	0.28	0.31	0.31	0.27	0.23	0.26	0.25	0.27	**0.27**	0.67
	1/25/2017	0.61	0.67	0.70	0.67	0.65	0.61	0.47	0.51	**0.61**	0.64
	2/9/2018	0.43	0.70	0.74	0.67	0.64	0.67	0.69	0.67	**0.65**	0.61
	3/12/2018	0.13	0.12	0.10	0.09	0.10	0.09	0.09	0.10	**0.10**	0.10
	5/10/2018	0.64	0.31	0.34	0.06	0.00	0.23	0.47	0.34	**0.30**	0.02
	7/20/2018	N/A	N/A	N/A	N/A	N/A	N/A	N/A	N/A	N/A	N/A

5. Conclusion

The unifying goals of the research in this dissertation were to 1). Characterize the drivers of estuarine carbonate system variability on time scales relevant for organismal fitness (i.e. "carbonate weather"), 2). Attribute the natural and anthropogenically-driven signals in present-day estuarine carbonate weather observations, and 3). Quantify the relative roles of atmospheric CO_2 and oceanic C_{anth} forcings in coastal acidification dynamics of estuarine systems. This research was focused in estuarine habitats known to be vitally important for the ecology of these systems. The majority of research on coastal acidification dynamics at the inception of this project was focused on shelf habitats and on ~seasonal time scales (Cai *et al.*, 2011; Ryan B Wallace *et al.*, 2014; Takeshita *et al.*, 2015; Waldbusser et al., 2011). The lack of mechanistic research in estuaries seemingly led to uncertainty as to whether rising atmospheric CO_2 would have a meaningful impact on estuarine carbonate chemistry (Duarte *et al.*, 2013, 2015; Waldbusser and Salisbury, 2014), with little work on quantifying how carbonate weather dynamics would change. To address this uncertainty and achieve the goals of my research, I combined high-frequency observations of estuarine biogeochemistry, high-quality discrete samples to constrain the inorganic carbon system, and relatively simple mechanistic models to understand interactions amongst natural and anthropogenic inorganic carbon cycling in estuarine habitats.

The primary conclusion from this work is that the addition of anthropogenic carbon to metabolically-intensive estuarine habitats will disproportionately enhance rates of acidification when compared with open-ocean settings. This enhanced acidification operates on multiple time scales, ranging from diel metabolic cycling to interannual

baseline pH decrease, and increases the magnitude, frequency, and duration that estuarine organisms are exposed to stressful chemical conditions. The findings that estuarine systems are prone to enhanced acidification due to their relatively low buffering capacities are not new (Egleston, Sabine and Morel, 2010; Cai *et al.*, 2011; Waldbusser *et al.*, 2011; Hu and Cai, 2013b), but the impacts had been poorly quantified in the past and often relied on conceptual understandings. Chapters 2 and 3 of this dissertation quantify how the magnitudes of diel and seasonal cycling of CO_2 in seagrass habitats have been altered by the addition of anthropogenic carbon, with important implications for organismal exposure and water quality standards. This work also highlights the temporal and spatial complexity of OA-related chemical impacts. The seagrass habitat sites in Puget Sound would be considered by many to be quite similar, yet showed significantly different OA trajectories driven by the interactions between habitat-specific metabolic CO_2 cycling and anthropogenic carbon. This spatial and temporal complexity of coastal acidification drivers is supported by the findings in the Tillamook Estuary work (chapter 4), where seasonal signals in the human perturbations of oceanic and watershed drivers alter not just the magnitude of chemical change, but also the "footprint" over which impacts are most severe.

The comparison of local drivers, including eutrophication, altered river discharge, warming water temperatures, and watershed land use change with the global atmospheric CO_2 forcing in controlling present-day and future changes directly addresses the previous uncertainty as to the importance of OA as a driver of estuarine chemical change. In both Puget Sound and Tillamook Estuary, rising atmospheric CO_2 is ultimately responsible for the majority of change presently realized in these habitats, as well as the change predicted

in end-of-century scenarios. Whether by local modification of CO_2 gas exchange fluxes, and/or mixing in of ocean waters with increased C_{anth} burdens, the ongoing anthropogenic perturbation of the carbon cycle on the global scale is a dominant signal in present-day CO_2 chemistry of these habitats. This may not be true for all coastal systems, as some have been shown to be heavily impacted by local drivers such as concentration of waste water discharges and eutrophication (e.g.Wallace *et al.*, 2014; Waldbusser et al., 2011). The findings of the research contained in this dissertation suggests a need to re-evaluate the relative importance of local versus global drivers in coastal acidification dynamics, however. Indeed, new research is showing that even in a system known to be heavily impacted by eutrophication such as the northern Gulf of Mexico, the global atmospheric CO_2 signal emerges as the primary driver of future acidification (Laurent *et al.*, 2018).

An important outcome of this work is the development of methodologies to address the efficacy of local policy and management actions in addressing water quality impacts of coastal acidification. In the habitats studied, the global OA signal is estimated to be the dominant driver of coastal acidification, with relatively small changes driven by local anthropogenic perturbations of water chemistry. This highlights the difficulties associated with local-scale management actions, such as nutrient reductions, in these habitats. However, this sort of attribution work improves our understanding of the magnitude of chemical changes, as well as the spatial and temporal dynamics of those changes. These findings providing relevant amelioration targets and guidelines for potential management plans addressing coastal acidification impacts and species conservation efforts.

Finally, the model techniques I have used are quite simple when compared to the power of current regional and global numerical models. However, these sorts of simple mechanistic models allow for easily recognizing and isolating the emergence of system properties and mechanisms that may be important at the organismal and/or habitat scale, but may be overlooked in coarse, large-scale regional and global models. Additionally, simple models may be more tractable for utilization in local-scale management decisions when fewer resources are available for complex model evaluations. I believe that the common aphorism "All models are wrong, but some models are useful" applies in this instance. It is my hope that the patterns of change predicted by the simple models of this dissertation can be used to inform new investigations of larger, more complex models capable of incorporating chemical and ecological feedbacks that are likely important modulators of future acidification trajectories and ecosystem responses. For instance, does seasonal amplification of carbonate chemistry emerge on the regional level in the Salish Sea and to the degree predicted by this work, or is this ameliorated by an environmental feedback not captured by my modeling techniques? While I have attempted to contextualize my findings with our current understanding of biological responses, an obvious shortcoming of the observational and attribution work I have done is its inability to translate in a meaningful way to organismal and ecosystem effects. New investigations with more complex models would also go a long way in bridging this divide between observations and projections of chemical change, with observations and projections of ecosystem change. Further development of this holistic understanding is vital if our society is to respond in a meaningful way to the impacts of ongoing climate

change through social, technological, and policy tools. It is my hope that the findings of this dissertation bring us one small step closer to that goal.

6. Bibliography

Adelsman, H. and Whitley Binder, L. (2012) *Ocean Acidification: From Knowledge to Action, Washington State's Strategic Response*. Olympia, WA.

Ainsworth, C. H. *et al.* (2011) 'Potential impacts of climate change on Northeast Pacific marine foodwebs and fisheries', *ICES Journal of Marine Science*, 68(6), pp. 1217–1229. doi: 10.1093/icesjms/fsr043.

Albright, R. *et al.* (2016) 'Reversal of ocean acidification enhances net coral reef calcification', *Nature*. Nature Publishing Group, 531(7594), pp. 362–365. doi: 10.1038/nature17155.

Amaral, V. *et al.* (2012) 'Moderate acidification affects growth but not survival of 6-month-old oysters', *Aquatic Ecology*, 46(1), pp. 119–127. doi: 10.1007/s10452-011-9385-5.

Banas, N. S. *et al.* (2015) 'Patterns of River Influence and Connectivity Among Subbasins of Puget Sound, with Application to Bacterial and Nutrient Loading', *Estuaries and Coasts*, 38(3), pp. 735–753. doi: 10.1007/s12237-014-9853-y.

Bandstra, L., Hales, B. and Takahashi, T. (2006) 'High-frequency measurements of total CO_2: Method development and first oceanographic observations', *Marine Chemistry*, 100(1–2), pp. 24–38. doi: 10.1016/j.marchem.2005.10.009.

Barnes, R. T. and Raymond, P. A. (2009) 'The contribution of agricultural and urban activities to inorganic carbon fluxes within temperate watersheds', *Chemical Geology*, 266, pp. 318–327. doi: 10.1016/j.chemgeo.2009.06.018.

Barton, A. *et al.* (2012) 'The Pacific oyster, *Crassostrea gigas*, shows negative correlation to naturally elevated carbon dioxide levels: Implications for near-term ocean acidification effects', *Limnology and Oceanography*, 57(3), pp. 698–710. doi: 10.4319/lo.2012.57.3.0698.

Barton, A. *et al.* (2015) 'Impacts of coastal acidification on the Pacific Northwest shellfish industry and adaptation strategies implemented in response', *Oceanography*, 28(2), pp. 146–159. doi: 10.5670/oceanog.2015.38.

Bates, N. R. *et al.* (2012) 'Detecting anthropogenic carbon dioxide uptake and ocean acidification in the North Atlantic Ocean', *Biogeosciences*, 9(7), pp. 2509–2522. doi: 10.5194/bg-9-2509-2012.

Baumann, H. *et al.* (2014) 'Large natural pH, CO_2 and O_2 fluctuations in a temperate tidal salt marsh on diel, seasonal, and interannual time scales', *Estuaries and Coasts*, pp. 220–231. doi: 10.1007/s12237-014-9800-y.

Baumann, H. and Smith, E. M. (2017) 'Quantifying metabolically driven pH and oxygen fluctuations in US nearshore habitats at diel to interannual time scales', *Estuaries and Coasts*, (October), pp. 1–16. doi: 10.1007/s12237-017-0321-3.

Bednaršek, N. *et al.* (2014) '*Limacina helicina* shell dissolution as an indicator of declining habitat suitability owing to ocean acidification in the California Current Ecosystem.', *Proceedings. Biological sciences / The Royal Society*, 281(1785), p. 20140123. doi: 10.1098/rspb.2014.0123.

Bednaršek, N. *et al.* (2016) 'Pteropods on the edge: Cumulative effects of ocean acidification, warming, and deoxygenation', *Progress in Oceanography*, 145, pp. 1–24. doi: 10.1016/j.pocean.2016.04.002.

Bednaršek, N. *et al.* (2017) 'Exposure history determines pteropod vulnerability to ocean acidification along the US West Coast article', *Scientific Reports*, 7(1), pp. 1–12. doi: 10.1038/s41598-017-03934-z.

Bender, E. A. *et al.* (1984) 'Perturbation Experiments in Community Ecology: Theory and Practice', *Ecology*, 65(651), pp. 1–13. doi: 10.2307/1939452.

Bianucci, L. *et al.* (2018) 'Sensitivity of the regional ocean acidification and carbonate system in Puget Sound to ocean and freshwater inputs', *Elem Sci Anth*, 6(1), p. 22. doi: 10.1525/elementa.151.

Borges, A. V. and Gypens, N. (2010) 'Carbonate chemistry in the coastal zone responds more strongly to eutrophication than ocean acidification', *Limnology and Oceanography*, 55(1), pp. 346–353. doi: 10.4319/lo.2010.55.1.0346.

Boyd, P. W. *et al.* (2016) 'Biological responses to environmental heterogeneity under future ocean conditions', *Global Change Biology*, pp. 2633–2650. doi: 10.1111/gcb.13287.

Boynton, W. R. *et al.* (2018) 'Oxygen and Nutrient Exchanges at the Sediment-Water Interface: a Global Synthesis and Critique of Estuarine and Coastal Data, Estuaries and Coasts', *Estuaries and Coasts*, pp doi: 10.1007/s12237-017-0275-5.

Brown, C. A. and Ozretich, R. J. (2009) 'Coupling between the coastal ocean and yaquina bay, oregon: Importance of oceanic inputs relative to other nitrogen sources', *Estuaries and Coasts*, 32(2), pp. 219–237. doi: 10.1007/s12237-008-9128-6.

Bruno, J.L. *et al.* (2015) 'Exploring the role of temperature in the ocean through metabolic scaling', *Ecology*, 96(12), pp. 3126-3140. doi: 10.1890/14-1954.1.

Busch, D. (2013) 'Potential impacts of ocean acidification on the Puget Sound food web', *ICES Journal of Marine Science*, 70, pp. 823–833. Available at: http://icesjms.oxfordjournals.org/content/70/4/823.short.

Busch, D. S. and McElhany, P. (2016) 'Estimates of the direct effect of seawater pH on the survival rate of species groups in the California current ecosystem', *PLoS ONE*, 11(8), pp. 1–28. doi: 10.1371/journal.pone.0160669.

Cai, W.-J. *et al.* (2011) 'Acidification of subsurface coastal waters enhanced by eutrophication', *Nature Geoscience*. Nature Publishing Group, 4(11), pp. 766–770. doi: 10.1038/ngeo1297.

Cai, W. J. *et al.* (2017) 'Redox reactions and weak buffering capacity lead to acidification in the Chesapeake Bay', *Nature Communications*, 8(1), pp. 1–12. doi: 10.1038/s41467-017-00417-7.

Carstensen, J. *et al.* (2018) 'Long-term and seasonal trends in estuarine and coastal carbonate systems', *Global Biogeochemical Cycles*. doi: 10.1002/2017GB005781.

Chan, F. *et al.* (2017) 'Persistent spatial structuring of coastal ocean acidification in the California Current System', *Scientific Reports*, 7(September 2016), p. 2526. doi: 10.1038/s41598-017-02777-y.

Chase, Z. (2002) 'Iron, nutrient, and phytoplankton distributions in Oregon coastal waters', *Journal of Geophysical Research*, 107(C10), p. 3174. doi: 10.1029/2001JC000987.

Christiaen, B. *et al.* (2017) 'Puget Sound Seagrass Monitoring Report Monitoring Year 2015'. Available at: http://www.dnr.wa.gov/programs-and-services/aquatics/aquatic-science/nearshore-habitat-publications%0AThis.

Clark, H. and Gobler, C. (2016) 'Do diurnal fluctuations in CO2 and dissolved oxygen concentrations provide a refuge from hypoxia and acidification for early life stage bivalves?', *Marine Ecology Progress Series*, 558, pp. 1–14. doi: 10.3354/meps11852.

Cloern, J. E. (2018) 'Patterns, pace, and processes of water-quality variability in a long-studied estuary', *Limnology and Oceanography*, pp. 1–17. doi: 10.1002/lno.10958.

Colbert, D. and McManus, J. (2003) 'Nutrient Biogeochemistry in an Upwelling-Influenced Estuary of the Pacific Northwest (Tillamook Bay, Oregon, USA)', *Estuaries*, 26(5), pp. 1205–1219.

Cyronak, T. *et al.* (2018) 'Short-Term Spatial and Temporal Carbonate Chemistry Variability in Two Contrasting Seagrass Meadows: Implications for pH Buffering Capacities', *Estuaries and Coasts*. Estuaries and Coasts, pp. 1–15. doi: 10.1007/s12237-017-0356-5.

Doney, S. C. *et al.* (2007) 'Impact of anthropogenic atmospheric nitrogen and sulfur deposition on ocean acidification and the inorganic carbon system.', *Proceedings of the National Academy of Sciences of the United States of America*, 104(37), pp. 14580–5. doi: 10.1073/pnas.0702218104.

Doney, S. C. *et al.* (2009) 'Ocean Acidification: The Other CO_2 Problem', *Annual Review of Marine Science*, 1(1), pp. 169–192. doi: 10.1146/annurev.marine.010908.163834.

Doney, S. C. and Schimel, D. S. (2007) 'Carbon and climate system coupling on timescales from the Precambrian to the anthropocene', *Annual Review of Environment and Resources*, 32, pp. 31–66. doi: 10.1146/annurev.energy.32.041706.124700.

Dove, S. G. *et al.* (2013) 'Future reef decalcification under a business-as-usual CO2 emission scenario.', *Proceedings of the National Academy of Sciences of the United States of America*, 110(38), pp. 15342–7. doi: 10.1073/pnas.1302701110.

Du, J. and Shen, J. (2016) 'Water residence time in Chesapeake Bay for 1980 – 2012 Water residence time in Chesapeake Bay for 1980 – 2012', *Journal of Marine Systems*. Elsevier B.V., 164 (December 2017), pp. 101–111. doi: 10.1016/j.jmarsys.2016.08.011.

Duarte, C. M. *et al.* (2010) 'Seagrass community metabolism: Assessing the carbon sink capacity of seagrass meadows', *Global Biogeochemical Cycles*, 24(4), pp. 1–8. doi: 10.1029/2010GB003793.

Duarte, C. M. *et al.* (2013) 'Is Ocean Acidification an Open-Ocean Syndrome? Understanding Anthropogenic Impacts on Seawater pH', *Estuaries and Coasts*, 36(2), pp. 221–236. doi: 10.1007/s12237-013-9594-3.

Dumbauld, B. R. *et al.* (2011) 'The Willapa Bay Oyster Reserves in Washington State: Fishery Collapse, Creating a Sustainable Replacement, and the Potential for Habitat Conservation and Restoration', *Journal of Shellfish Research*, 30(1), pp. 71–83. doi: 10.2983/035.030.0111.

Egleston, E. S. *et al.* (2010) 'Revelle revisited: Buffer factors that quantify the response of ocean chemistry to changes in DIC and alkalinity', *Global Biogeochemical Cycles*, 24(1), pp. 1–9. doi: 10.1029/2008GB003407.

Ekstrom, J. A. *et al.* (2015) 'Vulnerability and adaptation of US shellfisheries to ocean acidification', *Nature Climate Change*. Nature Publishing Group, 5(3), pp. 207–214. doi: 10.1038/nclimate2508.

Engle, V. D. *et al.* (2007) 'A Classification of U . S . Estuaries Based on Physical and Hydrologic Attributes', pp. 397–412. doi: 10.1007/s10661-006-9372-9.

Fassbender, A. J. *et al.* (2017) 'Nonuniform ocean acidification and attenuation of the ocean carbon sink', *Geophysical Research Letters*, 44(16), pp. 8404–8413. doi: 10.1002/2017GL074389.

Fassbender, A. J. *et al.* (2018) 'Seasonal Carbonate Chemistry Variability in Marine Surface Waters of the Pacific Northwest', *Earth System Science Data Discussions*, (March), pp. 1–49.

Feely, R. A. *et al.* (2010) 'The combined effects of ocean acidification, mixing, and respiration on pH and carbonate saturation in an urbanized estuary', *Estuarine, Coastal and Shelf Science*. Elsevier Ltd, 88(4), pp. 442–449. doi: 10.1016/j.ecss.2010.05.004.

Feely, R. A. *et al.* (2008) 'Evidence for upwelling of corrosive "acidified" water onto the continental shelf.', *Science*, 320(5882), pp. 1490–1492. doi: 10.1126/science.1155676.

Feely, R. A. *et al.* (2010) 'The combined effects of ocean acidification, mixing, and respiration on pH and carbonate saturation in an urbanized estuary', *Estuarine, Coastal and Shelf Science*. Elsevier Ltd, 88(4), pp. 442–449. doi: 10.1016/j.ecss.2010.05.004.

Feely, R. A. *et al.* (2016) 'Chemical and biological impacts of ocean acidification along the west coast of North America', *Estuarine, Coastal and Shelf Science*, pp. 1–11. doi: 10.1016/j.ecss.2016.08.043.

Feely, R. A. *et al.* (2018) 'The combined effects of acidification and hypoxia on pH and aragonite saturation in the coastal waters of the California current ecosystem and the northern Gulf of Mexico', *Continental Shelf Research*, 152(July 2017), pp. 50–60. doi: 10.1016/j.csr.2017.11.002.

Gazeau, F. *et al.* (2013) 'Impacts of ocean acidification on marine shelled molluscs', *Marine Biology*, 160(8), pp. 2207–2245. doi: 10.1007/s00227-013-2219-3.

Gimenez, I. *et al.* (2018) 'Ocean acidification stress index for shellfish (OASIS): Linking Pacific oyster larval survival and exposure to variable carbonate chemistry regimes', *Elementa Science of the Anthropocene*, 6(51). doi: 10.1525/elementa.306.

Gruber, N. *et al.* (2012) 'Rapid progression of ocean acidification in the California Current System', *Science*, 337(6091), pp. 220–3. doi: 10.1126/science.1216773.

Gruber, N., Sarmiento, J. L. and Stocker, T. F. (1996) 'An improved method for detecting anthropogenic CO2 in the oceans', *Global Biogeochemical Cycles*, 10(4), pp. 809–837.

Hagens, M. *et al.* (2015) 'Biogeochemical processes and buffering capacity concurrently affect acidification in a seasonally hypoxic coastal marine basin', pp. 1561–1583. doi: 10.5194/bg-12-1561-2015.

Hagens, M. and Middelburg, J. J. (2016) 'Generalised expressions for the response of pH to changes in ocean chemistry', *Geochimica et Cosmochimica Acta*. Elsevier Ltd, 187, pp. 334–349. doi: 10.1016/j.gca.2016.04.012.

Hales, B. *et al.* (2017) 'The Carbonate Chemistry of the "Fattening Line," Willapa Bay, 2011–2014', *Estuaries and Coasts*. Estuaries and Coasts, pp. 2011–2014. doi: 10.1007/s12237-016-0136-7.10.1007/s12237-016-0136-7.

Hales, B., Chipman, D. W. and Takahashi, T. T. (2004) 'High-frequency measurement of partial pressure and total concentration of carbon dioxide in seawater using microporous hydrophobic membrane contactors', *Limnology and Oceanography: Methods*, 2(Weiss 1974), pp. 356–364. doi: 10.4319/lom.2004.2.356.

Hauri, C. *et al.* (2013) 'The intensity, duration, and severity of low aragonite saturation state events on the California continental shelf', *Geophysical Research Letters*, 40(13), pp. 3424–3428. doi: 10.1002/grl.50618.

Hauri, C., Gruber, N., Vogt, M., *et al.* (2013) 'Spatiotemporal variability and long-term trends of ocean acidification in the California Current System', *Biogeosciences*, 10(1), pp. 193–216. doi: 10.5194/bg-10-193-2013.

Hettinger, A. *et al.* (2012) 'Persistent carry-over effects of planktonic exposure to ocean acidification in the Olympia oyster', *Ecology*, 93(12), pp. 2758–2768. doi: 10.1890/12-0567.1.

Hinga, K. R. (1992) 'Co-occurrence of dinoflagellate blooms and high pH in marine enclosures', *Marine Ecology Progress Series*, 86(2), pp. 181–187. doi: 10.3354/meps087181.

Hofmann, G. E. *et al.* (2011) 'High-frequency dynamics of ocean pH: a multi-ecosystem comparison.', *PloS one*, 6(12), p. e28983. doi: 10.1371/journal.pone.0028983.

Hofmann, G. E. and Todgham, A. E. (2010) 'Living in the Now: Physiological Mechanisms to Tolerate a Rapidly Changing Environment', *Annual Review of Physiology*, 72(1), pp. 127–145. doi: 10.1146/annurev-physiol-021909-135900.

Hönisch, B. *et al.* (2012) 'The Geological record of ocean acidification', *Science*, 335(6072), pp. 1058–1063. doi: 10.1126/science.1208277.

Hu, X. and Cai, W. J. (2013) ‘Estuarine acidification and minimum buffer zone - A conceptual study’, *Geophysical Research Letters*, 40(19), pp. 5176–5181. doi: 10.1002/grl.51000.

Hu, X. *et al.* (2017) ‘Effects of eutrophication and benthic respiration on water column carbonate chemistry in a traditional hypoxic zone in the Northern Gulf of Mexico’, *Marine Chemistry*. Elsevier, 194(April), pp. 33–42. doi: 10.1016/j.marchem.2017.04.004.

Iles, A. C. *et al.* (2012) ‘Climate-driven trends and ecological implications of event-scale upwelling in the California Current System’, *Global Change Biology*, 18(2), pp. 783–796. doi: 10.1111/j.1365-2486.2011.02567.x.

Joesoef, A. *et al.* (2017) ‘Seasonal variability of the inorganic carbon system in a large coastal plain estuary’, pp. 4949–4963.

Kelly, M. W., Padilla-Gamiño, J. L. and Hofmann, G. E. (2013) ‘Natural variation and the capacity to adapt to ocean acidification in the keystone sea urchin Strongylocentrotus purpuratus’, *Global Change Biology*, 19(8), pp. 2536–2546. doi: 10.1111/gcb.12251.

Kelly, R. P. *et al.* (2011) ‘Mitigating Local Causes of Ocean Acidification with Existing Laws’, *Science*, 332(6033), pp. 1036–1037. doi: 10.1126/science.1203815.

Kroeker, K. J. *et al.* (2013) ‘Impacts of ocean acidification on marine organisms: Quantifying sensitivities and interaction with warming’, *Global Change Biology*, 19(6), pp. 1884–1896. doi: 10.1111/gcb.12179.

Kroeker, K. J., Kordas, R. L. and Harley, C. D. G. (2017) ‘Embracing interactions in ocean acidification research: confronting multiple stressor scenarios and context dependence’, *Biology Letters*, 13(3), p. 20160802. doi: 10.1098/rsbl.2016.0802.

Kwiatkowski, L. and Orr, J. C. (2018) ‘Diverging seasonal extremes for ocean acidification during the twenty-first centuryr’, *Nature Climate Change*. Springer US, 8(2), pp. 141–145. doi: 10.1038/s41558-017-0054-0.

Landschützer, P. *et al.* (2018) ‘Strengthening seasonal marine CO 2 variations due to increasing atmospheric CO 2’. doi: 10.1038/s41558-017-0057-x.

Laurent, A. *et al.* (2018) ‘Climate Change Projected to Exacerbate Impacts of Coastal Eutrophication in the Northern Gulf of Mexico’, *Journal of Geophysical Research: Oceans*, pp. 3408–3426. doi: 10.1002/2017JC013583.

Lee, K. *et al.* (2010) ‘The universal ratio of boron to chlorinity for the North Pacific and North Atlantic oceans’, *Geochimica et Cosmochimica Acta*. Elsevier Ltd, 74(6), pp. 1801–1811. doi: 10.1016/j.gca.2009.12.027.

Lejart, M. *et al.* (2012) 'Respiration and Calcification of Crassostrea gigas: Contribution of an Intertidal Invasive Species to Coastal Ecosystem CO2Fluxes', *Estuaries and Coasts*, 35(2), pp. 622–632. doi: 10.1007/s12237-011-9462-y.

Li, F. *et al.* (2016) 'Physiological responses of coastal and oceanic diatoms to diurnal fluctuations in seawater carbonate chemistry under two CO_2 concentrations', *Biogeosciences Discussions*, (July), pp. 1–39. doi: 10.5194/bg-2016-281.

Long, M. H. *et al.* (2015) 'Seagrass metabolism across a productivity gradient using the eddy covariance, Eulerian control volume, and biomass addition techniques', *Journal of Geophysical Research: Oceans*, 120(5), pp. 3624–3639. doi: 10.1002/2014JC010352.

Lüthi, D. *et al.* (2008) 'High-resolution carbon dioxide concentration record 650,000-800,000 years before present.', *Nature*, 453(7193), pp. 379–382. doi: 10.1038/nature06949.

Mabardy, R. A. *et al.* (2015) 'Perception and Response of the U.S. West Coast Shellfish Industry to Ocean Acidification: The Voice of the Canaries in the Coal Mine', *Journal of Shellfish Research*, 34(2), pp. 565–572. doi: 10.2983/035.034.0241.

Marshall, K. N. *et al.* (2017) 'Risks of ocean acidification in the California Current food web and fisheries: ecosystem model projections', *Global Change Biology*, 23(4), pp. 1525–1539. doi: 10.1111/gcb.13594.

Matsumoto, K. and Gruber, N. (2005) 'How accurate is the estimation of anthropogenic carbon in the ocean? An evaluation of the ΔC* method', *Global Biogeochemical Cycles*, 19(3), pp. 1–17. doi: 10.1029/2004GB002397.

Mauger, G. S. *et al.* (2015) *State of Knowledge: Climate Change in Puget Sound*. doi: 10.7915/CIG93777D.

Mcgrath, T. *et al.* (2016) 'The Inorganic Carbon Chemistry in Coastal and Shelf Waters Around Ireland', pp. 27–39. doi: 10.1007/s12237-015-9950-6.

McNeil, B. I. and Sasse, T. P. (2016) 'Future ocean hypercapnia driven by anthropogenic amplification of the natural CO2 cycle.', *Nature*. Nature Publishing Group, 529(7586), pp. 383–6. doi: 10.1038/nature16156.

Meinvielle, M. and Johnson, G. C. (2013) 'Decadal water-property trends in the California Undercurrent, with implications for ocean acidification', *Journal of Geophysical Research: Oceans*, 118(12), pp. 6687–6703. doi: 10.1002/2013JC009299.

Miller, C. and Waldbusser, G. (2016) 'A post-larval stage-based model of hard clam Mercenaria mercenaria development in response to multiple stressors: temperature and acidification severity', *Marine Ecology Progress Series*, 558, pp. 35–49. doi: 10.3354/meps11882.

Miller, J. J. *et al.* (2016) 'Exposure to low pH reduces survival and delays development in early life stages of Dungeness crab (Cancer magister)', *Marine Biology*. Springer Berlin Heidelberg, 163(5), pp. 1–11. doi: 10.1007/s00227-016-2883-1.

Millero, F. J. (2010) 'Carbonate constants for estuarine waters', (Millero 2001), pp. 139–142.

Mohamedali, T. *et al.* (2011) *Puget Sound Dissolved Oxygen Model Nutrient Load Summary for 1999-2008, Washington Department of Ecology*. Available at: https://fortress.wa.gov/ecy/publications/documents/1103057.pdf.

Moore-Maley, B. L. *et al.* (2016) 'Locally driven interannual variability of near-surface pH and OmegaA in the Strait of Georgia', *Journal of Geophysical Research: Oceans*, (121), pp. 1600–1625. doi: 10.1002/2015JC011118.Received.

Moore-Maley, B. L. *et al.* (2018) 'The sensitivity of estuarine aragonite saturation state and pH to the carbonate chemistry of a freshet-dominated river', pp. 3743–3760.

Murray, J. W. *et al.* (2015) 'An inland sea high nitrate-low chlorophyll (HNLC) region with naturally high pCO_2', *Limnology and Oceanography*, 60(3), pp. 957–966. doi: 10.1002/lno.10062.

Oh, N. and Raymond, P. A. (2006) 'Contribution of agricultural liming to riverine bicarbonate export and CO 2 sequestration in the Ohio River basin', 20(August), pp. 1–17. doi: 10.1029/2005GB002565.

Pacella, S. R. *et al.* (2018) 'Seagrass habitat metabolism increases short-term extremes and long-term offset of CO_2 under future ocean acidification', *Proceedings of the National Academy of Sciences of the United States of America*, 115(15). doi: 10.1073/pnas.1703445115.

Paulsen, M.-L. *et al.* (2018) 'Temporal Changes in Seawater Carbonate Chemistry and Carbon Export from a Southern California Estuary', *Estuaries and Coasts*. Estuaries and Coasts, 41(4), pp. 1050–1068. doi: 10.1007/s12237-017-0345-8.

Pelletier, G. *et al.* (2018) 'Seasonal variation in aragonite saturation in surface waters of Puget Sound – a pilot study'.

Perrin, A., Probst, A. and Probst, J. (2008) 'Impact of nitrogenous fertilizers on carbonate dissolution in small agricultural catchments : Implications for weathering CO_2 uptake at regional and global scales', 72, pp. 3105–3123. doi: 10.1016/j.gca.2008.04.011.

Provoost, P. *et al.* (2010) 'Seasonal and long-term changes in pH in the Dutch coastal zone', *Biogeosciences*, 7(11), pp. 3869–3878. doi: 10.5194/bg-7-3869-2010.

Rasmuson, L. K. (2013) 'The biology, ecology and fishery of the dungeness crab, cancer magister', *Advances in Marine Biology*. doi: 10.1016/B978-0-12-410498-3.00003-3.

Raymond, P. A. *et al.* (2008) 'Anthropogenically enhanced fluxes of water and carbon from the Mississippi River', *Nature*, 451(7177), pp. 449–452. doi: 10.1038/nature06505.

Regnier, P. *et al.* (2013) 'Anthropogenic perturbation of the carbon fluxes from land to ocean', *Nature Geoscience*, 6(8), pp. 597–607. doi: 10.1038/ngeo1830.

Reimer, J. J. *et al.* (2017) 'Time series pCO2 at a coastal mooring: Internal consistency, seasonal cycles, and interannual variability', *Continental Shelf Research*. doi: 10.1016/j.csr.2017.06.022.

Reum, J. C. P. *et al.* (2014) 'Interpretation and design of ocean acidification experiments in upwelling systems in the context of carboante chemsitry co-variation with temperature and oxygen', *ICES Journal of Marine Science*, 71(3), pp. 528–536. doi: 10.1093/icesjms/fst176.

Riahi, K. *et al.* (2011) 'RCP 8.5-A scenario of comparatively high greenhouse gas emissions', *Climatic Change*, 109(1), pp. 33–57. doi: 10.1007/s10584-011-0149-y.

Richier, S. *et al.* (2018) 'Geographical CO_2 sensitivity of phytoplankton correlates with ocean buffer capacity', *Global Change Biology*, (December 2017), pp. 1–15. doi: 10.1111/gcb.14324.

Riebesell, U. *et al.* (2010) *Guide to best practices for ocean acidification research and data reporting, European commission*. doi: 10.2777/66906.

Robbins, L. L. and Lisle, J. T. (2018) 'Regional Acidification Trends in Florida Shellfish Estuaries : a 20 + Year Look at pH , Oxygen , Temperature , and Salinity'. Estuaries and Coasts, pp. 1268–1281.

Roegner, G. C. *et al.* (2011) 'Coastal upwelling supplies oxygen-depleted water to the columbia river estuary', *PLoS ONE*, 6(4). doi: 10.1371/journal.pone.0018672.

Sabine, C. L. *et al.* (2002) 'Distribution of anthropogenic CO2 in the Pacific Ocean', *Global Biogeochemical Cycles*, 16(4), pp. 30-1-30–17. doi: 10.1029/2001GB001639.

Sabine, C. L. *et al.* (2004) 'The oceanic sink for anthropogenic CO2', *Science*, 305(5682), pp. 367–371. doi: 10.1126/science.1097403.

Schoepf, V. *et al.* (2015) 'Limits to the thermal tolerance of corals adapted to a highly fluctuating, naturally extreme temperature environment.', *Scientific reports*. Nature Publishing Group, 5(November), p. 17639. doi: 10.1038/srep17639.

Shanks, O. C. *et al.* (2006) 'Basin-wide analysis of the dynamics of fecal contamination and fecal source identification in Tillamook Bay, Oregon', *Applied and Environmental Microbiology*, 72(8), pp. 5537–5546. doi: 10.1128/AEM.03059-05.

Shaw, E. C. *et al.* (2013) 'Anthropogenic changes to seawater buffer capacity combined with natural reef metabolism induce extreme future coral reef CO2 conditions', *Global Change Biology*, 19(5), pp. 1632–1641. doi: 10.1111/gcb.12154.

Shaw, E. C. *et al.* (2012) 'Impacts of ocean acidification in naturally variable coral reef flat ecosystems', *Journal of Geophysical Research: Oceans*, 117(3), pp. 1–14. doi: 10.1029/2011JC007655.

Shaw, E. C. *et al.* (2013) 'The role of CO2 variability and exposure time for biological impacts of ocean acidification', *Geophysical Research Letters*, 40(17), pp. 4685–4688. doi: 10.1002/grl.50883.

Small, D. P. *et al.* (2016) 'Temporal fluctuations in seawater pCO_2 may be as important as mean differences when determining physiological sensitivity in natural systems', *ICES Journal of Marine Science: Journal du Conseil*, 73, pp. 604–612. doi: 10.1093/icesjms/fsv232.

Sosdian, S. M. *et al.* (2018) 'Constraining the evolution of Neogene ocean carbonate chemistry using the boron isotope pH proxy', *Earth and Planetary Science Letters*. Elsevier B.V., 498, pp. 362–376. doi: 10.1016/j.epsl.2018.06.017.

Stets, E. G. *et al.* (2014) 'Long-term trends in alkalinity in large rivers of the conterminous US in relation to acidification, agriculture, and hydrologic modification', *Science of the Total Environment*. Elsevier B.V., 488–489(1), pp. 280–289. doi: 10.1016/j.scitotenv.2014.04.054.

Strong, A. L. *et al.* (2014) 'Ocean acidification 2.0: Managing our Changing Coastal Ocean Chemistry', *BioScience*, 64(7), pp. 581–592. doi: 10.1093/biosci/biu072.

Suchet, P. A. and Ludwig, W. (2003) 'Worldwide distribution of continental rock lithology : Implications for the atmospheric / soil CO 2 uptake by continental weathering and alkalinity river transport to the oceans', 17(2). doi: 10.1029/2002GB001891.

Sullivan, T. J. *et al.* (2005) 'Assessment of water quality in association with land use in the Tillamook Bay Watershed, Oregon, USA', *Water, Air, and Soil Pollution*, 161(1–4), pp. 3–23. doi: 10.1007/s11270-005-2443-7.

Sunda, W. G. and Cai, W. (2012) 'Eutrophication Induced CO 2 -Acidification of Subsurface Coastal Waters: Interactive Effects of Temperature, Salinity, and Atmospheric P CO 2', *Environmental Science & Technology*, 46(19), pp. 10651–10659. doi: 10.1021/es300626f.

Sutton, A. J. *et al.* (2016) 'Using present-day observations to detect when anthropogenic change forces surface ocean carbonate chemistry outside pre-industrial bounds', *Biogeosciences Discussions*, (March), pp. 1–30. doi: 10.5194/bg-2016-104.

Takeshita, Y. *et al.* (2015) 'Including high-frequency variability in coastal ocean acidification projections', *Biogeosciences*, 12(19), pp. 5853–5870. doi: 10.5194/bg-12-5853-2015.

U.S. E.P.A., O. of W. R. and S. (1986) *Quality Criteria for Water 1986 (EPA Publication No. 440/5-86-001)*. Washington, DC.

Tillamook Estuaries Partnership (2015) 'State of the Bays 2015: Health Report', pp. 1–58. Available at: http://www.tbnep.org/reports-and-publications.php.

Turi, G. *et al.* (2016) 'Climatic modulation of recent trends in ocean acidification in the California Current System', *Environmental Research Letters*. IOP Publishing, 11(1), p. 14007. doi: 10.1088/1748-9326/11/1/014007.

USDA-NASS (2012) 'Census of Agriculture County Profile Tillamook County – Oregon'.

Vano, J. a *et al.* (2008) 'Climate Change Impacts on Water Management in the Puget Sound Region, Washington, USA'.

Waldbusser, G. G. *et al.* (2011) 'Biocalcification in the Eastern Oyster (Crassostrea virginica) in Relation to Long-term Trends in Chesapeake Bay pH', *Estuaries and Coasts*, 34(2), pp. 221–231. doi: 10.1007/s12237-010-9307-0.

Waldbusser, G. G. *et al.* (2015a) 'Ocean acidification has multiple modes of action on bivalve larvae', *PLoS ONE*, 10(6). doi: 10.1371/journal.pone.0128376.

Waldbusser, G. G. *et al.* (2015b) 'Saturation-state sensitivity of marine bivalve larvae to ocean acidification', *Nature Climate Change*, 5(3), pp. 273–280. doi: 10.1038/NCLIMATE2479.

Waldbusser, G. G., Bergschneider, H. and Green, M. A. (2010) ‘Size-dependent pH effect on calcification in post-larval hard clam Mercenaria spp’, *Marine Ecology Progress Series*, 417(x), pp. 171–182. doi: 10.3354/meps08809.

Waldbusser, G. G. and Salisbury, J. E. (2014) ‘Ocean acidification in the coastal zone from an organism’s perspective: multiple system parameters, frequency domains, and habitats.’, *Annual Review of Marine Science*, 6, pp. 221–47. doi: 10.1146/annurev-marine-121211-172238.

Wallace, R. B. *et al.* (2014) ‘Coastal ocean acidification: The other eutrophication problem’, *Estuarine, Coastal and Shelf Science*. Elsevier Ltd, 148, pp. 1–13. doi: 10.1016/j.ecss.2014.05.027.

Wang, Z. A. *et al.* (2016) ‘Intertidal salt marshes as an important source of inorganic carbon to the coastal ocean’, *Limnology and Oceanography*, 61(5), pp. 1916–1931. doi: 10.1002/lno.10347.

Weisberg, S. B. *et al.* (2016) ‘Water quality criteria for an acidifying ocean: Challenges and opportunities for improvement’, *Ocean & Coastal Management*, 126, pp. 31–41. doi: 10.1016/j.ocecoaman.2016.03.010.

Xue, L. *et al.* (2017) ‘Sea surface aragonite saturation state variations and control mechanisms at the Gray’s Reef time-series site off Georgia, USA (2006–2007)’. doi: 10.1016/j.marchem.2017.05.009.

Yang, Z. *et al.* (2015) ‘Estuarine response to river flow and sea-level rise under future climate change and human development’, *Estuarine, Coastal and Shelf Science*. Elsevier Ltd, 156(1), pp. 19–30. doi: 10.1016/j.ecss.2014.08.015.

Zhang, S. *et al.* (2009) ‘Major ion chemistry and dissolved inorganic carbon cycling in a human-disturbed mountainous river (the Luodingjiang River) of the Zhujiang (Pearl River), China’, *Science of the Total Environment, The*. Elsevier B.V., 407(8), pp. 2796–2807. doi: 10.1016/j.scitotenv.2008.12.036.